Late Quaternary Stratigraphies from the Hebridean Continental Shelf and Margin, North West Scotland, United Kingdom.

A thesis submitted to the University of St Andrews
for the degree of Doctor of Philosophy

Lindsay Judith Wilson

School of Geography and Geosciences
University of St Andrews

Submitted September 2003

Declaration

i. I, Lindsay Judith Wilson, hereby certify that this thesis, which is approximately 40,000 words in length, has been written by me, that it is the record of work carried out by me and that it has not been submitted in any previous application for a higher degree.

Date 16/04/04. Signature of candidate ....

ii. I was admitted as a research student in October, 1999 and as a candidate for the degree of Ph.D. in October, 2000; the higher study for which this is a record was carried out in the University of St Andrews between 1999 and 2003.

Date 16/04/04. Signature of candidate .....

iii. I hereby certify that the candidate has fulfilled the conditions of the Resolution and Regulations appropriate for the degree of Ph.D. in the University of St Andrews and that the candidate is qualified to submit this thesis in application for that degree.

Date 16/04/04 Signature of supervisor .

Unrestricted

In submitting this thesis to the University of St Andrews I understand that I am giving permission for it to be made available for use in accordance with the regulations of the University Library for the time being in force, subject to any copyright vested in the work not being affected thereby. I also understand that the title and abstract will be published, and that a copy of the work may be made and supplied to any bona fide library or research worker.

Date 16/04/04. Signature of candidate .

Abstract

A detailed reconstruction of the behaviour of the last British Ice Sheet (BIS) during the last glacial period is obtained from two IMAGES cores (MD95-2006 and MD95-2007) from the Hebridean continental shelf and margin, north west Scotland.

A multiproxy approach has been adopted, involving the use of sediment grain size, calcium carbonate, stable isotope, radiocarbon and sediment colour analyses. Results obtained are used to relate the depositional environments of the continental margin and shelf to the behaviour of the ice sheet. A revised chronostratigraphy for the climatic events is established through detailed age-depth modelling.

The study of the high resolution cores enables the interpretation of the continental margin sediment accumulation pattern in terms of ice sheet fluctuation. Millennial and sub-millennial scale climate variability are recognised within this region of the North Atlantic during marine isotope stage (MIS) 3 to MIS 2. These cycles are particularly evident within MIS 3, where periodicities of 2- 3,000 years dominate. They correspond with the Dansgaard-Oeschger cycles which are clearly defined in the $\delta^{18}O$ record of the Greenland ice cores.

The BIS LGM is observed during MIS 2, within the period 21 - 17 ka BP. Deglaciation of the entire margin is complete by about 15 ka BP and the relatively rapid regional deglaciation of the Hebridean shelf took place prior to, or coincident

with Heinrich Event 1 (15.1-16.6 cal ka BP). The transition to the interstadial warming and the timing of the onset of the Younger Dryas cold phase are more difficult to define because of the uncertainties in radiocarbon dating, but the latter is observed at approximately 13 ka BP.

The main Heinrich events (HE) 1 to 5 are also evident through the associated meltwater events reflected in the $\delta^{18}O$ record and ice rafting detritus (IRD) peaks. However, a number of "non-Heinrich" IRD events are evident with similar magnitudes to the main HE. It is therefore proposed that an event stratigraphy based upon interstadial events would provide a more reliable means of correlating amphi-Atlantic climate change at such ice-proximal locations.

Acknowledgements

I would like to thank my supervisor Dr Bill Austin for his continued support, encouragement and invaluable discussions throughout my doctoral studies.

Also, external supervisor, Dr Charlotte Bryant, and her colleagues at the NERC Radiocarbon Laboratory, East Kilbride who supported the AMS dating programme and provided invaluable help in the early stages of the project.

I would like to thank Dave Gunn for his support while obtaining the spectrophotometry data at the Southampton Oceanography Centre and also Dr Mark Chapman (UEA) who provided useful advice on sediment colour.

I would also like to acknowledge the support of the European Union Marie Curie pre-doctoral fellowship and the University of Bergen in obtaining the stable isotope data. Professor Eystein Jansen and Professor Hans Petter Sejrup provided insightful comments and advice during my time in Norway. I also benefited from the assistance given by Rune Sørås in the operation of the mass spectrometer.

Thanks also to Colin Chilcott (University of Edinburgh) and the staff at the University of Bremen (Palaeoclimate) for running the additional stable isotope samples.

I am grateful to Dr John Hunt (GEMRU) who assisted with the geochemical analysis of the NAAZII tephra shards and provided invaluable comments during the discussion of NAAZII.

I benefited greatly from the guidance given by Graeme Sandeman (University of St Andrews) on the diagrammatic illustrations included within this thesis.

Thanks to Chris Byrne (University of Edinburgh) who permitted the inclusion of seven AMS ^{14}C dates from her Ph.D. and for her assistance with the cores at SOC. I would also like to thank Hayley Cawthorne (University of St Andrews) for her assistance with the tephra samples.

My gratitude also goes to David, Dan E, Andrew, Iain, Heather E, Carol, John and Laura Evans, Dan B and Danielle for making my time in St Andrews so enjoyable. Heather A and Danielle are thanked for their efforts in patiently verifying references and helping with the proof-reading of the text.

Finally, I would like to thank Katherine, Alasdair and my parents for their continued patience, encouragement, support and understanding.

Table of Contents

Figures

Tables

Chapter 1.

Introduction

1.1 The North Atlantic: Past, Present and Future

1.1.i Thermohaline Circulation: The global significance of the North Atlantic.

The oceans play an essential role in regulating the Earth's climate, transporting heat, nutrients and fresh water around the globe. This transportation is influenced by the inter-hemispheric circulation of the ocean and its interaction with the atmosphere. Heat transportation in the oceans has a significant impact on atmospheric temperatures, particularly at high latitudes, because the ocean's heat capacity is greater than the atmosphere by a 'factor of over thirty' (Stocker, 2000). The high heat capacity of the ocean enables it to affect temperatures daily, seasonally and annually (Clark *et al.*, 2002). The implications of this latitudinal transport for the climate system as a whole are profound (Ganachaud and Wunsch, 2000). Equally, the oceans represent the largest of the 'fast exchanging' carbon reservoirs (Stocker, 2000) and hence the rate of overturning (ventilation) will directly influence the global carbon cycle and its influence on climate.

Thermal forcing largely governs the freshwater forcing and meridional overturning of the ocean. The differential solar heating between the low and high latitudes generally forces warmer surface water towards the poles. In the Northern Hemisphere the warm surface water flows northwards to the high latitudes of the

northern North Atlantic, where it subsequently cools and sinks to form the southwards flow of salty, cold deep water. This southwards flow of dense water is termed the North Atlantic Deep Water (NADW). This 'ventilation' is achieved through a combination of cooling, high salinity and resultant increase in surface ocean water density. In its simplest conceptual form, this water eventually upwells in the Pacific and returns again to the North Atlantic via warm surface currents. Horizontal shallow and deep currents feed the vertical flows of this thermohaline circulation. It is the production of NADW which maintains the warm climate of the Atlantic basin, supplementing annual insolation at these latitudes by approximately 25 % (Lehman and Keigwin, 1992). It acts as a global heat conveyor, currently operating to balance water vapour transport through the atmosphere. If changes were to occur in the North Atlantic which disrupted thermohaline circulation, then severe climate change would very likely take place over NW Europe. An improved understanding of both the present and past operation of the ocean's thermohaline circulation will therefore inform the debate on the risk and impact of future rapid climate change.

1.1.ii The Palaeoceanography of the North Atlantic

The ocean is thought to act as a pacemaker for the abrupt millennial and sub-millennial climate changes observed in late Quaternary palaeoclimate archives. Broecker and Denton (1990) proposed that massive and abrupt climate change took place as a result of a change in the thermohaline circulation. The Atlantic conveyor

is thought to be a particularly vulnerable part of that system. For example, it has been suggested that a massive influx of freshwater stopped or at least slowed the conveyor and triggered the Younger Dryas cold phase (e.g. Broecker, 2003).

Ice sheet melting during the last deglacial period resulted in the release of freshwater equivalent to 120 m of global sea-level. The meltwater from the Laurentide ice sheet (LIS), the largest of the northern hemisphere's ice sheets, flowed down the Mississippi River to the Gulf of Mexico during most of the deglacial period (Broecker *et al.*, 1989). However, at ~12.5 cal ka BP (11 ^{14}C ka BP) a diversion took place as the retreat of the ice sheet led to a channel opening to the east from pro-glacial Lake Agassiz. This resulted in the release of large volumes of meltwater directly into the St Lawrence and the North Atlantic, close to the site of deep water formation. The impact of this freshwater input would have been to reduce surface water salinity and density, preventing water from sinking and thus decreasing the North Atlantic heat flux associated with the northwards advection of warm surface waters.

However, as Fairbanks (1989) has shown, the inferred discharge of meltwater during the Younger Dryas itself was significantly reduced. He used deglacial sea-level records from Barbados corals to propose that NADW production did not significantly decrease during this period. Jansen and Veum (1990) also challenged the question of NADW cessation; however, they remain in a minority

and numerous authors have suggested reduced NADW formation as the main controlling influence on Younger Dryas climates.

Global circulation models have been utilized to examine the effects of alterations within the freshwater budget on the stability of the thermohaline conveyor (e.g. Stocker and Wright, 1996). They suggest that the ocean did not return to the full glacial conditions observed at the Last Glacial Maximum (LGM) during the Younger Dryas (Keigwin *et al.*, 1991), thus suggesting that the THC has more than one stable operating mode (Stocker, 2000; Clark *et al.*, 2002) (Figure 1.1).

1. 2 Millennial-scale Climate Changes

The last glacial period is characterized by rapid fluctuations in climate on a number of time scales. This climatic variability is evident in ocean, terrestrial and ice core proxy records, indicating interaction between the ocean, atmosphere and ice sheets of the northern hemisphere at millennial and shorter time scales. However, the origin and mechanisms of these regular, and irregular oscillations remain largely unresolved.

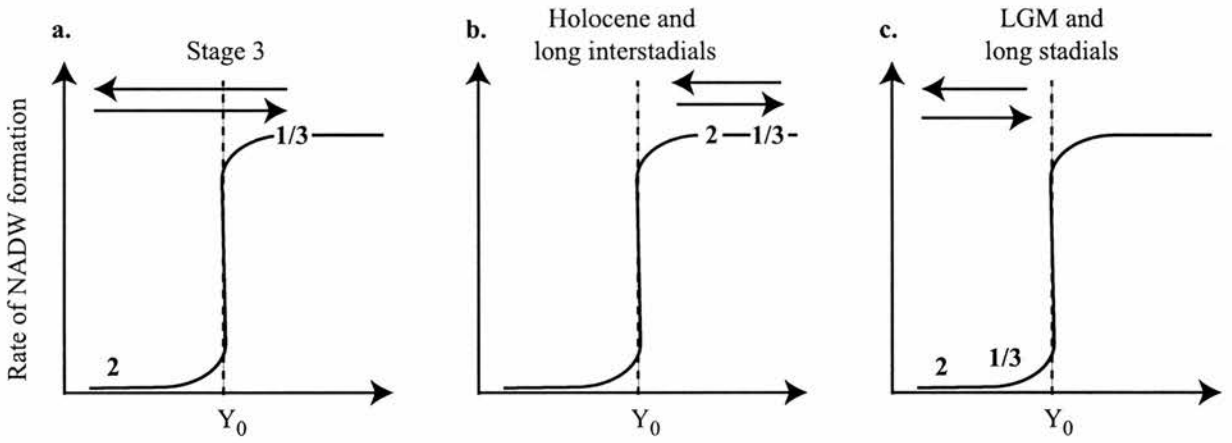

Figure 1.1. Modes of operation for the ocean system.
The arrows illustrate the changes in freshwater inputs and hence surface salinity fluctuations, where '**1**' is the initial state, '**2**' the new system equilibrium and '**3**' the final state. '$\mathbf{Y_0}$' represents the threshold value at which a mode switch in circulation occurs.

a. The increases in freshwater exceed the threshold value. The input of freshwater is short-lived therefore following each mode change the system returns to the initial state.

b. The freshwater fluxes do not exceed the threshold value, for example, an increase in salinity may have resulted in a more stable ocean within the glacial period. This could be applied to the Holocene or to the longer interstadials of the early glaciation.

c. The system is unable to return to its initial state due to the low surface salinity. This may be representative of the stadials during the last glaciation.

(Bond *et al.*, 1999, Figure 13, p.52)

1.2.i Millennial fluctuations in the Greenland Ice Cores: Dansgaard/Oeschger events

The millennial-scale climate fluctuations of the last glacial period are probably best known from the stable isotope records of the Greenland ice cores. Isotopic and geochemical analysis of the European GRIP (72° 34'N, 37° 37'W; elevation = 2321m) and the parallel US GISP2 (72.6°N, 38.5°W; elevation = 3200m) ice cores from central Greenland provide some of the highest resolution climate records for this period (Johnsen *et al.*, 1992; GRIP Members, 1993; Dansgaard *et al.* 1993; Taylor *et al.*, 1993). Annual, and even sub-annual layer counting has been carried out down-core from the surface for much of the Holocene and parts of the Lateglacial, largely revolutionizing climate research in recent decades (Alley, 2000).

The $\delta^{18}O$ of the precipitation locked in the ice of Greenland largely reflects the air temperature at the time of deposition. The fluctuations of $\delta^{18}O$ reveal a high degree of instability and abrupt climatic changes, notably within the last glacial period, particularly the 500 – 2,000 year Dansgaard/Oeschger (D/O) events (Figure 1.2) (Dansgaard *et al.*, 1993; Bond and Lotti, 1995; Bond *et al.*, 1999). These cycles (Johnsen *et al.*, 1992) of alternating warm to cold conditions give rise to the characteristic pattern of warm interstadials, followed by gradual cooling to stadials. The Greenland ice cores have recorded twenty-four D/O events between 115,000 and 14,000 yrs BP, each associated with an annual temperature variation of 5 to 8°C

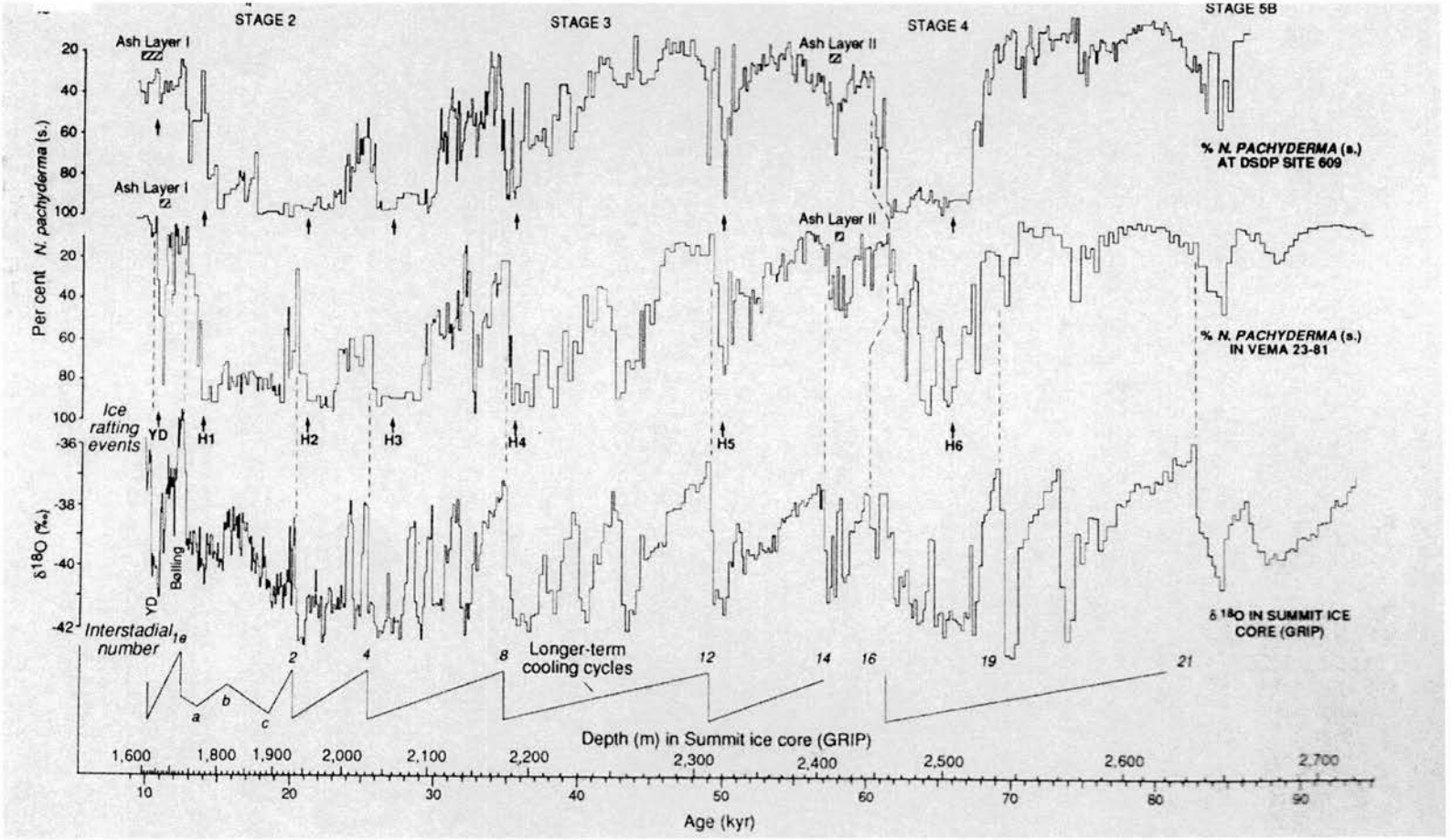

Figure 1.2. Bond *et al.*'s (1993) assignment of Heinrich Events 1-6 and groupings of Dansgaard-Oeschger cycles. Also shown is the correlation between the foraminiferal records from marine cores DSDP site 609 and V23-81 and, the GRIP $\delta^{18}O$ record.

(Bond *et al.*, 1993, Figure 3, p.145)

(Raymo *et al.*, 1998). These extremely rapid millennial-scale oscillations were particularly prominent during the middle and late phases of Marine Isotope Stage (MIS) 3, while cycle amplitudes diminished during MIS 2 around the time of the LGM (Bond *et al.* 1997). During MIS 2 and 4, the D/O cycles are associated with prolonged stadials and large global ice volumes, while the D/O cycles in early MIS 3 occur when ice volumes were lower and are associated with long, particularly warm interstadials. The mid to late MIS 3 period is characterised by intermediate ice volumes and 1-2 kyr D/O cycles (Bond *et al.*, 1999).

1.2.ii Millennial fluctuations in the North Atlantic Ocean: Heinrich Events

Millennial oscillations were first recorded in high resolution marine sediments in the 1970s and early 1980s (e.g. Ruddiman, 1977; Heinrich 1988; Broecker *et al.*, 1992), although interest was renewed following the seminal paper by Heinrich (1988). Prior to this date, climate variability studies had focussed largely on longer time periods and orbital-scale fluctuations.

1.2.ii.a The characteristics of Heinrich Layers

The major climate anomalies associated with 'barren' zones, i.e. devoid of planktonic foraminifera (Heinrich, 1988; Bond *et al.*, 1992) and coccoliths, were first recorded in marine sediment cores from the North Atlantic. These 'zones' within marine sediment cores were also characterised by high magnetic

susceptibility values (i.e. increased ferromagnetic and paramagnetic minerals, and a decrease in quartz or calcite) and increases in ice-rafted detritus (IRD) content (Grousset *et al.* 1993). This coarse lithic component (>150μm) consisted of particles or clasts which were deposited into a glacimarine environment from icebergs or sea ice. The size of the IRD deposited was partly dependent on the transportation agent and distance from source. In addition, marked decreases in $\delta^{18}O$ and faunal evidence indicated ocean surfaces were cooler and less saline during these intervals.

Six major intervals of increased IRD deposition were observed within the last glacial period between 14 and 70 ka BP (Heinrich, 1988) in the NE Atlantic. These were later termed 'Heinrich Events' (HE) by Broecker *et al.* (1992) (Figure 1.2). They were numbered HE6 through to the most recent, HE1. The sharp contacts between the IRD layers and the contrasting foraminifera-rich layers (Figure 1.3) indicates that each layer accumulated rapidly (Dowdeswell *et al.*, 1995). However, AMS ^{14}C dating evidence taken directly above and below each layer should be treated with caution due to a possible increase in the marine reservoir age during the Heinrich Events (Voelker *et al.*, 1998; Waelbroeck *et al.*, 2001).

The absolute timing of each HE therefore varies slightly between studies (e.g. Broecker *et al.*, 1992; Bond *et al.*, 1993, 1997; McIntyre and Molfino, 1996; Mayewski et al., 1997; Curry *et al.*, 1999) but the consensus indicates a periodicity of once every 7 ka to 10 ka. The HEs tend to be more closely spaced towards the LGM (Bond *et al.*, 1992; Bond *et al.*, 1999).

Figure 1.3.

a. Ice Rafted Detritus from Heinrich Event 4 in IMAGES core MD95-2006 (core depth = 2460 cm).
Image is approximately 4 cm across. DC= detrital carbonate

b. Foraminifera: typical North Atlantic Current assemblage, dominated by *Globigerina bulloides* (core depth = 20 cm; MD95-2006).
Similar foraminiferal assemblages occur between the IRD-rich horizons, in lighter coloured sediments, rich in foraminiferal carbonate and indicative of warmer sea surface temperatures (see Kroon *et al.*, 1997).
Image is approximately 4 mm across.

Ruddiman (1977) identified a zone of maximum IRD between 40°N and 55°N in the North Atlantic; a region often referred to as the "Ruddiman belt". This has recently been confirmed by Broecker *et al.* (1992), who observed these Heinrich layers in marine ODP site 609, and by Bond *et al.* (1992) who observed that the increased IRD input was associated with major coolings of the entire Northern Hemisphere. These results indicated that the IRD events were not purely a regional feature and raised questions regarding the stability of the circum-Atlantic ice sheets. Dowdeswell *et al.* (1995) carried out detailed analysis and reviewed over fifty sediment cores from the North Atlantic IRD 'belt'. An average layer thickness was recorded of 10-15cm, in association with a strong distance-decay pattern from the main Laurentide source, i.e. layer thickness decreased from the West to the East Atlantic.

1.2.ii.b The composition and provenance of Heinrich Layers

The composition of the lithic components within HEs gives an indication of the IRD source regions. Bond *et al.* (1992) observed that H1 and H2 consist predominantly of detrital carbonate derived from the limestone and dolomite bedrock of the Hudson Strait. Andrews *et al.* (1993, 1994) also observed that many of the Heinrich layers contain a high detrital carbonate content (20-25%). This corresponds to the Palaeozoic carbonate bedrock of the Hudson Bay and Hudson Strait, indicating that the source region of the IRD was one lobe of the Laurentide

Ice Sheet (LIS). The rapid discharges of icebergs therefore appear to be closely associated with a significant component of ice derived from an ice stream in the Hudson Strait which drained the central region of the LIS.

However, recent Sr-Nd isotope studies of HE3 and HE4 in a number of marine cores (38°N to 68°N) indicate that the icebergs were calved from a number of ice sheets from around the North Atlantic (Bond and Lotti, 1995; Snoeckx *et al.*, 1999; Grousset *et al.*, 2000, 2001). Heinrich events have now been observed outside the "Ruddiman belt", for example in the Norwegian Sea (Fronval *et al.*, 1995) and off the coast of Portugal (Robinson *et al.*, 1995). The isotopic evidence identifies the involvement of the Fennoscandian, Icelandic and Laurentide ice sheets in Heinrich layer sediment composition.

The term 'atypical' is applied to Heinrich events which exhibit (HE3, HE6) evidence for a clearer European derived provenance signal (Grousset *et al.*, 1993; Revel *et al.*, 1996, Snoeckx *et al.*, 1999) in addition to the later, less dominant LIS signal. The 'typical' Heinrich events (HE1, HE2, HE4, HE5) have a dominant LIS lithic component (Gwiazda *et al.*, 1996; Hemming *et al.*, 1998). It has therefore been suggested that the glaciological mechanisms at play may have differed between the 'typical' and 'atypical' HEs. It is possible that this variation in source may therefore provide further understanding of the timing of the events from the different amphi-Atlantic ice sheets.

Elliot *et al.* (1998) hypothesised that the European ice sheets may have fluctuated with a shorter oscillatory period (1-2 kyr) than the LIS (7.2 kyr); a feature which Knutz *et al.* (2001) demonstrated from IRD of BIS provenance. Heinrich Layer 3 is thought not to be synchronous throughout the North Atlantic due to the varying origins of composition, but may equally highlight the asynchronous nature of response within many of the circum-Atlantic ice sheets to external forcing.

1.2.ii.c Precursors to the Heinrich Events

A 'precursor' IRD signal of European and/or Icelandic composition has been proposed for H2 (Scourse *et al.*, 2000; Grousset *et al.*, 2001), which was immediately followed by the LIS-derived IRD signal. However, it is not yet known whether the behaviour of the European ice sheets was independent from the LIS, or whether it was in fact the European IRD signal which initiated the events leading to LIS surging (Grousset *et al.*, 2001). The implications of such sub-millennial IRD events, with distinctive regional signatures, are potentially significant for the synchronicity of the ice-rafting events and may help to elucidate possible circum-Atlantic forcing mechanisms.

1.2.iii Causal factors for millennial-scale fluctuations

Heinrich (1988) originally proposed a causal mechanism for IRD events primarily controlled and driven by the precession of the Earth's axis. The precessional cycle consists of summer and winter insolation minima to give a mean

periodicity of 11,000 $\pm$ 1,000yrs. This hypothesis has recently been further developed by McIntyre and Molfino (1996), who suggest that the existence of millennial-scale fluctuations in the Holocene record rule out a high-latitude forcing mechanism, such as modulations of the THC. During a time of reduced eccentricity, the precessional component of orbital variation produces a modulation in zonal wind-driven divergence in the tropics. This mechanism of millennial-scale variability remains highly controversial, with no evidence having been found of solar oscillations at the Dansgaard-Oeschger 1500 year scale.

In contrast, MacAyeal (1993) hypothesised that it took approximately 7,000 years for sufficient ice to accumulate for the required amount of heat to be generated to allow basal melting and surging. It has also been proposed that the iceberg discharges from Hudson Bay may be in response to climatic cooling (Bond *et al.*, 1992; Broecker *et al.*, 1992). Equally, if sea surface temperatures (SSTs) are reduced, icebergs will survive longer and may therefore lead to more widespread IRD events (Dowdeswell *et al.*, 1995). Alley and MacAyeal (1994) and MacAyeal (1993) hypothesised that the internal dynamics of the LIS were responsible for the initiation of the major calving events that produced HEs. They argued that the storage of geothermal heat by the ice cap would reach a critical point whereby basal melting took place over the unconsolidated sediment of the Hudson Bay. This enabled the LIS to surge periodically into the Labrador Sea, resulting in massive iceberg discharges. In contrast to many other mechanisms proposed to explain HEs,

the 'binge/purge' model of Alley and MacAyeal (1994) is based solely on the internal behaviour of the LIS and does not call upon external trigger mechanisms.

The involvement of IRD from different regional sources indicates that a number of ice sheets were therefore contributing to the HEs and a mechanism should therefore involve all these ice sheets. For example, the internally-driven geothermal model of Alley and MacAyeal (1994) cannot account for the presence of a European signal in early H4 (Snoeckx *et al.*, 1999). However, the thin ice lobes draining the circum-Atlantic ice sheets are particularly sensitive to both internal and external changes to the ice sheet. A small rise in relative sea-level, for example, would destabilise the margin, enabling the ice sheet to float, resulting in significantly increased iceberg calving. The initial rise in sea-level could result from the discharge of icebergs from any one of the major ice sheets; even those in the Southern Hemisphere. However, while smaller ice sheets such as the western BIS may have been highly sensitive to such forcing it would require a relatively large rise in sea-level to instigate the destabilisation of the major ice sheet margins.

A further causal factor could equally involve interactions between various elements of the climate system. Since it is the maritime margins of the ice sheets which are probably the most sensitive to climate forcing, it seems plausible that ocean circulation changes, particularly those linked to the formation of deep water, may play an important role in changing coastal temperatures and hence destabilising ice sheets.

Broecker *et al.* (1990), as discussed previously, proposed that a natural salt oscillation mechanism operated in the North Atlantic during the last glacial period. The formation of deep water, which involves the transport of salt to the deep ocean, coincides with the release of heat at high latitudes and therefore aids melting of the ice sheet margins. This melting results in an increased input of freshwater to the oceans thus reducing surface ocean salinity; in turn slowing the ocean's conveyor system. However, as salt removal is reduced due to the reduction of deep water formation at high latitudes, a resultant increase in salinity occurs at low latitudes. At the same time, there is some evidence to suggest that the tropics build-up a surplus of heat. Starved of heat, the volume of meltwater input to the mid- to high latitude North Atlantic gradually reduces and salinity levels eventually increase until deep water formation takes place again. This process has been successfully reproduced in modelling studies (e.g. Stocker and Wright, 1996; Rahmstorf, 1994) and the sudden turn-on of thermohaline convection during the last termination was termed the "super-conveyor" by Kroon *et al.* (1997).

Uncertainties remain regarding the precise underlying internal and/or external causal mechanism(s) of these sub-millennial-scale oscillations and in particular, the interaction between the circum-Atlantic ice sheets.

1.2.iv Correlation between the marine and ice core records of millennial-scale climate change

Several studies have illustrated the similarity between millennial-/sub-millennial scale climate changes in the marine and Greenland ice core records (Bond *et al.*, 1993; Elliot *et al.*, 1998). These show that a close correlation exists between the $\delta^{18}O$ record of the Greenland ice cores and the sea surface temperature (SST) fluctuations reflected by the polar/sub-polar foraminiferal records from the North Atlantic. Dating uncertainties mean that small lags or leads may exist between the records, but the records are generally assumed to be synchronous. However, the general pattern is still one of slow, gradual cooling followed by a rapid return to warm climatic conditions.

The $\delta^{18}O$ D/O shifts are less pronounced in the Southern Hemisphere Vostok ice core from E. Antarctica (Barnola *et al.*, 1987; Jouzel *et al.*, 1987). This suggests that while these variations in the climate system seem to have been global, they were centred on the North Atlantic. Indeed, they have been closely associated with North Atlantic Heinrich Events (HE); each HE occurring at the culmination of a series of D/O cycles to define the so-called Bond cycles (Bond *et al.*, 1992; 1993). The latter are thought to be associated with North Atlantic Deep Water (NADW) flow reduction and fluctuations in meltwater supply (Bond and Lotti, 1995; Bond *et al.*, 1999). Bond *et al.* (1999) also noted that each stadial within the D/O cycle package is associated with 'deep southward penetration of the polar front' (see also section

1.2.iii). The cold-to-warm transitions are particularly marked where a D/O culmination coincides with a HE (Figure 1.2).

1.3 The Last British Ice Sheet (BIS)

The offshore limits of the last BIS remain poorly defined, particularly around the NW continental margins. The evidence is particularly limited with regard to the limits of the ice sheet prior to the LGM and the timing of events during the last glacial period.

1.3.i Pre-LGM Limits

In fact, relatively little is known about the behaviour of the last BIS prior to it reaching its maximum extent. It was originally thought (Clapperton, 1997) that between the last interglacial and the Late Devensian that much of Britain and Ireland were free of ice. However, research now suggests that an ice sheet advanced and retreated on several occasions between 40 ka BP and the LGM (Last Glacial Maximum) (Bowen *et al.*, 2002). The evidence to support this on land and on the surrounding continental shelves is poorly preserved due to the increased erosional activity of the ice as it expanded to its maximum extent. However, offshore, around the glaciated margins of NW Scotland, there are "proximal" glacimarine deposits which preserve this record of early glaciation.

1.3.ii LGM Limits

If one accepts that LGM ice sheet limits are sometimes poorly dated then the maximum extent of the last ice sheets need not necessarily coincide with any formal definition of LGM timing, hence a different approach is called for.

Evidence from the North Sea suggests that during the Middle and Late Pleistocene Scotland supported at least four periods of major glacial activity (Bowen *et al.*, 1986). The LGM of the last BIS margin in the North Sea Basin has been inferred as the junction between the glacial Wee Bankie moraine and the Marr Bank formation (Thomson and Eden, 1977; Sutherland, 1984; Stoker, *et al.*, 1985). Sejrup *et al.* (1994, 2000) suggest that during this period (between 29.4 and 22 ka BP) the BIS and Scandinavian ice sheets were in contact with one another.

In the northern North Sea a possible independent ice cap over the Shetland Isles (Flinn, 1978) may not have been coalescent with the Scandinavian ice sheet. It was originally thought that the whole Scottish mainland and the north and central parts of the North Sea Basin were glaciated during the Late Devensian. However, the stratigraphic analysis of Toa Glason and Crossbrae Farm sites (Hall, 1984; Sutherland, 1984) indicate that some areas of the NE Scottish mainland were ice free, e.g. Caithness and Orkney, (Smith, 1997, 2000; Benn, 1997). A general dearth of radiocarbon dates limits the evidence for this hypothesis although Hall and Bent

(1990) infer an offshore ice limit extending to its maximum at the Bosies Bank moraine complex.

The extent of ice in the offshore area of NW Scotland is also open to debate. The original proposal hypothesised that the last Scottish ice sheet extended northwards directly across the Outer Hebrides to the continental shelf edge (Geikie, 1873; 1878; Jehu and Craig, 1934). However, it is now widely accepted that the Outer Hebrides supported an east and south-east flowing independent ice cap (Flinn, 1978; von Weymarn, 1979; Peacock *et al.*, 1980; Peacock, 1984, 1991).

In the offshore region of NW Scotland Late Devensian ice is long thought to have had a limit near to the continental shelf edge (Boulton *et al.*, 1977; Anderson, 1981). Recent offshore investigations have suggested that the mainland ice streams may have been confluent in the Minches with the Outer Hebrides ice cap and possibly the northernmost part of the Irish ice cap. These ice streams may then have flowed north of Lewis (von Weymarn and Edwards, 1973; Sutherland and Walker, 1984; Stoker and Holmes, 1991; Sutherland, 1991) and south to the Hebrides platform on the continental shelf (Davies *et al.*, 1984; Selby, 1989; Peacock *et al.*, 1992).

Opinions remain divided over whether the Hebrides ice cap terminated on north Lewis or whether mainland ice flowed onto the island (Flinn, 1978; Peacock, 1991; Sutherland and Walker, 1984). Hall (1995) suggests that the whole of Lewis

was glaciated during this period. Dating evidence obtained from an organic layer which overlies glacial till suggests the presence of either local ice, or a combination of local and mainland ice on the island after ~ 31.5 cal ka BP [27.3 ^{14}C ka BP] (von Weymarn and Edwards, 1973) thus supporting interstadial conditions in Scotland at this time. Whittington and Hall (2002) re-examined the organic sediment beneath the Tolsta Head Till. They dated interstadial events from ~38.1 cal kyr BP (32.8 ^{14}C kyr BP) to ~32 cal kyr CP (28.7 ^{14}C kyr BP) as the build-up of Late Devensian ice began.

The extent of the last ice sheet at the LGM has also been examined through the identification of periglacial trimlines on mainland NW Scotland and the Outer Hebrides (Ballantyne *et al.*, 1998). Trimlines are interpreted as having been cut by the glacier around former nunataks when the ice was at its maximum thickness. The transition between the frost-weathered detritus and the glacially-scoured bedrock is typically observed over a few tens of metres (Ballantyne *et al.*, 1998). The reconstructed ice sheet altitudes range from >950m on the mainland to 425-450m on the Outer Hebrides. Ballantyne *et al.* (1998) confirmed the presence of an independent ice cap on the Outer Hebrides at the LGM, and suggested that the trimlines indicated a thinner ice sheet was present in this region compared to the previous proposal by Lambeck (1995). The idea of a thinner last glacial ice sheet has now been adopted as the most likely scenario.

1.3.iii The timing of the LGM

Only a relatively small number of radiocarbon dates have been obtained for reconstructing the chronology of the BIS at the LGM, although many more exist through the deglacial period. The timing of these events tend to vary on a regional scale, often specific to the local ice sheet conditions, but sufficient exist to reveal a general pattern.

Rose (1985) proposed the Dimlington Stadial as the chronostratigraphic name for the period of maximum ice sheet extent during the Late Devensian. A type site on the coast of East Yorkshire related this phase to the period between 26 and 13 ^{14}C ka BP (Catt, 1987). The LGM in eastern England was suggested to have been between 18 to 16 ^{14}C ka BP.

Sejrup *et al* (1994, 2000) constructed a glaciation curve, based on lithostratigraphic, seismic and geotechnical data, for the Late Weichselian period in the North Sea. It suggests that the area was ice-free around 30ka BP but at some period between 22 and 29ka BP the Scottish ice and SIS were confluent. At 22 ka BP the Scandinavian ice sheet (SIS) occupied the Baltic, Scandinavia and sections of Denmark and North Europe and this is taken to represent the LGM.

The ages obtained for the British LGM ice sheet limits should be treated with caution. Recent evidence from ^{36}Cl and ^{14}C dating suggests a slightly revised

chronology for the British and Irish ice sheet (BIIS) LGM (Bowen *et al.*, 2002). The BIIS is now thought to have reached its maximum extent at approximately 22 ka BP (Bowen *et al.*, 2002) when the BIS and SIS were no longer in contact.

1.3.iv Deglacial characteristics of the BIS

The precise chronology of the last deglacial period is equally difficult to establish. The decay of the LIS at approximately 17.2 to 17.6 cal kyr BP may have led to the collapse of the other circum-Atlantic ice sheets (McCabe and Clark, 1998), but dating uncertainties make it difficult to resolve some of these important phasing issues.

In the North Sea region the confluent BIS and Fennoscandian ice fronts receded after 22 ka BP (Sejrup *et al.*, 1994). Deglaciation of the Scandinavian ice sheet is characterised by a two-step process. In a marine core study off the coast of Tromsø, Jansen and Erlenkeuser (1985) dated the first termination to approximately ~14.7 cal ka BP (13 ^{14}C ka BP) while the second termination coincided with the Younger Dryas/Holocene boundary at approximately ~11 cal ka BP (10 ^{14}C ka BP).

Lehman *et al.*, (1991) carried out AMS ^{14}C dating and isotope analysis on rapidly deposited supra-till from Troll 3 (60° 46.7'N, 3° 42.8'E) in the central Norwegian Channel. The measurements indicated the retreat of the southern margin of the Fennoscandian ice sheet by 15 kyr BP, while freshwater/IRD discharge into

the channel continued until 13.5 kyr BP. The recalibration of existing ^{14}C dates indicates deglaciation in the Norwegian Sea region from 18 cal ka BP onwards.

The North Sea Plateau and parts of the Norwegian Trench were ice-free by ca. 19 ka BP, prior to a brief readvance between 18.5 to 15.1 ka BP. Sejrup *et al.* (1994, 2000) contested the 14.7 ka BP date proposed by Lehman *et al.* (1991) for the deglaciation of the Norwegian Trench, favouring a slightly earlier date of 15.1 ka BP. However, the history of deglaciation between Scotland and Fladen remains unresolved (Sejrup *et al.*, 1994).

The last deglacial period of the BIS took place as the ice sheet margin fluctuated in response to major changes in the climate and ocean systems (Austin and Kroon, 1996; Knutz *et al.*, 2001). The retreat-advance-retreat pattern observed for the LIS was, apparently, also reflected in the behaviour of the BIS. McCabe and Clark (1998) hypothesise that since the LIS and Fennoscandian ice sheets were retreating at this time, the BIS was merely responding to the collapse of the LIS. This readvance is dated at ca. 16.1 kyr BP in the northern Irish Sea. The Irish Sea glacier is one of the major drainage conduits of the last BIS and it is thought to have undergone at least five oscillations at its margins between 25.4 and 16.2 cal ka BP (22 and 14 ^{14}C ka BP) (McCabe and Clark, 1998). The BIIS was particularly dynamic during its retreat and exhibited unstable behaviour. Bowen *et al.* (2002) utilised ^{36}Cl and ^{14}C ages to propose an early deglacial pulse at approximately 21.8 ka BP. Deglaciation was widespread by 17.4 $\pm$0.4 ka BP (Bowen *et al.* 2002),

however, terrestrial evidence from NE Ireland indicates the ice sheet retreat phase was interrupted by a readvance which correlates with the H1 event (McCabe and Clark, 1998). It has therefore been proposed that the deglacial phase was partially reversed by H1 at ca. 15.8-16.9 ka BP (McCabe and Clark, 1998). This link between the ice sheet readvance and H1 has also been suggested on the mainland of NW Scotland (Benn, 1997).

1.4 The Hebridean continental shelf and margin

1.4.i Regional Setting

The dynamic nature of the last British ice sheet has fundamentally influenced the characteristics of the depositional environment in the offshore region (Stoker, 1995). The sensitive offshore margins of the BIS to the NW of Scotland are sited in an ideal location to respond to changes caused by sea-level fluctuations and alterations in moisture supply and heat flux in the thermohaline circulation. The Late Devensian ice sheet extended close to the shelf break around St Kilda before calving into the deeper waters of the North Atlantic (Davies *et al.*, 1984). Therefore, the continental shield and slope in this region are ideally situated to provide the sedimentary record that will reflect this dynamic history.

1.4.ii The Barra Fan

The Barra Fan advances westwards, encroaching onto the Hebrides Terrace Seamount before extending out towards the Rockall Trough (Holmes *et al.*, 1998) (Figure 1.4). It passes between the Geikie Bulge to the north and the Donegal platform to the south (Armishaw *et al.*, 1998). The Barra Fan, together with the Donegal Fan, comprises a single fan complex which covers an area of approximately 6,300 km^2. This fan complex is one of the southernmost well-developed glacigenic fan systems on the European continental margin (Knutz *et al.*, 2001).

Stoker *et al.* (1994), Holmes *et al.* (1998) and Armishaw *et al.* (1998) have recently reviewed the geometry and structure of the Barra Fan and its seismostratigraphic setting. The base of the Barra Fan is identified by an unconformity which has been tentatively correlated with the mid-Miocene (Stoker, 1998). This unconformity extends westwards into the Rockall Trough. A date obtained from just above this layer, in the British Geological Survey (BGS) borehole 90/13, estimates an average of 10.1 Ma corresponding to the Late-Miocene. Deposition along this margin is punctuated by a series of slide failures, many of which correspond with the Peach mega slide, located further to the south (Armishaw *et al.*, 1998).

Stoker *et al.* (1994) utilised seismostratigraphic, biostratigraphic, lithologic and magnetostratigraphic analyses to propose a sub-division of the Hebrides slope

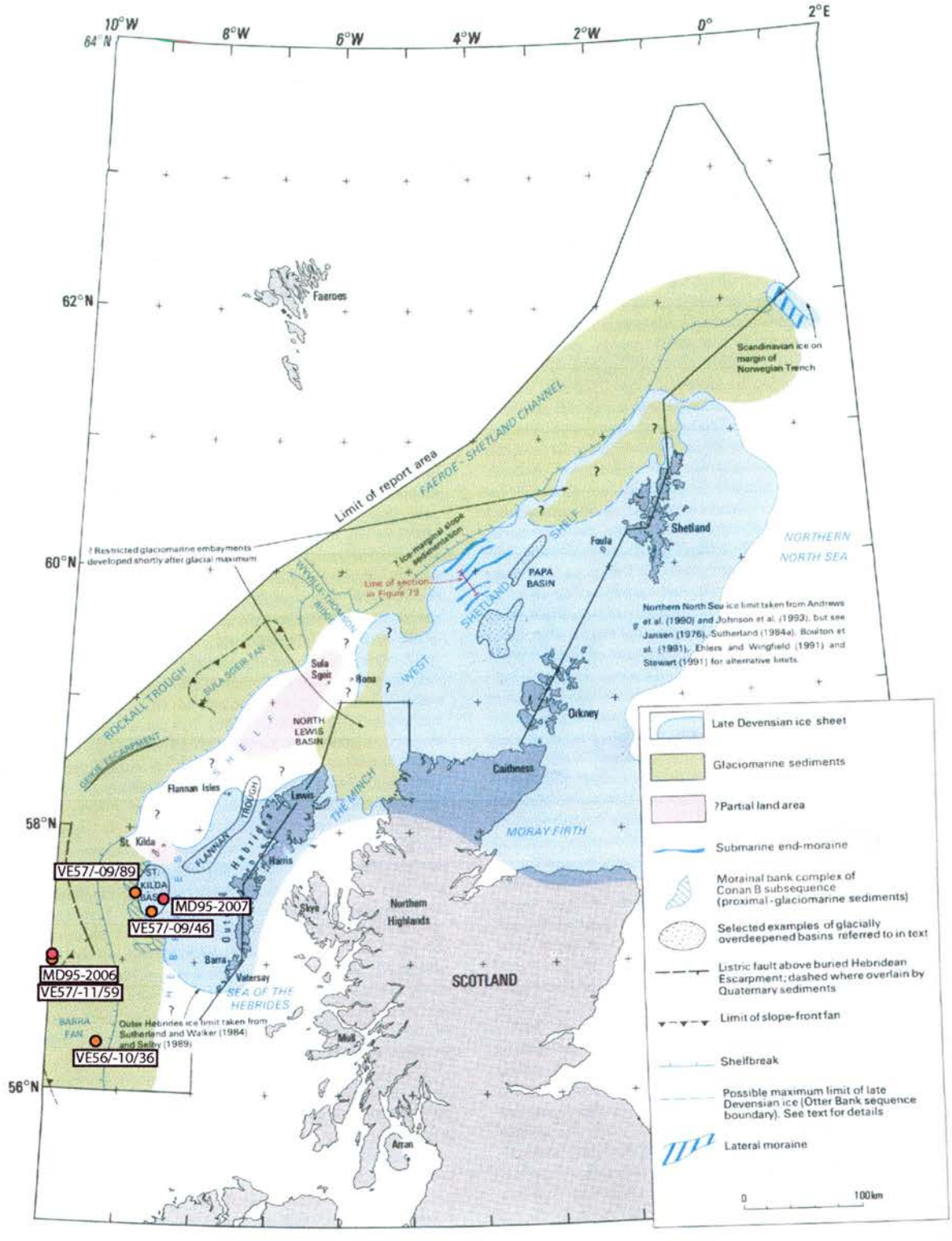

Figure 1.4. Schematic reconstruction illustrating the inferred extent of the late Devensian ice sheet around the last glacial maximum.

(Stoker *et al.*, 1997, Figure 78, p.114)

deposition. The sandstone and igneous basement rock is overlain by Pliocene to mid-Pleistocene age deposits of the non-glacial Lower MacLeod Sequence and the glacigenic Upper MacLeod Sequence. A 50-60 m deposit of Upper Pleistocene sediment and a thin Holocene sedimentary layer no more than 20-50 cm thick comprise the Gwaelo and MacAulay Sequences (Stoker *et al.*, 1994; Armishaw *et al.*, 2000). These sequences consist of predominantly distal glacimarine and marine deposits and are deposited on the Barra Fan and NE Rockall Trough respectively.

The Barra Fan is therefore composed of rapidly deposited complex Neogene sands and mid- to early-Pleistocene glacigenic sediment (Stoker *et al.*, 1994; Armishaw *et al.*, 1998). The latter consists of material derived from the NW of Britain, which was transported over the shelf and downslope to the Barra Fan by ice-marginal processes (Stoker, 1995). The Lower Pleistocene deposits are overlain by a 'sub-horizontal glacigenic erosional surface' (Armishaw *et al.*, 1998), which is itself overlain by a series of mid-Pleistocene through to Holocene sediment (Selby, 1989). The glacially derived sediment is predominantly distal in character (Stoker, 1995).

Following deposition of sediment from glacial outlets onto the slope-front fan (Stoker, 1990; Stoker, 1995; Howe *et al.*, 1998; Armishaw *et al.*, 1998), material is influenced by downslope (gravitational) and alongslope (geostrophic) sediment transport (Huthnance, 1986; Armishaw *et al.*, 1998; Knutz *et al.*, 2000).

1.4.iii The St Kilda Basin

Through the mid- to late Pleistocene the Hebridean shelf was subject to a series of glaciations (Stoker, 1995) during which time grounded ice probably extended to the shelf edge and deposited sediment onto the upper continental slope. The well-defined Hebridean Shelf is a constituent of the European continental margin (Armishaw *et al.*, 2000) (Figure 1.4). It is comprised of the basement rock platform (inner), the deep shelf area west of the platform (middle) and the area to the shelf break (outer zones) (Selby, 1989).

The St Kilda Basin is a large 30-40 km wide depression located on the middle Hebridean shelf (Selby, 1989; Peacock *et al.*, 1992). It was eroded by glacial overdeepening during the development of the Hebridean ice mass. The Otter Bank rise forms a boundary to the south, the St Kilda platform marks the northern limit (Selby, 1989) and a series of morainal banks lie to the west. It is from these that the maximum offshore position of the grounded Late Devensian ice mass has been inferred (Selby, 1989).

The thick layers of Quaternary sediments consist of glacimarine and glacial deposits (Davies *et al.*, 1984) which record fluctuations of the ice margin. Binns *et al.* (1974) carried out some of the early stratigraphical research in the Hebridean Sea. They proposed the deposition of four sedimentary formations which were deposited during the retreat of the ice mass from its LGM limits. This analysis has

more recently been revised by Davies *et al.* (1984) with the suggestion of eight formations based on seismostratigraphical and borehole data. They suggested that the temperate Skerryvore and the overlying Malin Formations were pre-Devensian deposits. The Canna Formation was possibly also of pre-Devensian origin. The proposed late Devensian sequence consisted of the glacimarine Stanton Formation, the Late Devensian glacial maximum Hebrides Formation and the Barra Formation.

A more recent scheme by Selby (1989) suggested the lodgment and melt-out till of the Caoilte Sequence represented deposits from the grounded ice cap of the last glacial maximum. A floating ice margin then deposited the St Kilda Basin Oisein Sequence. An absence of subglacial melting led to reduced sediment accumulation in this low energy environment. As the ice cap rapidly retreated to the inner shelf the seismically laminated Fionn Sequence was deposited into the basin.

During the Holocene the shelf was characterised by sediment winnowing and transportation particularly by the action of strong bottom currents (Howe *et al.*, 1998; Armishaw *et al.*, 1998).

1.4.iv The Hebridean continental shelf and margin; Previous studies.

The Hebridean shelf and slope region off NW Scotland provide potentially valuable sites for high resolution palaeoclimate studies, being in close proximity to the largest central mass of the last BIS and at a latitude which is ideally located to

capture the stadial/interstadial variability in the strength of THC. This potential was previously demonstrated by investigations of short vibrocores collected as part of a regional mapping programme by the BGS (Stoker *et al.*, 1993). Micropalaeontological, stable isotope, lithological and sedimentary evidence were obtained from two shallow cores recovered from the Hebridean shelf. Core VE 57/-09/89 (57°30.11'N, 08°42.52'W; 155m water depth) and core VE 57/-09/46 (57°19.30'N, 08°30.04'W; 156m water depth) (Figure 1.4) were recovered from the eastern margins of a morainal bank on the western edge of the St Kilda Basin and from the infilled St Kilda Basin respectively. The core sites are close to the proposed maximum extent of the late Devensian BIS and provide evidence for the pattern and timing of regional deglaciation (Austin, 1991; Peacock *et al.*, 1992; Austin and Kroon, 1996). It has been proposed that the St Kilda Basin became ice free from about 17.6 cal ka BP (15.2 ^{14}C ka BP) after which the cold, low salinity water continued to bathe the site until 15.6 cal ka BP (13.5 ^{14}C ka BP). After 15.6 cal ka BP the warm seas of the interstadial period were fully established and remained present until the initial cooling trend into the Younger Dryas from about 13 cal ka BP (11.6 ^{14}C ka BP). The fully developed conditions of the Younger Dryas stadial were observed from 12.5 cal ka BP (11 ka ^{14}C BP) until a precursor warming at approximately 11 cal ka BP (10.2 ^{14}C ka BP). Holocene temperatures were then established before 10.9 cal ka BP (10 ka ^{14}C BP), but records of the Holocene itself are generally poor from this region.

Two vibrocores were recovered from the Barra Fan on the continental slope of NW Scotland. Core 57/-11/59 (57 ° 01'N, 10 ° 01'W; 2089m water depth) and core 56/-10/36 (56 ° 43'N, 09°19'W; 1320m water depth) (Figure 1.4) first studied in detail during the NEAPACC (NE Atlantic Paleoceanography and Climate Change) Special Topic funded by the Natural Environmental Research Council (NERC) (Kroon *et al.*, 1997; Kroon *et al.*, 2000; Austin and Kroon, 2001). Sedimentological, geochemical and micropalaeontological evidence from these cores identified the presence of sub-Milankovitch scale climatic oscillations during the last deglaciation and Late Devensian Lateglacial period. Kroon *et al.* (1997) obtained a sea surface temperature (SST) record from core 56/-10/36. The SST and salinity estimates together with the benthic foraminiferal $\delta^{13}C$ records from nearby core 57/-11/59 (Austin and Kroon, 2001) suggested a strengthening of NADW formation during the Bølling-Allerød period and a reduction in strength during the Younger Dryas period.

The transition between the cold glacial period and the warm interstadial was dated at ~14.1 cal ka BP (12.6 ^{14}C ka BP) while a decrease in temperature shortly after 14.1 cal ka BP implied the onset of cooling which culminated in the Younger Dryas stadial. However, the limited sampling resolution for the radiocarbon dating from these cores did not allow confirmation of the events with their corresponding timing in the GISP2 record. Kroon *et al.* (1997) argue that a visual comparison of the GISP2 $\delta^{18}O$ and core 56/-10/36 SST provided a more robust age-modelling approach, but this assumes synchronicity in the records.

1.5 Scientific Rationale

Continental margins are the '*transition zones between markedly different domains of land masses and deep-ocean basins*' (p.1. Evans *et al.*, 1998). They are important zones of sediment flux, where the input and subsequent transport of material during the last glacial period were governed by climate change, glacier extent, the glacier drainage system, sediment supply, relative sea-level and ocean currents (Kroon *et al.*, 2000). These high sedimentation rate sites offer the potential for the recovery of high resolution sediment records from both shelf (Scourse and Austin, 2002) and slope (Kroon *et al.*, 1997) on which multiproxy analyses can be undertaken.

However, the majority of studies have concentrated on the North Atlantic deep sea record (Duplessy *et al.*, 1981; Ruddiman and MacIntyre, 1981; Jansen and Veum, 1990) and until recently, there have been relatively few high-resolution studies of the last glacial period from these North Atlantic marginal marine sites. Because these depositional environments are often associated with highly dynamic ice margins they are ideally located to record regional sediment and IRD fluctuations. However, they are less useful on their own within the context of an integrated record of amphi-Atlantic ice margin variability. The problem does not derive from their distal location to the LIS, but from the proximal location of the BIS to the Barra Fan, i.e. there is a danger that it will be '*impossible to see the glaciers for the icebergs*' (Scourse, *pers. comm.* 2001).

1.5.i The IMAGES Programme

The IMAGES (International Marine Global Change Study) programme is a marine component of the PAGES (Past Global Changes) project within the IGBP (International Geosphere-Biosphere Program). The fundamental objectives of IMAGES are to quantify climate and chemical variability of the ocean on time scales of oceanic and cryospheric processes, to identify and determine its sensitivity, to identify internal and external forcing, and to determine its role in controlling atmospheric CO_2 (PAGES Workshop Report, Series 94-3). In addition, the program aims to encourage the integration of marine sediment core records with the ice core records of Greenland and Antarctica. The high resolution marine cores obtained by the R/V *Marion Dufresne* commonly have sedimentation rates greater than 10 cm/kyr.

1.5.ii IMAGES core MD95-2006

Kroon *et al.* (2000), Knutz *et al.* (2001, 2002a) and Boessenkool (2001) have previously carried out analyses on sediment from the giant piston core MD95-2006 (57°01.82 N, 10°03.48 W; 2120m water depth) (Figure 1.4, Figure 1.5). This continental slope core consists of 30 m of distal glacimarine sediment from the northern edge of the Barra Fan, NW Scotland. The average accumulation rate is greater than 0.5 m/ka (Kroon *et al.* 2000; Knutz *et al.* 2001). Kroon *et al.* (2000) and

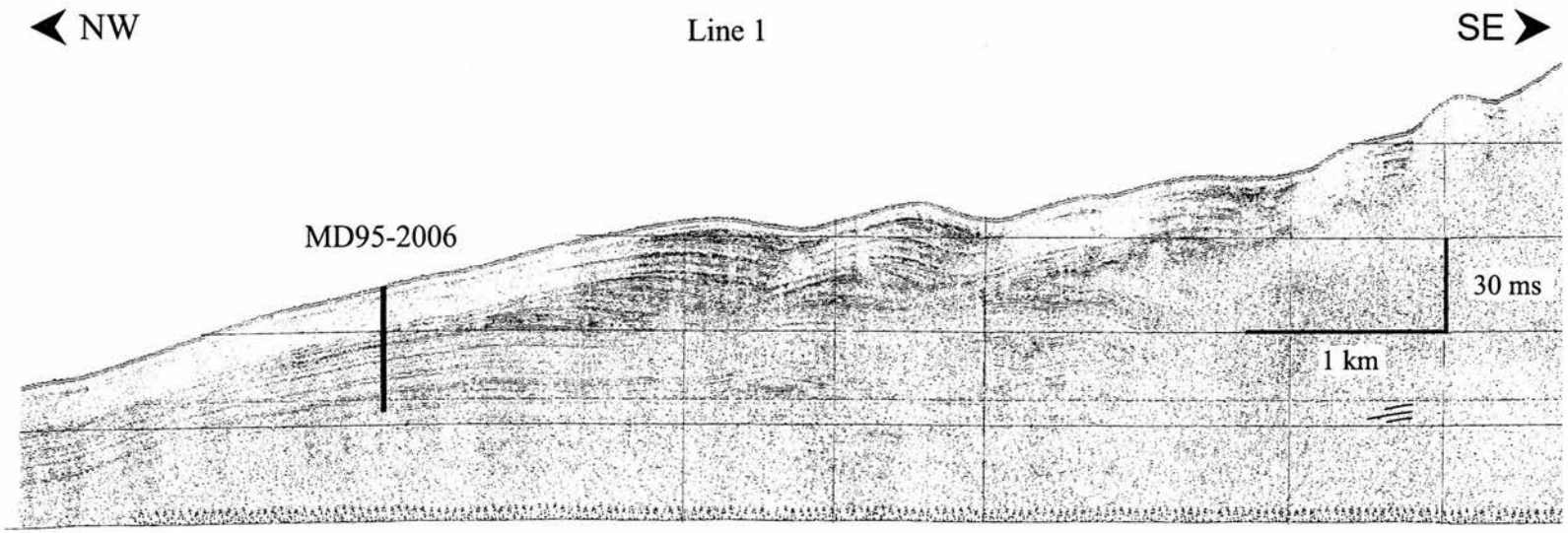

Figure 1.5. Deep-tow boomer line 1 aligned SE-NW across the Barra Fan, N.W. Scotland. The location of core MD95-2006 is marked .Figure courtesy of Knutz *et al.* (2002).

Knutz *et al.* (2001, 2002a) examined the lithological evidence while Boessenkool (2001) examined the limited pollen evidence. These investigations demonstrate that this marine core records the fluctuations of the last BIS and highlights the potential for the study of rapid (i.e. century-to-millennial-scale) climatic oscillations. However, the original chronological sampling was carried out at a relatively low resolution and the investigations concentrated only upon the general depositional pattern (Kroon *et al.*, 2000) and the IRD signature of the core (Knutz *et al.* 2001). Therefore, evidence for the timing of the events of the last glacial period and the identification of the characteristics associated with the expansion and contraction of the last BIS remained limited for the offshore region of NW Scotland at the outset of this study.

1.5.iii IMAGES core MD95-2007

Core MD95-2007 lies approximately 115 km from MD95-2006. The 19.35 m of sediments in giant piston core MD95-2007 (57°31.057'N, 08°23.171'W; 158 m water depth) were recovered from the St Kilda Basin, North West Scotland (Figure 1.4, Figure 1.6). This glacially overdeepened basin contains well-preserved, thick Quaternary deposits (Davies *et al.*, 1984) from a shelf region which is believed to have been glaciated during the last glacial maximum of the BIS (Selby, 1989; Austin, 1991; Peacock *et al.*, 1992; Lambeck, 1995). The initial range-finder dates obtained by W. Austin confirmed the presence of a highly expanded Lateglacial

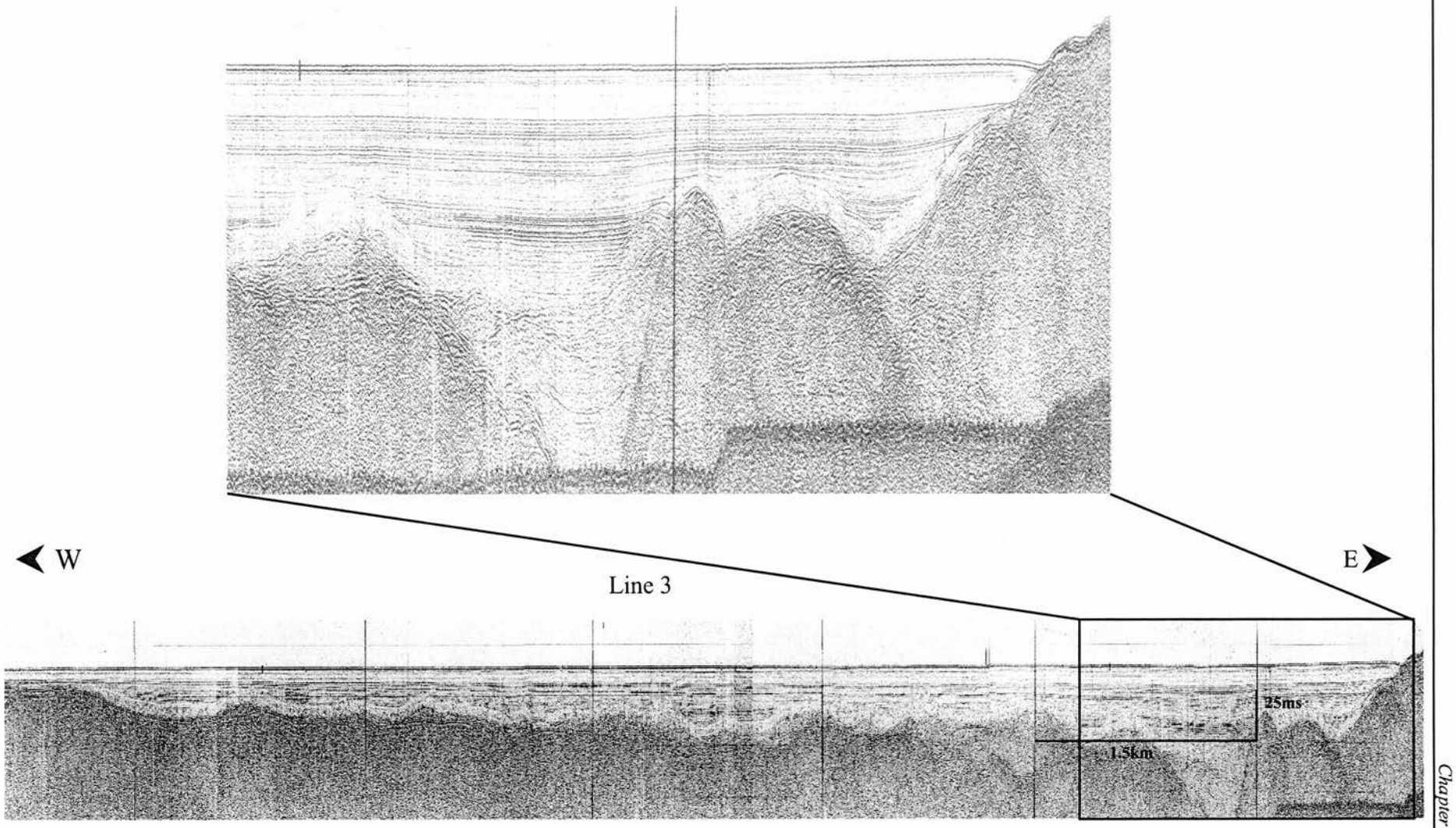

Figure 1.6. British Geological Survey 85/07 line 3, Huntec deeptow boomer profile aligned E-W across the St Kilda Basin, N.W. Scotland. The inset figure illustrates the over-deepened nature of the basin, with a clearly draped seismic unit possibly reflecting sub-glacial deposition ad a seismically laminated unit representing the postglacial fill of the basin. Water depth= 159 m.

sequence consisting of fine sand-silt-clay-rich muds with an average sedimentation rate of >0.5 m/ka.

Bioturbation processes are one of the major hurdles in reconstructing sub-millennial scale palaeoclimate oscillations, particularly in the deep sea where sediment accumulation rates tend to be low (typically <10 cm kyr^{-1}). They act to 'smooth' the palaeoclimate record, particularly the amplitude of palaeoclimate proxies. However, Austin *et al.* (1995) demonstrated that the Lateglacial sedimentation rates in the St Kilda Basin were sufficiently high to overcome most of the detrimental effects of sediment bioturbation.

This continental shelf record, which lies within the BIS LGM limits, therefore has the potential to yield new insights into the timing of deglaciation of the BIS and should allow comparison to the deglacial records of the adjacent Barra Fan and deeper North-East Atlantic.

1.6 Thesis aims and objectives

The main aim of this thesis is to establish a detailed chronostratigraphy for the climatic events of the last glacial period on the Hebridean continental shelf and margin, NW Scotland. The characterisation of the sediments and the identification of the behaviour of the last British ice sheet during this period is placed into a wider amphi-Atlantic setting through detailed age-depth modelling. The investigations

have focused on two high resolution sediment cores, namely MD95-2006 (Barra Fan) and MD95-2007 (St Kilda Basin).

This thesis takes the form of a series of four papers, together with an introduction (Chapter 1), materials and methods section (Chapter 2) and general discussion (Chapter 7). Chapter 3 focusses on the identification of millennial-scale events in the offshore record from North West Scotland and involved collaboration with W. Austin (University of St Andrews). It was published in the *Geological Society Special Publication*, volume 207, in 2002. Chapter 4 focusses on the behaviour of the last BIS on the continental margin of NW Scotland from MIS 4 to MIS 2 and was published in *Polar Research*, volume 21, in 2002. My co-authors, E. Jansen (University of Bergen) and W. Austin assisted in generating the $\delta^{18}O$ data. A manuscript is in preparation from Chapter 5. It concentrates on the chronology of regional deglaciation of the BIS on the Hebridean Shelf. Chapter 6, on the age and chronostratigraphic significance of North Atlantic Ash Zone II (NAAZ2), was submitted to a special issue on Quaternary Chronology in the *Journal of Quaternary Science* in November 2002 and is currently under review. My co-authors, J. Hunt (GEMRU) and W. Austin assisted with the identification and geochemical analysis of the NAAZ2 samples.

Sample preparation, and processing, for the foraminiferal oxygen isotope analysis and the radiocarbon dates from core MD95-2006 were obtained by L.Wilson. The molluscan radiocarbon dates from core MD95-2007 were also

processed by L. Wilson. Spectrophotometer measurements on core MD95-2006 were also carried out as was the preparation of the higher resolution residues for the identification of the NAAZ2 tephra. The tephra slides for MD95-2006 were prepared by L Wilson while the tephra shard preparation for core MD95-2007 was carried out by H. Cawthorne under the supervision of W. Austin and L. Wilson.

The objectives of the thesis can be summarised as follows:

- To characterise the pattern of sediment accumulation on the Hebridean continental margin during the last 60 ka within the context of a finely resolved age-depth model, and relate this pattern to ice sheet dynamics.

- To characterise millennial and sub-millennial scale events during marine isotope stages 2 and 3.

- To examine the timing of ice sheet fluctuations, reflected in IRD and related proxies, in the context of amphi-Atlantic climate changes.

- To develop an integrated account of the extent and timing of deglaciation of the last major ice sheet on this margin.

Chapter 2.

Materials and Methods

2.1 Sediment Samples

2.1.i Core Acquisition

Marine sediment cores MD95-2006 (30 m in length) and MD95-2007 (19.35 m in length) were recovered in 1995 using the giant piston (Calypso) corer aboard the research vessel *Marion Dufresne* as part of the International Marine Global Change Study (IMAGES) programme. The Calypso corer weighs between 8 to 10 tons, depending upon the conditions of deployment and consists of a 40-60 m lance and an internal high pressure PVC liner (10 cm diameter).

Calypso giant piston coring (Figure 2.1) is commonly associated with potential over-sampling or stretching in the upper core sections (Skinner and McCave, 2003). This over-sampling is exacerbated in certain lithological types and at greater depths. This is due to the recoil of the Kevlar cable resulting in greater volumes of sediment being sampled at certain core depths. By contrast, an open barrel gravity corer tends to under-sample basal sediments. Skinner and McCave (2003) have therefore proposed the use of a combination of corers during sampling, i.e. a piston corer could be used to obtain sediments at depth, while a gravity corer could be used for the upper 10-12 m, thus overcoming the sampling errors of each coring method. However, a comparison of the upper sections of the IMAGES cores, MD95-2006 and MD95-2007, with previously obtained vibrocores from the St Kilda

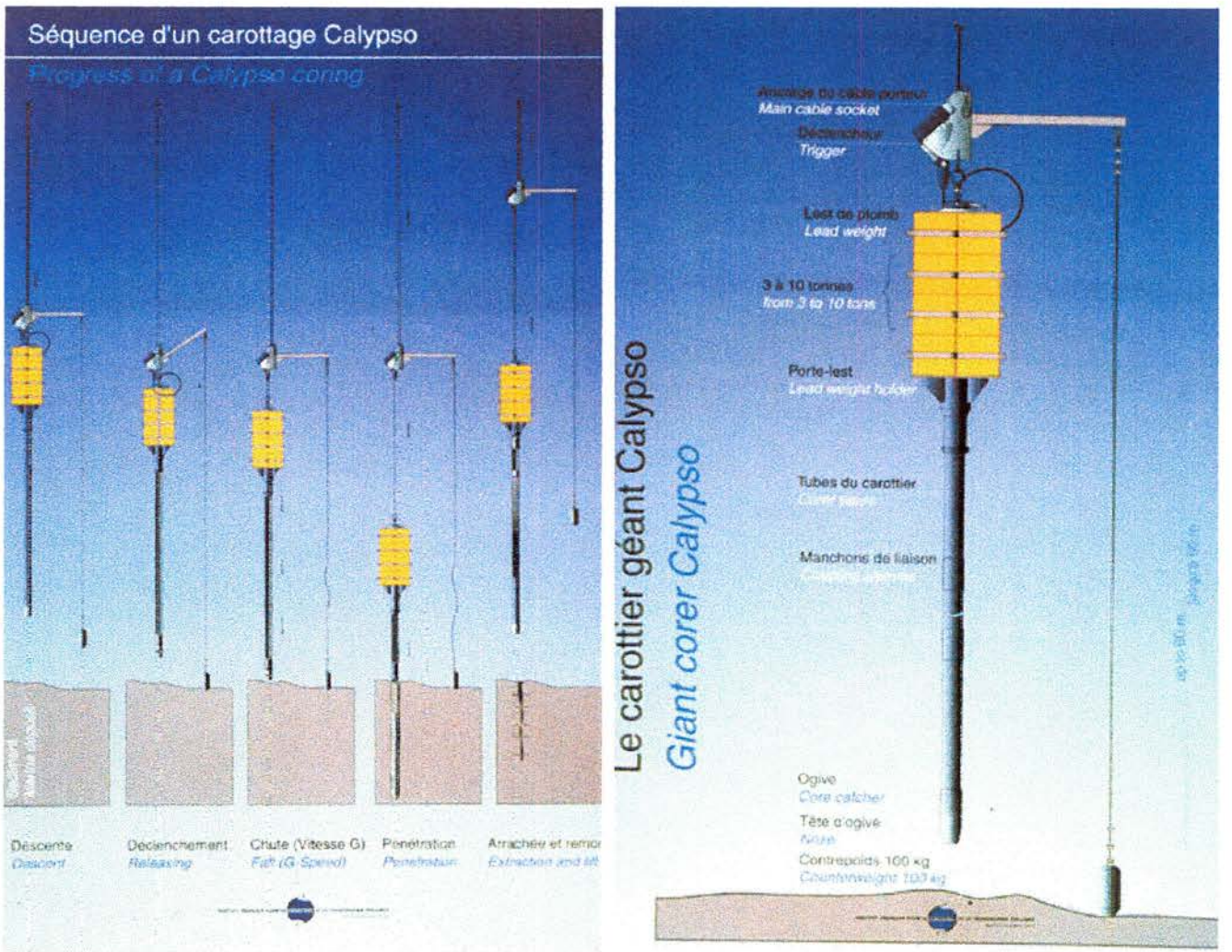

Figure 2.1. Schematic diagram to illustrate the design and deployment of the giant Calypso (piston) corer (Image courtesy of IPEV; French Polar Institute).

Basin (VE 57/-09/46 and VE 57/-09/89) and Barra Fan (VE 56/-10/36 and VE 57/-11/59), suggest that 'core-stretching' is not a major problem in these cores.

The PVC core linings were cut ship-board into 1.5 m sections. The core sections are numbered from section 1 to 20 (MD95-2006) and section 1 to 13 (MD95-2007). In addition, the depth range and orientation of each section is marked on the core tube. The 1.5 m sections of MD95-2006 were logged onboard ship with the GEOTEK^{TM} multi-sensor track system (i.e. magnetic susceptibility, p-wave velocity and γ density) prior to splitting in half. This was not possible for MD95-2007, given the limited time available between core recovery and disembarkation.

The core surfaces are protected with polythene film and each core section is sealed in a polythene tube. Both cores were transferred from the ship and stored in Stornoway for five days at 4°C and subsequently transferred to cold storage at the University of Edinburgh. The cores were split lengthways with a bench-mounted router system and thin nylon cord, and each section length was designated as a 'working' or 'archive' half. The archive sections of cores MD95-2007 and MD95-2006 were logged (GEOTEK^{TM} system) by E.J.Jones at the Southampton Oceanography Centre.

The archive core halves are currently at the Southampton Oceanographic Centre and the working sections are presently held in cold storage (4°C) at the School of Geography and Geosciences at the University of St Andrews.

2.1.ii Core sampling strategy

The working core sections from MD95-2006 and MD95-2007 were initially sampled every 10 cm and 5 cm respectively. The 10 cm^3 plugs (Ocean Drilling Program type) were removed by William Austin and Cecilia Taylor for micropalaeontological counts, AMS (accelerator mass spectrometer) ^{14}C samples, IRD (ice-rafted detritus) lithic counts and carbon and oxygen isotope samples. In addition, 6 cm^3 cubes were removed for water content, combined bulk density, environmental magnetics and, eventually, grain size and bulk sediment geochemical analysis. Further sub-sampling was undertaken where a higher resolution sampling strategy was required (e.g. sampling at 1cm intervals across the North Atlantic Ash Zone II horizon, see chapter 6). Care was taken to avoid taking samples close to the plastic core tubing as this sediment may have been contaminated by down-core smearing during the core retrieval process (Austin, 1994).

2.1.iii Residue preparation

Samples were initially stored as wet sediment at ca. 4°C, and subsequently oven-dried at 40°C to constant weight. The drying temperature is kept low to prevent damage to the enclosed foraminifera as the sediment shrinks and high temperatures (> 60°C) may alter shell chemistry when further analyses are intended. These sub-samples were subsequently weighed (sediment dry weight) and soaked in Calgon

(sodium hexametaphosphate) overnight to encourage disaggregation. Samples were washed over 2 mm and 63 μm stacked sieves. The 2 mm sieve prevented larger clasts from damaging the foraminiferal assemblages retained on the 63 μm sieve. Between each sample Methylene blue was added to stain any remaining carbonate contamination on the sieve. A light water spray was utilised to ensure thorough washing of the sample which is particularly important for foraminiferal analysis since small particles may become lodged within or adhere to the foraminiferal tests. Sediment contamination has a detrimental effect on radiogenic and non-radiogenic isotope analyses and makes subsequent cleaning more time-consuming. The coarse residues (>2 mm, >63μm) were washed with distilled water and oven-dried at 40°C for 24 hours. The dry residue weights were recorded to two decimal places on a digital balance for each sample and then placed in labelled glass bottles. These samples were prepared by W. Austin and C. Taylor at the Grant Institute University of Edinburgh and by L. Wilson at the School of Geography and Geology, University of St Andrews.

2.1.iv Foraminiferal analyses

Samples were prepared for the extraction of planktonic foraminifera by dry sieving (mesh size 150 μm)the dry coarse residue (>63 μm/2 mm). This dry fraction was dispersed thinly and evenly across the 42 square divisions of a brass counting tray. A fine artist's paint brush and a mounted steel pin were utilised to remove or manipulate specimens under a Zeiss Stemi SV11 binocular microscope.

Approximately ten planktonic foraminifera were removed from each sample for stable isotope analysis. Samples of approximately 1,000 monospecific specimens of either the polar species *Neogloboquadrina pachyderma* (sinistral) [*N.p.* (s)] or the sub-polar species *Globigerina bulloides* [*G.b*] were required for each AMS ^{14}C analysis. The quantitative foraminiferal counts were undertaken on a square-by-square basis, i.e. all samples within one square are picked and/or identified before proceeding to the next. In addition, squares were counted across the tray from left to right until the required numbers of specimens were achieved. Specimen samples that were removed were placed on card microscope slides and covered with a glass slide to avoid contamination during storage.

2.2. Isotope Stratigraphy

2.2.i Radiocarbon dating

AMS ^{14}C sample preparation was carried out at the NERC Radiocarbon Laboratory, East Kilbride by L.Wilson under the direction and supervision of C. Bryant and M.Currie. The ^{14}C samples consisted of planktonic foraminifera (MD95-2006) and assorted bivalve molluscan species (MD95-2007). Mollusc specimens were identified by J.D.Peacock (British Geological Survey, retired). An AMS ^{14}C date from a foraminiferal sample requires approximately 1,000 monospecific specimens in order to yield ca. 10-12 mg of shell material. However, foraminiferal abundance was low within some residue samples, indicating that further sub-sampling of the core was required in order to reach the required counts. Therefore,

extra 1 cm slices were processed from the core, alternating on either side of the original sample until the required number of specimens were obtained. However, wherever possible foraminifera were sampled around local abundance maxima.

In addition to the dating problems associated with bioturbation mixing and down-slope reworking of older material, sample contamination may also occur. Care was therefore taken to clean foraminiferal samples sufficiently well to remove any fine biogenic calcite grains from the internal chamber cavities. All foraminiferal samples analysed at East Kilbride are normally photographed under a binocular microscope to check for contamination prior to analysis.

In preparing the mollusc samples for dating, the shell surface was acidified with dilute HCl in order to remove the potentially contaminated outer layers of the shell (etched) in accordance with its weight. The foraminiferal or molluscan sample was then rinsed in distilled water and crushed using a pre-cleaned (10% HCl, DDH_2O) agate pestle and mortar. The powder obtained was then weighed. Where 'etched' mollusc samples were used, one standard was pretreated as described above and one standard was processed without acid etching.

Prior to sample reaction, the complete hydrolysis vessels were attached to a vacuum rig and pumped down to $0.05x10^{-1}$ Torr to check for leaks. One 5 ml beaker per sample was placed with the sample onto filter paper on a calibrated weighing balance. The sample weight was accurately noted and a small piece of glass filter

paper was placed over the beaker to prevent sample loss during vacuum. Each beaker was then placed into a labelled hydrolysis vessel. A disposable pipette was used to transfer 85% orthophosphoric acid into the arm of each hydrolysis vessel and the top of each vessel secured with a large metal clip. Each vessel was attached to the rig and pumped through a water trap to extract the air and any residual moisture. The time taken to expel the air may be reduced by carefully heating the vessel with a blowtorch. However, care must be taken to avoid a premature reaction of the carbonate sample and any acid vapour generated.

The hydrolysis vessel was equilibrated with a water bath at a constant temperature of 25 °C over approximately 30 minutes. The vessel was then tipped manually to react the acid with the carbonate sample. To ensure a complete reaction of the carbonate the vessel was rotated on its side, and returned to the water bath to remain overnight at 25 °C.

The next day the vacuum rig pressure was reduced to 0.05×10^{-1} Torr. A series of limestone standards, prepared according to the above method, were run prior to each series of samples on the vacuum rig. This enables the identification of any potential contamination, which would affect the subsequent samples. Before opening the hydrolysis vessel to the evacuated rig, an IMS/CO_2 (isopropanol/dry ice) slush trap was raised on the water trap and a liquid nitrogen dewar raised on the CO_2 trap. In this way, after manually closing the valves on the rig, the evolved water and CO_2 are separated.

The volume of CO_2 obtained was calculated from a pressure transducer and noted. One aliquot (~2.0 mls) of CO_2 was allowed to enter a glass tube and the CO_2 gas was then reduced by heating with hydrogen and iron filings (catalyst) to a graphite (carbon powder) target (Gagnon and Jones, 1993). These graphite targets were sent to the University of Arizona NSF-AMS radiocarbon laboratory for radioisotope analysis on the Accelerator Mass Spectrometer (AMS). Details of the dated samples, including their unique laboratory codes, are provided in chapters 3, 4 and 5.

2.2.ii Calibration of radiocarbon ages

Radiocarbon dates reported as conventional ages (^{14}C yr BP), have been calibrated (calendar year BP) using the MARINE98.14C calibration option in the CALIB4.2 programme (Stuiver and Reimer, 1993; Stuiver *et al.*, 1998). The marine calibration dataset, which is limited to the age range 460-20,760 ^{14}C yr BP, is based on the INTCAL98.14C calibration (Stuiver *et al.*, 1998) as an input for modelled ocean carbon exchange. A mean global ocean reservoir correction of 402 years for AD1850 is also used. The MARINE98.14C calibration dataset (Figure 2.2) comprises 1) a marine decadal model dataset (0-8,800 cal yr BP), 2) a marine coral and varve data spline (8,800-15,585 cal yr BP) and 3) linear approximation of coral data (15,585-24,000 cal yr BP + 1,000 linear extension for the estimation of cal ages

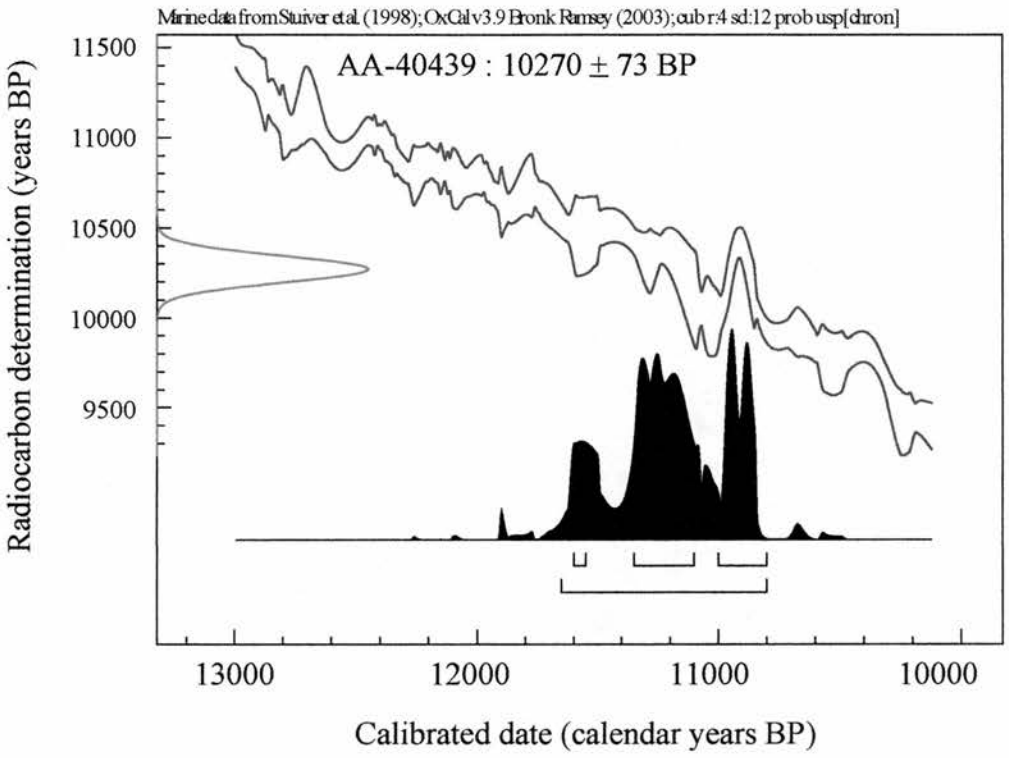

Figure 2.2. An example of radiocarbon calibration using the OxCal v. 3.9 programme (Bronk Ramsey, 2003). The marine calibration dataset is based upon Stuiver et al (1998) and incorporates a marine reservoir age correction of 400 years (i.e. $\Delta R = 0$). The horizontal lines associated with the calibrated ages represent the 68.2% and 95.4% probability distributions. In this case, a marine ^{14}C age of 10,270 ±73 years BP yields the following age solutions:

68.2 % probability
11600 BP (2.5%) 11550 BP
11350 BP (42.6%) 11100 BP
11000 BP (23.1%) 10800 BP
95.4 % probability
11650 BP (23.1%) 10800 BP

only). Any ages older than 20,760 ^{14}C yr BP are calibrated using marine coral U/Th ages and the second order polynomial equation (equation 2.1) of Bard *et al.* (1998), which statistically extends the current coral calibration dataset of Stuiver *et al.* (1998):

$$[\text{cal age BP}] = -3.0126 \times 10^{-6} \times [^{14}\text{C age BP}]^2 + 1.2896 \times [^{14}\text{C age BP}] - 1005$$

{equation 2.1}

However, extreme care should be taken with the interpretation of these older calibrated ages (see chapters 3, 6 and 7).

2.2.iii Stable isotopes

Planktonic foraminifera (*N.p.* (s) and *G.b.*) from core MD95-2006 core were hand-picked from the >150μm dry-sieved fraction of the coarse residues (>63 μm/<2 mm). Sample weights range between 0.090mg and 0.105mg (i.e. approximately 10 foraminiferal tests). The foraminifera are crushed in cleaned glass vials using a glass rod before adding a few drops of methanol. They were then placed in an ultrasonic bath for approximately 60 seconds and a syringe was used to decant the excess methanol and any fine dissagregated material that may have been attached to the foraminiferal tests. The samples were then placed in an oven (40°C) overnight to ensure they are completely dry. The tops of the glass tubes were

checked for dust and cleaned if necessary before being placed into the autosampler of a Kiel device attached to ThermoFinnigan MAT 251 IRMS (Isotope Ratio Mass Spectrometer). Results were reported with respect to Vienna Pee Dee Belemnite (VPDB) standard through calibration with the NBS (National Bureau of Standards) 19 standard.

Stable isotope measurements were carried out by L. Wilson at the University of Bergen, Norway. Reproducibility of the system for samples within the weight range ca. 60-100 μg is typically 0.07‰ for $\delta^{18}O$ and 0.06‰ for $\delta^{13}C$, based on replicate measurements of the NBS 19 standard (0.1 ± 0.05 mg).

2.3 Spectrophotometry

The moisture content of cores is problematic when spectrophotometer measurements are taken directly after their recovery (e.g. ODP cores, Blum, 1997). MD95-2006 and MD95-2007, obtained in 1995, have since been stored in a cold room at 4°C. Oxidation takes place shortly after the core is split and is generally evident through a lightening of the sediment surface. This process results in an increase in light reflectance values over time. The time between core retrieval from the cold store (4°C) and the recording of spectrophotometry measurements should therefore be kept as constant as possible for each core section (Blum, 1997). Both MD95-2006 and MD95-2007 undisturbed archive sections were measured approximately 10 minutes after removal from the cold storage during a visit to Southampton Oceanography Centre in February 2000.

A hand-held Minolta Spectrophotometer CM-2002 (Figure 2.3) was utilised to obtain spectral reflectance data from the split-core surface of MD95-2006 and MD95-2007. It has a '*double-beam feedback system, monitoring the illumination on the specimen at the time of measurement and automatically compensating for any changes in the intensity or spectral distribution of the light*' (Blum, 1997). The sediment surface is viewed at an angle of 2^{o} normal to the surface and is diffusely illuminated. The viewing beam width is 7.4^{o}. The geometry may be set at SCI (specular component included) or SCE (specular component excluded). The latter, SCE, is recommended for general all-purpose use by Minolta. The SCE geometry is also thought to reduce the effects of any moisture variation which are known to exist; measurements on both cores were therefore made using the SCE setting.

Calibration data must be entered into the spectrophotometer prior to the recording of any measurements. A white ceramic cap has been factory-calibrated at 'intervals of 10 nm between 400-700 nm against the primary standard consisting of pressed $BaSO_4$' at the United Kingdom National Physical Laboratory (Blum, 1997). This white calibration is carried out immediately after the camera is switched on and establishes the maximum reflectance as 100%. This procedure must be repeated throughout use, in order to minimise the effect of temperature variations on instrument readings.

Figure 2.3. The hand-held Minolta Spectrophotometer CM-2002 used to obtain spectral reflectance data from the split-core surfaces.
(http://www.minoltaeurope.com/ii/gb/cms/products/spectrophotometers.html).

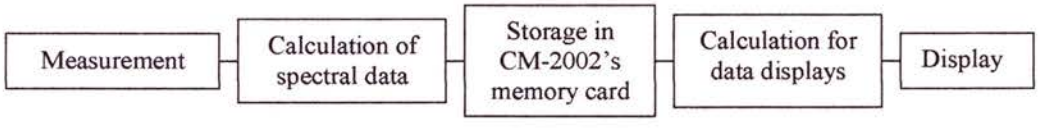

Figure 2.4. Data Flow at time of measurement (CM2002 Technical Guide).

It is also essential to execute a 'zero' calibration, which is achieved by removing the protective cap and pointing the spectrophotometer into the air. The instrument should be 1 metre clear of any surrounding objects and held in this position until three 'zero' measurements are taken. This compensates for any stray light arising from flare characteristics such as dust or stains (Blum, 1997). Calibrations should be undertaken approximately every 12 hours during use.

A measurement procedure was established based on the Ocean Drilling Program's use of the Minolta CM-2002 (Blum, 1997). Once white and zero calibrations were completed, the core surface was cleaned using a sharp-edged, clean spatula. The split-core surface was covered in clear plastic film (Note: the same brand of Clingfilm was used throughout). Care should be taken to avoid creases in the film to ensure a uniform transition of light. A single measurement was recorded for each position of the instrument on the core surface. These measurements were taken on a single track along the centre of the core. The sampling interval was set to 5 cm and was decreased to 1 or 2 cm where higher resolution records were required, e.g. an obvious visible band of differing colour or bands highlighted in other proxy studies.

Measurements should be avoided at any large detectable cracks or breaks in the sediment since these are likely to produce invalid results. It is important that the time taken between core cleaning and the recording of each reading is kept to a constant throughout. It should also be noted that the aperture of the

spectrophotometer was cleaned between each sample to avoid sediment contamination. The data was stored on the spectrophotometer memory card (Figure 2.4). Information may then be read directly from the instrument's LCD or downloaded into a spreadsheet on an external computer. This data may be displayed in a number of formats, all of which are obtainable from the single measurement at each sampling interval (Table 2.1).

Data was recorded as L*a*b* measurements to enable comparisons with other studies, since this is the most commonly employed colour indicator in palaeoceanography. L* indicates lightness ($\simeq$ grayscale reflectance) where, on a scale of zero to one hundred, zero is black and one hundred is white. a* and b* are chromaticity co-ordinates, where a* is indicative of a colour shift from red (+60) to green (-60) and b* illustrates a colour shift from yellow (+60) to blue (-60). It should also be noted that the a*, b* co-ordinate 0,0 is achromatic (i.e. no spectral colour separation) and as the values deviate from 0 colour saturation intensity will increase. However, spectral reflectance data, over the various bandwidths (the Minolta CM2002 records reflectance every 50 nm from 400-700 nm) may enable more detailed analyses of results when correlated with other proxies, such as obtaining optimum reflectance spectra for determining $CaCO_3$ content.

Abbreviation	Data Display
ABS	Absolute measured data
Δ	Difference between measured data and target data
XYZ	XYZ tristimulus values
Yxy	CIE 1931 Yxy colour system
L*a*b*	CIE 1976 L*a*b* colour system
$L^*C^*H^0$	CIE 1976 $L^*C^*H^o$
Lab	Hunter Lab colour system
L*u*v*	CIE 1976 L*u*v* colour system
SPECTRAL	Graph of spectral reflectance
COLOR Gr.	Graph of colour-difference data in the L*a*b* colour system
MUNSELL	Munsell colour notation
MI	Metamerism index
WI (E313)	ASTM E 313 whiteness index
WI (CIE)	CIE whiteness index
YI (E313)	ASTM E 313 yellowness index
YI (D1925)	ASTM D 1925 yellowness index
CMC (2:1)	CMC colour difference with l=2 and c=1
CMC (1:1)	CMC colour difference with l=1 and c=1
FMC2	FMC-2 colour difference

Table 2.1. Data Displays available on the Minolta CM-2002 hand-held spectrophotometer (CM2002 Technical Guide).

2.4 Magnetic Susceptibility

The down-core magnetic susceptibility measurements were obtained using the procedure outlined by Dearing (1999). Volumetric magnetic susceptibility was measured down core in 1 cm increments using a Bartington Instruments magnetic susceptibility meter (Model MS1, adapted with a MS2F probe) with an operating frequency of 0.58 Hz (Figure 2.5). The results are reported as 1 x 10^{-6} SI Units.

The susceptibility sensor is used in a stable, 'quiet' environment (Dearing, 1999), away from strongly magnetic materials, electromagnetic fields and the machine's transformer and mains cable. There must be no draughts in the vicinity and it should be used within a constant temperature environment, out of direct sunlight.

The sensor was zeroed and a background reading recorded prior to measurement. Each sediment reading was obtained twice before a background reading was again recorded. The drift during measurements was obtained by calculating the difference between the two background readings. Because the sensitivity of the probe will reduce with distance from the sediment, care must be taken not to push the probe into the sediment to differing depths, ideally only the tip of the sensor will be in contact with the sediment surface. In the Bartington

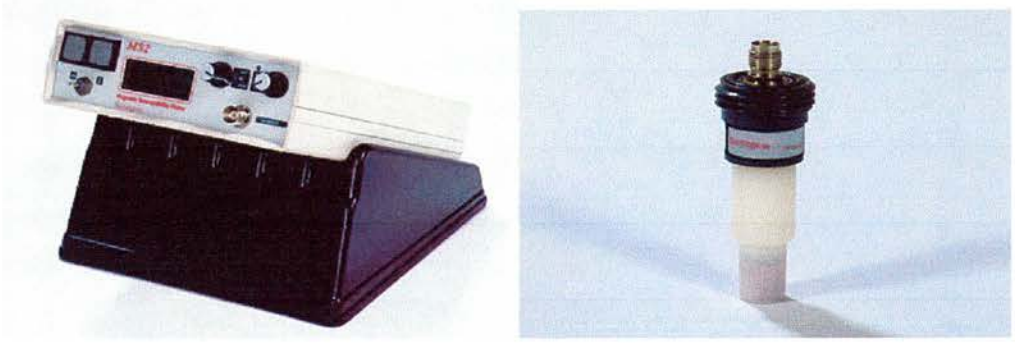

Figure 2.5. The Bartington Instruments magnetic susceptibility meter (Model MS1 [left], adapted with a MS2F probe [right]). The probe has a diameter of 15 mm.
(www.bartington.com)

Instruments magnetic susceptibility meter the F probe sensor is affected by materials within a maximum distance of 5 mm.

2.5 Calcium Carbonate

Calcium carbonate ($CaCO_3$) content was determined using a modified back titration method (Grimaldi *et al.* 1966) and was described by Austin and Kroon (1996). 0.5 g of dry sediment was accurately weighed and treated with an excess of acid (25 ml of 0.5 M HCl solution). 0.5 ml of bromophenol blue indicator was added and the solution was back-titrated against 0.35M NaOH solution until the yellow to violet end-point was reached. The calcium carbonate content was calculated using equation 2.2., where the weight is given in grams and the volume in litres (e.g. Austin and Kroon, 1996; Austin and Evans, 2000):

$$\%CaCO_3 = 100\ [(\text{vol. HCl} \times \text{molarity HCl} \times 1.007225) - (\text{vol. NaOH} \times \text{molarity NaOH})] \times (2 \times \text{sample weight})^{-1} \times 100. \quad \{\text{equation 2.2}\}$$

2.6 Grain Size Distributions

Grain size measurements were carried out on decalcified sediment samples from cores MD95-2006 and MD95-2007. All samples were processed using a

Coulter LS230 Particle Size Machine (PSM) at the Grant Institute, University of Edinburgh by W. Austin and C. Taylor.

A dissolution procedure was used to remove biogenic carbonate in order to determine the non-carbonate, lithogenic particle size components of the samples. Distilled water was added to approximately 0.55-0.60 g of 'wet' sediment and the excess liquid was decanted after the samples were centrifuged; this ensured the dissolution and removal of salt crystals. The additional water was removed by oven-drying the samples overnight (40°C). A 20% acetic acid solution was added to decalcify the samples overnight. Following centrifuging the excess solution was decanted and distilled water was added; this process was repeated twice. Sodium hexametaphosphate solution was added to disperse the sample before it was transferred to the PSM (e.g. Austin and Kroon, 2001).

2.7 Tephra Analysis

Tephra shards were handpicked using a fine artist's brush (size 0000) under a binocular microscope (see 2.1.i) from the >150 μm dry residue fraction. They were then separated into a number of types on the basis of their colour, texture and morphology. The number of shards per gram of dry sediment was calculated (the procedure is very similar to that for foraminifera: see 2.1.iv). Maximum shard

dimensions were determined using a Zeiss Stemi SV11 binocular microscope with a calibrated eye-piece graticule (see chapter 6).

It is important to determine the specific eruption from which the tephra were dispersed. The shards were therefore mounted on frosted glass slides in clear Araldite™ fixative, set on a hot plate to harden and then ground to approximately 50 μm in thickness to expose the grain surface. The slides were vacuum coated with evaporated carbon and a strong electrical contact was obtained through the application of a graphite paint. Tephra shard geochemistry was obtained on a twin spectrometer Cambridge Instruments Microscan V electron microprobe at the University of Edinburgh by W.Austin and J.Hunt (GEMRU). This is a reliable method of analysis for small grains and low abundances (Hunt *et al.* 1995). The instrument operated at an accelerating potential of 20 kV and a probe current of 15 nA, with an exposure time of 50 seconds based on a 10 second counting interval per element. Pure oxides and simple silicates were used as standards while an andranite garnet acted as a secondary standard. Corrections were made for counter dead-time, atomic number effects, fluorescence and absorption, using a ZAF procedure described by Sweatman and Long (1969).

Chapter 3.

"Millennial and sub-millennial-scale variability in sediment colour from the Barra Fan, NW Scotland: implications for British ice sheet dynamics"[3.1]

Abstract

Sediment colour, together with other proxy data, provides a novel, rapid and non-destructive tool in the investigation of glacier-influenced sedimentation on the Barra Fan, NW Scotland. Lightness (L*) and reflectance (400 – 700 nm) measurements at this site provide a quantitative estimate of changes in calcium carbonate and clay content. Interstadials are carbonate-rich/clay-poor (higher L* and reflectivity), while stadials are carbonate-poor/clay-rich (lower L* and reflectivity). Detailed sedimentological investigations suggest that the last British Ice Sheet (BIS) extended to the outer continental shelf-break shortly after 30 ka BP. This climatic response of the BIS to global cooling at the Marine Isotope Stage 3 – 2 transition marks a significant increase in sediment delivery to the Barra Fan. Prior to 30 ka BP, strong Dansgaard/Oeschger (D/O) cyclicity dominates the record. After 30 ka BP,

[3.1] This chapter is based upon the following published work: Wilson, L. J. and Austin, W.E.N. 2002. Millennial and Sub-millennial variability in sediment colour from the Barra Fan, NW Scotland: implications for British ice sheet dynamics. *In:* Dowdeswell, J.A. and O'Cofaigh, C (eds.) *Glacier-Influenced Sedimentation on High-Latitude Continental Margins*, Geological Society, London, Special Publications, **203**, 349-365.

shorter periodicities prevailed as the BIS reached its maximum extent. Glacier dynamics plays a significant role in the delivery of ice-rafted debris (IRD) across this margin, highlighting the inherent difficulties of correlating millennial-scale IRD events when the IRD is derived from different ice sheets. An event stratigraphy based upon carbonate-rich interstadials provides a more robust means of amphi-Atlantic correlation during this interval.

3.1 Introduction

3.1.i Background

During much of the late Pleistocene, glacier-influenced sedimentation was the dominant depositional feature of the North East Atlantic margins (e.g. Andrews *et al.*, 1996). Marine sediment records recovered from the 'open' North Atlantic provide the basis for a significant body of literature describing glacial variability at millennial time-scales during this period (e.g. Bond *et al.*, 1992, 1993, 1999). However, there are relatively few well-dated continental margin records predating the last glacial maximum (LGM), particularly from formerly glaciated regions, which provide this millennial-scale detail.

During the past 60,000 years, periods of increased ice-rafting, the so-called 'Heinrich Events' (after Heinrich, 1988), punctuate and dominate the 'open' ocean record (Bond *et al.*, 1992). Early provenance studies linked the carbonate-rich ice-

rafted debris (IRD) of these Heinrich layers to the Laurentide Ice Sheet (LIS) (e.g. Andrews and Tedesco, 1992). However, glacier-influenced sedimentation at these oceanic sites represents an integrated record of IRD from numerous potential source regions (e.g. Dowdeswell *et al.*, 1995; Revel *et al.*, 1996) and compositional differences may have climatic implications (e.g. Bond and Lotti, 1995). More recently, there has been considerable debate concerning the origin and timing of the emplacement of detrital material within Heinrich Events (e.g. Gwiazda *et al.*, 1996; Grousset *et al.*, 2000).

In addition to the Heinrich Events, the last glacial period is characterised by rapid warm to cold climate transitions (Dansgaard/Oeschger (D/O) events), occurring with periodicities of 500-2000 years (e.g. Dansgaard *et al.*, 1993; Bond *et al.*, 1999). There is growing evidence to suggest that these cycles are a persistent feature of the North Atlantic's climate system, albeit with considerably diminished Holocene cycles (Bond *et al.*, 1997). The freshwater forcing mechanism of D/O events suggested by Broecker *et al.* (1990) has recently been discussed by Bond *et al.* (1999), who propose that cooling phases caused freshening of surface waters in the glacial North Atlantic through increased rates of iceberg discharge.

There is, as yet, limited understanding of the contribution made by the last British ice sheet (BIS) to North Atlantic IRD (see Richter *et al.*, 2001). However, Scourse *et al.* (2000), in a detailed investigation of Heinrich Event 2 at the Goban Spur, demonstrated a precursor event of British origin, predating the main

Laurentide IRD signature. On the Barra Fan, NW Scotland, Knutz *et al.* (2001) documented the general pattern of ice-rafting during Marine Isotope Stage (MIS) 2–3 and suggested a strong regional IRD signature closely coupled to the D/O climate cycle. Since this region represents the major depo-centre of the last BIS, it is well placed to record the dynamic response of this climatically-sensitive ice margin (Boulton, 1990).

3.1.ii Sediment colour

Colour is 'the perception of the visible light-reflectance spectrum of an object' (Deaton, 1987). The earliest procedure used for identifying colour variations was the Munsell Renotation System (Munsell, 1941). This is based on colour deduction by the naked eye and is therefore dependent on the colour perception of the individual. The development of simple colorimeters and later spectrophotometers, has allowed uniform colour values to be represented by a single quantitative measurement. Measurements are rapid and non-destructive, so that data can be generated at a very high sampling resolution (density) (Chapman and Shackleton, 1998a).

Late Pleistocene marine sediment cores from the open North Atlantic Ocean commonly contain carbonate-rich (light-coloured) and clay-rich (dark-coloured) sediment layers (e.g. Nagao and Nakashima, 1992). Sediment colour and reflectance

provide a useful tool in this region, not only in characterising intervals of enhanced IRD deposition (e.g. Grousset *et al.*, 1993), but also in characterising sediment biogenic carbonate content (e.g. Cortijo *et al.*, 1995; Ortiz *et al.*, 1999; Helmke and Bauch, 2001). Rapid temperature fluctuations (Dansgaard/Oeschger cycles) identified in the ice core records of Greenland (e.g. Dansgaard *et al.*, 1993) have clear parallels within the colour variations observed in N. Atlantic sediment records (Bond *et al.*, 1992; Cortijo *et al.* 1995). Sediment colour has also been used as a proxy for changing North Atlantic circulation intensity (e.g. Chapman and Shackleton, 1998a). The potential therefore exists for the identification of sediment composition changes and, hence, fluctuations in environmental conditions through the analysis of marine sediment colour variations. Few studies, however, have investigated this methodology in a continental margin setting, partly because of the complexity of the depositional systems involved.

3.1.iii Giant piston core MD95-2006

Giant piston core MD95-2006 (57°01.82 N, 10°03.48 W, water depth 2,120 m) was recovered in 1995 by the RV *Marion Dufresne* from the northern limits of the Barra Fan, NW Scotland as part of the IMAGES programme (Figure 3.1). The Barra Fan extends from the Hebridean continental slope to the deep-water basin of the NE Rockall Trough (Holmes *et al.* 1998). It is primarily composed of Neogene sands and Pleistocene glacigenic sediment from NW Britain (Armishaw *et al.* 1998). This latter component is thought to have been deposited when locally grounded ice

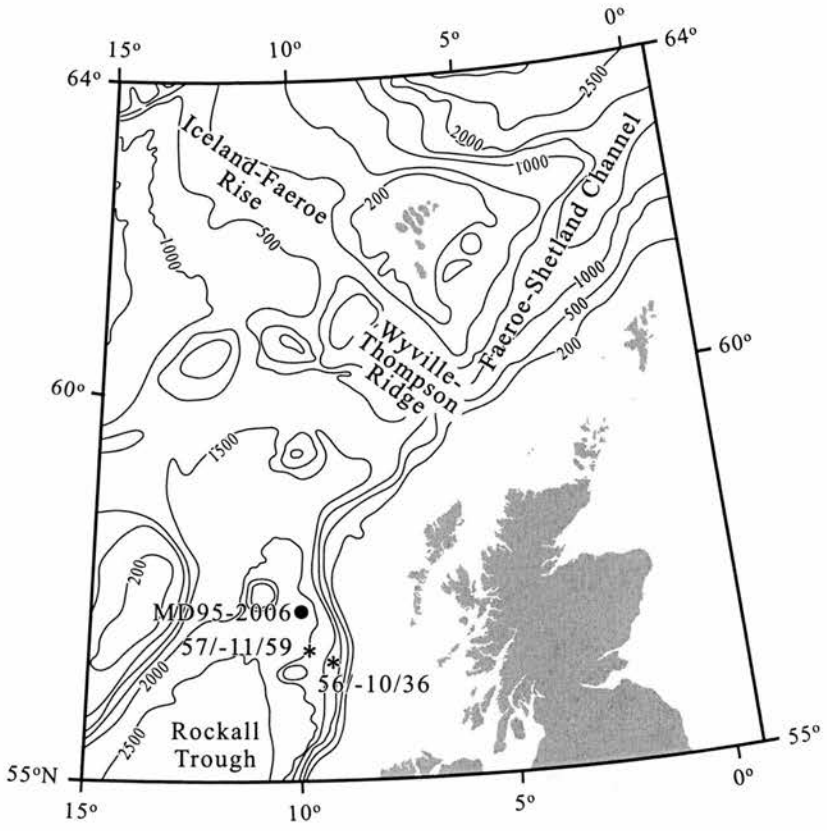

Figure 3.1. Location map of core MD95-2006 (57°01.82 N, 10°03.48 W, water depth 2,120 m), Barra Fan, NW Scotland. Nearby cores 56/-10/36 (Kroon *et al.*, 1997) and 57/-11/59 (Austin and Kroon, 2001) are located. Bathymetric contours are shown in metres.

reached the shelf edge. Further evidence of late Pleistocene glacial activity is present on the shelf margin in the form of morainal banks (Selby, 1989; Stoker, 1995) and iceberg plough marks (Kenyon, 1987). A 400-700 m undisturbed shelf-margin wedge forms the bulk of the landward depocentre of the Barra Fan (Stoker, 1995; Holmes *et al.* 1998).

Two vibrocores (57/-09/89 and 57/-09/46) from the St. Kilda Basin of the Hebridean Shelf have documented the timing of the last deglaciation of NW Scotland and provide an exceptionally high resolution record of the Younger Dryas cold phase (Austin, 1991; Peacock *et al.* 1992; Austin *et al.*, 1995; Austin and Kroon, 1996). In addition, two short cores from the Barra Fan (56/-10/36 and 57/-11/59) have established the detail of deglaciation along this margin within the context of surface (Kroon *et al.*, 1997) and deep water circulation changes (Austin and Kroon, 2001). Piston core MD95-2006 recovered 30 m of distal glacimarine sediments with average accumulation rates of greater than 0.5 m/ka (Kroon *et al.*, 2000; Knutz *et al.*, 2001). It therefore exhibits the potential for higher resolution marine sediment studies over MIS 2 and 3, from a continental margin setting which is known to record the major fluctuations of the last British ice sheet.

The characterisation of millennial-scale events by spectrophotometry is evaluated at this site and the significance of the MD95-2006 record is discussed in the context of amphi-Atlantic climate change. The aims of this paper are to present a new and revised radiocarbon-based age:depth model for core MD95-2006 and to

determine the response of the British ice sheet through the MIS3 to MIS2 transition using sediment colour and reflectance measurements.

3.2 Methods

3.2.i Spectrophotometry

The cleaned split-core surfaces of the MD95-2006 archive sections were analyzed with a hand-held Minolta CM-2002 spectrophotometer. A calibration and measurement procedure was established based on the Ocean Drilling Program's use of the Minolta CM-2002 (Blum, 1997). The illumination system was set at an angle of 2° and spectral reflectance measurements were made on the SCE (secular component excluded) setting (Balsam *et al.* 1997).

Polyethylene film was placed over the sediment surface in accordance with the methodology of Chapman and Shackleton (1998a). Measurements were taken on a single track along the centre of the core, with the spectrophotometer held orthogonal to the sediment surface. The sampling interval was set at 5 cm and was increased to 1 or 2 cm where higher resolution records were required, i.e. at a clearly visible transition between two colours, or, at bands highlighted within other proxy studies. The time interval between core cleaning and recording of each reading was kept to a minimum.

The recorded data is displayed using the Commission Internationale de l'Eclairage (CIE) L*a*b* colour space, the most commonly employed colour indicator in palaeoceanography in recent times (Merrill and Beck, 1996). This colour definition was established in 1931 as a standard component in aiding international colour matching. In this study L* indicates lightness (~greyscale reflectance) where, on a scale of zero to one hundred, zero represents black and one hundred is white. In addition to L*, colour reflectance data is presented every 100 nm from 400-700 nm (i.e. within the visible spectrum).

3.2.ii Particle size measurements

Particle size distributions were measured from samples of core MD95-2006 on a Coulter LS 230 Particle Size Machine (PSM). Sediment sub-samples were treated for the removal of carbonate through dissolution. The decalcified results obtained reflect the lithogenic (non-carbonate) particle size distribution of the sample. The biogenic opal content of the sediments is generally <5% and was estimated from smear slides.

Decalcified data were obtained from approximately 0.55-0.60 g of 'wet' sediment, which were placed in a test tube with distilled water and then centrifuged, before excess fluid was decanted. To remove all traces of salt crystals this procedure was repeated twice. Following decalcification of the sediment overnight in a 20% solution of acetic acid, samples were centrifuged to allow settlement of all fine

particles. Excess fluid was decanted, distilled water was added and the procedure repeated twice. A fixed volume of sodium hexametaphosphate was then transferred to the sample and this solution was added to the PSM and the grain size distributions recorded. This methodology is consistent with Austin and Kroon (2001).

3.2.iii Calcium carbonate

Calcium carbonate content was determined downcore at 10 cm intervals using a modified back titration method (Grimaldi *et al.* 1966) as described in Austin and Kroon (1996) and Austin and Evans (2000). 0.5g of dry sediment was accurately weighed and treated with an excess of acid (25ml of 0.5M HCl solution). 0.5ml of bromophenol blue indicator was added and the solution was back-titrated against 0.35M NaOH solution until the yellow to violet end-point was reached. The calcium carbonate content was calculated (weight in grams, volume in litres) by:

$$\%CaCO_3 = 100\ [(\text{vol. HCl} \times \text{molarity HCl} \times 1.007225) - (\text{vol. NaOH} \times \text{molarity NaOH})] \times (2 \times \text{sample weight})^{-1} \times 100.$$

{equation 3.1}

3.2.iv Magnetic Susceptibility

The volumetric magnetic susceptibility was measured down-core in SI units in 1cm increments using a Bartington Instruments magnetic susceptibility meter (Model MS2, adapted with a MS2F probe with an operating frequency of 0.58Hz). The results are reported as 1 x 10^{-6} SI Units.

3.3 Results

3.3.i Lithostratigraphy

Five lithological units were identified in core MD95-2006 which may be sub-divided into six lithofacies, based upon sedimentary structure, texture, colour and carbonate content (Figure 3.2) (Kroon *et al.* 2000; Knutz *et al.* 2001). The sequence consists of soft, light grey-brown silts and clays, which are interspersed with occasional clasts and thin sandy horizons, tending to exhibit sharp bases and gradational upper contacts (typically < 1 cm; maximum = 5 cm). The latter are interpreted as turbidite layers and are most prevalent through the interval 14-22 m. Well-developed dark blue-black monosulphide streaks were common between 7-13 m. Lighter grey-pale blue horizons, corresponding to higher carbonate contents, are visible between 22-24 m.

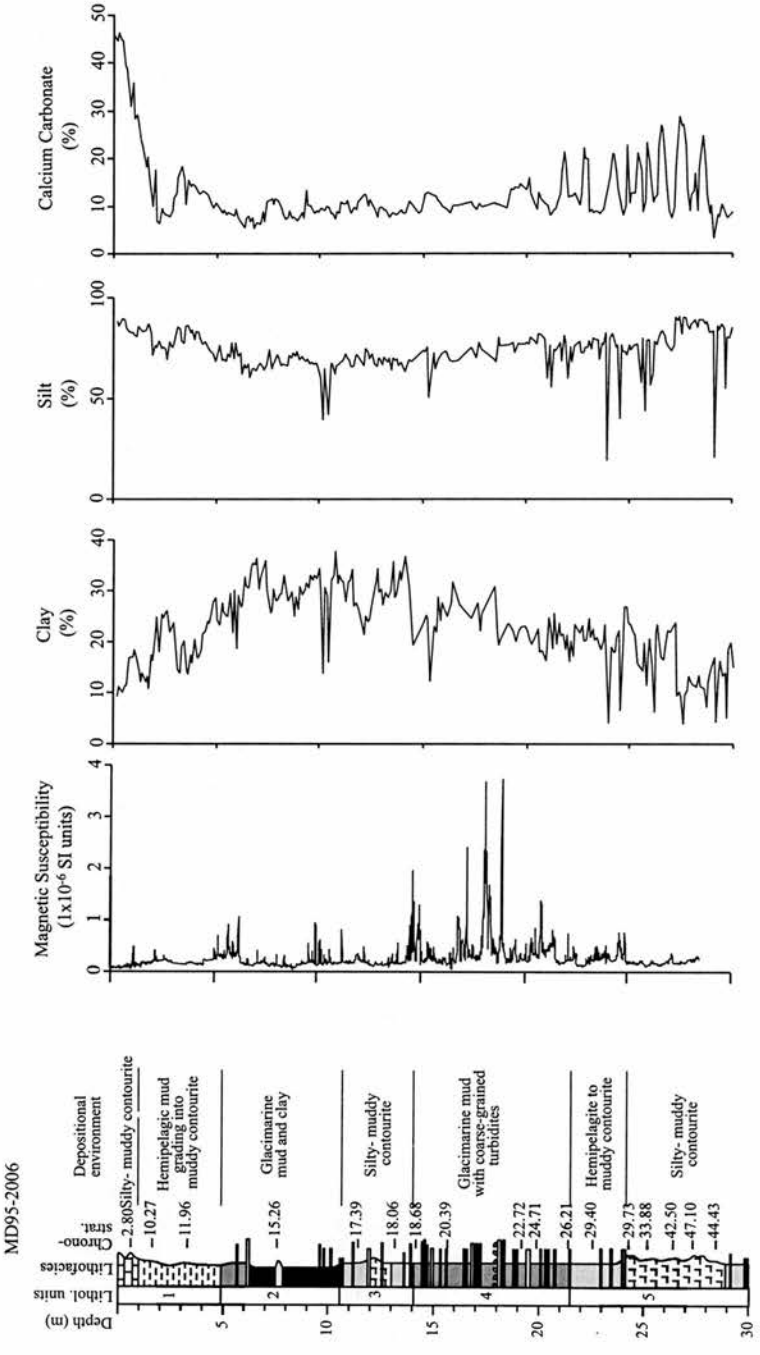

Figure 3.2. Lithological summary of core MD95-2006. General log modified after Kroon *et al.* (2000) with additional radiocarbon ages indicated (^{14}C ka BP). Clay and silt values (lithogenic) are volume %, calcium carbonate is weight %.

Magnetic susceptibility (ms) measurements reveal significant down-core variability. Below 5 m the first in a series of marked peaks in ms are observed, many coincide with silty to sandy muds containing dropstones. Prior to this, small ms peaks are observed between 1 and 3 m core depth. The most pronounced ms events are recorded at approximately 10 m, 15 m, 17-19 m, 21 m and 24.5 m. Between 14 to 24 m core depth, the silty to sandy muds are interspersed with numerous sandy turbidites and occasional gravel layers.

Silt content is typically greater than 60% throughout MD95-2006, as previously shown by Kroon *et al.* (2000). Below 20 m, there appears to be considerable variation in % silt, coinciding with low ms and variable $CaCO_3$. Above approximately 6-7 m, silt content rises steadily, coinciding with an increase in $CaCO_3$ and general decrease in % clay. Clay content varies between 10% to 35% and exhibits a very clear long-term trend. Lowest values are observed at the base of the core, increase steadily through a series of cycles to a maximum at approximately 6-7 m, and decline in a cyclical manner towards the core top.

Calcium carbonate data were reported for MD95-2006 by Kroon *et al.* (2000), with maximum core top values of approximately 20%. The data presented here suggest that near-surface values range from approximately 10% to 50%, which agree with Holocene data reported by Austin and Kroon (2001) on nearby core 57/-11/59. The $CaCO_3$ % data reported by Kroon *et al.* (2000) are actually Ca weight

data since they were measured by sediment XRD. Calcium carbonate values in MD95-2006 are generally low between 6-19 m, coinciding with an interval of prominent ms peaks and increased clay content. Below 19 m, values exhibit a pronounced cyclicity, ranging between 10-25 % calcium carbonate content.

3.3.2 Chronostratigraphy

Seventeen ^{14}C AMS radiocarbon dates were obtained from core MD95-2006, based upon monospecific foraminiferal samples of sub-polar *Globogerina bulloides* and polar *Neogloboquadrina pachyderma* (sinistral) (Table 3.1). Samples were prepared to graphite at the NERC Radiocarbon Laboratory, East Kilbride, and ^{14}C analysis was carried out at the University of Arizona NSF-AMS facility. One tephra layer (1 Thol. 2 Ash) was identified to further constrain the Younger Dryas period. This is a constituent of North Atlantic Ash Zone 1 (Kvamme *et al.,* 1989) and provides a useful chronostratigraphic marker within an interval of significant radiocarbon dating uncertainty (e.g. Austin *et al.*, 1995). Seven ^{14}C ages were calibrated into calendar ages using the Calib 4.2 programme (Stuiver and Reimer, 1993; Stuiver *et al.*, 1998) which incorporates a 400 year correction for the modern surface ocean reservoir effect at this latitude. This calibration of ^{14}C ages was only applied to radiocarbon dates younger than 21,000 ^{14}C years; the calibration data set available beyond this age is limited and has significantly decreased reliability. The nine remaining ^{14}C dates were calibrated using the U/Th ages and second-order

Laboratory Number	Core depth (cm)	Conventional radiocarbon age (^{14}C yr BP ±1σ)	Calendar age (years)	Species
VE 56/-10/36				
AA-13902*	72.5	10,040 ± 80	11062, 10984, 10834	*G. bulloides*
AA-13899*	75.5	10,585 ± 85	11674	*N. pachyderma (sinistral)*
AA-13900*	355	12,055 ± 100	13476	*G. bulloides*
AA-13898*	431.5	13,020 ± 115	15123, 14701, 14393	*G. bulloides*
VE 57/-11/59				
AA-23932*	2.5	2,535 ± 45	2183	*G. bulloides*
AA-23933*	21.5	5,540 ± 60	5910	*G. bulloides*
AA-23934*	51.5	7,175 ± 80	7639	*G. bulloides*
AA-23935*	71.5	9,010 ± 65	9619	*G. bulloides*
AA-24177*	180.5	11,725 ± 95	13161	*G. bulloides*
AA-24179*	224	12,720 ± 170	14144	*G. bulloides*
AA-24178*	282	12,940 ± 90	14355	*G. bulloides*
MD95-2006				
AA-40438*	0.5	2,799 ± 44	2526	*G. bulloides*
AA-40439*	164.5	10,270 ± 73	11153	*G. bulloides*
AA-40440*	323	11,960 ± 120	13442	*G. bulloides*
AA-22347*	770	15,260 ± 140	17664	*N. pachyderma (sinistral)*
AA-35119*	1175.5	17,390 ± 190	20115	*N. pachyderma (sinistral)*
AA-22348*	1340	18,060 ± 130	20886	*N. pachyderma (sinistral)*
AA-35120*	1411	18,680 ± 130	21600	*N. pachyderma (sinistral)*
AA-35121**	1591.5	20,390 ± 150	23567	*N. pachyderma (sinistral)*
CAMS-60835**	1941.5	22,720 ± 130	26740	*N. pachyderma (sinistral)*
AA-22349**	2020.5	24,710 ± 280	29022	*N. pachyderma (sinistral)*
AA-32312**	2173.5	26,210 ± 270	30726	*N. pachyderma (sinistral)*
AA-32313**	2288	29,400 ± 370	34305	*G. bulloides*
AA-32314**	2418.5	29,730 ± 470	34672	*G. bulloides*
AA-22350**	2539	33,880 ± 610	39229	*G. bulloides*
AA-35122**	2653.25	42,500 ± 1,800	48361	*G. bulloides*
AA-35123**	2728.5	47,100 ± 3,000	53052	*G. bulloides*
AA-35124**	2860	44,430 ± 2,000	50345	*G. bulloides*

Table 3.1. Radiocarbon ages of Barra Fan cores VE 56/-10/36, VE 57/-11/59, and MD95-2006. Samples marked * have been calibrated using Calib 4.2 (Stuiver and Reimer, 1993; Stuiver *et al.*, 1998); samples marked ** have been calibrated using U/Th ages and second-order polynomial equation (Bard *et al.*, 1998) but have not been corrected for the 400 year marine reservoir effect.

polynomial equation of Bard *et al.* (1998) which statistically extends the current coral calibration set of Stuiver *et al.* (1998):

$$[\text{cal age BP}] = -3.0126 \times 10^{-6} \times [^{14}\text{C age BP}]^2 + 1.2896 \times [^{14}\text{C age BP}] - 1005$$

{equation 3.2}

An age-depth model was constructed for core MD95-2006 using 14 of the calibrated AMS ^{14}C dates and the one tephra date (1 Thol. 2 Ash) (Figure 3.3). The oldest three dates obtained (AA35122, AA35123 and AA35124) were not used in the construction of the age-depth model due to the large dating uncertainty beyond 40,000 ^{14}C years BP. These dates lie close to the routine ^{14}C detection limit and are not statistically distinguishable at the 95% confidence level (Table 3.1, Figure 3.3). Contrasting age-depth models may yield significant age differences, particularly at the greatest core depths, where dating uncertainties are greater.

The first age-depth modelling approach employs the 14 calibrated AMS ^{14}C dates and the dated tephra horizon to fit two third-order polynomial curves to the data (Figure 3.3). From 0 – 323 cm, the well-dated record of nearby core 57/-11/59 (Austin and Kroon, 2001) provides an excellent constraint and test of the following

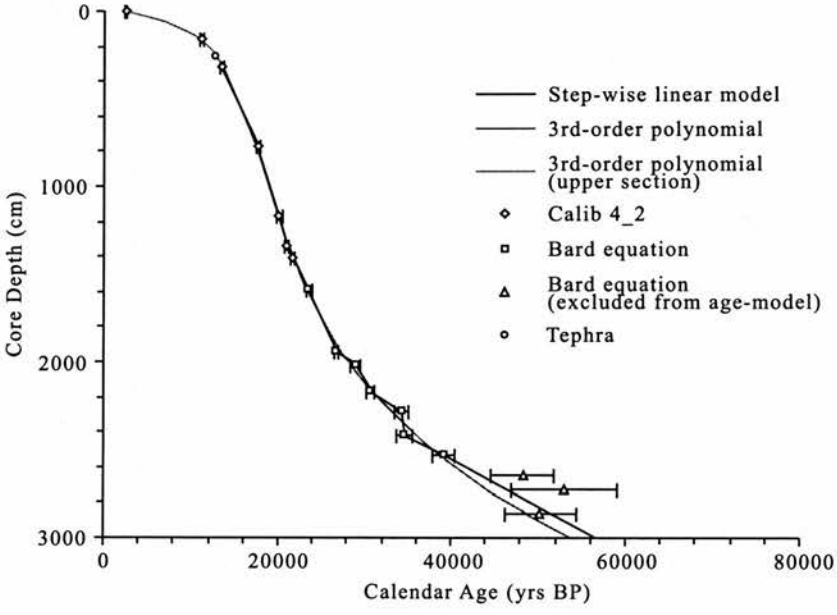

Figure 3.3. Age-depth models of core MD95-2006. Dated levels shown are calibrated radiocarbon ages (years BP ± 1σ); see text for explanation of calibration procedure.

equation (equation 3) for the age-depth relationship (r = 1):

$$[\text{cal age BP}] = 2482.2 + 87.78 \times [\text{core depth}] - 0.263 \times [\text{core depth}]^2 + 3.04e^{-4} \times [\text{core depth}]^3$$

{equation 3.3}

Equation 3.3 is based upon three calibrated AMS ^{14}C dates and dated tephra horizon at 262.5 cm. From 323 cm to the bottom of the core, the following equation for the age-depth model is employed (r = 0.995):

$$[\text{cal age BP}] = 9929.9 + 13.528 \times [\text{core depth}] - 7.0233e^{-3} \times [\text{core depth}]^2 + 2.4709e^{-6} \times [\text{core depth}]^3$$

{equation 3.4}

Using the above relationship (equation 3.4), the bottom of the core, at a depth of 3000 cm, yields an age estimate of 53,800 years BP. This differs from the previously published date of 45,000 years BP reported in Knutz *et al.* (2001) and emphasises the significance of the new dates reported here (Table 3.1)[3.2].

[3.2] See further discussion and revision of age-depth model in Chapter 6.

The second age-depth modelling approach assumes a constant sedimentation rate between the calibrated AMS ^{14}C ages, enabling the construction of a step-wise linear age-depth relationship (Figure 3.3). The age of the core bottom was inferred by fitting a linear regression line through three calibrated ages between 34,000 and 39,000 years BP (AA32313, AA32314 and AA22350), but excluding the oldest three dates obtained (i.e. AA35122, AA35123 and AA35124). This yields an age estimate of 56,661 years BP at the base of the core (i.e. 3000 cm).

There is therefore relatively little age difference between the two modelling approaches (Figure 3.3). The third-order polynomial age-depth models yield good statistical fits to the age control points. Large changes in sediment accumulation rates can arise in step-wise linear age-depth models as an artifact of dating uncertainties and sample density. Given the very rapid, sub-millennial changes of sediment accumulation defined during the last deglaciation at this site (Kroon *et al.*, 2000), the third-order polynomial age-depth model is preferentially applied in all further age-depth calculations.

3.3.iii Colour variability

The stratigraphic record of lightness (L*) and reflectance (400 – 700 nm) is presented in Figure 3.4. Three major subdivisions of the record are very clearly observed within the sequence. These can be defined as (1) a basal zone of highly

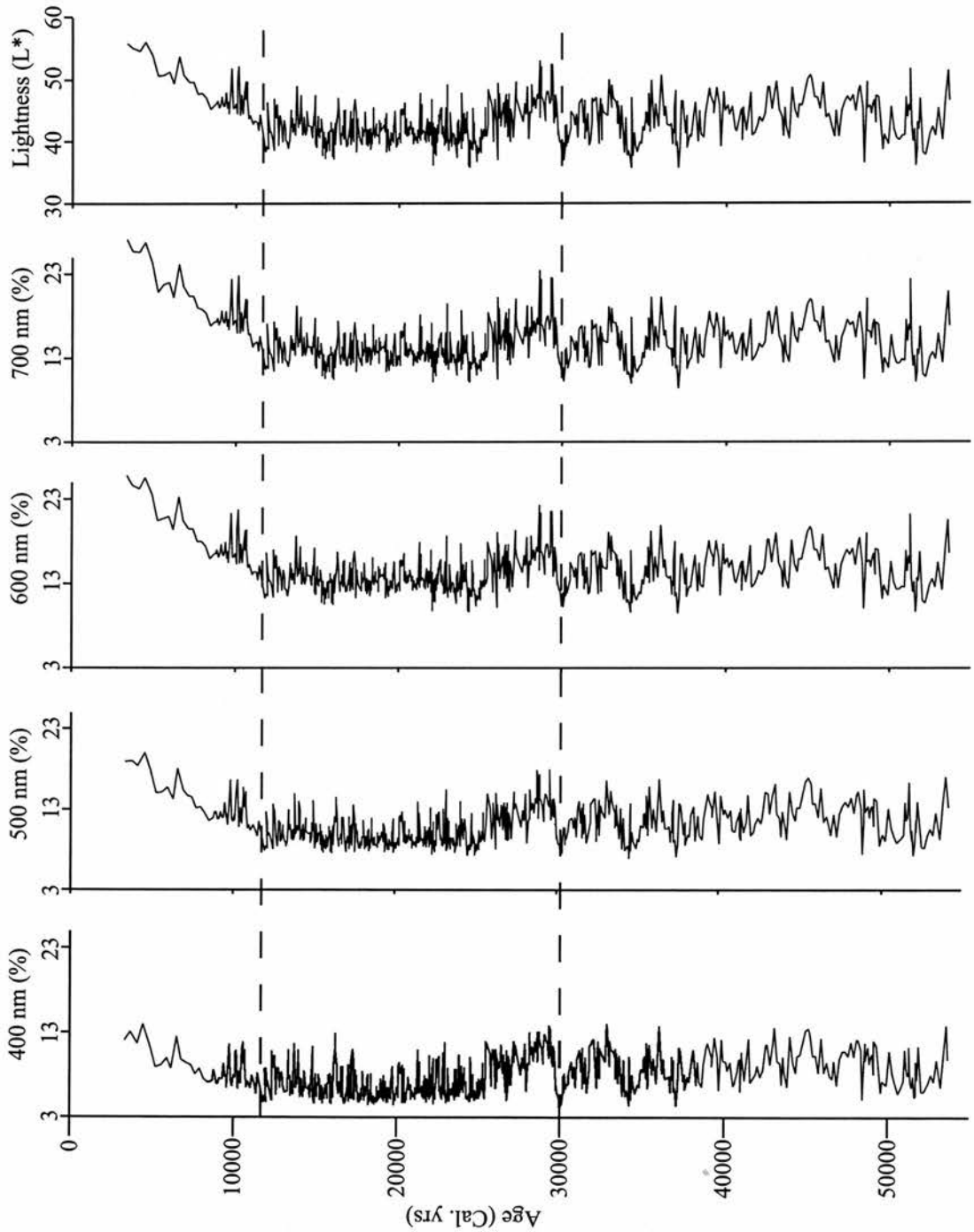

Figure 3.4. Stratigraphic summary of sediment reflectance (400-700 nm) and lightness (L*) of core MD95-2006. Age is calendar years BP.

variable L* and reflectance, pre-dating a transition beginning at about 30,000 years BP to (2) a zone of darker, lower amplitude variability in L* and reflectance, which gives way to (3) a light coloured, high reflectance zone postdating approximately 11,000 years BP. Colour variability pre-dating approximately 30,000 years BP exhibits an apparent cyclicity of about 3,000 years. Between 11,000 to 30,000 years, L* and reflectance show high frequency variability. After 11,000 years, L* and reflectance are less variable and show a steady increase towards the top of the core; the latter is particularly evident at 600 and 700 nm.

Reflectance spectra, L* and percentage clay results have been plotted against percentage bulk calcium carbonate to investigate relationships between these variables (Figure 3.5). A clear positive relationship is observed between L* and calcium carbonate ($r = 0.66$, Figure 3.5a), confirming that lighter coloured sediments have a higher calcium carbonate content. However, carbonate contents are generally low throughout much of the sequence and the relationship with L* is less clearly defined when calcium carbonate values fall below 15 – 20 %. Within the same range of observed L*, there also exists a negative relationship with sediment clay content ($r = 0.53$, Figure 3.5b). Therefore, in general, we observe high L* when clay content is low and calcium carbonate content is high and *vice versa*.

Specific reflectance wavelengths (400 - 700 nm) coinciding with the visible spectrum reveal positive relationships with the calcium carbonate content of the sediments (Figure 3.5c-f). The strongest correlations ($r = 0.73$) are observed at

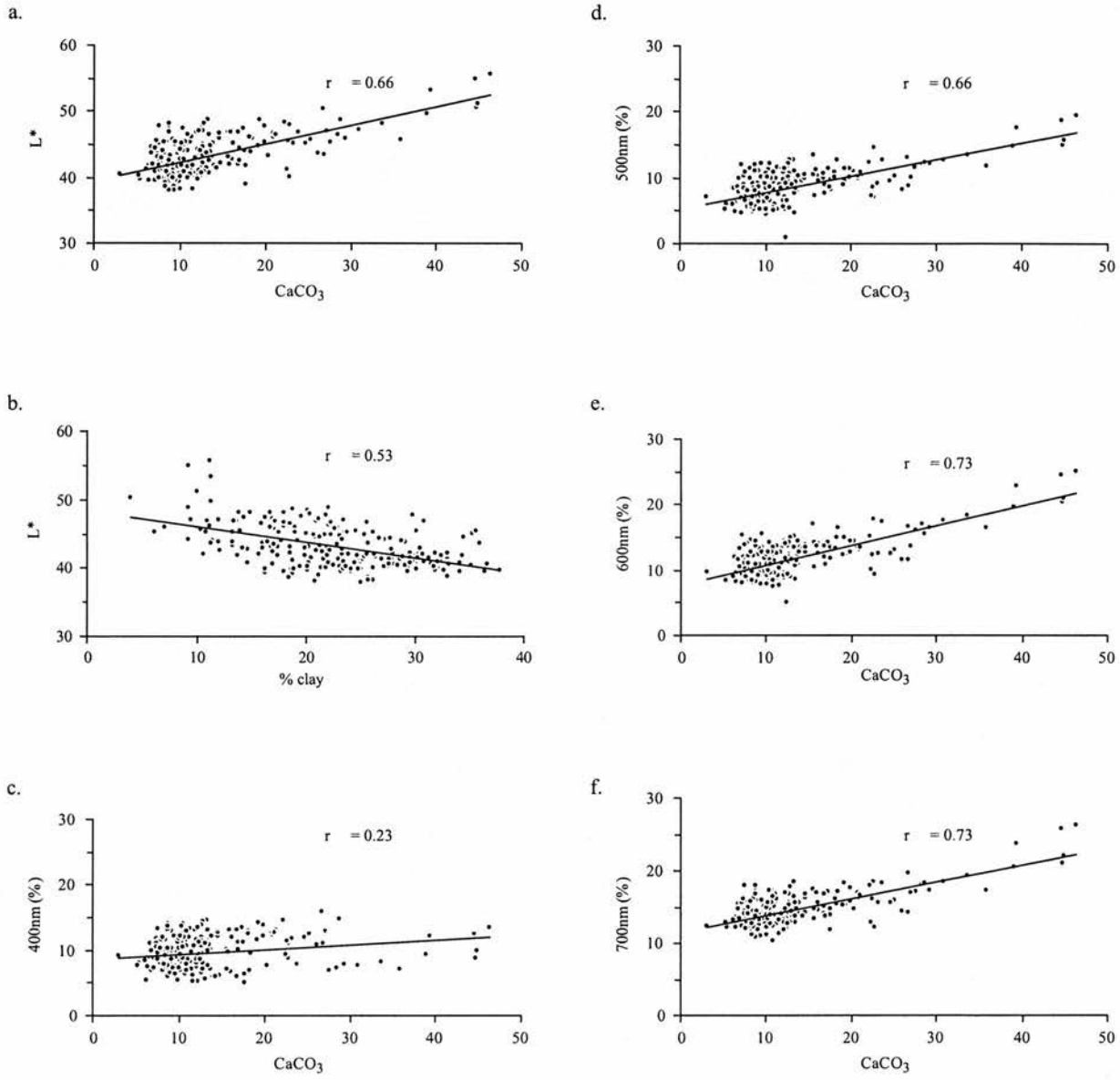

Figure 3.5. Summary plots of sediment reflectance and lightness against calcium carbonate (weight %) and clay (volume %) from core MD95-2006. Best-fit linear regression lines shown.

600 nm and 700 nm (Fig. 3.5e-f), corresponding to blue light reflectance. A weaker correlation (r = 0.23) is noted for red light reflectance at 400 nm (Figure 3.5c).

3.3.iv Spectral analysis

Spectral analysis of the data (L*, 400-700 nm reflectance, % clay and % $CaCO_3$) were carried out using the Blackman-Tukey method in the Analyseries 1.1 programme (Paillard *et al.*, 1996). The results were compiled for two distinct chronostratigraphic intervals, corresponding to 15-22 ka BP and 30-50 ka BP (Figure 3.6). These intervals were chosen as periods of relative signal stability and avoid some of the major transitions in depositional pattern, notably after 15 ka BP and between 22-30 ka BP.

In the interval 30-50 ka BP, a strong periodicity is observed at 3077 years, notably in the following proxies: 500 nm, 600 nm, 700 nm, CaCO3. L* and 400 nm reflectance exhibit a strong periodicity at 3125 years. Longer periodicities, notably in % clay and % silt, are also observed through this interval, with greatest power at 4878 and 9524 years, respectively. In addition, a periodicity of 1980 years is observed in all the proxies investigated between 30-50 ka BP, although at a reduced power.

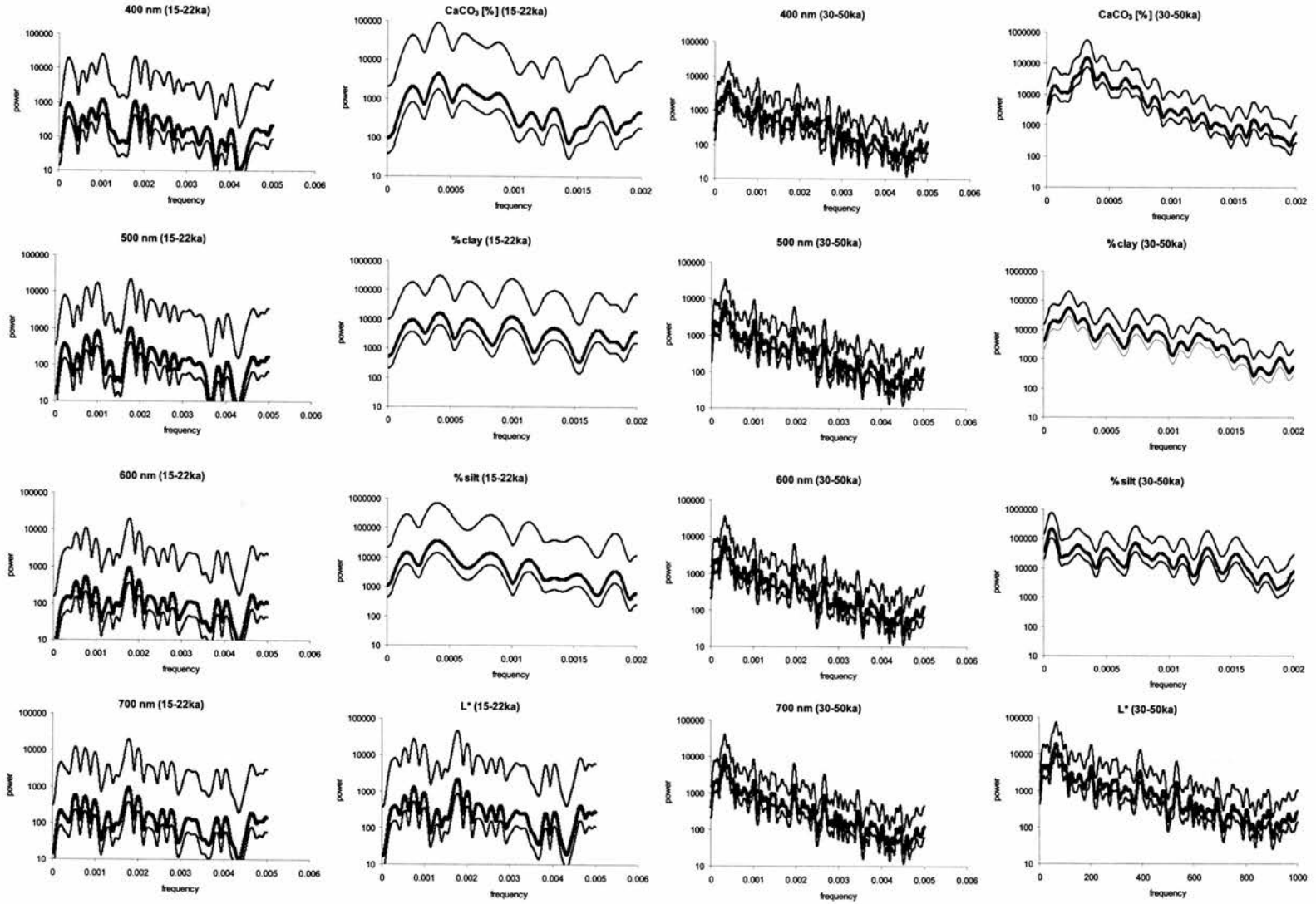

Figure 3.6. Summary figures illustrating power spectra of various sedimentological proxies from the intervals 15-22 ka BP and 30-50 ka BP from MD95-2006. Spectral analysis employs the Blackman-Tukey method in the AnalySeries 1.1 programme (Paillard *et al.*, 1996). Upper and lower confidence limits (80%) are illustrated by thin lines.

In the interval 15-22 ka BP, periodicities generally exhibit reduced power and higher frequency. The most common periodicities observed typically range from approximately 1000 to 2500 years. Many of the proxies investigated, notably L* and reflectance, exhibit numerous periodicities of similar power. However, % clay, % silt and % $CaCO_3$ show maximum power at a consistent periodicity of approximately 2500 years.

3.4 Discussion

The lithostratigraphy of core MD95-2006 was originally defined by Kroon *et al.* (2000) and Knutz *et al.* (2001). Kroon *et al.* (2000) describe the general depositional setting at this site, emphasising the rapidity of sub-millennial scale changes in the depositional cycles observed. Knutz *et al.* (2001) concentrated upon the IRD signature and its implications for fluctuations along the western limits of the last British ice sheet, postulating a coupling between BIS-derived IRD and D/O cyclicity. Here, the dynamics of this ice sheet are investigated in the context of a refined age-depth model, allowing the response of the depositional pattern along this margin to be quantified through the last glacial period. Of particular note is the marked increase in sediment accumulation rate at approximately 30 ka BP, which suggests the sedimentological response is in-phase with the climatological transition of the MIS 3 – 2 boundary. The timing of this transition agrees with the age estimate from GISP2 and VM19-30 reported by Bond *et al.* (1997, 1999), but is 6,000 years

older than estimated in the original definition of the MIS 3 –2 boundary by SPECMAP (Martinson *et al.*, 1987).

The refined age-depth model of core MD95-2006 (Figure 3.3) represents a significant improvement in constraining the depositional features at this site on the Barra Fan. In particular, the age at the bottom of core (ca. 3000 cm) is estimated to be 53.8 ka BP, considerably older than the previous age estimate of 45 ka BP. This finding has implications for some of the previously reported IRD correlations, notably the position of H5, which was not recognised by Knutz *et al.* (2001). The latter has been tentatively assigned here to the quartz-rich IRD interval at approximately 28 m, defined as BF16 by Knutz *et al.* (2001).

The equivalent of the Heinrich Event stratigraphy of the open NE Atlantic (e.g. Bond *et al.*, 1992) can be identified along this margin, despite some uncertainty regarding H2, H3 and H5 (Table 3.2). Only one of the IRD events (H4 at 24.7 m) has the characteristically high concentration of distinct pale yellow dolomitic carbonate (G. Bond, *pers. comm.*, 2000). Since the timing of H1 is well constrained in this and other NW European records (e.g. McCabe and Clark, 1998; Scourse *et al.*, 2000), the interval of intense ice-rafting identified between 15.1-16.6 ka BP is confidently assigned to this event. However, there are numerous additional IRD events in the MD95-2006 record which do not coincide with Heinrich Events, most of which lack a distinctive Laurentide signature. At this site, these IRD lithologies

Heinrich Event	Curry et al. 1999	GISP 2	This study
1	16.5	15.8-16.5	15.1-16.6
2	24.3	24	24-24.8
3	31.6	30.2	30.8-29.3
4	39.9	38.5-39.6	38.0-36.7
5	46	45.5-46.2	46.4

Table 3.2. Age estimates of Heinrich Events 1 to 5. The GISP 2 data are derived from Grootes and Stuiver (1997).

are dominated by basaltic grains in the lithic sand-sized fraction, supporting the interpretation that they are derived from the Tertiary provinces of the NW British Isles (Austin and Kroon, 1996; Knutz *et al.*, 2001). Given this strong regional IRD signal, derived from a relatively small ice sheet, amphi-Atlantic correlations based on the IRD events described at this site are extremely difficult. These significant "non-Heinrich" IRD events highlight the problem of IRD correlation and asynchronous deposition at sites distal to the main Laurentide IRD belt (Dowdeswell *et al.*, 1999), yet proximal to, for example, the BIS.

In this study, a more promising approach to amphi-Atlantic correlation is the use of clearly defined cycles of carbonate-rich sediment in defining interstadial events. These cycles have been investigated through the analysis of sediment colour variability. Lightness (equivalent to grey-scale measurements) and blue colour reflectance measurements provide a useful proxy for calcium carbonate content (Figure 3.5). In an attempt to provide a quantitative estimate of % $CaCO_3$, we have simplified the multiple regression approach of Ortiz *et al.* (1999) and applied the following regression equation:

$$\text{Proxy \% } CaCO_3 = 1.7733R_{600} - 7.7483$$

{equation 3.5}

This approach provides a rapid means of estimating calcium carbonate content and has the potential to resolve the fine detail of the interstadial events within MIS 3.

The clay content of the sediment plays a significant role in carbonate dilution, so that interstadial events correspond to lower % clay, associated with lower sediment accumulation rates (Figure 3.7). Stadials, which have low calcium carbonate contents, are characterised by higher % clay, reflecting higher sediment accumulation rates. This depositional pattern is consistent with a switching mechanism between hemipelagic and hemiturbiditic sedimentation (e.g. Stow and Tabrez, 1998) during stadials, when ice margin sediment supply is high and bottom current activity reduced. During the interstadials sediment accumulation rates are reduced, due to glacier retreat and sediment entrapment on the continental shelf and shelf break. In addition, enhanced bottom current activity may act to winnow fine particles and hence reduce clay content. In response, carbonate content increases. There is some evidence in the literature which suggests enhanced ventilation during the interstadials (e.g. Curry *et al.*, 1999) of MIS 3. Alternatively, a change in the actual mechanism of convection between interstadials and stadials (e.g. Dokken and Jansen, 1999), would also be consistent with our interpretation of the data.

Spectral analysis of the data reveals a marked difference in periodicities pre- and post-30 ka BP, corresponding to the transition from MIS 3 to 2. Prior to 30 ka BP, there is a strong 3077 year periodicity, which is somewhat longer than the well-

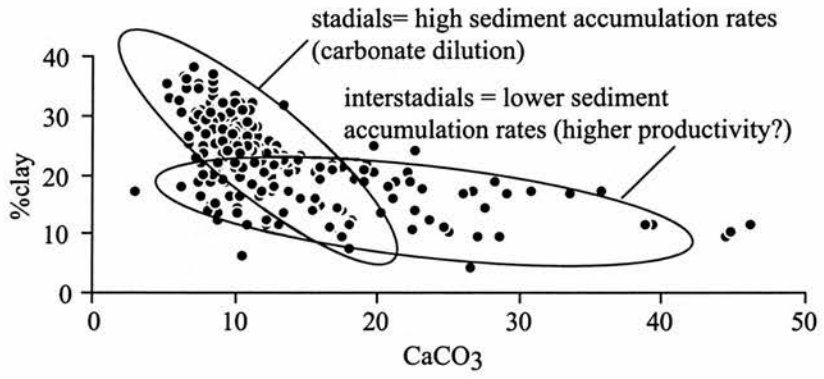

Figure 3.7. Summary plot showing clay (volume %) against calcium carbonate (weight %) from core MD95-2006. Stadial intervals are characterised by high sediment accumulation rates; interstadials by lower sediment accumulation rates.

known Dansgaard/Oeschger cycles (Dansgaard *et al.*, 1993, Bond *et al.*, 1993). However, the most persistent cycle observed within this interval has a frequency of 1980 years, which does correspond rather more closely to the Dansgaard/Oeschger frequency (e.g. Bond *et al.*, 1997). This quantitative observation compares well with a visual inspection of the data (Figure 3.8), where 10 distinct peaks in calcium carbonate are recorded within the interval 30-50 ka BP. These 10 peaks, having an average periodicity of approximately 2000 years, allow us to assign Greenland interstadial events 5-14 (Dansgaard *et al.* 1993) to our stratigraphic record. The correlation of these interstadial events gives us additional confidence in our age-depth model (since the age estimates are independently derived) and suggests that the reported problems of radiocarbon dating this time period (e.g. Voelker *et al.*, 1998) have not significantly affected this record[3.3].

After 30ka BP, the observed periodicities in our proxy data do not appear to coincide with those reported from the Greenland ice core record (Grootes and Stuiver, 1997) or open North Atlantic (Bond et al., 1997). The higher frequency variability recorded, often at considerably lower power, within the interval 15-22 ka BP suggests that changes in the prevailing depositional environment were more dynamic than during MIS 3. This quantitative observation may be anticipated, given the marked transition in numerous sedimentological proxies at 30 ka BP (Figure 3.8). During MIS 2, ice sheets surrounding NW Europe reached their maximum extent at or shortly before 22 ka BP (e.g. Sejrup *et al.*, 1994). Regional mapping of

[3.3] Please refer to Chapter 7 for further discussion of this MIS 3 dating uncertainty.

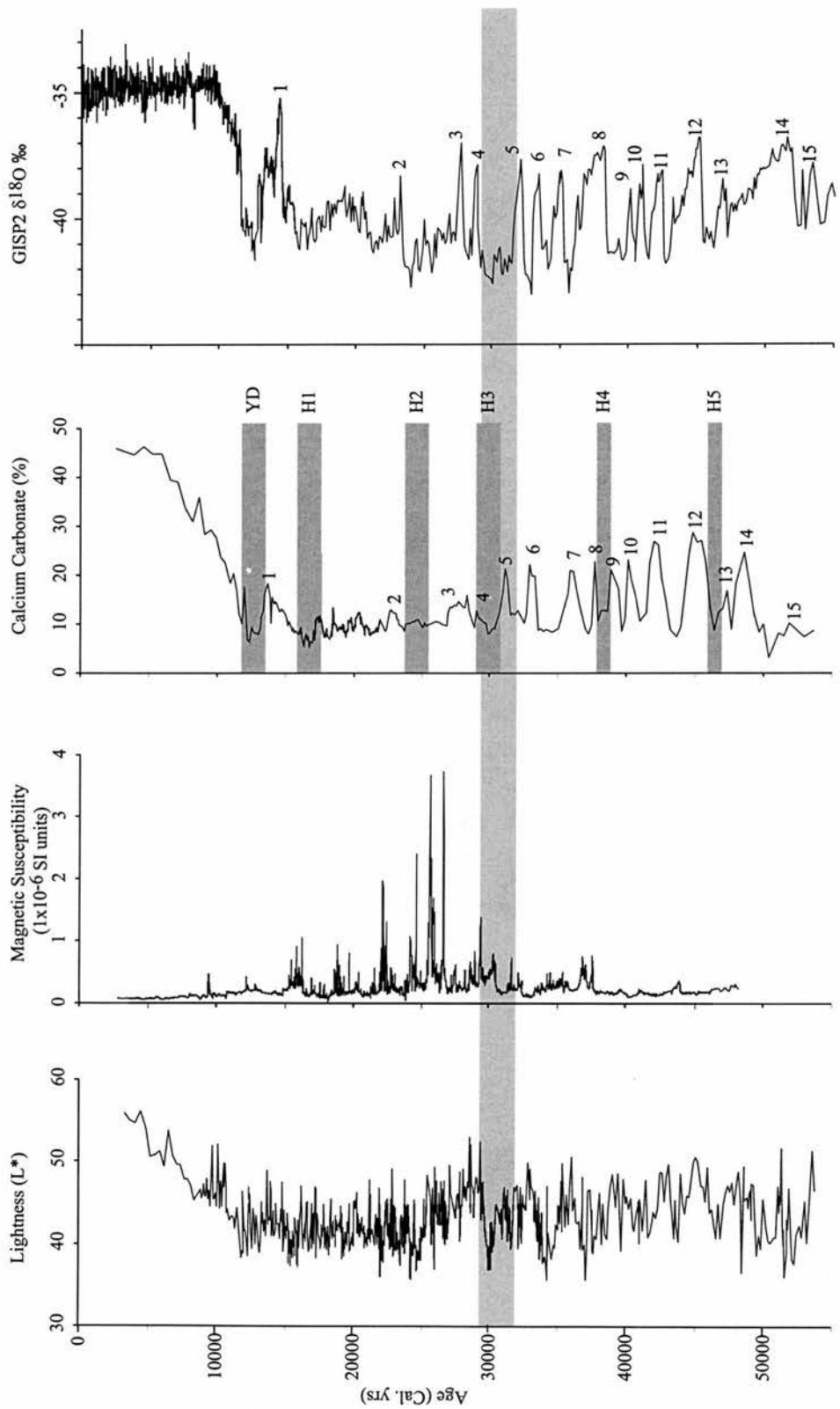

Figure 3.8. Stratigraphic summary of core MD95-2006 and Greenland Ice Sheet Project (GISP2) ice core $\delta^{18}O$ (Grootes *et al.*, 1993). Interstadial events are numbered after Dansgaard *et al.* (1993) and corresponding intervals of increased calcium carbonate content are identified. Light shading represents the transition in depositional environment from MIS3 to MIS2 at approximately 30,000 years BP.

extensive submarine moraine ridge complexes on the Hebridean shelf suggests that the BIS extended to the outer shelf during this period (Selby, 1989, Stoker, 1995). At its maximum extent, lying on deformable sediments, the last BIS had the potential to respond rapidly to both internal and external forcing mechanisms. The exact driving mechanism of the observed periodicities at this time remains uncertain, but it is apparent that glacier-influenced sedimentation was not operating with a clear D/O cyclicity.

As the ice sheet extended across the continental shelf during the MIS 3-2 transition, enhanced sediment delivery across the shelf-slope break resulted in rapidly increasing accumulation rates (Figure 3.3). During this period small, discrete turbidite horizons appear in the record and are associated with intervals of IRD (Knutz *et al.*, 2001) (Figure 3.2). This suggests that large volumes of sediment were being deposited on the upper slope of the Barra Fan, providing a source material for the generation of turbidites. One potential trigger mechanism, which may have acted to destabilise the sediment-laden upper slopes of the Barra Fan, would have been iceberg scouring. Iceberg scours, extending to depths of over 400 m, are well known along this margin (e.g. Belderson *et al.*, 1972, Kenyon, 1987, Armishaw *et al.*, 1998). Therefore, at a time of maximum ice-sheet extent and sediment delivery to a proximal site, strong periodicities in sediment proxies are likely to have been weaker. This observation further illustrates the difficulty in correlating millennial-scale IRD events deriving from major ice sheets, particularly during the last glacial maximum.

3.5 Summary and Conclusions

The combined use of sediment colour with other proxy data provides a powerful tool in the detailed analysis of highly expanded sediment sequences. Sediment colour, while widely used in deep ocean records, has not commonly been utilised in the investigation of high latitude continental margin records. Despite difficulties associated with low calcium carbonate contents, the potential exists to investigate depositional processes at an extremely high resolution and in a non-destructive manner. The records obtained from MD95-2006 reveal how ice sheet extent influences sediment delivery rates across the shelf-slope break. The response of the BIS across the MIS 3-2 transition is clearly defined in a large number of sedimentological proxies and illustrates the highly responsive nature of this ice sheet to external climate forcing at about 30 ka BP. Sediment colour allows the characterization of rapid, sub-millennial-scale variability, suggesting a shift at about 30 ka BP to lower amplitude, higher frequency in all the proxies investigated.

Numerous IRD intervals within MD95-2006, which do not coincide with Heinrich Events, have a clear BIS provenance. These "non-Heinrich" IRD events are similar in magnitude to the IRD events correlated with H1 to H5 and appear to have a pacing which matches the D/O cyclicity (Knutz *et al.*, 2001). While the local, Heinrich-equivalent events may have been triggered by instabilities in the BIS generated as a direct response to massive iceberg discharges from the LIS, this

mechanism is unlikely to have generated all the observed IRD throughout the MD95-2006 record. Unfortunately, the absence of a distinctive LIS geochemical signature in the Barra Fan record make amphi-Atlantic correlations extremely difficult. As such, the recent debate concerning so-called "precursor" events of European origin (Grousset *et al.*, 2000; Scourse *et al.*, 2000), predating the major Heinrich Events, may require further consideration of the numerous IRD events characterising North Atlantic sediment records at the millennial and sub-millennial-scale. In particular, the MD95-2006 record suggests that IRD originating from the last BIS during MIS 2 is a pervasive sub-millennial-scale feature, operating at higher frequencies than the D/O cycle. Care should therefore be taken when identifying "precursor" events for H1 to H3, since these may simply reflect a background signal of sub-millennial ice-rafting.

Despite the difficulties in radiocarbon chronologies and the problems which exist in the determination of lead-lag relationships between the marine, terrestrial and Greenland ice core records, reliable amphi-Atlantic correlations can still be achieved from an event stratigraphy based on interstadials.

Chapter 4.

"The Last British Ice Sheet: growth, maximum extent and deglaciation."[4.1]

Abstract

The growth, maximum lateral extent and deglaciation of the last British Ice Sheet (BIS) has been reconstructed using sediment, faunal and stable isotope methods from a sedimentary record recovered from the Barra Fan, NW Scotland. During a phase of ice sheet expansion postdating the early 'warmth' of Marine Isotope Stage 3 (MIS 3), ice-rafting events, operating with a cyclicity of approximately 1,500 years, are interspersed between warm, carbonate-rich interstadials operating with a strong Dansgaard/Oeschger (D/O) cyclicity. The data suggest that the BIS expanded westwards to the outer continental shelf-break shortly after 30 ka BP (before present) and remained there until about 15 ka BP. Within MIS 2, as the ice sheet grew to its maximum extent, the pronounced periodicities which characterise MIS 3 are lost from the record. The exact timing of the Last Glacial Maximum (LGM) is difficult to define in this record; but maxima in *N.pachyderma* (sinistral) $\delta^{18}O$ are observed between 21 – 17 ka BP. A massive discharge of ice

[4.1] This chapter is based upon the following published work: Wilson, L.J., Austin, W.E.N. and Jansen, E. 2002. The Last British Ice Sheet: growth, maximum extent and deglaciation. *Polar Research*, **21**, 243-250.

rafted detritus (IRD), coincident with Heinrich event 1, is observed at about 16 ka BP. Deglaciation of the margin is complete by about 15 ka BP and surface waters warm rapidly after this date.

4.1 Background

The growth and decay of northern Hemisphere ice sheets is a persistent feature of the late Pleistocene and glacier-influenced sedimentation is therefore a characteristic depositional feature of the North East Atlantic margins (e.g. Andrews *et al.*, 1996). Continental margin sediments which predate the last glacial maximum (LGM) have the potential to provide millennial-scale records of ice sheet dynamics (Bond and Lotti, 1995; Knutz *et al.*, 2001). These regional records highlight the significance of local ice sheet variability, set in the wider context of North East Atlantic ice rafting and palaeoclimate changes.

Rapid warm to cold climate transitions (Dansgaard-Oeschger (D/O) events), occurring with periodicities of 500-2000 years (e.g. Dansgaard *et al.*, 1993; Bond *et al.*, 1999), characterise the last glacial period. These persistent cycles of the North Atlantic's climate system, coupled to fresh water forcing mechanisms, may explain the global significance of such ice-rafting events (Broecker *et al.*, 1990; Bond *et al.*, 1999).

The contribution of the last British ice sheet (BIS) to North Atlantic IRD and fresh water forcing mechanisms is unlikely to be large, yet the BIS may serve as a

sensitive indicator of climate forcing upon northern hemisphere glacier response (e.g. Boulton, 1990). Richter *et al.* (2001), in a review of the BIS contribution to North Atlantic IRD, have shown how IRD records can be related to late Devensian (~30 ka BP) ice advances from the south west sector of the BIS. In a detailed investigation of Heinrich Event 2 at the Goban Spur, Scourse *et al.* (2000) demonstrated a precursor event of British origin, predating the main Laurentide IRD signature. This dynamic response of the last BIS has also been documented by Knutz *et al.* (2001), who suggested a strong regional IRD signature closely coupled to the D/O climate cycle.

The aim of this paper is to present evidence for the dynamic nature of the BIS during the last glacial period. In addition, the chronology of the main MIS transitions and the related growth, maximum extent and collapse of the ice sheet is evaluated from marine sediment core MD95-2006.

4.1.i Giant piston core MD95-2006

Giant piston core MD95-2006 (57°01.82 N, 10°03.48 W, water depth 2,120 m) was recovered in 1995 by the RV *Marion Dufresne* from the northern limits of the Barra Fan, NW Scotland as part of the International Marine Past Global Changes Project (IMAGES) programme (Figure 4.1). Evidence of late Pleistocene glacial activity is present on the shelf margin in the form of morainal banks (Selby, 1989; Stoker, 1995, Austin and Kroon, 1996) and iceberg plough marks (Kenyon, 1987).

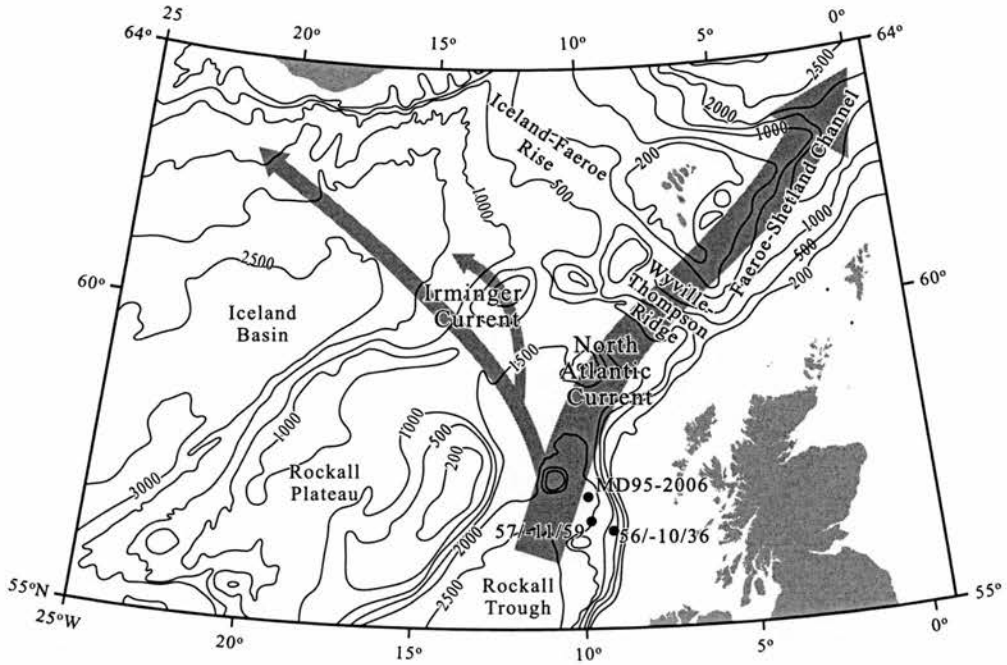

Figure 4.1. Location of marine core MD95-2006 (57°01.82N, 10°03.48 W, water depth 2,120m) from the Barra Fan, NW Scotland modified from Kroon *et al.* (1997). British Geological Survey cores 56/-10/36 and 59/-11/59 are also shown.

Two vibrocores from the St. Kilda Basin of the Hebridean Shelf (57/-09/89 and 57/-09/46) document the timing of the final deglaciation of the shelf from this region of NW Scotland and provide an unprecedented record of the Younger Dryas cold phase (Austin, 1991; Peacock *et al.* 1992; Austin *et al.*, 1995; Austin and Kroon, 1996). The detailed record of deglaciation from two short cores on the Barra Fan (56/-10/36 and 57/-11/59) which postdate 15 ka BP are documented by Kroon *et al.* (1997) and the associated deep water circulation changes by Austin and Kroon (2001). Piston core MD95-2006 recovered 30 m of distal glacimarine sediments with average accumulation rates of greater than 0.5 m/ka (Kroon *et al.*, 2000; Knutz *et al.*, 2001). It therefore exhibits the potential for high resolution marine sediment studies over MIS 2 and 3 from a continental margin setting which is known to record the major fluctuations of the last British ice sheet. This paper presents new planktonic foraminiferal stable isotope data from core MD95-2006 and a refined interpretation of BIS dynamics within the context of NE Atlantic palaeoceanography.

4.2 Methods

4.2.i Calcium carbonate

Calcium carbonate content was determined downcore at 10 cm intervals using a modified back titration method (Grimaldi *et al.* 1966) as described in Austin

and Kroon (1996) and Austin and Evans (2000). 0.5 g of dry sediment was accurately weighed and treated with an excess of acid (25 ml of 0.5M HCl solution). 0.5 ml of bromophenol blue indicator was added and the solution was back-titrated against 0.35M NaOH solution until the yellow to violet end-point was reached. The calcium carbonate content was calculated (weight in grams, volume in litres) by:

$$\%CaCO_3 = 100\ [(\text{vol. HCl} \times \text{molarity HCl} \times 1.007225) - (\text{vol. NaOH} \times \text{molarity NaOH})] \times (2 \times \text{sample weight})^{-1} \times 100. \quad \{\text{equation 4.1}\}$$

4.2.ii Magnetic Susceptibility

The volumetric magnetic susceptibility was measured down core in SI units in 1 cm increments using a Bartington Instruments magnetic susceptibility meter (Model MS2, adapted with a MS2F probe with an operating frequency of 0.58 Hz). The results are reported as 1×10^{-6} SI Units.

4.2.iii Stable Isotopes

Stable isotope measurements were performed on a Finnigan MAT 251 mass spectrometer at the University of Bergen, Norway. The $\delta^{18}O$ isotope results were obtained from the analysis of the planktonic foraminifera *Neogloboquadrinia pachyderma* (sinistral) and *Globigerina bulloides*. The foraminifera were processed from the >63μm washed residues and picked from the size range > 150μm from the

dry sieved residues. Sample weights, typically 10 specimens, were in the range 0.090-0.105 mg. Results are reported with respect to Vienna Pee Dee Belemnite (VPDB) standard through calibration with the National Bureau of Standards (NBS) 19 standard. The reproducibility of the system for $\delta^{18}O$ is ± 0.07 ‰ based on replicate measurements of an internal carbonate standard (0.1 ± 0.05 mg).

4.3 Results

4.3.i Lithostratigraphy

The lithostratigraphy of core MD95-2006 is summarised in Figure 4.2 (see Kroon *et al.* 2000; Knutz *et al.* 2001; see section 3.3.ii).

Down-core variability is highlighted by magnetic susceptibility measurements. Below 5 m, the first in a series of marked peaks in magnetic susceptibility are observed, many of these coinciding with silty to sandy muds, containing dropstones and previously interpreted as IRD events (Knutz *et al.*, 2001). The most pronounced magnetic susceptibility events are recorded at approximately 10 m, 15 m, 17-19 m, 21 m and 24.5 m. Between 14 to 24 m core depth, the silty to sandy muds are interspersed with numerous sandy turbidites and occasional gravel layers. Calcium carbonate values in MD95-2006 are generally low (<15%) between 6-19 m, coinciding with an interval of prominent magnetic susceptibility peaks and

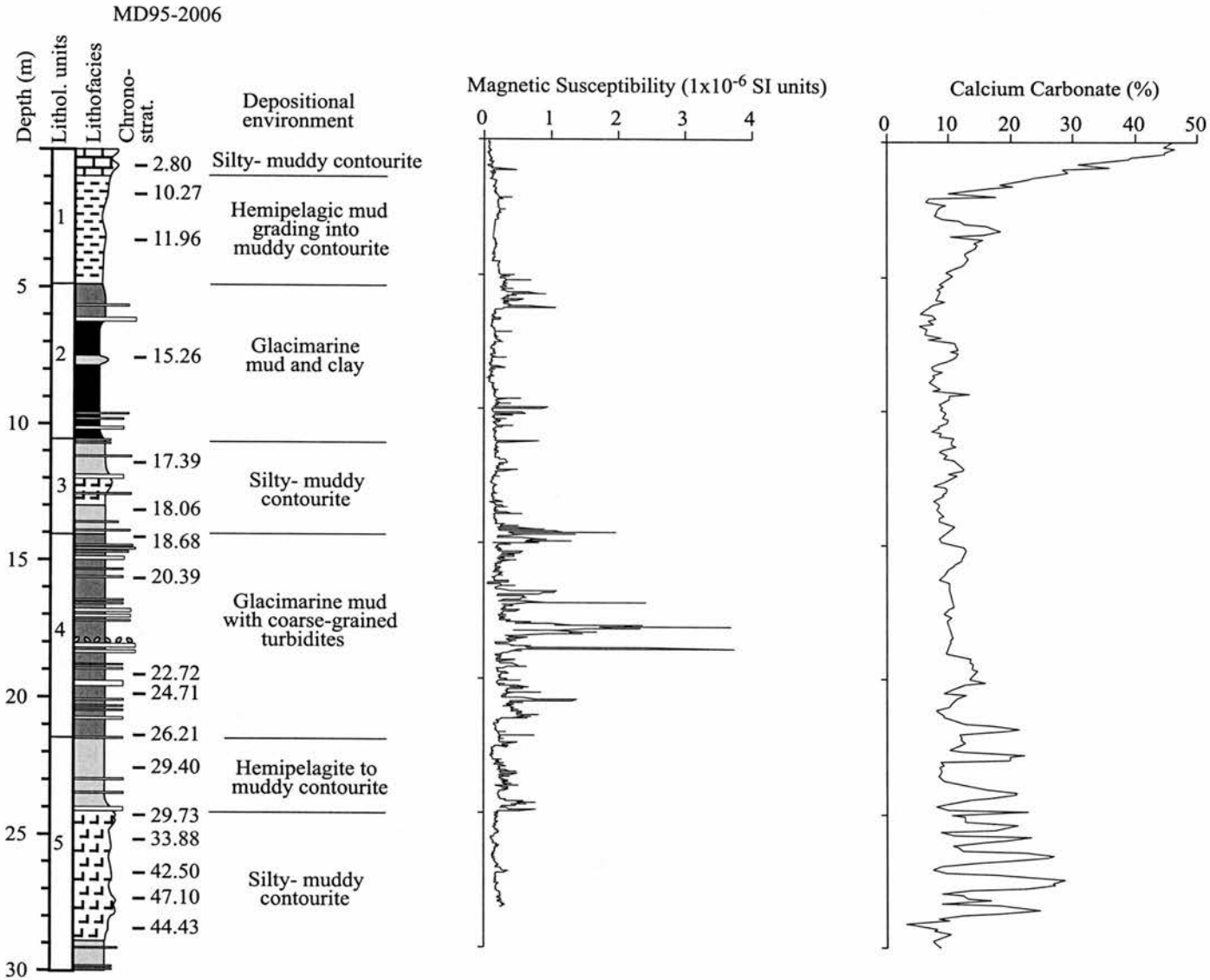

Figure 4.2. Lithological log modified from Kroon *et al.* (2000) with additional radiocarbon ages (^{14}C ka BP) indicated. Calcium carbonate is weight %.

increased clay content. Below 19 m, values exhibit a pronounced cyclicity, ranging between 10-25 % calcium carbonate content (Figure 4.2). These carbonate-rich intervals are observed to contain increased abundances of *Globigerina bulloides* and other temperate planktonic foraminifera.

4.3.ii Chronostratigraphy

Seventeen ^{14}C AMS dates were obtained from core MD95-2006 (Figure 4.3), based upon monospecific foraminiferal samples of sub-polar *Globogerina bulloides* and polar *Neogloboquadrina pachyderma* (sinistral). Samples were prepared to graphite at the NERC Radiocarbon Laboratory, East Kilbride, and ^{14}C measurements were made at the University of Arizona NSF-AMS facility. One tephra layer (1 Thol. 2 Ash) was identified to further constrain the Younger Dryas period. This is a constituent of North Atlantic Ash Zone 1 (Kvamme *et al.,* 1989) and provides a useful chronostratigraphic marker within an interval of significant radiocarbon dating uncertainty (e.g. Austin *et al.*, 1995). Five ^{14}C ages were calibrated into calendar ages using the Calib 4.2 programme (Stuiver and Reimer, 1993; Stuiver *et al.*, 1998) which incorporates a 400 year correction for the modern surface ocean reservoir effect at this latitude. This calibration of ^{14}C ages was only applied to radiocarbon dates younger than 21,000 ^{14}C years; the calibration data set available beyond this age is limited and has significantly decreased reliability. The nine remaining ^{14}C dates were calibrated using the U/Th ages and second-order polynomial equation of Bard *et al.* (1998) which statistically extends the current

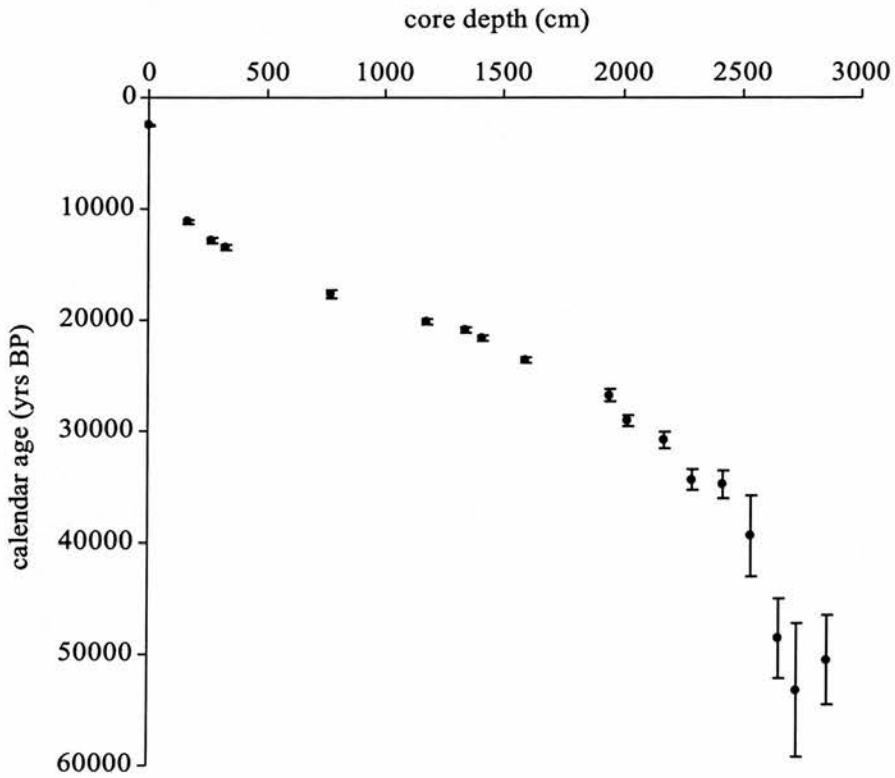

Figure 4.3. Age-depth model of core MD95-2006 modified from Chapter 3, Figure 3.3.

coral calibration set of Stuiver *et* al. (1998). Full chronostratigraphic details of this record are included in Chapter 3.

4.3.iii Stable isotopes

The $\delta^{18}O$ stratigraphy of core MD95-2006 is presented in Figure 4.4. A marked decrease in $\delta^{18}O$, with a mid-point at about 52 ka BP is interpreted to represent the MIS 4/3 transition. This transition is also characterised by a prominent minimum in $\delta^{13}C$ (Wilson, unpublished data, Appendix A). The early part of MIS 3 is characterised by a series of cycles in $\delta^{18}O$, corresponding to marked changes in planktonic foraminiferal assemblage composition. The transition to MIS 2 is not prominent in the $\delta^{18}O$ record at this site, but can be defined from other proxies, such as the increase in IRD at about 30 ka BP (section 3.4). Planktonic foraminiferal $\delta^{18}O$ reach their most positive values within the latter part of MIS2, between 20.5-17.5 ka BP, which is consistent with other North Atlantic records (e.g. V29-204, Curry *et al.*, 1999). The first in a series of marked shifts towards lighter $\delta^{18}O$ occur shortly after 17 ka BP and herald the onset of Termination 1. The deglacial $\delta^{18}O$ record of MD95-2006 agrees well with previously published records postdating 15 ka BP from this margin (e.g. Kroon *et al.*, 1997; Austin and Kroon, 2001). Whilst the MIS stage boundaries are not used as control points in the age-depth model of core MD95-2006, they do provide a valuable check on the calendar ages derived from the corrected and calibrated AMS ^{14}C dating.

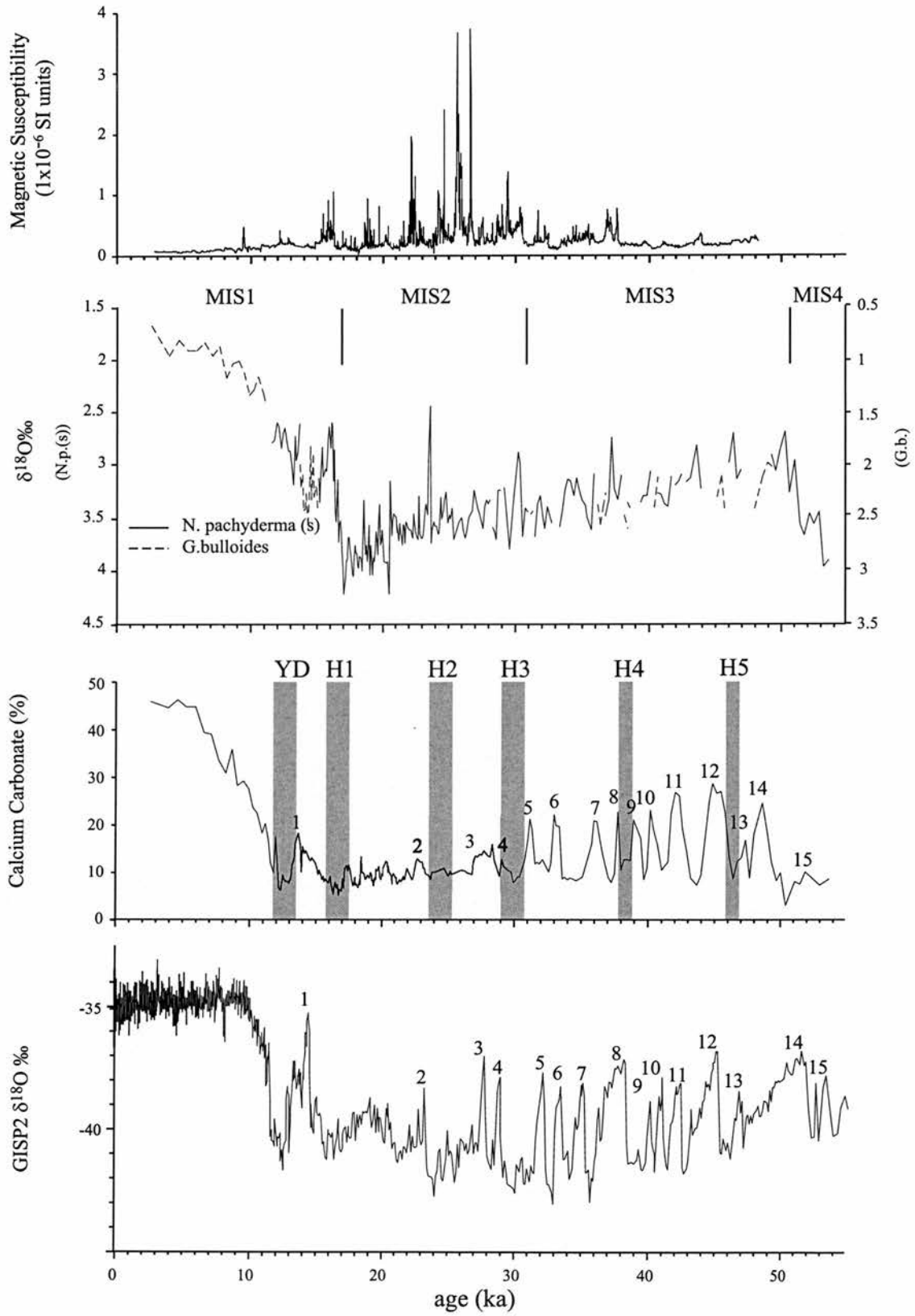

Figure 4.4. Summary figures of magnetic susceptibility, calcium carbonate content and uncorrected planktonic foraminiferal $\delta^{18}O$ from core MD95-2006 with Greenland Ice Sheet Project (GISP2) ice core $\delta^{18}O$ (Grootes *et al.*, 1993). Interstadials are numbered after Dansgaard *et al.* (1993). Shading represents the Heinrich Events as defined by Bond *et al.* (1999). MIS1-4 are indicated, after Martinson *et al.* (1997). Ages for MD95-2006 are calibrated (ka BP).

4.4 Discussion

Despite recent speculation on BIS variability through the last glacial period (e.g. Bowen *et al.*, 2002), there remains considerable uncertainty regarding the dynamics of the last ice sheet prior to the last glacial maximum (Clapperton, 1997). The offshore record of core MD95-2006 provides an opportunity to investigate the distal sedimentological response of glacimarine processes at this margin over the last 55,000 years. The lithostratigraphy of core MD95-2006 has been published previously by Kroon *et al.* (2000) and Knutz *et al.* (2001). These investigations demonstrate the significance of the IRD signature, interpreted from clast counts, magnetic susceptibility and spectrophotometry, and highlight the dynamic nature of the last BIS. Here, the growth, maximum extent and deglaciation of the BIS are discussed within the context of a complete planktonic foraminiferal $\delta^{18}O$ record.

In general, $\delta^{18}O$ exhibits an overall cooling trend through MIS 3, from an initial warm phase above the MIS 4/3 transition (Figure 4.4). However, because of major planktonic foraminiferal assemblage changes, the $\delta^{18}O$ signal alternates between two species, *Neogloboquadrina pachyderma* (sinistral) and *Globoquadrina bulloides*. These assemblage changes reflect surface watermass transitions above the core site, comparable to those described for the last deglaciation (Kroon *et al.*, 1997). Ten well-defined concentration peaks in calcium carbonate content are observed within MIS 3, with an average periodicity of 2000 years. These interstadial

events were assigned to Greenland interstadial events 5-14 (Dansgaard *et al.* 1993) in section 3.4.

Sediment accumulation rates are reduced during the MIS 3 interstadials because glacier retreat would have led to sediment entrapment on the continental shelf and shelf break. There is some evidence in the literature which suggests enhanced ventilation during the interstadials of MIS 3 (e.g. Curry *et al.*, 1999), which would also act to increase bottom current strength, reduce clay contents, and therefore increase relative carbonate content (see chapter 3 for further discussion).

The stadials of MIS 3 are characterised by clearly defined IRD events, which carry a BIS signal (Knutz *et al.*, 2001). This record, constrained by planktonic $\delta^{18}O$, illustrates the dynamic nature of the BIS within MIS 3. This stadial/interstadial pattern of IRD-rich/carbonate rich deposits demonstrates the nature of the North Atlantic 'Bond Cycle' (Bond *et al.*, 1993; Bond and Lotti, 1995). In addition, Heinrich Events H1 to H5 are identified at this site (Figure 4.4) and clearly correspond to low planktonic $\delta^{18}O$ values. These IRD events and low $\delta^{18}O$ excursions suggest significant meltwater influence.

A transition, at approximately 30 ka BP, from silty- muddy contourites to hemipelagite to muddy contourite sediments marks the transition from MIS 3 to MIS2 (Knutz *et al.*, 2001). The timing of the transition in MD95-2006 agrees with the age estimate from GISP2 and VM19-30 reported by Bond *et al.* (1997, 1999).

Interestingly, Bond *et al.* (1999) note a discontinuous record of Icelandic glass below 400 cm (about 32 ka) in core VM23-81, which they interpret as being outside ("downstream") the main Ruddiman IRD belt (Ruddiman, 1977). It is also likely that the quantity of IRD from the smaller NE Atlantic ice sheets (e.g. BIS, Iceland) was considerably less prior to regional ice sheet expansion after 30 ka BP.

Sejrup *et al.* (1994, 2000) identified the maximum Weichselian glaciation in the northern North Sea between 29.4 and 22 ka BP. Bowen *et al.* (2002) follow the recommendation of the EPILOG project, which defines the LGM between 19 and 23 ka BP. The precise timing of the LGM is difficult to define in core MD95-2006. At this location the advance of the last BIS ice margin can be seen approaching the shelf break at 30ka. Delivery of IRD to the core site is greatly enhanced as the ice sheet reaches its maximum extent. The *N.pachyderma* (sin.) $\delta^{18}O$ show maxima (cold, polar water) between 21-17 ka BP.

At its maximum extent, lying on deformable sediments, the last BIS had the potential to respond rapidly to both internal and external forcing mechanisms. Factors such as sea level rise, coupled with glacier dynamics, would have generated a very unstable response at the ice margin. This instability is convincingly illustrated by two major MIS 2 IRD events (Figure 4.4), which coincide with pronounced $\delta^{18}O$ minima (H2 at 24 ka BP; H1 at 16.5 ka BP).

Deglaciation, following H1, is rapid, but is punctuated by a clear return to polar conditions, before the incursion of North Atlantic Current waters at 15 ka BP. After this time, surface waters warm rapidly and our records are generally consistent with those of Kroon *et al.* (1997) which describe the Lateglacial period in greater detail. A final, minor phase of ice rafting is resolved during the Younger Dryas stadial, but this is unlikely to derive from the BIS, which at this time is believed to have been restricted to the mountain valleys of NW Scotland (Benn, 1997).

4.5 Summary and Conclusions

The records obtained from MD95-2006 reveal how ice sheet extent influences sediment delivery rates across the shelf-slope break. The response of the BIS across the MIS 3-2 transition is clearly defined in a large number of sedimentological proxies and illustrates the highly responsive nature of this ice sheet to external climate forcing and climate cooling at about 30 ka BP. Major ice rafting events indicative of Scottish IRD provenance, coincident with the North Atlantic Heinrich Events, are clearly defined in this record and are synchronized with low $\delta^{18}O$ events. The LGM is not clearly resolved, but can be inferred from $\delta^{18}O$ maxima between 21-17 ka BP. Deglaciation of the margin is largely achieved through H1, but climate remains cold until about 15 ka BP, when a transition from polar to North Atlantic Current assemblages is identified.

Chapter 5.

"The last Deglaciation of the Hebridean Continental Shelf, N.W. Scotland"

5.1 Background

The EPILOG (Environmental Processes of the Ice age: Land, Oceans, Glaciers) Project proposed that the Last Glacial Maximum (LGM) took place between 19 and 23 cal ka (Mix *et al.*, 2001). The date for the LGM has been continually discussed and challenged, particularly in view of the increasing evidence of spatial and temporal differences for the growth and retreat of the last major ice sheets around the globe. The last British Ice Sheet (BIS) was particularly dynamic in this region during the Late Devensian (e.g. Austin and Kroon, 1996; Knutz *et al.*, 2001). Bowen *et al.* (2002) suggest the BIS LGM event took place ~22 cal ka. However, the exact chronology and ice sheet dimensions during the last glaciation, and perhaps to a lesser extent the subsequent, relatively rapid, deglaciation, remains open to debate. The timing of deglaciation at the regional scale is particularly critical in determining the decay characteristics of the smaller ice sheets.

5.1.i The last deglacial period

5.1.i.a Global deglaciation

Fairbanks's (1989) Barbados coral sea level curve indicated that sea level did not increase smoothly through the deglacial period. During the LGM sea level was about 121 ±5 m below present (Peltier, 2002; Lambeck *et al.*, 2002). However, the deglacial sea level rise operated with a step-wise rhythm. The fluctuations in meltwater discharge into the northeast Atlantic led to alterations in NADW production (see section 1.1.ii). A 'fast-slow-fast' pattern took place with two periods of rapid sea level rise; the first increase immediately prior to 14 ka (Th/U or calendar) yrs ago and a second after 12 ka. Northern hemisphere ice sheet decay was probably rapid during the two main "meltwater events"; meltwater pulse 1A (mwp-1A) (12 ^{14}C ka BP, i.e. before ca. 13.7 cal ka BP and younger than ca. 14.2 cal ka BP) and meltwater pulse 1B (mwp-1B) (9.5 ^{14}C ka BP) (Fairbanks, 1989; Bard *et al.*, 1990a, 1990b). At these times surface water salinities in the northeast Atlantic were lowered. The timing of mwp-1A remains debatable (Clark and Mix, 2002). These events are also recognized in the Greenland ice cores as minima within the δ^{18}O record.

The rate of sea level rise slowed between 14 and 12 ka BP before the final major melt phase in the early Holocene. This latter 'lull' in ice sheet melt is

coincident with the Younger Dryas oscillation in the North Atlantic and Europe, when temperatures returned to almost full glacial conditions.

Changes in relative sea level, in part, reflect the fluctuating, growth and decay, behaviour of ice sheets (Lambeck *et al.*, 2002). They vary spatially and temporally and are dependent on interactions between the ocean-ice system and the terrestrial environment. Therefore, observations of sea-level change cannot be directly related to ice volume, particularly in formerly glaciated regions. Glacio-hydro-isostasy models enable the essential corrections to be made and these models depend on reliable ice sheet reconstructions.

5.1.i.b Regional deglaciation

The last deglaciation was an episode of extremely variable climatic and oceanographic fluctuations in the NE Atlantic (Austin and Kroon, 2001). Lambeck (1995a) produced isostatic models from theoretical isobases to predict the temporal and spatial variations of sea-level, and thus ice sheet limits, through the last deglacial period. The Lateglacial model predictions were then compared to observations. Crustal rebound in the north of the British Isles and meltwater release into the global ocean were largely responsible for the observed changes. Additional rebound from the Fennoscandian and N. American ice sheets also influenced the British sea-level record, although to a lesser extent. The BIS differed from the major ice sheets in terms of its unloading history. For example, in the Irish and Celtic Seas a land bridge was predicted to have formed from 20-13 ^{14}C ka BP. Scottish ice is

believed to have extended across the northern Irish Sea until 14 ^{14}C ka BP. There is some disagreement between the models and observations, most notably in the north of Scotland and Ireland where ice sheets may have been thicker than those assumed in the Lambeck model (Ballantyne *et al.*, 1998).

Marine cores from the Nordic Sea indicate that ice receded from the Norwegian Shelf by approximately 15,000 yrs BP (Rochon *et al.*, 1998). On the Iceland Plateau warming took place from 16 ^{14}C ka BP and evidence from the Faeroe area shows a deglacial signal from 15.5 – 15.1 ^{14}C ka BP (Lassen *et al.*, 2002). The marine-based margins of the Barents Sea and Fennoscandian Ice sheets began retreating around 14.7 to 15 ^{14}C kyr BP from their maximum position, which had probably been maintained since the LGM (McCabe and Clark, 1998).

It appears, from much of the available information, that initial deglaciation of the major northern hemisphere ice sheets therefore took place approximately synchronously from ca. 15 ka ^{14}C BP (Zaragosi *et al.*, 2001; McCabe and Clark, 1998). However, this is still open to debate, and the question of whether ice sheet margins were synchronous in their initial deglaciation remains controversial.

The fluctuations in meltwater discharge into the North Atlantic surface ocean lead to variations in the production of North Atlantic Deep Water (NADW) and changes in oxygen isotope chemistry recorded in marine biogenic carbonates

(Fairbanks, 1989). The Barbados corals indicated that the last deglaciation was accelerated at ~15 ^{14}C ka BP, correlating with deep-sea core δ^{18}O records (Duplessy *et al.*, 1986; Broecker *et al.*, 1988). North Atlantic foraminiferal and diatom records of sea surface temperature also record the two-step deglacial process seen in δ^{18}O records (Bard *et al.*, 1994; 1987). Bard *et al.* (1987) observed that by 13 ^{14}C ka BP or a little later, the oceanic polar front lay to the north of the British Isles resulting in more temperate climatic conditions. This was followed by cooler conditions during the Younger Dryas when the oceanic polar front again extended southwards to the Portuguese margin.

5.1.ii The last British Ice Sheet

During the Middle and Late Pleistocene, Scotland and the surrounding offshore regions were originally thought to have been glaciated during four or five separate events, the most recent of these being the Devensian (Sutherland, 1991). The last British Ice Sheet may well have been a sensitive indicator of palaeoclimate change due to its proximity towards the western limits of the last glaciation of NW Europe (Boulton, 1990). The Late Devensian (26-10ka BP) incorporated two distinct periods of glaciation in Scotland; the so-called *Dimlington Stadial* and the Loch Lomond Stadial (Younger Dryas). The final significant phase of growth and decay of the last BIS took place within the first of these divisions. During this period a number of major upland ice centres expanded on the high ground of western Grampian, Northern Highland, Lake District, Snowdonia and southern Wales.

Smaller, minor ice caps formed over lowland areas, including the Cairngorms and the southeast Grampians and the Pennines (Sutherland, 1991).

Patterns of glacial erosion and deposition have been mapped to determine the generally westerly to northwesterly pattern of ice-sheet movement on the northwest coast of Scotland (Ballantyne, 1990). Periglacial trimline evidence has defined the upper limits of the LGM mainland ice sheet in North West Scotland (Ballantyne, 1990). Evidence is also present for minor readvances of the ice sheet, e.g. in South West Scotland a readvance took place at ~13 ka BP (Sutherland, 1991). This final, Younger Dryas, ice readvance was, however, limited to the mountain valleys of NW Scotland (Benn *et al.*, 1992; Benn, 1997).

The chronology of the deglacial period implies that retreat of the last ice sheet took place under cold climatic conditions, indicated by the presence of polar waters surrounding the British Isles (Ruddiman and McIntyre, 1981; McCabe and Clark, 1998). The BIS does therefore seem to be an extremely sensitive indicator of climate change due to its maritime position towards the southern limit of the last glaciation of NW Europe (Knutz *et al.*, 2001).

The previously weak geochronological control for the LGM and subsequent events have recently been revised by Bowen *et al.* (2002). It was previously thought, from the last interglacial through to the Late Devensian, that Britain and Ireland remained ice free (Mitchell *et al.*, 1973). The BIS was also thought to have been

relatively static through this latter period. However, the ice sheet was sensitive and mobile, fluctuating several times at its north west margins (Selby, 1989; Kroon *et al.*, 1997; Knutz *et al.*, 2001). Cosmogenic nuclide surface-exposure dating, aminostratigraphy, AMS radiocarbon dating and marine sediment core evidence have been combined to develop the chronological sequence suggested by Bowen *et al.* (2002). ^{36}Cl and ^{14}C data show that the British and Irish Ice Sheet (BIIS) reached its LGM position around 22 ka BP following Heinrich Event 2. At this time the BIIS and the Scandinavian Ice Sheets were not in contact and were probably out of phase, given their differences in size and location. An initial deglaciation pulse was recorded at 21.4 $\pm$1.3 ka BP, followed by a more extensive period of deglaciation around 17.4 $\pm$ 0.4 ka BP prior to Heinrich Event (HE) 1 (Bowen *et al.*, 2002). The ice sheet advanced during HE1, surging forwards although it did not reach the LGM limits (McCabe *et al.*, 1998). Terrestrial moraines indicate the readvance and rapid retreat of the ice sheet during this period. (Zaragosi *et al.*, 2001; Clapperton, 1997). The last British Ice Sheet therefore remained active during its retreat phase.

The Outer Hebrides and Faroe Islands were each glaciated by small ice caps independent from the mainland ice sheet (Davies *et al.*, 1984; Bowen *et al.*, 1986; Peacock, 1991). By contrast, the two ice caps centred over the Outer Hebrides were probably adjoined to the mainland ice sheet to the east. Glacial and glacimarine deposits on the neighbouring shelf provide further, minimal, evidence of ice sheet fluctuations. However, the extent of the northwest margins of the BIS on the continental shelf are particularly controversial (Stoker and Holmes, 1991).

The western continental shelf is generally smooth and flat-lying with a series of ridges or moraines defining the possible Late Devensian ice limit (Sutherland, 1991). High-resolution seismic profiles identified a submarine morainal bank (Selby, 1989, Stoker and Holmes, 1991; Peacock *et al.*, 1992) at the shelf edge west of the Outer Hebrides and south of St Kilda. The moraine indicates two phases of local glaciation of the North Hebrides and West Shetland shelf. The timing of these phases of glaciation remains uncertain; however, it is suggested that the older glacial event pre-dates the last BIS while the younger deposit *may* be indicative of the late Devensian ice sheet activity.

The lateral dimensions and offshore ice sheet limits remain uncertain for many areas of the British Isles (Boulton *et al.*, 1985, 1991; Lambeck, 1993a, 1993b, 1995a). Despite the fact that glacimarine deposits accumulated in offshore areas and provide a record of sedimentological change during the last deglacial period, defining exact ice limits remains problematic.

Recent work (Knutz *et al.*, 2002a) on the Rockall Trough indicates the sensitivity of the BIS to changes in thermohaline transport. A warming pulse denotes the earliest sign of deglaciation which led to a number of ice rafted debris (IRD) peaks. The resulting discharge of meltwater at 17,500 years BP can be linked to ice sheet collapse and a reduction in NADW ventilation. The comparatively small size of the BIS in relation to the LIS and SIS (Scandinavian Ice Sheet) means the

fluctuations of the BIS in the North East Atlantic respond relatively rapidly to thermohaline and polar front changes.

The rapid fluctuations of temperature and salinity during the Younger Dryas cold period may be indicative of changes in the water masses present at this latitude. Kroon *et al.* (1997) suggest that a warm water mass shifted north as far as 56°N on at least three occasions during the Younger Dryas, replacing the cooler, polar water mass. The rate of NADW production is closely linked to the presence of glacial or interglacial climatic conditions (Broecker *et al.*, 1988). A reduction in NADW, possibly due to the decreased transport of deep water from the Nordic Seas into the North Atlantic and an accompanying reduction in surface ocean salinity, is therefore associated with a glacial climate (Keigwin *et al.*, 1991; Lassen *et al.*, 2002). It has been suggested that a severe "shutdown" of the conveyor system triggered the Younger Dryas and resulted in the North Atlantic polar front reaching its southernmost limit since the LGM. Broecker *et al.* (1988) suggested that during the Younger Dryas (~11,000 yrs BP) NADW production was terminated when meltwater from the southern margin of the LIS was diverted from the Gulf of Mexico to the N. Atlantic (Broecker *et al.*, 1989).

Surface waters in the NE Atlantic are thought to have largely been affected by local iceberg melting (Kroon *et al.*, 1997). Austin and Kroon (2001) analysed marine sediment cores from the continental slope off NW Scotland and suggested that the formation of NADW strengthened in the *Bølling-Allerød* period. Regional SST and SSS fell following the global meltwater event (MWP-1A) (Fairbanks,

1989). At a time when global ice sheet decay stabilized, around 13 ^{14}C ka BP, Austin and Kroon (2001) suggest that maximum ocean ventilation was established at intermediate depths in the NE Atlantic. A fall in temperature (approximately 7°C) and salinity marked the onset of the Younger Dryas on the adjacent Barra Fan (Kroon *et al.*, 1997). Ventilation appears to have reduced rapidly and weakened significantly during the Younger Dryas cold phase, but benthic δ^{13}C values are not as low as they were during the LGM.

5.1.iii Continental shelf studies of the last deglacial period

Recent marine sediment studies have concentrated on continental slope sites due to their high sediment accumulation rates (Andrews *et al.*, 1996). As a result there have been few high-resolution studies focussing on the extremely dynamic continental shelf environment (Scourse and Austin, 2002).

One exception was the Hald and Vorren (1987) study of Norwegian continental shelf records, which radiocarbon dated Termination 1a and 1b. The warm conditions of Termination 1a, >14-13.5 kyr BP, were followed by a meltwater pulse near 13 kyr BP. Then, as temperatures increased, warm, saline Atlantic Water replaced the glacially influenced shelf water. Termination 1b therefore relates to the Holocene-Pleistocene boundary and ranges from 10.3 to 9.7 kyr BP in this region of northern Norway (Hald and Vorren, 1987). Conditions then remained relatively stable throughout the Holocene.

These shallow marine sites do provide potentially high resolution records of the last deglaciation. They enable analysis of the marine reservoir effect (e.g. Austin *et al.*, 1995; Eiriksson *et al.*, 2000) and provide sea-level index points for glacio-hydro-isostatic models (Lambeck, 1995a, 1996). Sedimentation rates are often greater than in the deep ocean records, providing an ideal sampling opportunity to compare land-ocean proxy records.

5.1.iv Previous work on the Scottish continental shelf

The island of St Kilda shows evidence of only limited local glaciation, however, seismic evidence does suggest that an ice margin reached the St Kilda Plateau during the late Quaternary (Sutherland *et al.*, 1984). The St Kilda Basin is a shallow depression up to 40 km in width and –160 m at its deepest, lying between a series of morainal banks to the west and an undulating rock platform to the east (Figure 5.1). It is enclosed to the south by the 10 m high, east-to-west aligned ridge of the Otter Bank.

BGS Seismostratigraphic evidence suggests the basin is probably infilled with Late Quaternary sedimentary successions which were deposited from suspension in a low-energy depositional environment (Selby 1989; Peacock *et al.*,

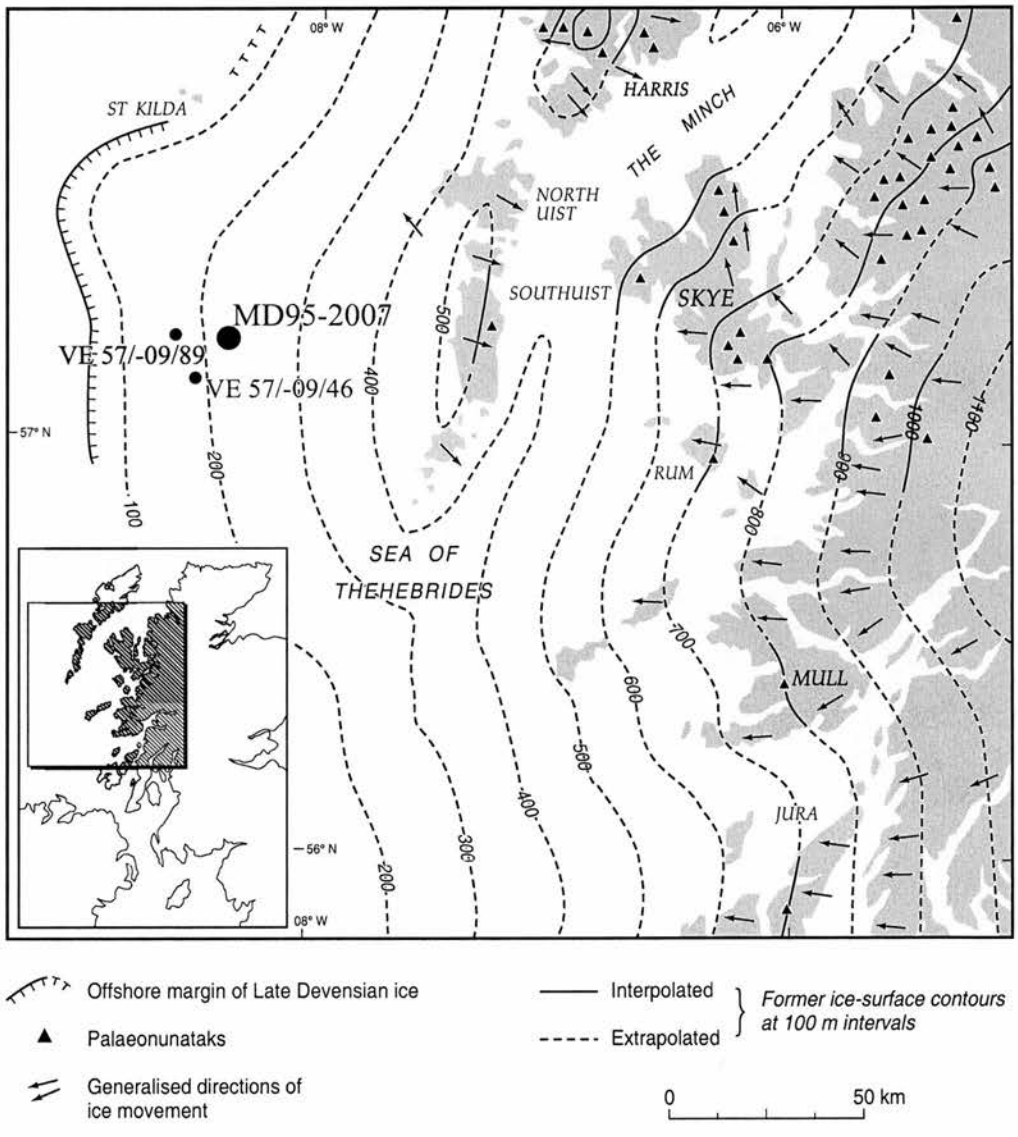

Figure 5.1. Location map of core MD95-2007, St Kilda Basin, NW Scotland. Vibrocores and are also shown. Reconstructed former ice surfaces are shown by the dashed lines. Reproduced with permission from C.K. Ballantyne.

(Ballantyne and Hallam, 2001)

1992). Previous work has shown that, approximately 60-80 km to the north of St Kilda, moraines are present near or at the shelf break. They are thought to pre-date the Late Devensian (Stoker, 1988). It has been suggested that the maximum extent of the Late Devensian grounded ice sheet was also marked on the continental shelf to the west of the St Kilda Basin by a series of morainal banks (Selby, 1989). This is further supported by the presence of an AMS ^{14}C dated marine bivalve, *Yoldiella lenticula* (AMS ^{14}C age = 22 480 $\pm$ 300 yr BP), in glacimarine sediment deposited west of the morainal banks. No such radiocarbon dates exceeding ca. 15 ka BP on *in situ* marine bivalves have been obtained to the east of the morainal banks (i.e. within the proposed Late Devensian maximum).

Austin (1991), Peacock *et al.* (1992) and Austin and Kroon (1996) provided faunal, stable isotope, lithological and sedimentary evidence for the timing of regional deglaciation from two BGS shallow marine cores recovered from the Hebridean shelf off NW Scotland. Core VE 57/-09/89 (57°30.11'N, 08°42.52'W, 155 m water depth) was recovered from the eastern margins of a morainal bank on the western edge of the St Kilda Basin, and core VE 57/-09/46 (57°19.30'N, 08°30.04'W, 156 m water depth) was from the in-filled St Kilda Basin. The two cores lie a short distance within the maximum position of the Late Devensian ice sheet. Peacock *et al.* (1992) state the basin became ice free *after* 17.6 cal ka BP (15.2 ^{14}C ka BP), however, this would not account for the deposition of the marine bivalve in Core VE 57/-09/89 from which the radiocarbon date was obtained. Hence deglaciation must have taken place *before* or close to 17.6 cal ka BP.

Shortly after 15.6 cal ka BP (13.5 ^{14}C ka), and before 14.7 cal ka BP (13 ^{14}C ka BP), a cold period of low salinity persisted. Higher energy, temperate climatic conditions then marked the interstadial warming of these shallow seas. The warmer conditions continued until a marked faunal cooling from 13 cal ka BP (11.6 ^{14}C ka BP) (Peacock *et al.*, 1992). Full Younger Dryas conditions were present from 12.5 cal ka BP (11 ^{14}C ka BP) until a warming at 11 cal ka BP (10.2 ^{14}C ka BP) before rapid warming and increased sedimentation rates mark the onset of the Holocene.

Reconstructed water depths for vibrocores VE57/-09/89 and VE 57/-09/46 (Peacock *et al.*, 1992; Lambeck *et al.*, 1995b) suggest water depths (Figure 5.2a) at approximately 13000 yr BP in the St Kilda Basin were shallower than the global average determined from the Barbados sea-level record (Fairbanks, 1989). In addition, predicted sea-level variations (Figure 5.2b) for the core sites do not indicate the rapid sea-level rise observed in the coral records (Peacock *et al.*, 1992; Lambeck *et al.*, 1995b).

Such data are potentially useful in event stratigraphy discussions and, with new results from IMAGES core MD95-2007, will allow the regional deglaciation of N.W. Scotland to be placed in a wider North Atlantic context. In particular, relatively few shelf sea records exist where the timing of regional deglaciation can be documented with confidence.

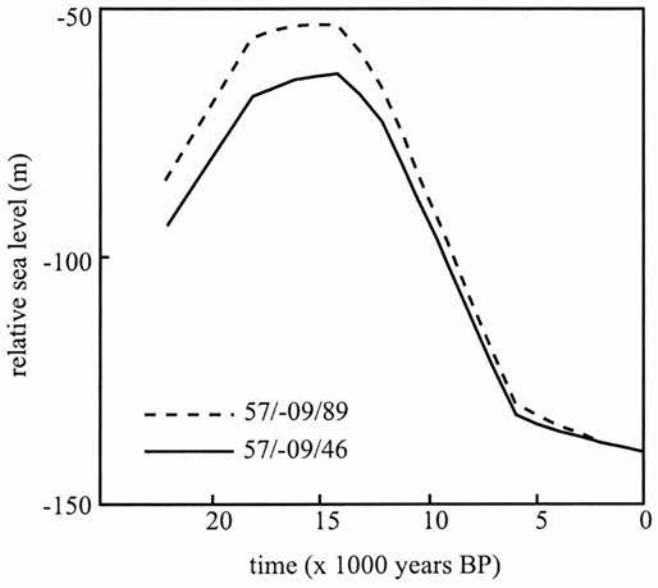

a

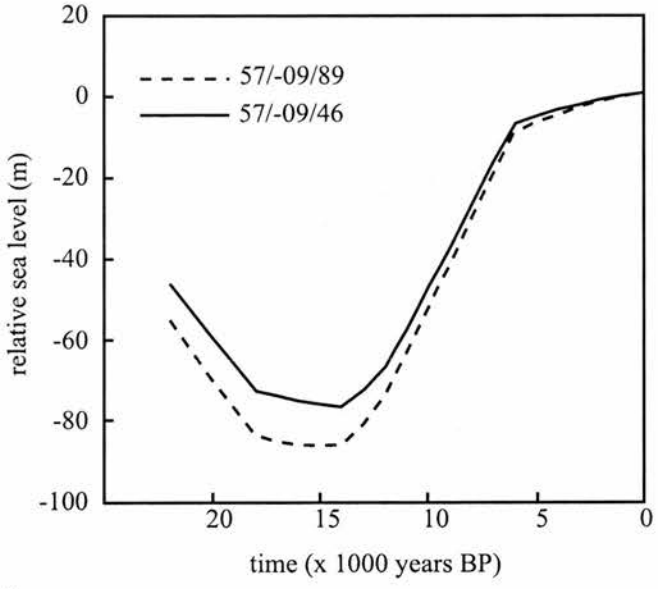

b

Figure 5.2. (a) Predicted water depths in the St Kilda Basin at two core locations (VE 57/-09/89 and 57/-09/46), from the end of the last glacial maximum at about 22 000 yr BP to the present.
(b) Predicted sea-level variations at the two locations, based on the glacio-hydro-isostatic model of rebound and eustacy (Lambeck, 1995b).

(Lambeck, 1995b, Figure 1, p83)

5.1.v Aims and Objectives

It is difficult to define a precise date for the thermal onset of the Lateglacial maximum within marine records. The chronology of the glaciation and deglaciation of the BIS are very poorly established for many sectors of the ice sheet. While it is beyond the scope of this chapter to reconstruct detailed paleoenvironments, the major lithological transitions of the Lateglacial period will be investigated. This chapter will therefore attempt to constrain the phase of glacial marine influence on one of the most sensitive maritime margins of the British Ice Sheet, the St Kilda Basin. In addition, it will aim to resolve the timing of regional deglaciation. The focus is therefore on setting the regional record into a wider, N. Atlantic Ocean context.

Synchronicity in North Atlantic climates during the Lateglacial period is now widely accepted (e.g. Björck *et al.*, 1998); this record offers the potential to investigate the impact of such changes at the land-ocean transition zone and will complement existing investigations from the adjacent continental slope (MD95-2006) (Chapters 3 and 4).

In previous work (Kroon *et al.*, 1997), variations in sea surface temperatures from the Barra Fan co-varied closely with the $\delta^{18}O$ records of GRIP and GISP2 (Johnsen *et al.*, 1992; Stuiver *et al.*, 1995). Analyses of the nearby vibrocores from the St Kilda Basin (Austin and Kroon, 1996) have illustrated the potential of

correlation with other records and the possibility of comparison between the MD95-2007 record and the Greenland ice cores is evaluated here. The regional pattern of deglaciation can therefore be set in the wider context of N. Atlantic climate change.

5.2 MD95-2007

Core MD95-2007 forms the basis of a detailed study of the Lateglacial sediment stratigraphy from the Hebridean Shelf, N.W. Scotland (Figure 5.1). The semi-enclosed St Kilda Basin was formed by the activity of the advancing last glacial ice sheet across the middle shelf (Selby, 1989). At this point the continental shelf break is located at a water depth of approximately 300 m. The eroded glacial overdeepening of the St Kilda Basin provided a depositional centre from which nearly 20 m of Lateglacial sediment have been recovered.

IMAGES (International Marine Global Change Study) core MD95-2007 was recovered from a water depth of 158 m from the St Kilda Basin, NW Scotland (57°31.057'N, 08°23.171'W). The core, 19.35 m in length, consists of soft, dark brown fine sand-silt-clay-rich muds with occasional clasts, most notably at the base of the core. A single, large clast was reported from the core-catcher at the time of core recovery (W. Austin, pers. comm). Initial range-finder AMS ^{14}C dating of the core confirms a highly expanded Lateglacial sediment sequence with average sedimentation rates of 506 cm/kyr. MD95-2007 is therefore one of the most highly expanded Lateglacial sedimentary sequences ever recovered from a continental shelf setting.

5.3 Methodology

5.3.i Lightness

Reflectance measurements were obtained every 2-5 cm along core MD95-2007 using a hand-held Minolta CM-2002 spectrophotometer. The calibration and measurement procedure was based upon the Ocean Drilling Program's methodology (Blum, 1997). The measurements were taken through polyethylene film on a single track along the centre of the core. L* indicates lightness ($\simeq$ greyscale reflectance) on a scale from zero (black) to one hundred (white).

5.3.ii Particle Size Measurements

The particle size distribution of the fine material (<400 μm) from core MD95-2007 were measured on a Coulter LS 230 Particle Size Machine (PSM). To obtain the non-carbonate, lithogenic components the biogenic carbonate was removed from the sub-samples through dissolution. The 'wet' sediment (approximately 0.55-0.60 g) was placed in a test tube with distilled water and then centrifuged, before excess fluid was decanted.

A 20% solution of acetic acid was added to decalcify the samples. The residues were then centrifuged and the excess solution was removed and distilled water added. This procedure was repeated twice before a fixed volume of sodium

hexametaphosphate was added to the sample. This solution was then transferred to the PSM and the grain size distributions recorded.

5.3.iii Molluscan Radiocarbon Measurements

Sixteen mollusc samples (Table 5.1) were extracted from the MD95-2007 >63 μm sediment fraction. The species of each sample was, where possible, identified by J. D. Peacock and processed by LJW at the NERC Radiocarbon laboratory at East Kilbride (Table 5.1). The molluscan samples included *Timoclea ovata, Portlandia arctica, Nuculana pernula, Jupiteria minuta* and *Abra alba* (Table 5.1). Where possible samples from known species were used, however, unknown fragments were used for three dates (AA-41754, AA-41762, AA-41763).

The samples were prepared to graphite at the NERC Radiocarbon Laboratory, East Kilbride, and ^{14}C analysis was undertaken at the University of Arizona NSF-AMS facility. The Accelerator Mass Spectrometer (AMS) ^{14}C dates were calibrated using the Calib 4.2 programme (Stuiver and Reimer, 1993; Stuiver *et al.*, 1998), which incorporates a global mean surface ocean reservoir effect of 400 years. The modern surface ocean reservoir correction at this latitude in the North Atlantic is most commonly quoted as 405 $\pm$ 40 years (Harkness, 1983), but significant changes in Lateglacial reservoir age are known from this latitude (Bard *et al.*, 1994; Austin *et al.*, 1995; Haflidason *et al.*, 1995). To simplify matters, a zero

Laboratory Number	Core depth (cm)	Conventional radiocarbon age (^{14}C yr. BP ±1σ)	Calendar age (years)	Species
VE 57/-09/89				
OxA-2780	55	5960 ± 80	6378	*Timoclea ovata*
OxA-2871	72.5	11040 ± 110	12779, 12754, 12634	*Nuculoma belloti*
OxA-2782	197	11440 ± 120	12977	*Parvicardium ovale*
OxA-2783	230	12030 ± 120	13468	*Nucula nucleus*
OxA-2784	252.5	13920 ± 140	16122	*Portlandia arctica*
OxA-2785	310	15650 ± 160	18113	*Portlandia arctica*
VE 57/-09/46				
OxA-2786	49	10380 ± 100	11326, 11236, 11205	*Acanthocardia echinata*
OxA-2787	117.5	10580 ± 100	11671	*Nuculoma belotti*
TO-3127	207.5	10610 ± 70	11869, 11690	*Nuculoma belotti*
TO-3128	231.5	10970 ± 70	12612, 12487, 12370	*Nuculoma tenuis*
OxA-2788	490	11420 ± 120	12966	*Nuculoma belotti*
TO-3126	566.5	11400 ± 70	12945	*Nuculana pernula*
MD95-2007				
AA-41753	21	2279±36	1879	*Timoclea ovata*
AA-41754	121	10664±65	11909, 11829, 11736	*Unknown fragments*
AA-41762	375.5	11353±62	12907	*Unknown*
AA-41755	396.5	11299±66	12890	*Portlandia arctica*
AAR-2602	425	11500±90	13000	*Portlandia arctica*
AA-41763	442.5	11296±77	12889	*Unknown*
AA-41756	556.5	11471±62	12990	*Nuculana*
AA-41757	741.5	12353±74	13832	*Nuculana pernula*
AAR-2603	826	12630±100	14109	*Nuculana pernula*
AAR-2604	974.5	12790±120	14289	*Nuculana pernula*
AA-41758	1008.5	12789±88	14289	*Jupiteria minuta*
AA-41759	1345.5	12953±74	14957, 14847, 14361	*Abra alba*
AAR-2605	1663	13810±170	15995	*Nuculana pernula*
AA-41760	1674	13020±110	15123, 14701, 14393	*Nuculana pernula*
AAR-2606	1815.5	14250±150	16502	*Portlandia arctica*
AA-41761	1821	13950±130	16157	*Portlandia arctica fragments*

Table 5.1. AMS ^{14}C ages for the St Kilda Basin cores VE 57/-09/89, VE 57/-09/46 and MD95-2007. The conventional radiocarbon ages were calibrated using the Calib4.2 programme (Stuiver and Reimer, 1993; Stuiver *et al.*, 1998).

deviation ($\Delta R = 0$) from the global mean surface ocean reservoir age has been employed throughout.

Two tephra layers (Vedde Ash and 1 Thol. 2) were identified. These distinct correlatable horizons act as time-parallel (isochronous) markers. They are particularly useful to test for any temporal or spatial variations in reservoir ages between different core locations.

5.3.iv Magnetic Susceptibility

Volumetric magnetic susceptibility was measured downcore on split core sections. Measurements were obtained at 5 cm intervals using a Bartington Instruments magnetic susceptibility meter (Model MS2) at the University of Edinburgh. The results are reported as 1×10^{-6} SI Units.

The water content was calculated in 5 cm increments from the >63μm residue samples. Results are presented as weight percentages.

5.3.v Tephra Analysis

A number of shards, from each tephra horizon (see section *5.4.iii*) and representative of each major morphological type, were handpicked from the dry residue (>150 μm) using a fine artist's brush (size 0000) under a Zeiss Stemi SV11

binocular microscope with a calibrated eye-piece graticule. The number of shards per gram of dry sediment was calculated.

The shards were mounted in Araldite™ fixative on glass slides and left to harden on a hot plate. The samples were ground down to thin sections (approximately 50 μm in thickness). The slides were vacuum coated with evaporated carbon and a graphite paint was applied to obtain a strong electrical contact. Geochemical analyses were carried out by H. Cawthorne and D. Herd on a JEOL JCXA733 electron microprobe at the University of St Andrews. This method enables the identification of individual tephra peaks through the geochemical analyses of a series of elements. The instrument operated at an accelerating potential of 20 kV and a probe current of 15 nA, with an exposure time of 50 seconds based on a 10 second counting interval per element.

5.4 Results

5.4.i Lithostratigraphy

Based on the particle size variations five lithological units are identified within core MD95-2007 (Figure 5.3). The sequence consists of soft, dark brown fine

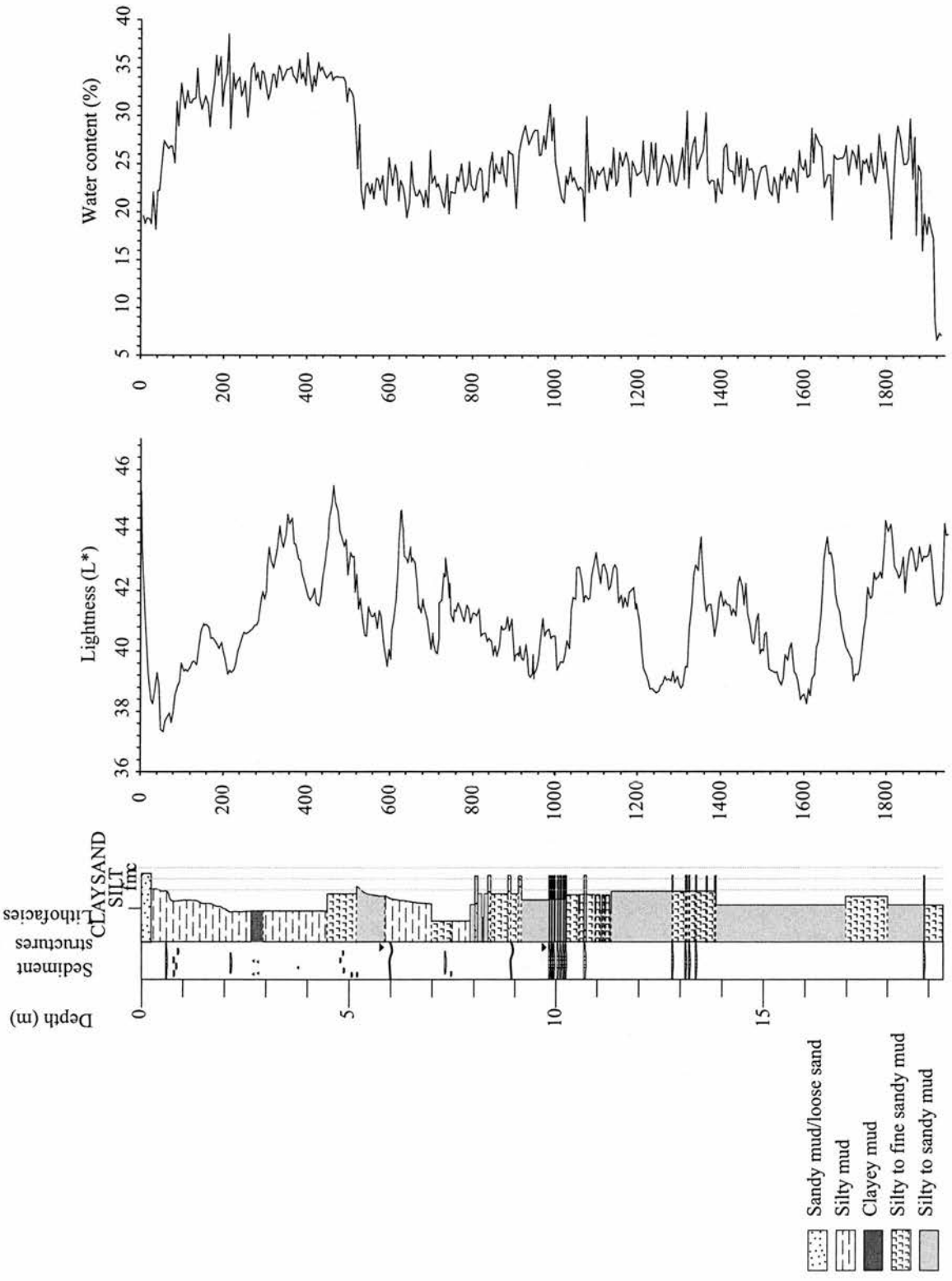

Figure 5.3. Lithological summary of core MD95-2007. Water content (%) and Lightness (L*) values are also shown.

sand-silt-clay-rich muds with occasional small clasts. A single sub-rounded, elongate clast >15cm long was observed at the base of the core. A series of fine to medium sand horizons were noted towards the middle of the core. The contacts are gradational between all sedimentary units with the most notable exception being the sand layers at a depth of approximately 10 m. Munsell colour chart observations vary from light olive brown (2.5 YR 5/3) to very dark olive grey (2.5 YR 3/3). The olive grey sediments are present between 5 to 9 m. The lightest coloured sediments are observed towards the core top.

Variations in water content (Figure 5.3) may reflect changes in core lithology. Water content values are relatively low (~6%) at the base of the core before switching rapidly to higher values at 18.56 m (~24%). Values remain relatively constant, fluctuating between ~16% to 26% prior to a slight increase in values at 10.00 m. Values increase rapidly at 5 m and remain high until a more gradual switch back towards lower values at 3.6 m.

Variations in the magnetic susceptibility (ms) signal (Figure 5.4) also indicate variations in lithofacies through the core. Ice rafted detritus can deliver lithic material of diverse mineralogy to the seabed over relatively short periods of time. Below 10 m the ms signal exhibits relatively high frequency, low amplitude variability, with the exception of the two pronounced peaks at 15.36 m and 10.71 m. The first occurs in silty to sandy muds while the latter peak coincides with a narrow sand layer. The ms values fall at 10.21 m before rising sharply again at 9.26 m. This

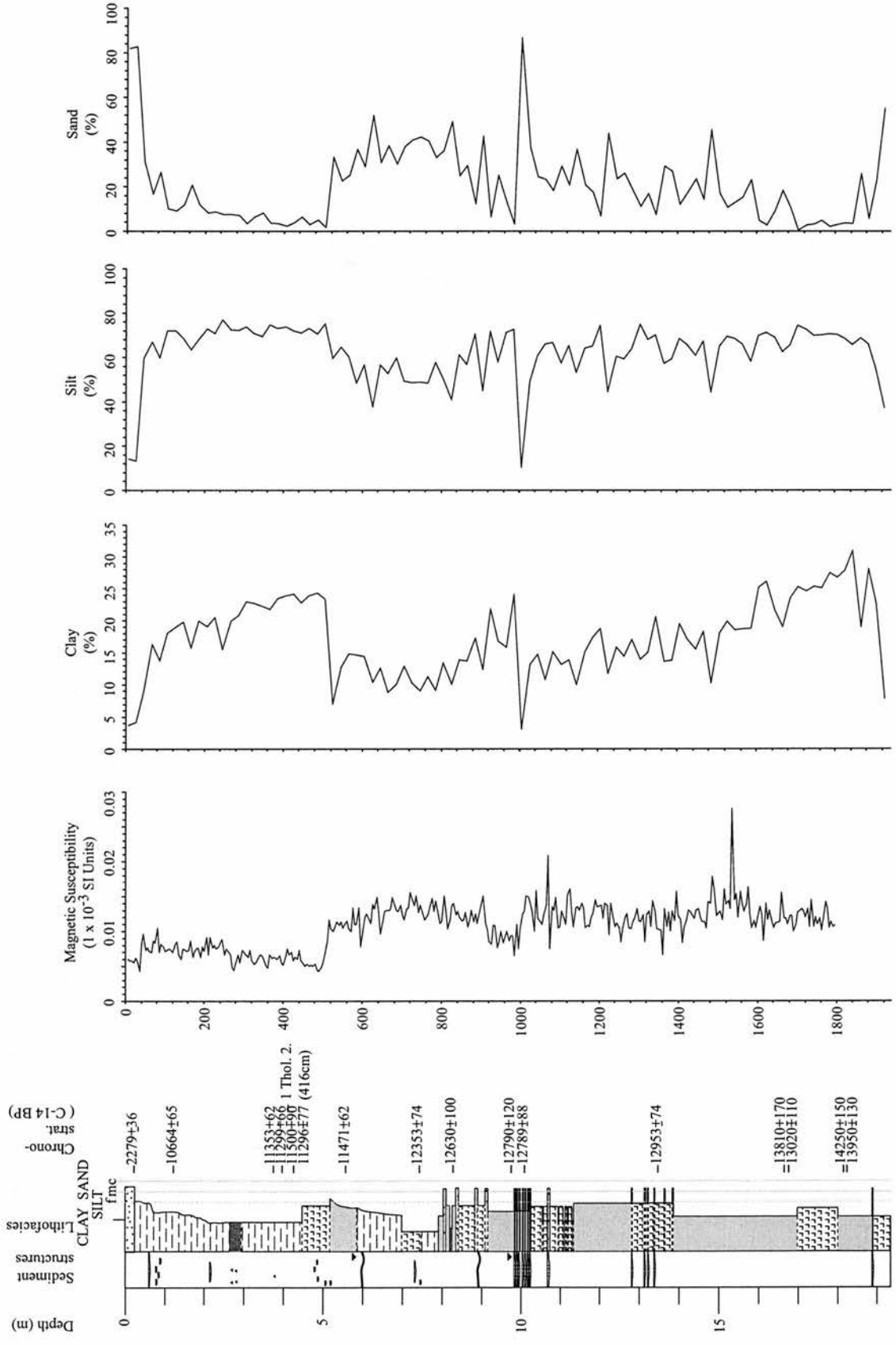

Figure 5.4. Lithostratigraphy with radiocarbon ages. Clay, silt and sand values are expressed as volume %.

rise coincides with a series of silty to fine sandy muds. Between 9.06 m and 5.16 m, ms events remain at relatively high values before falling rapidly at 5.16 m. Values remain low through a series of low amplitude cycles to 0.4 m, when they decrease briefly before a slight increase towards the core top.

Clay content varies between 3 and 30% through core MD95-2007 and despite the generally low clay values, large fluctuations are evident (Figure 5.4). At the base of the core a sharp increase in clay content to 30% is followed by a slow, steady decline to ~3% at 10 m. This sequence is repeated between 10 m and 5.2 m with a rapid rise in clay content at 5.2 m. Clay content remains relatively high until 0.8 m, followed by a marked decline to 3.5%.

Silt content (Figure 5.4) typically remains high with average values fluctuating between 40% and 80%. The lowest values are observed at the base of the core (40%), at 10 m (10%), and at the core top (12%). In addition, values between 10 m and 5.2 m show a gradual decrease to 7.4 m, followed by an equally gradual increase to 5.2 m. Values remain relatively stable at around 75 % between 5 m and 0.6 m.

Sand content fluctuates greatly throughout the core, varying between 2% and 88% (Figure 5.4). As clay and silt content increases at the base of the core, sand content decreases. A general trend of gradually increasing sand content is observed through to a marked peak at 10 m. This peak coincides with a series of sharply

defined sandy horizons. Above 10 m, sand content gradually increases to around 6 m and then decreases through to approximately 5 m, after which values remain low until a particularly marked increase at 0.6 m.

5.4.ii Lightness (L)*

The stratigraphic record of lightness (L*) from spectrophotometer measurements is presented in Figure 5.3. Values range from approximately 37.2 to 45.2 where the lower value indicates darker coloured sediments. Within this narrow range L* is highly variable. At the base of the core values are initially dark before switching briefly to slightly lighter values. A series of uneven cycles, between light and dark values (i.e. L* values between approximately 44 and 37), continues up core. Each of these 'cycles' contains minor high frequency, low amplitude fluctuations. From 10 m to 6.4 m L* values increase steadily through very low amplitude fluctuations, towards lighter coloured sediments. A rapid change to darker sediments is followed by a more gradual return to lighter material at approximately 6.1 m. From 4.6 m to 0.6 m values decrease, through high amplitude fluctuations, prior to a sharp return to light sediments at the core top.

5.4.iii Tephra

5.4.iii.a Identification of tephra horizons

In addition to the molluscan AMS ^{14}C dates, two tephra horizons (Vedde Ash and 1 Thol. 2) were identified to further constrain the chronostratigraphic framework

of the core. Ash layers, particularly primary ash-fall deposits, act as geologically instantaneous marker horizons within the marine and terrestrial record. They enable time-synchronous (isochrone) correlations between different locations and depositional settings (Haflidason *et al.*, 1995). These tephra layers are particularly useful during the last deglaciation and early Holocene as event markers during periods where radiocarbon dating is hindered by radiocarbon plateaux (see section 5.5.iii.a). However, the marine tephra stratigraphic record is regarded as problematic in some quarters (e.g. Bond *et al.*, 2001), with relatively few known tephra layers present within this last deglacial period.

Geochemical analyses of the clear, acidic shards, many exhibiting a 'winged' morphology, suggested they were representative of the Vedde Ash (Hunt *et al.*, 1995). The Vedde Ash is a component of North Atlantic Ash Zone 1. Two transport mechanisms were proposed for the shards; direct airfall at the core site or transportation by sea ice (Peacock *et al.*, 1992; Austin *et al.*, 1995). The shallow water of the continental shelf and large grain size of the basic tephra suggested deposition from drifting sea ice was the most plausible mechanism, although an airfall origin was not ruled out for shards <300 μm.

Figure 5.5a shows the number of shards/gram from the >63μm residue of core MD95-2007. Three tephra shard types have been identified; basaltic, pumice and rhyolitic. Tephra shards are present in core MD95-2007 between 0.65 m and 4.4 m. The basaltic tephra exhibit a rapid rise to a peak in concentration at 4.1 m, falling

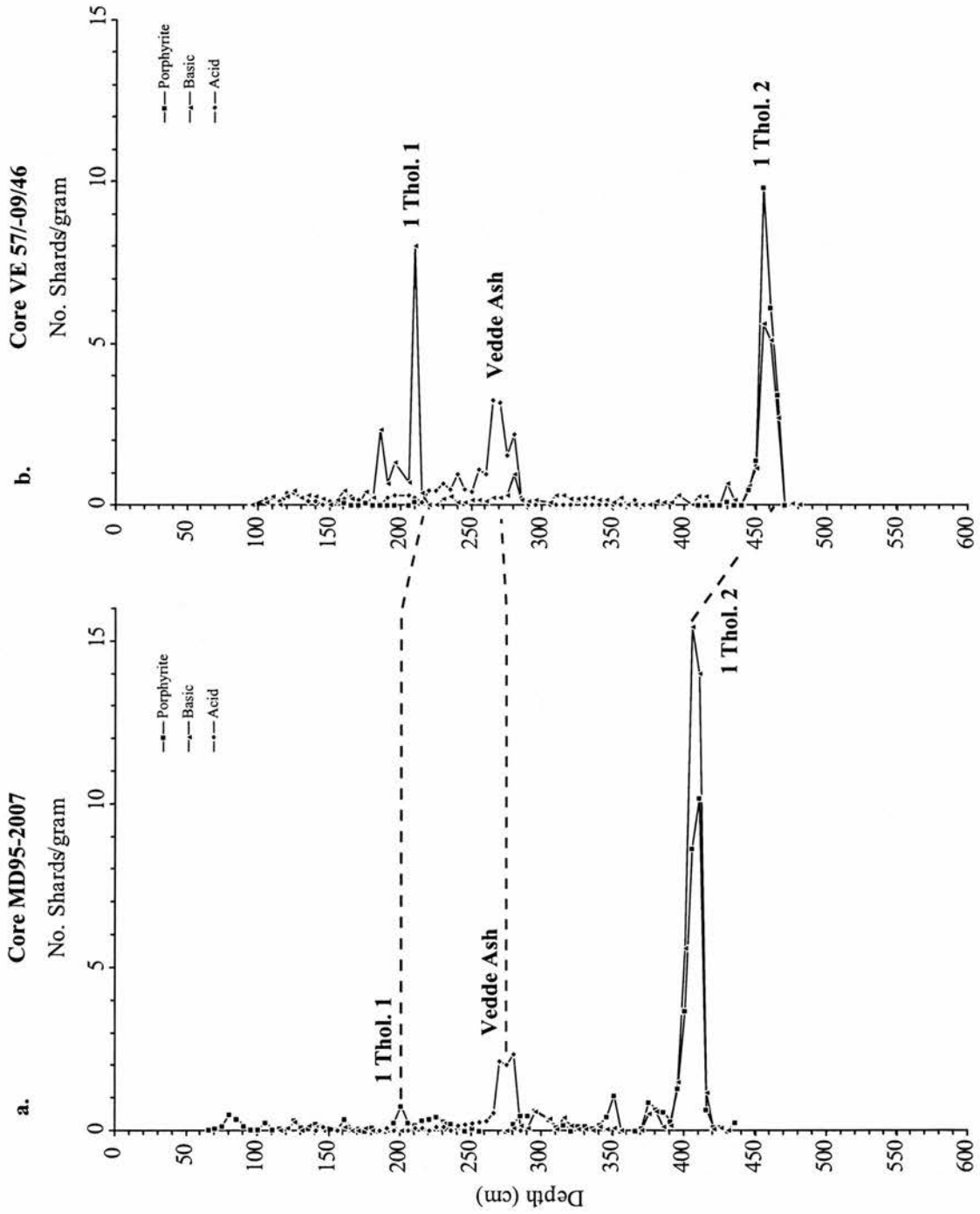

Figure 5.5. Tephra shard distribution for (a) core MD96-2007 and (b) core VE 57/-09/46 (Austin and Kroon, 1996).

away slowly to almost zero at 3.9 m. Concentration levels remain low, with a small peak of basalt and pumice shards at 3.8 m and two small basalt peaks at 3.5 m and 2.0 m. The pumice follows a similar pattern at the base of the core, with a major peak at 4.0 m which falls away rapidly by 3.9 m. The most prominent rhyolitic peak is present between 2.9 m and 2.5 m.

Low concentrations of Icelandic volcanic ash were previously identified in St Kilda vibrocore core VE 57/-09/46 (Austin *et al.*, 1995; Hunt *et al.*, 1995). The presence of these geochemically identified ash horizons enables correlations with core MD95-2007 (Figure 5.5b). Concentration counts for the Vedde Ash are fractionally lower in core MD95-2007, while basaltic counts relating to the 1 Thol. 2 horizon are slightly lower in VE 57/-09/46. The shard concentrations, particularly the ratio of basaltic glass to porphyritic grains within 1 Thol. 2, and their equivalent depths in both VE 57/-09/46 and MD95-2007 are remarkably similar. The basaltic tephra peak of 1 Thol. 1 is easily identified in VE 57/-09/46 compared to the minor basaltic peak in MD95-2007. This ash horizon has therefore not been used in the age-depth model.

5.4.iii.b Tephra geochronology

The rhyolitic tephra peak in North Atlantic marine cores (Ruddiman and Glover, 1972) correlates with the Vedde Ash in Ålesund, W. Norway identified in lacustrine sediments by Mangerud *et al.* (1984). Mangerud *et al.* (1984) assigned the

terrestrial ash deposit an age of 10,600. More recently Austin and Kroon (1996) assigned a ^{14}C age of 10,939 AMS ^{14}C BP to the marine deposited ash horizon, which is equivalent to a true calibrated age of 11,980 ka BP. This was based upon the identification of the Vedde Ash horizon in core 57/-09/46 which was recovered from the St Kilda Basin, approximately 23 km from core MD95-2007 (Austin and Kroon, 1996). It is important to remember that the ^{14}C dating of an ash eruption is not carried out directly on the tephra shards (e.g. Austin *et al.*, 1995) but on material, e.g. molluscan and/or foraminifera, present within the same stratigraphic level. For this reason, there will be an age uncertainty of unknown amount associated with the ^{14}C age of the tephra.

A second marker horizon is correlated to the 1 Thol. 2 Ash which is another constituent of North Atlantic Ash Zone 1 (Kvamme *et al.*, 1989). It is particularly useful in further constraining the Younger Dryas period, where dating uncertainty associated with the radiocarbon method is significant (Austin *et al.*, 1995). A calibrated age of 12,760 cal. BP (11,293 AMS ^{14}C) is assigned here to the 1 Thol. 2 ash layer in accordance with Kroon *et al.* (1997).

5.4.iv Chronostratigraphy

An age-depth model for core MD95-2007 is produced by utilising the two tephra horizons and the mollusc AMS ^{14}C ages. However, because of inverted age-depth relationships, it is not feasible to include all sixteen molluscan ages in the

model. It is possible that age differences may exist between samples from different species at the same core depth, and that different mollusc species may live at different depths below the sea floor sediment.

Therefore, where slight age reversals occur and samples were taken from approximately the same depth, averages were calculated for the corresponding ages. This approach was used for the dates from 1821 cm and 1815.5 cm, 1674 cm and 1663 cm and 1008.5 cm and 974.5cm. Between 442.5 cm and 375.5 cm a series of four different samples are present with approximately the same AMS ^{14}C age. This may reflect 1) a radiocarbon plateau or 2) a very rapid phase of sediment accumulation. Austin *et al.* (1995) discuss the presence of an increased marine ^{14}C reservoir age from the North Atlantic surface ocean during the Younger Dryas. 1 Thol. 2 lies within this series of dates. An average age is therefore taken incorporating the four molluscan ages. A step-wise linear age-depth model (Figure 5.6) is adopted with a linear sedimentation assumed between each date. By extending the linear regression line between the two oldest dates an age of 17,501 cal BP is obtained for the base of the core at 1935 cm. Unfortunately no molluscan samples were present at the top of the core to obtain a core top age. The nearby St Kilda Basin core 57/-09/89 indicates a Holocene date of approximately 6.3 cal ka BP (5,960 ^{14}C ka BP) at a depth of 0.5-0.6 m. The nearest surface age for core MD95-2007 is 1.9 cal ka BP (2,279 ^{14}C ka BP) at 0.21 m (Figure 5.6).

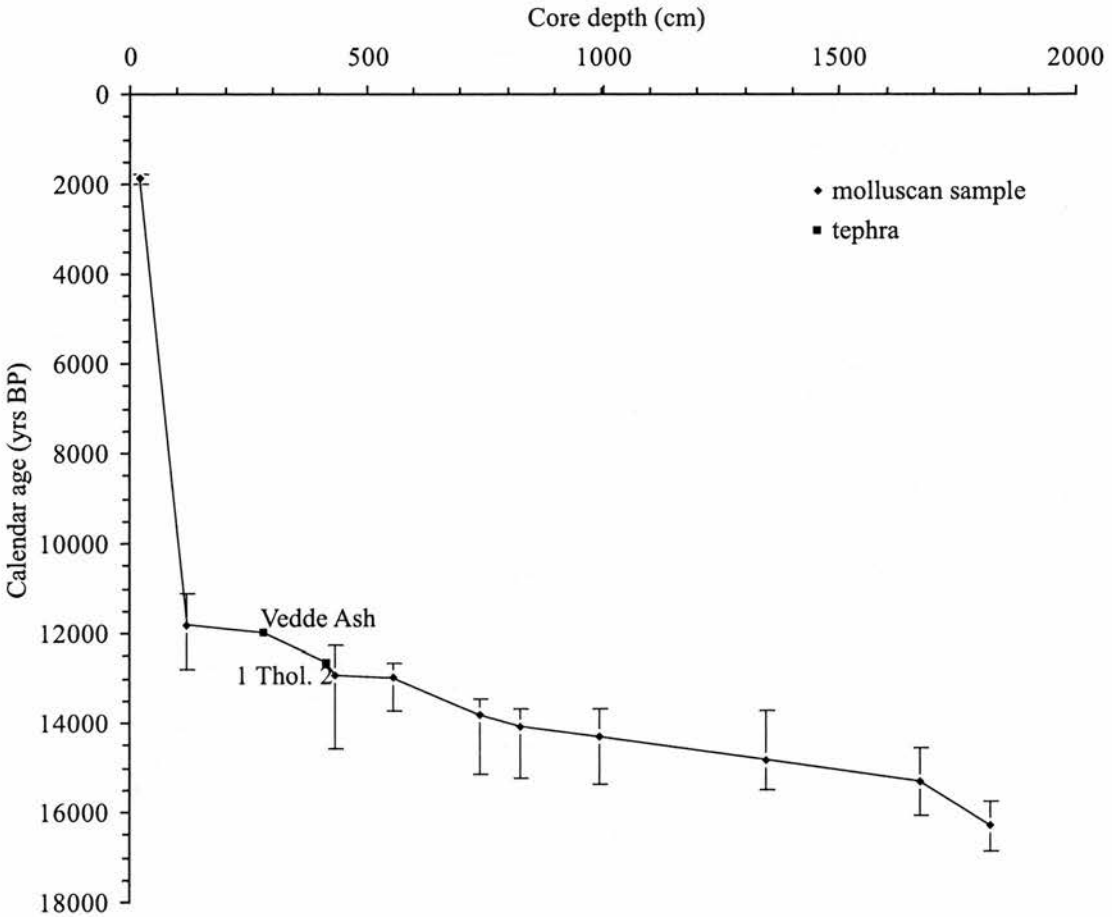

Figure 5.6. Age-depth model of core MD95-2007.

5.5 Discussion

5.5.i BIS limits and MD95-2007

The identification of palaeonunataks, in the form of periglacial trimlines, are used to infer Hebridean ice cap altitude and subsequently constrain ice sheet dimensions within this region during the last glacial maximum. The assumption that trimlines over this part of NW Scotland were cut by the last ice sheet while at its maximum thickness is supported by careful cosmogenic isotope dating (Ballantyne *et al.*, 1998). A single, high-level weathering limit exists at altitudes ranging from 425-450 m over much of the Outer Hebrides suggesting an independent ice cap. On the Scottish mainland contemporaneous, high-level weathering limits extend to above 1000 m (Ballantyne *et al.*, 1998). Despite this improved vertical resolution of the BIS LGM limits, the lateral limits, particularly in the offshore regions to the north and west of Scotland, are not well constrained.

In addition to the limited data available on both lateral and vertical limits, the chronology of the glaciation and deglaciation of the last BIS, particularly in the offshore regions, remains limited. Studies of the palaeoclimate record from the Barra Fan, to the west of the St Kilda Basin, have demonstrated the dynamic nature of the last BIS, particularly at its western extremity (Knutz *et al.*, 2002a; Chapter 4). The most recent evidence from the Barra Fan (section 4.4) suggests that the BIS

extended towards the outer continental shelf shortly after 30ka BP. An LGM date, between 21-17 ka BP, was observed from maxima in the *N. pachyderma* (s) $\delta^{18}O$ record. This concurs with the Bowen *et al.* (2002, 1996) report of the EPILOG BIS LGM date of ca. 22ka BP, ie. shortly after Heinrich Event 2.

Peacock *et al.* (1992) observed that vibrocores VE57/-09/46 and VE57/-09/89, from the St Kilda Basin, are located approximately 15-30 km inside the maximum position of the Late Devensian ice sheet limits. The St Kilda IMAGES MD95-2007 core, at approximately the same proximal site to the BIS as VE 57/-09/46, therefore also lies within the inferred limits of the LGM. It has the potential to provide a valuable record of the deglaciation of the St Kilda Basin and on the timing of deglaciation on this very sensitive maritime margin of the last BIS.

5.5.ii Timing and pattern of regional deglaciation

In the Nordic Seas initial deglaciation has been observed between 15 and 13 ^{14}C ka BP. Initial deglaciation of the LIS appears to have taken place earlier, sometime between ca. 17.2-17.6 cal kyr BP. It has previously been proposed that the various stages of collapse of the LIS initiated changes in the behaviour of the other ice sheets surrounding the North Atlantic, including the BIS. Bowen *et al.* (2002) document the initial pulse of deglaciation of the BIS at 21.4 $\pm$1.3 ka BP, followed by an extensive deglacial phase at ca. 17.4 $\pm$ 0.4 ka BP, just prior to an advance during HE1. Knutz *et al.* (2002a) identified two periods of ice sheet advance between 30

and 22 kyr, and 17-16 kyr, with the latter corresponding to HE1. The BIS readvance around 17-16 kyr also corresponds with the last readvance of the Irish Sea Margin (McCabe *et al.*, 1998).

McCabe and Clark (1998) constrain the age of the readvance of the BIS in the northern Irish Sea at ca. 16 cal kyr BP based on terrestrial evidence from the Irish Sea Basin (ISB) region. The ISB acted as one major conduit for the drainage of the BIS during the last deglaciation (Scourse *et al.*, 2000). The sequence of events in the ISB indicate that a widespread deglaciation of the southern margin of the BIS preceded the major readvance at 16 cal ka BP. Marine mud deposits record the initial widespread deglaciation of the southern parts of the ice sheet between ca. 19.3 and 17 cal ka BP (16.7 and 14.7 ^{14}C) kyr. The melting of the BIS was then initiated again ca. 13.8 ka ^{14}C BP (McCabe and Clark, 1998). The terrestrial records show that during H1, ice accumulated and advanced rapidly along the northern margins of the BIS. McCabe and Clark (1998) suggest that this readvance of the BIS resulted from the cooling of the North Atlantic due to the collapse of the LIS. However, the relatively thin ice sheet margin on the Hebridean shelf would have been equally highly sensitive to sea-level change as it would to climate forcing at this time.

Detailed AMS ^{14}C dating of marine mollusc shells suggest that the Hebridean Shelf core, MD95-2007, provides a continuous sediment record through the Lateglacial period. The highly expanded nature of the sedimentary record

provides the potential for analysing and constraining the complex regional pattern of deglaciation and subsequent palaeoenvironmental evolution.

5.5.iii Comparisons to the BGS vibrocores

Regional mapping programmes, conducted by the British Geological Survey, of the UK's continental shelf seas have provided an excellent opportunity to investigate the late Quaternary stratirgaphy of the Hebridean Shelf. The deglacial behaviour of the BIS has previously been demonstrated by the study of vibrocores VE 57/-09/89 and VE 57/-09/46 from the St Kilda Basin (e.g. Austin and Kroon, 1996). The main phase of deglaciation reportedly took place from 17.6 cal ka BP to 15.6 cal ka BP (Peacock *et al.*, 1992). This deglaciation is marked in core VE 57/-09/89 by a period of increased clay and silt input and very low sand content. The oldest date obtained from this core records this critical deglacial transition at ca. 17.6 cal ka BP (15.2 ^{14}C ka BP) which corresponds with a cold, low salinity period of glacial retreat inferred from sedimentology, faunal evidence and stable oxygen isotope stratigraphy.

The oldest dates obtained from core MD95-2007 (16.1 and 16.5 cal ka BP) are slightly younger than the transitional phase previously dated by Peacock *et al.* (1992). The deglacial transition in the St Kilda Basin core MD95-2007 also appears to be marked by an increase of fine silt and clay input into the basin. Based on

extrapolation from the age-depth model of the core, this transition corresponds to an age of ca. 16.8 cal ka BP.

Faunal and isotopic data from the BGS vibrocores support the argument that cold water persisted in the basin until approximately 15.6 cal ka BP (13.5 ^{14}C ka BP). At a corresponding age in MD95-2007 there is a lithological transition as sand content gradually increases in conjunction with a slight decrease in clay and silt content. This suggests a transition from a low energy, muddy environment to one with fewer fines and possibly increased bottom current strength. The dominance of the fine-grained silt and clay material prior to 15.6 cal ka BP may be indicative of a continued meltwater influence following the decrease in IRD content (Figure 5.7).

From 15.6 cal kyr BP a gradual decrease in fine material corresponds to the return of warmer conditions observed in vibrocore 57/-09/89. This lithology persists through to a marked input of silt and clay at ca. 14.2 cal ka BP.

The low silt and clay content from approximately 14.3 cal kyr BP marks a change in sedimentary facies which is coincident with the establishment of full interstadial conditions in MD95-2007. Lithological character during the interstadial fluctuates slightly, although the overall dominance of coarse-grained sand suggests a shallow marine environment of high depositional energy. The sediment accumulation rates fall through this interval, probably because high current velocities limit deposition. In vibrocore 57/-09/89 initial interstadial conditions of

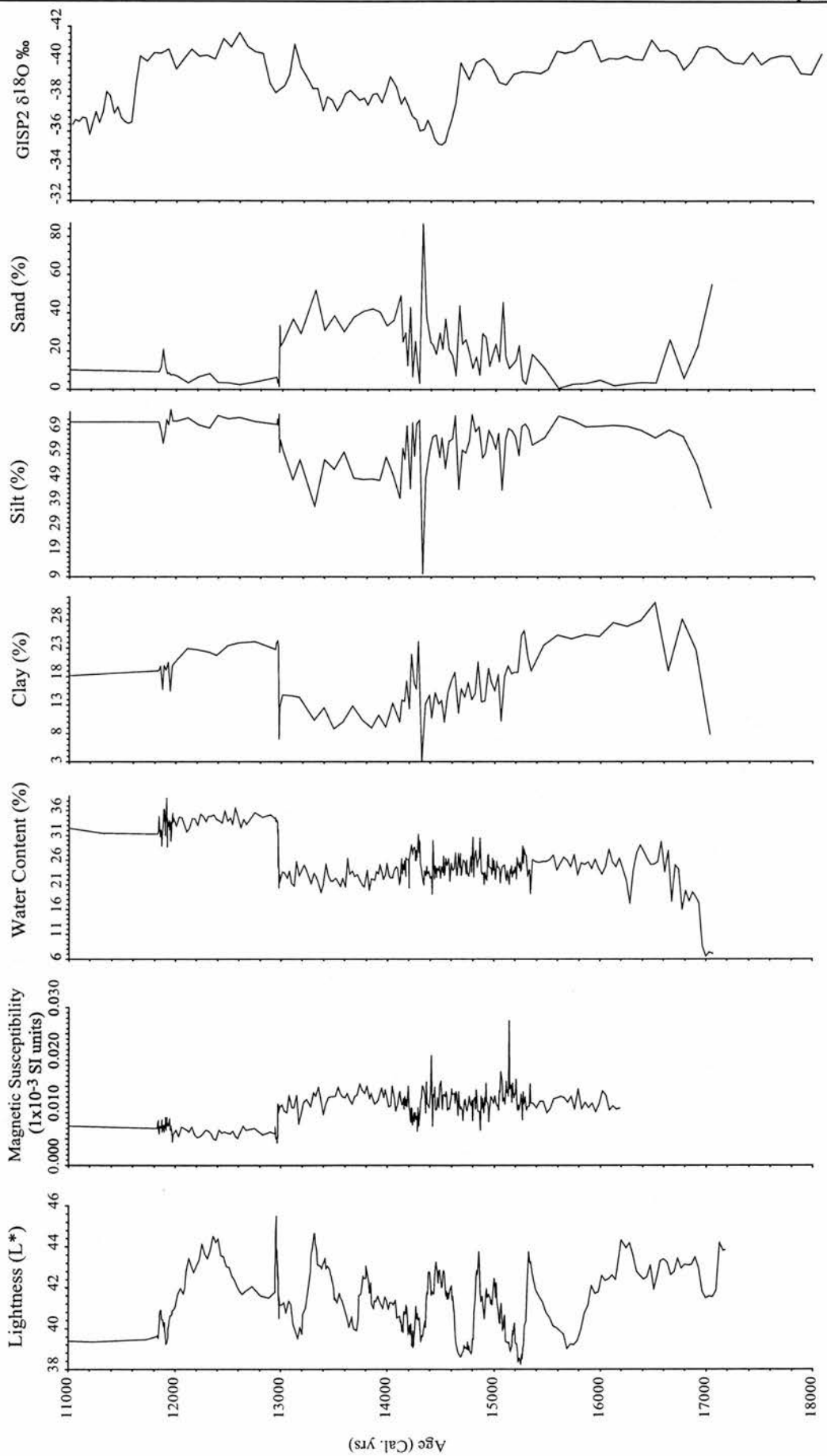

Figure 5.7. MD95-2006 stratigraphic summary and Greenland Ice Sheet Project (GISP2) ice core $\delta^{18}O$ (Grootes *et al.*, 1993).

climate amelioration are recorded between approximately 15.6 to 14.7 cal kyr BP (13.5 and 13 ^{14}C ka BP) (Austin and Kroon, 1996). The Barra Fan core VE 56/-10/36 indicates the final warming took place from 14 cal kyr BP (Kroon *et al.*, 1997). Core V23-81 (Ruddiman and McIntyre, 1981), to the west of Ireland, records full warm conditions by ca. 14.3 cal ka BP (12.9 ka ^{14}C BP); while further offshore Koç *et al.* (1996) propose a synchronous surface water warming for the North Atlantic of ca. 15.5 cal kyr BP (13.4 ka ^{14}C BP).

5.5.iv Problems associated with radiocarbon dating the Younger Dryas cold phase

In the marine sediment record of the Barra Fan, Kroon *et al.* (1997) observed a large decrease in SST prior to the onset of the Younger Dryas stadial. This possible precursor cooling would have marked a further period of ice rafting in the region. The MD95-2007 water content record indicates a lithological transition possibly marking the onset of the Younger Dryas cold phase at approximately 13 cal kyr BP. This corresponds to the same lithological (and faunal) transition observed in core VE 57/-09/89. The influx of coarse material into the St Kilda Basin remains low throughout this period. In comparison, the finer silt and clay material remains high probably because of the influence of iceberg melt during this period of climate deterioration. Throughout the YD cold phase, ice sheet readvance is restricted to valley glaciers on the Outer Hebrides and to the high mountain valleys of the Scottish mainland (Sutherland, 1984; Benn, 1997). However, the supply of sediments to the continental shelf, particularly fine sediments out in the St Kilda Basin, is likely to have increased dramatically as climates deteriorated.

Sediment accumulation rates are relatively high throughout the Younger Dryas period. However, the exact timing of the transitions associated with this phase are difficult to establish due to the limitations associated with the presence of Younger Dryas ^{14}C plateaux (Ammann and Lotter, 1989; Wohlfarth, 1996; Rochon *et al.*, 1998). The series of AMS ^{14}C dates obtained for core MD95-2007 are not in exact stratigraphic order. Five of the molluscan AMS radiocarbon dates (from 11,535± 62 to 11,471± 62 ^{14}C yr BP) fall within the stratigraphically accepted limits of the Younger Dryas period (e.g. Ruddiman and McIntyre, 1981; Peacock and Long, 1994). However, it is impossible to determine the precise start or end of this otherwise well-dated period because of the presence of the radiocarbon plateau. An average age and depth is therefore determined for these five dates for use in the age-depth model (Figure 5.6), but this must be treated with some caution.

These episodes of apparent near-constant radiocarbon ^{14}C age occur throughout the Last Glacial-Interglacial transition. They indicate periods when the atmospheric ^{14}C concentration increased, possibly due to reduced deep ocean ventilation (e.g. Hughen *et al.*, 1998). The large deviations in the ^{14}C chronology of the last glacial-interglacial transition explain why it is necessary to calibrate ^{14}C ages prior to age-depth modelling. If this is not done, large, artificial 'jumps' in sedimentation rate may appear. There are a number of these episodes within the Lateglacial and Holocene period, ranging in duration from a hundred to several hundred years. Kromer and Becker (1993) identified plateaux at 8,250, 8,750, 9,600

and 10,000 yr BP from chronological records from German oak and pine. Hughen *et al.* (1998) observed plateaux at 9.6, 11.4 and 11.7 ^{14}C ka BP in addition to the 'sloping' plateau between 10 and 10.4 ^{14}C ka BP. Ammann and Lotter (1989) observed two plateaux within annually varved lake sediments in Switzerland, at 12,700 yr BP and at 10,000 yr BP. The Younger Dryas-Holocene Transition falls within the latter of these plateaux, reducing the ^{14}C dating precision for the end of the Younger Dryas. In addition, the duration of the Younger Dryas and the events within this interval are difficult to resolve based on the current limited proxy data available from MD95-2007. Precise dating chronology can only be achieved through higher resolution sampling for AMS ^{14}C dating measurements.

Johnsen *et al.* (1992) estimate a duration of 1,150 calendar years for the Younger Dryas cold phase from the Greenland Summit ice core. These periods of rapidly changing ^{14}C age during the Lateglacial are not well resolved in some of the ^{14}C calibration data sets, particularly those which extend beyond the dendrochronology timescales. Tephrochronology, which provides important isochrones through this interval (Lowe and Walker, 2000) aids correlation between marine, ice and terrestrial records. The Vedde Ash (Bard *et al.*, 1994) is present within North Atlantic marine sediments and *may* coincide with the 10.4 -10.3 ^{14}C ka BP plateau (Ammann and Lotter, 1989; Hughen *et al.*, 1998). One of the two distinct tephra layers identified in MD95-2007 is identified as the Vedde Ash. This ash layer has also been identified in nearby core VE 57/-09/46. The ash layers therefore act as

chronostratigraphic markers within the record, excluding some, but not all, of the uncertainties associated with radiocarbon plateaux.

Further ^{14}C dating problems of marine materials arise because of the assumption that the 'apparent' age of the surface water, relative to the atmosphere, has remained constant over time (e.g. Waelbroeck *et al.*, 2001). However, the radiocarbon composition of the ocean does differ from that of the atmosphere and the apparent age (or 'reservoir' age) of surface ocean water reflects an exchange history between atmospheric CO_2 and the ocean. In the North Atlantic, a correction factor of 405 $\pm$ 40 yrs is generally applied to marine AMS ^{14}C ages to enable comparisons to terrestrial records (Harkness, 1983). The ^{14}C reservoir age of 300-400 $\pm$ 100 years at lower latitudes increases to 1200 years at the higher latitudes of the N. Pacific and Southern Ocean (Austin *et al.*, 1995; Reimer, 2003[5.1]). However, various authors (e.g. Bard *et al.*, 1994; Haflidason *et al.*, 1995) have reconstructed a marine reservoir age of ca. 800 years in the North Atlantic and the Norwegian Sea during the Younger Dryas. This is probably due to variations in ocean circulation and atmospheric ^{14}C production during the last deglacial period, i.e. the carbon reservoirs differed greatly from the modern day (Austin *et al.*, 1995). Specifically, changes in the rate and location of deep sea ventilation and sea-ice distribution led to varying ^{14}C distributions (Austin *et al.*, 1995). Waelbroeck *et al.* (2001) reconstructed the apparent surface water ages for the deglacial North Atlantic of 1,180$\pm$630 to 1,880$\pm$750 years at the end of Heinrich 1 (*ca.* 14,500 yrs BP) and by

[5.1] http://www.qub.ac.uk/arcpal/marine

930±250 to 1,050±230 towards the end of the Younger Dryas. Austin *et al.* (1995) observed increased marine ^{14}C Younger Dryas reservoir ages in North Atlantic surface waters from paired terrestrial and marine AMS ^{14}C dates. Vibrocore VE 57/09/46, from the St Kilda Basin, recorded a Younger Dryas ^{14}C reservoir age of *ca.* 700 yrs. This spatial and temporal variation in Younger Dryas reservoir age will have implications for comparisons between marine records. Table 5.2 illustrates the effect of this 'increased' 700 year marine reservoir effect above the modern 400 year correction, but given the transient nature of reconstructed atmospheric ^{14}C (e.g. Hughen *et al.*, 1998, 2000), no single Younger Dryas marine reservoir age correction will be appropriate.

The Holocene/Younger Dryas transition in core MD95-2007 is marked in the lithology by a rapid increase of sand and a corresponding decrease in clay and silt content, reflecting a change in sediment supply into the St Kilda Basin. As temperatures increased during the early Holocene, the supply of sediment into the basin decreased and stronger tidal currents probably produced the coarse and highly compressed Holocene sequence. This change in lithology takes place over a very short period of time according to Austin and Kroon (1996).

5.5.v Offshore records and the timing of H1

Low water content and stiff, clast-rich diamicts at the base of core MD95-2007, coinciding with a high sand content, marks the presence of a grounded ice sheet on the Hebridean shelf. Together, the low water content, high shear strength

Laboratory number	Core depth (cm)	Conventional radiocarbon age (^{14}C years BP ±1σ)	Conventional radiocarbon age (^{14}C years BP ±1σ) 405 yr reservoir correction	Conventional radiocarbon age (^{14}C years BP ±1σ) Incorporating 700 yr reservoir correction for Younger Dryas (shaded samples)
MD95-2007				
AA-41753	21	2279±36	1874	1874
AA-41754	121	10664±65	10259	10259
AA-41762	375.5	11353±62	10948	10653
AA-41755	396.5	11299±66	10894	10599
AAR-2602	425	11500±90	11095	10800
AA-41763	442.5	11296±77	10891	10596
AA-41756	556.5	11471±62	11066	10771
AA-41757	741.5	12353±74	11948	11948
AAR-2603	826	12630±100	12225	12225
AAR-2604	974.5	12790±120	12385	12385
AA-41758	1008.5	12789±88	12384	12384
AA-41759	1345.5	12953±74	12548	12548
AAR-2605	1663	13810±170	13405	13405
AA-41760	1674	13020±110	12615	12615
AAR-2606	1815.5	14250±150	13845	13845
AA-41761	1821	13950±130	13545	13545

Table 5.2. AMS ^{14}C ages for the St Kilda Basin core MD95-2007. The shaded box indicates the ages corrected for a 700 year marine reservoir correction through the Younger Dryas cold phase.

and matrix supported, clast-rich diamicts suggest the presence of sub-glacial, overconsolidated sediments (Selby, 1989). A transition to finer grained sediments with higher water content indicates the transition to a deglacial phase, with a change from sub-glacial conditions as the ice sheets floated and broke up. The ice sheet margin would have been very susceptible to external forcing; a small increase in sea level, for example, would have resulted in destabilization of the margin and increased iceberg calving.

The nearby Barra Fan core, MD95-2006, records an age of 16.1 ka cal. BP for the mid-point of Heinrich Event 1. However, there is no obvious evidence for the presence of H1 in MD95-2007. A large clast at the base of the core was recorded on retrieval of the core-catcher and the corer itself probably stopped at a depth of 19.35m due to the presence of these clast-rich, highly consolidated sediments. Two molluscan radiocarbon dated samples from MD95-2007 yield an average calibrated age of approximately 16.3ka BP at a depth of 18.2 m. This age, together with the known age of H1 from the adjacent continental margin and elsewhere in the NE Atlantic (e.g. Curry *et al.*, 1999), may indicate that the lithological transition at the base of the core is infact coincident with H1 in the offshore record.

These findings have important implications for the timing of the deglaciation of the BIS in the wider context of the amphi-Atlantic ice rafting events. The Hebridean margin appears to have deglaciated in phase with the main LIS-sourced H1 event, and was therefore probably in phase with one stage of the deglaciation of

the LIS. McCabe and Clark (1998) suggested that the LIS initiated the changes in other circum-Atlantic ice sheets and this seems a likely scenario, at least for deglaciation of the sensitive margins of the last BIS. It is however probable that on the smaller, sub-millennial, time-scales the BIS did not respond in phase due to the sensitivity of the ice sheet margins. The basal section of core MD95-2007 illustrates the retreat of grounded ice at the time of HE1, but does not itself resolve the issue of possible regional ice advance at this time.

5.6 Summary

The St Kilda Basin record provides evidence for the timing of the ice sheet response to climate fluctuations at its margin. The lithological changes in core MD95-2007 correlate closely with those observed in the shorter St Kilda cores VE 57/-09/89 and VE 57/-09/46. The lithological transition observed in core MD95-2007 water content measurements indicates regional deglaciation of the BIS at this offshore margin takes place at *ca.* 16.7 cal ka BP. The receding ice sheet led to an increase in the deposition of fine glacimarine material onto the shelf. The transition from the end of the Interstadial warming to the onset of the Younger Dryas cooling is more difficult to determine due to the inherent complexities and the age uncertainties of the AMS ^{14}C dating method. However, a marked lithological change indicates an approximate age of 13 cal ka BP for this cooling transition. Following this increase of silt and clay to the basin, a marked increase in sand coincides with the return to warmer conditions recorded in nearby core VE 57/-09/46, marking the onset of the Younger Dryas-Holocene transition.

This chapter has focussed primarily on the timing of regional deglaciation of the BIS. However, it has also served to illustrate the highly expanded nature of the MD95-2007 Lateglacial record compared to the previously published vibrocore studies. The potential exists for future faunal and stable isotope studies to focus on the variability within the stadial and interstadial oscillations of this record, e.g. the interstadial warming prior to the Younger Dryas cold phase which appears defined in the lithological record (Figure 5.4). This is perhaps best illustrated by a *tentative* correlation of the MD95-2007 lithology to the GISP2 $\delta^{18}O$ record (Figure 5.7). Kroon *et al.* (1997) indicated that rapid oscillations observed during the last deglacial period on the Barra Fan, NW Scotland were similar to those observed in $\delta^{18}O$ from the Greenland ice cores. The data from MD95-2007 show that variations in sediment size, which appear to mark the main climatic transitions of the Lateglacial, closely coincide with the same transitions in the GISP2 $\delta^{18}O$ record. Further work on the climate proxies of MD95-2007 may therefore provide a valuable tool in the correlation of these archives on a centennial or possibly decadal timescale.

The exact forcing mechanism that led to the deglaciation of the BIS is, at present, unknown. However, once deglaciation had started it appears to have been a rapid process on the shelf margin, with the floating ice sheet quickly becoming unstable. New observations from core MD95-2007 indicate that regional deglaciation of the outer Hebridean shelf took place immediately prior to or coincident with H1, if an age of 15.1-16.6 cal kyr BP is inferred for H1. An

additional core, MD95-2006, on the Hebridean continental slope indicates that the ice sheet remained on the outer continental shelf, supplying IRD with similar lithologies (Knutz *et al.*, 2001), until shortly before 15 cal kyr BP (see section 3.4).

The MD95-2007 St Kilda marine sediment core, within dating uncertainties, therefore suggests that grounded ice on the Hebridean shelf withdrew at the same time as the main Laurentide-sourced H1 event was deposited in the North Atlantic. This regional ice sheet response may be coincident across the entire North Atlantic due to the strong coupling between ocean circulation and ice sheet margins. The BIS therefore probably responded in phase with the LIS during this particular phase of the deglaciation. However, the dating uncertainties associated with the timing of these events on both sides of the Atlantic Ocean makes it impossible to determine the exact sequence of events.

Chapter 6.

"The age and chronostratigraphic significance of North Atlantic Ash Zone II"

Abstract

Rhyolitic tephra with the geochemical characteristics of North Atlantic Ash Zone II are described from the giant piston core MD95-2006 from the NE Atlantic Ocean. Shard size distribution indicates that the tephra represent a wind-sorted, primary air-fall deposit, but with a mode close to 200 μm they are too coarse to be air-fall deposits at the core site which lies ca. 1,000 km from the possible tephra source. Randomly sampled shards reveal a single geochemical population belonging to the Icelandic transitional alkali magma series, suggesting that they are unlikely to represent ice rafted debris derived from Icelandic icebergs. The tephra probably represent air-fall deposits, transported to the core site by sea ice within the NE Atlantic gyre. The NAAZ II peak coincides with the rapid climate transition (cooling) at the end of interstadial 15, which can be assigned an age of 53,260 ± 2,660 yr BP from direct correlation with the Greenland ice core (GISP2) record. A comparison of the MD95-2006 *N.pachyderma* (sinistral) relative abundance and GISP2 $\delta^{18}O$ records, relative to the NAAZ II isochron, suggests that this climatic event was synchronous across the North Atlantic. By direct correlation of interstadial maxima between the two records, the GISP2 timescale is transferred to MD95-2006. Comparison of corrected and calibrated radiocarbon ages derived from

monospecific foraminifera with the GISP2 ages at the same stratigraphic horizon suggest major age differences. These probably result from large variations in atmospheric ^{14}C concentration and highlight the significant uncertainties associated with radiocarbon calibration during MIS 3.

6.1 Background

Tephrochronology is a powerful tool in the correlation and dating of Quaternary sedimentary sequences, providing a direct link between marine, terrestrial and ice core stratigraphies (e.g. Haflidason *et al.*, 2000). Within the sub-polar North Atlantic, the tephra providing the basis for this stratigraphic scheme are largely derived from explosive Icelandic eruptions. However, because of the presence of an extensive sea ice cover and the calving of Icelandic glaciers rich in volcanic material, care should be taken in the application of tephrochronology to late Quaternary NE Atlantic sediment records.

Three major zones of Mid- to Late-Pleistocene marine tephras have been reported throughout the North Atlantic region: North Atlantic Ash Zones - NAAZs I, II, and III (Ruddiman and Glover, 1972) or Zones – Zs 1, 2 and 3 (Sigurdsson, 1982). The detailed geochemistry of these zones has subsequently been presented by Kvamme *et al.* (1989) and Lacasse *et al.* (1996); with geochemical reference made to Sigurdsson's (1982) data to verify correlation.

North Atlantic Ash Zone II (NAAZ II) was originally correlated and mapped as far south as 45°N (Ruddiman and Glover, 1972). The earliest age estimates for NAAZ II are 64,700 ± 3,500 yr BP (Kellogg, 1973), later revised by Smythe *et al.* (1985) to 57,500 yr BP from oxygen isotope stratigraphy. More recently, NAAZ II has been correlated with the Thórsmörk ignimbrite in southern Iceland, which has been dated by $^{40}Ar/^{39}Ar$ of K-feldspar crystals to 54.5 ± 2 kyr (Sigurdsson *et al.*, 1998). The discovery of NAAZ II tephra, amongst numerous others, in the GRIP and GISP2 ice cores from Summit, Greenland (Grönvold *et al.*, 1995; Zielinski *et al.*, 1997) adds a valuable isochron to tie ice-ocean records within Marine Isotope Stage (MIS) 3. The mid-point of NAAZ II occurs in GISP2 at a depth of 2,464.275 m, corresponding to an age estimate of 53,260 ± 5% (± 2,660) yr BP on the Meese/Sowers timescale (Meese *et al.*, 1994; Bender *et al.*, 1994). As such, the presence of NAAZ II in marine sequences provides a chronological anchor beyond the normal limitations of radiocarbon dating and provides a test of the stadial-interstadial correlation commonly used in age model construction (e.g. Bond *et al.*, 1993).

This study examines the geochemical, stratigraphic and depositional context of NAAZ II in a very expanded, high-resolution marine core: MD95-2006 (57°01.82'N, 10°03.48'W), collected at a water depth of 2,120 m from the Barra Fan, NW Scotland in 1995 as part of the IMAGES programme (Figure 6.1). The core is

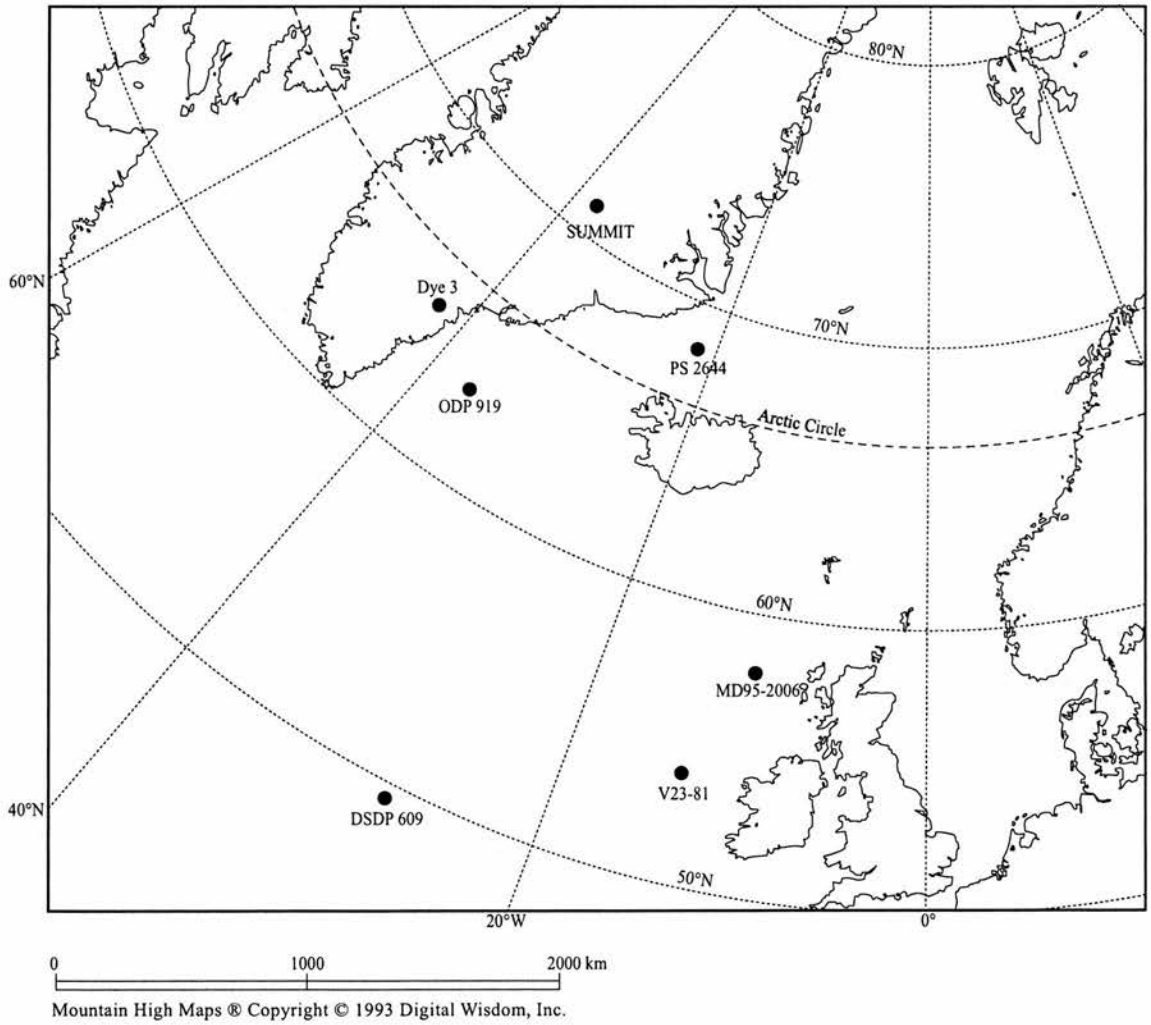

Figure 6.1 Location Map, showing the position of core MD95-2006 and other cores cited in this study.

nearly 30 m long and provides a centennial to sub-millennial-scale record of sediment accumulation on this margin over at least the last 60 kyr (see section 3.3.iii, section 3.4 and section 4.4). One objective of this study was to examine and compare the exact timing of NAAZ II emplacement within NE Atlantic sediments (MD95-2006) and Greenland ice (GISP2) and evaluate its reliability as a chronostratigraphic anchor (isochron) within NE Atlantic sediment records.

6.2 Methods

6.2.i Foraminifera and Tephra

Sampling was initially conducted at a 10 cm spacing resolution throughout the core and consisted of removing 20 cm^3 plugs. These were dried to constant weight at 40°C and sub-sampled for various analyses (see Kroon *et al.*, 2000; see Chapter 2). Approximately 20 g was processed by wet sieving on a 63 μm sieve, retaining the coarse residues for further analysis. Further sub-sampling at a continuous 1 cm interval was undertaken between 2786-2844 cm. Tephra were counted from the total dry-sieved residue >150 μm and classified as either basic or silicic glass on the basis of gross morphology and colour. Tephra counts are normalized to number per gram sediment dry weight. Individual shard measurements (>300), from the >63 μm dry residue, were made using a Zeiss Stemi SV11 binocular microscope with a calibrated eye-piece graticule to determine

maximum shard dimensions. The estimated size error, based on the calibration procedure and the magnification employed, is ± 10 μm.

Foraminifera were also counted from the fraction >150 μm and are presented as % *Neogloboquadrina pachyderma* (sinistral), expressed as a fraction of the total foraminiferal count (>100 specimens).

6.2.ii Tephra Geochemistry

Sub-samples of the tephra were mounted on a frosted glass slide and embedded in clear Araldite™, allowed to harden and the sample was ground to c. 50 μm thickness prior to polishing on coarse and fine diamond laps. The slides were then vacuum-coated with evaporated carbon, and conductivity enhanced using aquadag contacts. Glass shard geochemistry was determined on the twin spectrometer Cambridge Instruments Microscan V electron microprobe at the Grant Institute, University of Edinburgh. Instrumental conditions were as detailed by Hunt and Hill (1993, 1996, 2001), namely operating at an accelerating potential of 20 kV and a probe current of 15 nA, with an exposure time of 50 seconds based on a 10 second counting interval per element. Pure oxides and simple silicates were used as standards. Corrections were made for counter dead-time, atomic number effects, fluorescence and absorption, using a ZAF procedure described by Sweatman and Long (1969). An andradite garnet was used as a secondary standard. Assessment of sample stability under the electron beam is normally made using the Lipari obsidian

secondary standard as recommended by Hunt and Hill (1996, 2001) and Hunt *et al.* (1998). Unfortunately, this was unavailable at the time of analysis and the potential implications of this are discussed later. Data are presented in Table 6.1.

6.3 Results

6.3.i The distribution, size and composition of NAAZ II tephra

Typical bubble wall fragments of clear glass shards representative of NAAZ II silicic (rhyolitic) tephra in core MD95-2006 are illustrated in Figure 6.2. The stratigraphic distribution of this shard type within the core interval 2786-2844 cm is limited to 2810-2819 cm, with a maximum of 74 shards g^{-1} at 2817 cm, defining the abundance peak of a typical deep-sea asymmetric concentration profile (e.g. Berger and Heath, 1968). Within the maximum abundance peak at 2817 cm, the shard frequency size curve of NAAZ II (Figure 6.3) suggests a very well-sorted sample, with a clearly defined mode at 178 μm. The maximum observed shard size is 890 μm, but there are relatively few shards >350 μm present.

Data from the shards analysed in this study are presented in Table 6.1 and are compared with published data (Lacasse *et al.,* 1996; Sigurdsson, 1982) for Zones 1, 2 and 3 (Figure 6.4a-f). Only data with analytical totals >94% have been used from this study; analyses exhibiting lower totals have been excluded. For graphical comparisons with published tephras we have not used normalized data.

Probe Sample ID (MD95-2006)	SiO_2	TiO_2	Al_2O_3	FeO*	MnO	MgO	CaO	Na_2O	K_2O	Total Oxides	Total Alkalis
MD95:2006 1:B	72.08	0.08	11.42	2.48	0.09	0.00	0.34	3.92	3.94	94.35	7.86
MD95:2006 1:B	72.07	0.10	11.49	2.51	0.10	0.08	0.37	4.12	3.52	94.36	7.64
MD95:2006 1:B	72.22	0.15	11.61	2.59	0.12	0.08	0.33	3.84	3.69	94.63	7.53
MD95:2006 1:B	72.91	0.16	11.48	2.54	0.12	0.00	0.40	3.79	4.13	95.53	7.92
MD95:2006 1:B	72.68	0.11	11.70	2.53	0.08	0.00	0.41	4.02	3.79	95.32	7.81
MD95:2006 1:B	73.11	0.14	11.58	2.54	0.07	0.00	0.36	4.25	3.85	95.90	8.10
MD95:2006 1:B	73.66	0.11	11.54	2.43	0.10	0.00	0.36	4.17	3.94	96.31	8.11
MD95:2006 1:B	73.17	0.11	11.55	2.49	0.10	0.00	0.39	4.43	4.25	96.49	8.68
MD95:2006 1:B	72.43	0.11	11.29	2.54	0.09	0.00	0.35	3.90	4.07	94.78	7.97
MD95:2006 1:B	72.55	0.14	11.55	2.58	0.11	0.00	0.40	4.06	4.06	95.45	8.12
MD95:2006 1:B	73.60	0.16	11.68	2.64	0.11	0.00	0.33	4.33	3.90	96.75	8.23
MD95:2006 1:C	71.77	0.15	11.39	2.60	0.05	0.00	0.34	3.93	3.88	94.11	7.81
MD95:2006 1:C	71.93	0.15	11.45	2.48	0.10	0.00	0.35	3.92	3.87	94.25	7.79
MD95:2006 1:C	72.85	0.17	11.77	2.56	0.05	0.00	0.37	4.12	3.87	95.76	7.99
MD95:2006 1:C	73.03	0.17	11.48	2.45	0.08	0.00	0.39	3.90	4.08	95.58	7.98
MD95:2006 1:C	73.05	0.11	11.53	2.51	0.13	0.00	0.41	4.37	3.91	96.02	8.28
MD95:2006 2:B	72.43	0.14	11.52	2.45	0.07	0.00	0.31	3.92	3.86	94.70	7.78
MD95:2006 2:B	72.64	0.14	11.52	2.47	0.06	0.00	0.34	3.95	3.95	95.07	7.90
MD95:2006 2:B	72.49	0.13	11.40	2.49	0.05	0.00	0.38	4.08	4.01	95.03	8.09
MD95:2006 2:B	73.82	0.14	11.76	2.55	0.08	0.00	0.33	4.43	4.08	97.19	8.51
MD95:2006 2:B	72.75	0.13	11.47	2.55	0.08	0.00	0.36	3.97	3.88	95.19	7.85
MD95:2006 2:B	72.03	0.10	11.49	2.41	0.09	0.00	0.41	3.87	3.73	94.13	7.60
MD95:2006 2:B	72.36	0.12	11.44	2.40	0.06	0.00	0.40	4.08	3.75	94.61	7.83
MD95:2006 2:B	74.00	0.11	11.45	2.44	0.10	0.00	0.38	4.36	4.07	96.91	8.43

Table 6.1 Electron microprobe analyses of rhyolitic glass from NAAZ II in core MD95-2006. Number of analyses = 24.

Figure 6.2 Bubble wall fragments of clear glass shards representative of NAAZ II silicic (rhyolitic) tephra in core MD95-2006. Photomicrograph scale 600 μm x 600 μm.

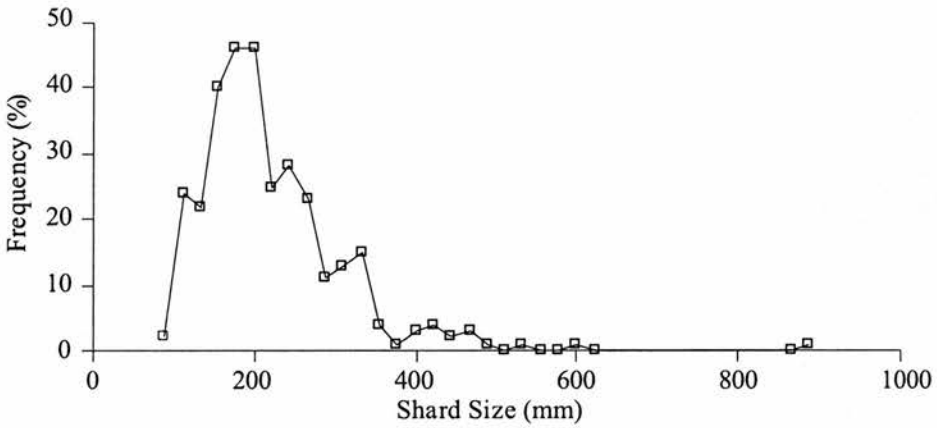

Figure 6.3 Shard frequency size curve from the maximum abundance peak (2817 cm) of NAAZ II tephra in core MD95-2006. The frequency (%) is calculated from the measurement of the maximum grain dimension (μm) of >300 randomly selected grains from the sieved residue >63 μm. The maximum shard diameter measured = 890 μm, median = 200 μm, mode = 178 μm (n = 316).

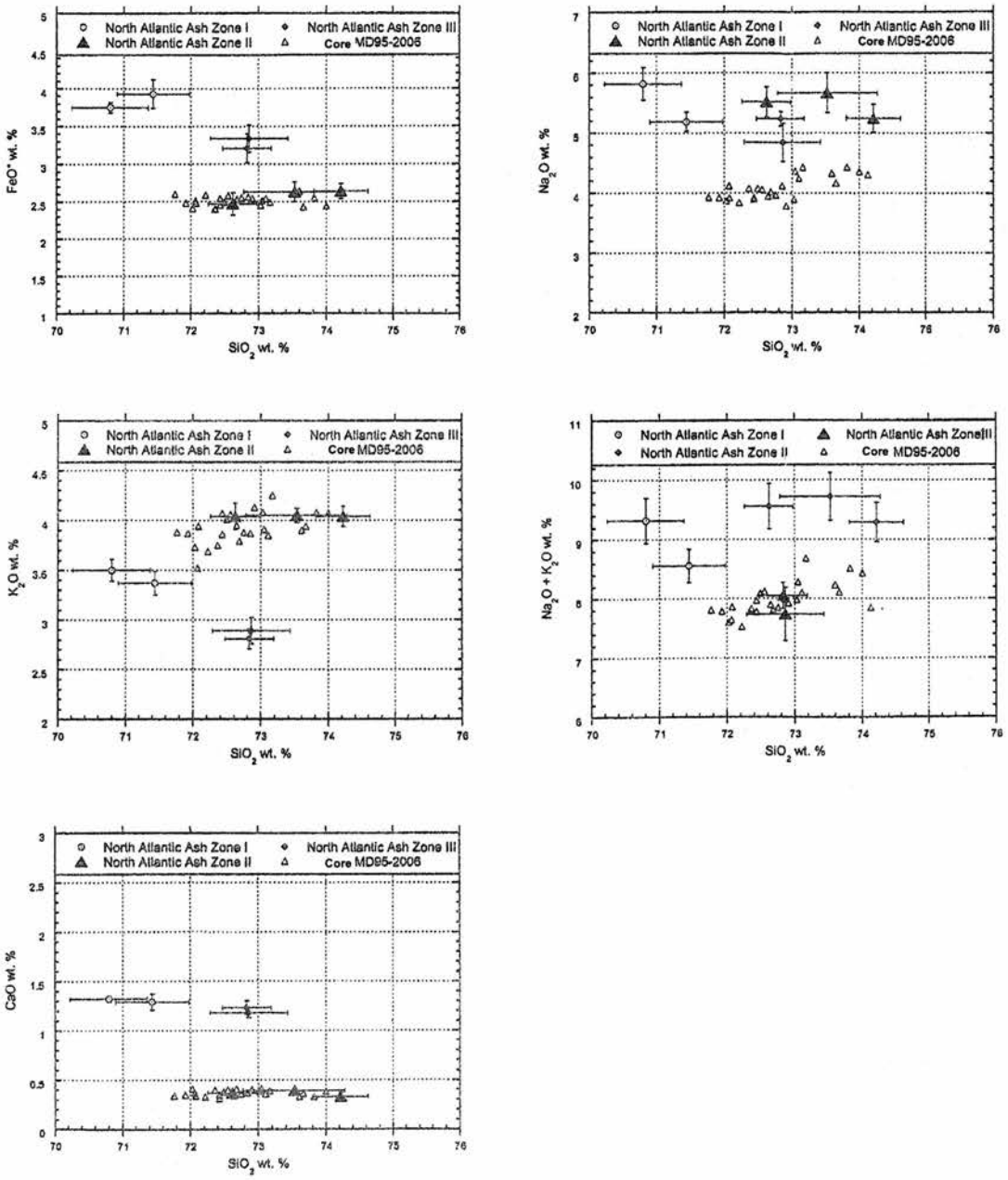

Figure 6.4. Variation diagrams of major elements against silica.

Normalization, unless an absolute necessity, is not deemed desirable (Hunt and Hill, 1993) because it can mask poor data. In this instance, where some data are published solely as means ± standard deviations (Sigurdsson, 1982; Lacasse *et al*, 1996), normalization may be problematical.

The data indicate that tephrogeochemistry of shards found in core MD95-2006 (2810-2819 cm) is rhyoltic (comendite – *sensu* Le Maitre 1989) within the Icelandic transitional alkali magma series. The geochemistry is strongly supportive of correlation with NAAZ II / Z2 as the latter zone is readily distinguished from NAAZ III / Z3 and NAAZ I / Z1 on the basis of its comparatively low FeO (<2.8%), CaO (<0.5%), Al_2O_3, TiO_2 and MgO (< detection threshold) content and its higher K_2O content.

However, Lacasse *et al.* (1996) indicate that NAAZ Z2 is also characterized by comparatively high Na_2O and total alkalis. Initially, our data do not support such a conclusion. This may reflect anomalies in relation to the analysis of Na_2O itself. The problem of sodium mobility has been rehearsed in detail elsewhere (see Nielsen and Sigurdsson, 1981; Hunt and Hill, 1993, 1996, 2001). In addressing these problems different and valid approaches have been used by both probe centres supplying data for comparison in this study (Brown University: Lacasse *et al.,* 1996; University of Edinburgh: our data). Published inter-laboratory comparability data (Hunt *et al.,* 1998) confirm that both approaches produce similar results. The approach used by Lacasse *et al.* (1996) and by Sigurdsson (1982) involves back-

projection of the sodium decay curve to Time, T = 0, whereas the Edinburgh probe uses a defocussed beam and beam-blanking to minimize sodium mobility. However, there is a suggestion (Hunt, 1997) that the back-projection method which is reliant on less precise data (sequential two second counting periods) and the assumption that mobility begins immediately after initial electron bombardment, may slightly over-estimate the initial sodium content. Conversely, the Edinburgh approach, monitored by repeated analysis of the Lipari obsidian secondary standard, may slightly under-represent sodium. In this study, the absence of the Lipari standard to assess beam-impact may have led to marginally less favourable conditions for sodium analysis and hence a partial under-representation. In combination, these two opposing influences may account for a larger than anticipated difference between sodium data from our results and those published for NAAZ II / Z2 (see Figure 6.4b-c). The departure, although sufficient to lead to potential association with published NAAZ III/ Z3 data, is less significant than that indicated in the Kvamme *et al.* (1989) data for NAAZ II in which Na_2O is typically <2/3%.

Despite the forgoing, the overall element signature for the MD95-2006 tephra is strongly indicative of correlation with NAAZ II / Z2 (see Table 6.2). We are therefore confident with the correlation and this confidence is reinforced by important, independent stratigraphic evidence provided by biostratigraphical and oxygen isotope data.

	Z1	Z2	Z3	MD95-2006
Z1	1.00			
Z2	0.64	1.00		
Z3	0.80	0.73	1.00	
MD95-2006	0.63	0.91	0.72	1.00

Table 6.2 Similarity coefficients (Borchardt *et al.*, 1972; Sarna-Wojcicki *et al.*, 1987) comparing published normalized data (Sigursson, 1982; Lacasse *et al.*, 1996) with normalized data from this study. The similarity coefficients indicate the best match is between MD95-2006 and Z2/NAAZ II. Values are not as high as reported in correlations by Lacasse *et al.* (1996) because of differences in the measurement of sodium between these studies.

6.3.ii Chronostratigraphy

The chronology of core MD95-2006 is constrained by seventeen accelerator mass spectrometer (AMS) radiocarbon dates on monospecific foraminiferal samples of the sub-polar *Globigerina bulloides* and polar *Neogloboquadrina pachyderma* (sinistral); typically 1,000 specimens (>250 μm) (Table 6.3). Seven of the ^{14}C ages were calibrated into calendar ages using Calib 4.2 (Stuiver and Reimer, 1993; Stuiver *et al.*, 1998), which incorporates a 400 yr surface ocean reservoir correction for this latitude in the NE Atlantic Ocean. Beyond about 21 kyr BP, the calibration procedure is less well constrained and has significantly decreased reliability. The older dates were calibrated using the U/Th ages and second-order polynomial equation of Bard *et al.* (1998), which extends the current coral calibration data set of Stuiver *et al.* (1998).

Chapter 3 (section 3.3.ii) discusses the various age-depth modelling approaches to the ^{14}C-derived chronology of core MD95-2006. Particularly problematic are age assignments at the bottom of the core beyond the normal limits of the radiocarbon method (about 45 ^{14}C kyr BP). Calibrated age estimates at a depth of 3000 cm ranged from 53,800 to 56,700 yr BP, depending on the age-depth model used (section 3.3.ii). The MIS assignments in core MD95-2006 (section 4.4), whilst not used as age-depth control points, do provide a check on the calendar ages derived from the corrected and calibrated AMS ^{14}C dating. In addition, the large,

Laboratory Number	Core Depth (cm)	Conventional radiocarbon age (^{14}C yr BP $\pm 1\sigma$)	Calendar age (years)	Species
AA-40438	0.5	2910 ± 130*	2526	*G. bulloides*
AA-40439	164.5	10376 ± 73*	11153	*G. bulloides*
AA-40440	323	12067 ± 120*	13442	*G. bulloides*
AA-22347	770	15260 ± 140*	17664	*N. pachyderma* (sinistral)
AA-35119	1175.5	17390 ± 190*	20115	*N. pachyderma* (sinistral)
AA-22348	1340	18060 ± 130*	20886	*N. pachyderma* (sinistral)
AA-35120	1411	18680 ± 130*	21600	*N. pachyderma* (sinistral)
AA-35121	1591.5	20390 ± 150*	23567	*N. pachyderma* (sinistral)
CAMS-60835	1941.5	22720 ± 130**	26278	*N. pachyderma* (sinistral)
AA-22349	2020.5	24710 ± 280**	28565	*N. pachyderma* (sinistral)
AA-32312	2173.5	26210 ± 270**	30273	*N. pachyderma* (sinistral)
AA-32313	2288	29400 ± 370**	33860	*G. bulloides*
AA-32314	2418.5	29730 ± 470**	34227	*G. bulloides*
AA-22350	2539	33880 ± 610**	38794	*G. bulloides*
AA-35122	2653.25	42500 ± 1800**	47948	*G. bulloides*
AA-35123	2728.5	47100 ± 3000**	52649	*G. bulloides*
AA-35124	2860	44430 ± 2000**	49936	*G. bulloides*

Table 6.3 Radiocarbon (conventional, non-reservoir age corrected) and calibrated (calendar) ages for monospecific samples of *G.bulloides* and *N.pachyderma* (s) from core MD95-2006. A reservoir age correction of 405 years is applied prior to calibration. Ages marked * are calibrated using Calib 4.2 (Stuiver and Reimer, 1993; Stuiver *et al.*, 1998) and older ages marked ** are calibrated using an U/Th calibration curve (Bard *et al.*, 1998).

well-known variations in atmospheric ^{14}C concentration during MIS 3 (e.g. Voelker *et al.* 1998; Beck *et al.*, 2001) raise significant calibration problems at this time.

To overcome some of these problems, we have constructed a calendar age model for core MD95-2006 based on the Meese/Sowers timescale of GISP2 (Meese *et al.*, 1994; Bender *et al.*, 1994). Tie points (Table 6.4), based largely on the prominent interstadial maxima, characterize both ice core and marine records (e.g. Bond *et al.*, 1993; 1999; Voelker *et al.*, 1998). Through the densely sampled core interval from 2786-2844 cm, anchored by NAAZ II at 2817 cm, the □^{18}O record of GISP2 (Grootes and Stuiver, 1997) provides a direct correlation with the relative abundance changes of *Neogloboquadrina pachyderma* (sinistral) in core MD95-2006 (Figure 6.5). Despite the excellent correlation between the two records, it is important to remember the 5% error estimate for GISP2 chronology through this interval (Alley *et al.*, 1997).

6.4 Discussion

6.4.i The transport and deposition of NAAZ II

Two major processes are responsible for the dispersal of tephra from Icelandic explosive eruptions: ash fallout, predominantly to the east from stratospheric plumes (see Lacasse, 2001) and ice rafting to southerly latitudes during cold stages (e.g. Ruddiman and Glover, 1972; Lackschewitz and Wallrabe-Adams,

Interstadial (IS) number & tie-points	Depth in MD95-2006	GISP2 age of IS	Depth in GISP2 (m)
IS3	2010.5	27736	2054
IS4	2060	28941	2074
IS 5	2184	32123	2124
IS 6	2233.5	33455	2144
IS 7	2278	35417	2174
IS 8	2418.5	38201	2228
IS 9	2493	40134	2254
IS 10	2539	41091	2274
IS 11	2587	42486	2302
IS 12	2653.25	45283	2356
IS 13	2728.5	46911	2380
IS 14	2747.25	51608	2448
NAAZII	2817	53260	2464.28
IS 15	2823	53497	2466
IS 16	2860	56238	2488

Table 6.4 Tie points, based on the position of interstadial maxima and NAAZ II, used to construct the calendar age model for core MD95-2006. The GISP2 ages are based on the "Meese/Sowers" timescale (Meese *et al.*, 1994; Bender *et al.*, 1994).

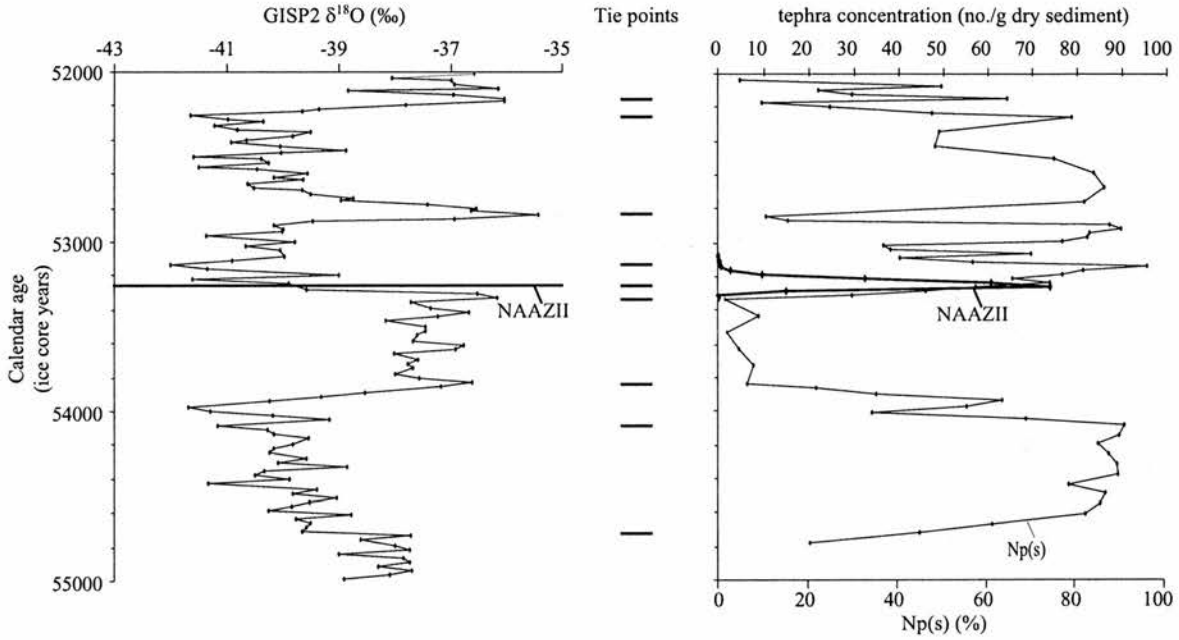

Figure 6.5 Expanded portion of the GISP2 $\delta^{18}O$ record compared with *N.pachyderma* (s) from core MD95-2006. The maximum abundance peak of clear glass shards (>150 μm) defines the stratigraphic position of NAAZ II during the cooling transition at the end of ice core interstadial 15. Calendar ages (ice core years) are based on the GISP2 time scale (Meese *et al.*, 1994; Bender *et al.*, 1994), which was transferred into the MD95-2006 record using the tie points defined in Table 6.3.

1997). Normal ice rafting processes implicate icebergs as the most significant transporters of ice rafted detritus (IRD), whereas sea-ice is not generally implicated (Andrews, 2000). However, when ash fallout occurs offshore, around Iceland, most of the ash that does not fall directly onto open water will fall onto sea-ice rather than directly onto calved icebergs. Modern glaciers on Iceland, such as the Vatnajökull ice cap, contain tephra layers from numerous eruptions (e.g. Larsen *et al.*, 1998). Whilst calving from Icelandic ice-sheets may produce icebergs rich in tephra, and might also produce varying IRD concentrations, these are highly unlikely to account for the distinctive geochemistry which characterizes primary ash horizons (e.g. Larsen, 1981) or the very well size-sorted distribution of the tephra, characteristic of distal airfall processes (e.g. Sparks *et al.*, 1981).

Recent high-resolution investigations reveal that Icelandic tephra are a distinctive component of North Atlantic IRD (e.g. Bond *et al.*, 1999). If they are to be successfully used as time-markers in marine stratigraphies, their depositional history must be carefully considered as a function of the mechanism by which they are delivered. One of the criteria which may usefully distinguish between eruptions onto sea-ice and icebergs derived from calving glaciers, is the geochemical signature of a randomly sampled population of shards. In this study, the geochemical characteristics of tephra from an abundance peak are largely consistent with other records of NAAZ II and strongly suggest a single geochemical population present (Table 6.1). In addition, the frequency size curve for these tephra is well-sorted (Figure 6.3), with a well-defined mode <200 μm, suggesting that they were

originally deposited some considerable distance from source, but being too coarse to be primary air-fall deposits at the core site. Such a size distribution and loss of a coarse "tail" fraction is typical (e.g. Sparks *et al.*, 1981) and arises when particles settle-out according to size and density from a wind-transported plume. For example, the maximum shard diameter of NAAZ II glass in the Dye 3 ice core from southern Greenland (1190 km west from source, Figure 6.1) is 300 μm (Ram and Gayley, 1991). Maximum shard diameter of NAAZ II glass in the GISP2 core (1260 km northwest from source, Figure 6.1) is 100 μm (Ram *et al.*, 1996). The significantly larger (silicic = 740 μm; Lacasse *et al.*, 1998) than expected shards at ODP Site 919 in the Irminger Basin (910 km from source, Figure 6.1) may reflect an ice-rafting rather than fallout origin for NAAZ II (Lacasse, 2001).

In late Quaternary sediments from the Reykjanes Ridge, Lackschewitz and Wallrabe-Adams (1997, 221) note "*strong correlation between IRD and ash particles suggest ... a mix from different volcanic provinces on Iceland because ash particles from different eruptions can be expected to be found in an ice-berg. Particles are both subglacial, englacial and supraglacial, and represent a variety of sources*". The NAAZ II tephra in core MD95-2006 clearly have a different origin. They are consistent with primary air-fall onto sea-ice, transport within the NE Atlantic gyre (Ruddiman and Glover, 1972) and subsequent deposition at the core site. A recent investigation of IMAGES core MD01-2461, to the west of Ireland and considerably further from the Icelandic source, suggests an almost identical shard size distribution to NAAZ II (V. Peck, pers. comm. 2002).

6.4.ii The timing of NAAZ II emplacement in MD95-2006

Having established that NAAZ II in core MD95-2006 was transported and deposited from sea-ice after initial air fall deposition close to Iceland, it would be useful to re-evaluate its chronostratigraphic value in NE Atlantic sediments. Was there a significant delay between the eruption event (and initial air fall) and subsequent deposition at the core site?

The nearby record of core 56/-10/36 (56°43'N, 09°19'W; water depth 1320 m) suggests that summer sea surface temperatures (SSTs) varied by as much as 10°C during the major stadial-interstadial transitions of the last deglaciation (Kroon *et al.*, 1997). While the SST reconstructions of Kroon *et al.* (1997) use the SIMMAX modern analogue method (Pflaumann *et al.*, 1996), based on total planktonic foraminiferal assemblage data, relative abundance changes of *Neogloboquadrina pachyderma* (sinistral) still provide valuable SST information. For example, the marked changes from >95% to <5% *Neogloboquadrina pachyderma* (sinistral) observed around NAAZ II in core MD95-2006 (Figure 6.5) suggest summer SSTs of >12°C to <4°C, respectively (Pflaumann *et al.*, 1996 and references therein).

Irrespective of the common tie points between MD95-2006 and GISP2 (Table 6.4), we note that NAAZ II occurs in both records mid-way through the interstadial-stadial transition which marks the end of interstadial 15 (Dansgaard *et*

al., 1993; Taylor *et al.*, 1993). In GISP2, this and other interstadial-stadial climate transitions, observed in $\delta^{18}O$, are largely complete in about 80 years (e.g. Stuiver and Grootes, 2000). Since NAAZ II is recorded at the MD95-2006 core site mid-way through the same climate transition, defined by changing relative abundances of *Neogloboquadrina pachyderma* (sinistral), it seems unlikely that it was deposited more than a decade or two after the air fall event recorded in GISP2. This argument assumes synchroneity in the major climate transitions between the summer SSTs of the NE Atlantic Ocean and air temperature over Greenland. Given the assymetric distribution of shard concentration within core MD95-2006 and its likely origin as a consequence of sediment bioturbation (e.g. Berger and Heath, 1968), the age differences between the emplacement of NAAZ II in these two records is probably <10 years.

Has NAAZ II in core MD95-2006 been assigned to the correct interstadial-stadial climate transition? If deposition of the tephra was delayed, possibly through complex sea-ice transport mechanisms, it is possible that they reached the site during a later cooling phase. Given the rapidity of the millennial-scale Dansgaard-Oeschger climate cycles throughout MIS3 and the fact that the dating uncertainties through this interval exceed the periodicity of the signal, this is not a trivial issue. However, because of the sub-millennial to centennial-scale resolution of the MD95-2006 record, high-frequency features of the GISP2 $\delta^{18}O$ record (e.g. the short-lived "warm" event at 52,800 yr BP, between interstadials 15 and 14; Figure 6.5) can be

resolved and confirm that NAAZ II occurs in core MD95-2006 at the interstadial-stadial transition marking the end of interstadial 15.

6.4.iii The chronostratigraphic significance of NAAZ II

The last glacial-interglacial transition (Termination I) in the North Atlantic region has been discussed extensively; many authors (e.g. Björck *et al.*, 1998; Walker *et al.*, 1999) arguing that an event stratigraphy provides a reliable framework for correlation. For example, Kroon *et al.* (1997) used an "event" approach to directly correlate the SST record of Termination I in core 56/-10/36 to the GISP2 □^{8}O ice core record. Since surface waters have likely advected northwards past this region of NW Europe throughout much of the late Quaternary (e.g. Koc *et al.* 1993), there are good reasons to expect a close relationship with air temperature over Greenland. As one might expect, such correlations east-west across northern Europe are less likely to be synchronous (Lowe, 2001). However, proving synchrony between the records is rather more difficult, largely because of the uncertainties associated with most dating methods.

The stratigraphic resolution of NAAZ II in core MD95-2006 at the interstadial 15-stadial transition (Figure 6.5) provides a strong case in support of synchronized climate records during the last glacial period. While such correlations have long been accepted (e.g. Bond *et al.*, 1993), decadal-scale correlation and

synchrony between the surface North Atlantic and Greenland air temperature has not previously been established.

The location and geochemical characterization of NAAZ II tephra in core MD95-2006 provides a valuable chronostratigraphic anchor at the end of interstadial 15, approximately 53,300 yr BP. To illustrate the age uncertainty associated with the dating of MIS 3, the corrected and calibrated radiocarbon ages (Table 6.3) are compared with the GISP2 calendar ages of the interstadial maxima through the same core interval (Figure 6.6). Despite the evidence presented above for decadal-scale correlation and synchrony between the records, the transferred GISP2 ages have their own age uncertainty, estimated at about 5% through this interval (Alley *et al.*, 1997). The fitted curves suggest a tendency of the corrected and calibrated radiocarbon ages to underestimate the calendar timescale between about 30-40 kyr BP and overestimate before 45 kyr BP; although larger statistical uncertainties of the older record are not significant at 95% confidence limits.

The limited number of radiocarbon dates through this interval in core MD95-2006 support recent observations suggesting large variations in atmospheric ^{14}C concentration during MIS 3 (e.g. Voelker *et al.* 1998; Beck *et al.*, 2001). The data highlight the significant uncertainties associated with radiocarbon calibration and illustrate the value of the NAAZ II isochron near the very limit of the radiocarbon dating method.

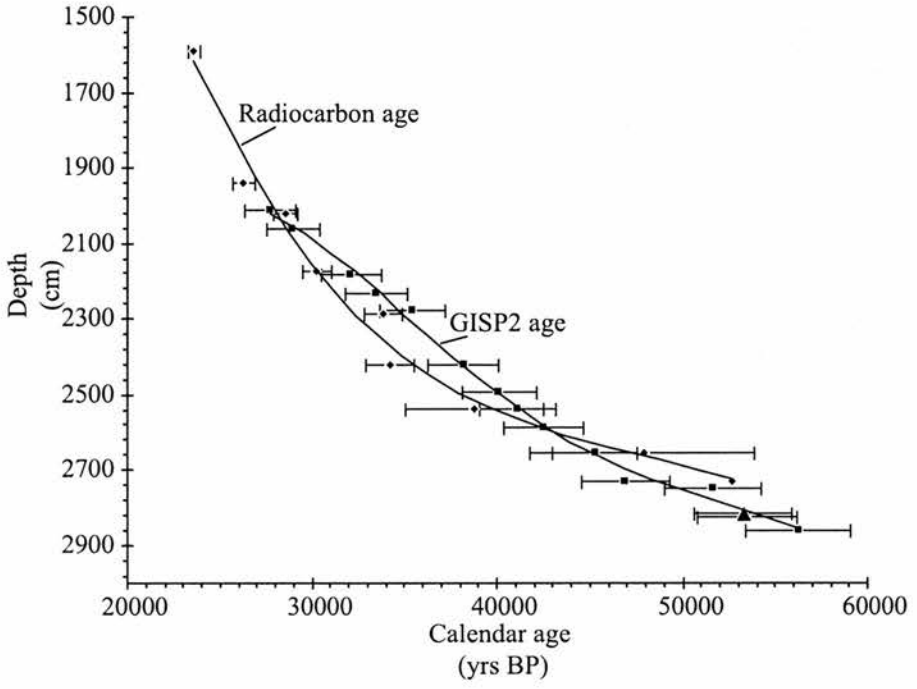

Figure 6.6 Calendar age-depth model for MIS 3 in core MD95-2006. Radiocarbon ages (open diamonds) are corrected and calibrated (see Table 6.2). Interstadial maxima (modified after Chapter 3 and 4) and their GISP2 calendar ages (open squares) are based on the GISP2 time scale (Meese *et al.*, 1994) and summarized in Table 6.4. The depth of the maximum abundance peak of NAAZ II (2817 cm) is plotted against the GISP2 age (closed square), together with the 5% error estimate for GISP2 chronology through this interval (Alley *et al.*, 1997).

6.5 Conclusions

The stratigraphic position, size distribution and characterization of tephra in core MD95-2006 suggest that they represent a wind-sorted, primary air-fall deposit with a geochemical signature closely correlated with NAAZ II. The shards are too coarse to be primary air-fall deposits at the core site and were probably transported there by sea ice within the NE Atlantic gyre. They are unlikely to be derived from Icelandic icebergs, because of their well-sorted size distribution and the single geochemical population present.

Maximum NAAZ II tephra abundances in core MD95-2006 are observed within an interval which defines the interstadial-stadial transition at the end of interstadial 15; about 53,260 ± 2,660 yr BP. The correlation of the MD95-2006 *N. pachyderma* (sinistral) and GISP2 □^{18}O records, suggests that this climate transition was synchronous. The rapidity of the Dansgaard-Oeschger climate cycles throughout MIS 3 and the large dating/calibration uncertainties associated with the radiocarbon method, make it particularly important to "tie" marine and ice core chronologies with isochrons such as NAAZ II. By direct correlation of interstadial maxima between the two records, the GISP2 timescale is transferred to MD95-2006. Comparison of the corrected and calibrated radiocarbon ages with the GISP2 ages at the same stratigraphic horizon suggest major age differences. These are likely the result of large variations in atmospheric ^{14}C concentration and highlight the significant uncertainties associated with radiocarbon calibration during MIS 3.

Chapter 7.

General Discussion

There are relatively few continuous, truly high-resolution records of the last glacial to present interglacial transition from marine continental margin settings. High sedimentation rates (>0.5 m/ka) within the IMAGES long giant piston sediment cores MD95-2006 from the Barra Fan, and MD95-2007 from the St Kilda Basin, NW Scotland, enabled detailed studies to constrain the timing and magnitude of last glacial period climatic events on the Hebridean continental shelf and margin. These records are variously composed of marine and glacier-influenced sediment deposited over the last ca. 60 cal ka BP and both cores contain records of high temporal resolution. The Barra Fan core MD95-2006 provides a continuous record for the whole of this period, while the St Kilda Basin records, which include MD95-2007, provide evidence on the timing and pattern of regional deglaciation on the Hebridean shelf. They are therefore ideally located to record the fluctuations and final deglaciation of the north west ice margin of the last BIS. This study has therefore focused in particular on the behaviour and characteristics of the last BIS through MIS 3 and 2 and during Termination I, i.e. the last deglacial period. During this time the ice sheet would have been influenced by internal and external forcing mechanisms (see section 1.2.ii) and may have been particularly sensitive to some forms of external forcing when at its maximum extent.

The sediment core sites are also located along the main track of the North Atlantic's thermohaline circulation. The ocean forms a linked system with the atmosphere and ice sheets and the glaciers along NW Europe's Atlantic margins are ideally placed to respond to ocean forcing mechanisms. The revised age models presented here enable results from these cores to be related to the wider, amphi-Atlantic, setting and have important implications for understanding the dynamics of both the European and Laurentide ice sheets.

7.1. The establishment of a high resolution chronological record

7.1.i The chronology of sediments accumulating on the Hebridean slope during the last glacial period

There are two versions of the MD95-2006 age-depth model, which have evolved during the course of this work; these have developed from those of Kroon *et al.* (2000) and Knutz *et al.* (2001). Kroon *et al.* (2000) and Knutz *et al.* (2001) constructed a chronostratigraphic framework for core MD95-2006 from 7 radiocarbon dated foraminiferal samples and the 1 Thol. 2 ash layer, reporting a basal age of 45 cal ka BP. Chapter 3 and 4 introduced a third age-depth model which used new AMS ^{14}C dates. A fourth age-depth model, presented in chapter 6, has further refined the chronostratigraphy with the identification of NAAZII towards the bottom of the core.

The age-depth model derived from the new sampling of core MD95-2006 is based upon the use of 14 AMS ^{14}C dates and the dated tephra horizon (1 Thol. 2) (Chapter 3 and Figure 4.3). This model gives a revised basal age of ca. 53,800 cal yr BP. The new dates, combined with the down-core stable isotope stratigraphy, enable the tentative identification of the marine isotope stage 3/4 transition within core MD95-2006 (Figure 4.4) and thus resolves some of the uncertainties inherent in the age-depth model reconstruction, particularly at the limit of the radiocarbon method (Figure 7.1).

7.1.i.a A revised age model for core MD95-2006

The geochemical identification of a new Icelandic tephra horizon, North Atlantic Ash Zone II (NAAZII), enabled further refinement to the age-depth relationship through the basal sector the core MD95-2006. The discovery of NAAZII in core MD95-2006 indicates that the basal age of the core is older than either of the previous models suggested. The direct correlation of the NAAZII horizon in MD95-2006 with the same event in the GISP2 ice core record enables the assignment of an age of 53,260 $\pm$ 2,660 yr BP at an MD95-2006 core depth of 2817 cm.

In addition to NAAZII, the position of H4 is confirmed at a core depth of 2460 cm from the identification of detrital carbonate in the corresponding residue

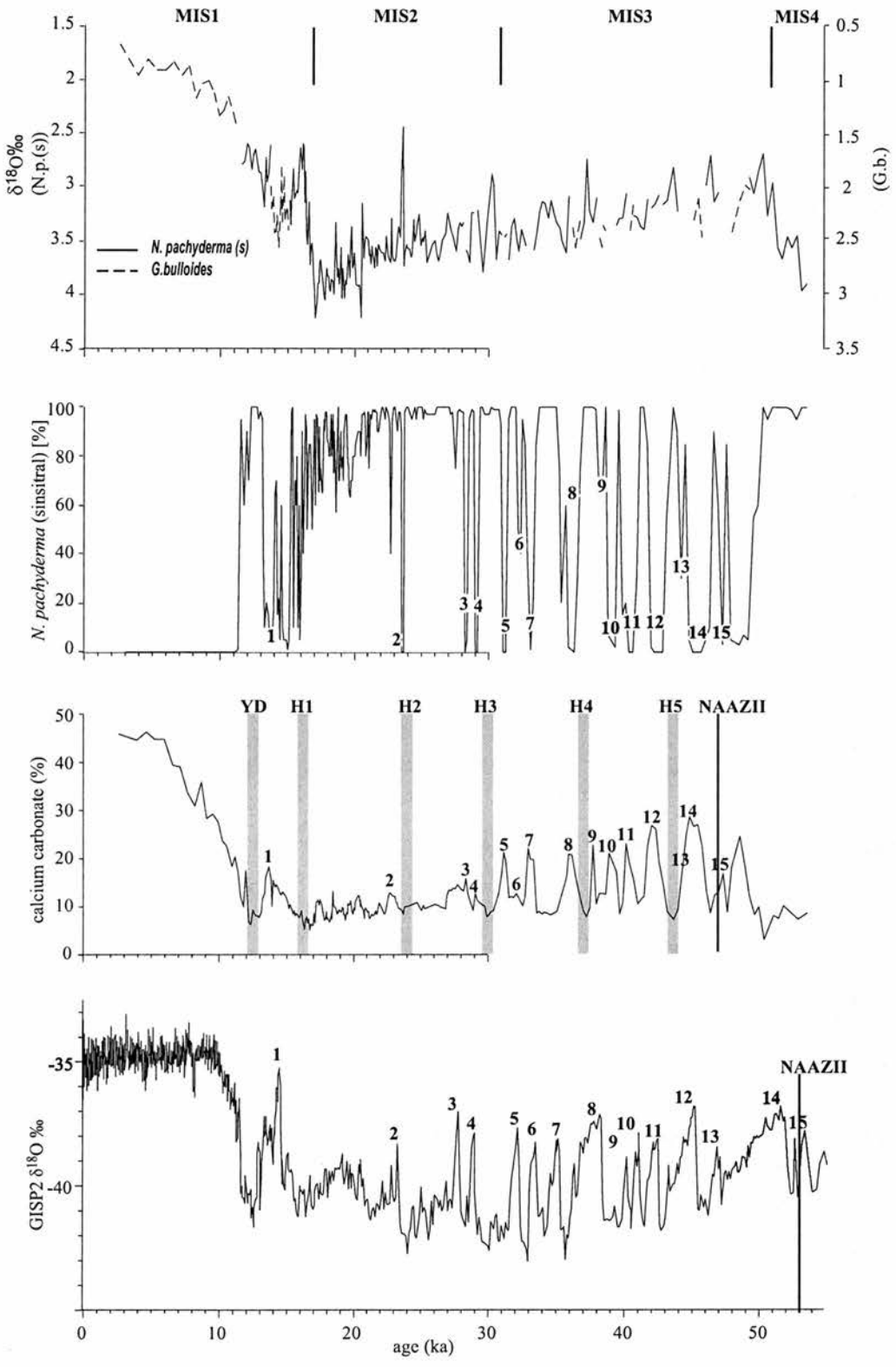

Figure 7.1. Stratigraphic summary of core MD95-2006 and Greenland Ice Sheet Project (GISP2) ice core $\delta^{18}O$ (Grootes and Stuiver, 1997). Interstadial events are modified from figure 3.8 following the identification of NAAZII. The age-depth model presented in Chapter 3 therefore highlights the previous age uncertainty towards the base of the core (>30 cal ka BP).

sample and additional magnetic susceptibility (ms) measurements and a clearly defined excursion in planktonic foraminiferal $\delta^{18}O$. A high ms peak can be clearly correlated with the North Atlantic Heinrich Event in this lower section of the core where 'non-Heinrich Event' IRD signals of likely BIS origin are less frequent and generally of lower amplitude than those observed during MIS 2 (Chapter 3).

The identification of the position of these two events, in conjunction with recently obtained down-core measurements of percentage *N.pachyderma* (sinistral), enables a refinement of the original labelling (Figure 3.8) of the interstadial events within core MD95-2006 (Figure 7.1). The older ages now established at the base of the core suggest that a total of 17 interstadial events, as opposed to 15, are recorded. Interstadial 13, for example, is now resolved in the percentage *N. pachyderma* (s) but its position was not reflected in the low-resolution (10cm) $CaCO_3$ record.

The established variations in atmospheric ^{14}C (Chapter 2.2.ii) result in problems when calibrating radiocarbon dates. The calibration of AMS ^{14}C dates has been achieved through the use of the Calib 4.2 programme (Stuiver and Reimer, 1993; Stuiver *et al.*, 1998) and, for dates older than 21,000 ^{14}C ka BP, the paired U/Th and ^{14}C ages fitted to a second-order polynomial equation by Bard *et al.* (1998) are employed. An additional calibration programme is OxCal[7.1] (Figure 7.2). The resulting OxCal multiplot highlights the uncertainty associated with the Younger Dryas cold phase. The probability distribution plots for the calibration of

[7.1] http://www.rlaha.ox.ac.uk/orau/06_ind.htm

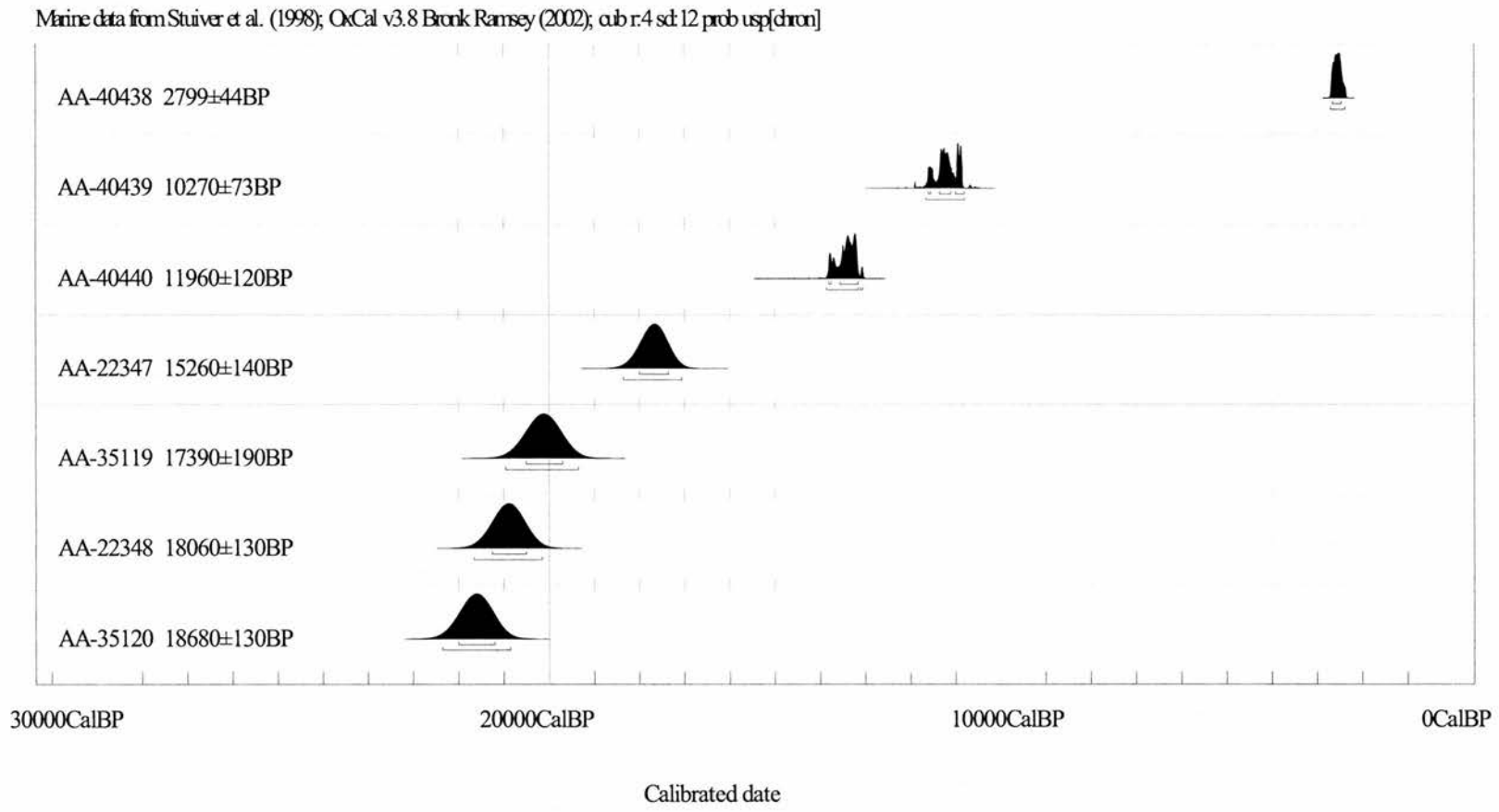

Figure 7.2. Probability distributions for the MD95-2006 AMS ^{14}C ages. The OxCal programme highlights the uncertainty surrounding the ages derived from material deposited within the Younger Dryas cold phase and equally highlights the limited temporal resolution of the pre-Younger Dryas calibration curve.

10,270 ± 73 ^{14}C ka BP and 11,960 ± 120 ^{14}C ka BP (Figure 7.2) demonstrate the problems in the associated calibration data and likelihood of obtaining multiple calibration solutions. Equally, due to the limited temporal resolution of the radiocarbon calibration dataset prior to the Younger Dryas, earlier radiocarbon dates have broad probability distributions once calibrated.

Recently, 11 AMS ^{14}C[7.2] dates within the upper eight metres of the core have become available and these reinforce the confidence in the original age-depth model to perform well through this interval (Table 7.1).

7.1.i.b A late Quaternary event stratigraphy

Mangerud *et al.* (1974) attempted a formal reclassification of the stratigraphic record of the late Quaternary in NW Europe with the proposal of a common chronostratigraphic classification. However, since the adoption of this classification scheme in the late 1970's higher resolution records have been obtained from terrestrial, marine and lacustrine environments. The framework of Mangerud *et al.* (1974) has subsequently been applied to a wide range of environmental records and sites for which its use as a strictly chronostratigraphic scheme was not originally intended.

[7.2] Chris Byrne, a PhD student at the Grant Institute, University of Edinburgh, obtained seven of the AMS ^{14}C dates in 2002 (RCL Allocation No. 927.0501). L. Wilson obtained five AMS ^{14}C in 2002.

Laboratory Number	Core Depth (cm)	Conventional radiocarbon age (^{14}C yr BP ±1σ)	Calendar age (years)	Species
AA-40438	0.5	2799 ± 44	2526	*G. bulloides*
AA-51687	11.5-16.5*	3031 ± 55	2774	*G. bulloides*
AA-51685	39.5- 44.5*	5113 ± 37	5468	*G. bulloides*
AA-51688	40	4897 ± 77	5256	*G. bulloides*
AA-49015	45	4790 ± 55	5035	*G. bulloides*
AA-51686	50.7-56*	6808 ± 65	7319	*G. bulloides*
AA-49016	74	9014 ± 45	9621	*G. bulloides*
AA-40439	164.5	10270 ± 73	11153	*G. bulloides*
AA-49017	202.5	10050 ± 48	10982	*G. bulloides*
AA-49018	285	11457 ± 55	12985	*G. bulloides*
AA-49019	312.5	11790 ± 57	13177	*G. bulloides*
AA-40440	323	11960 ± 120	13442	*G. bulloides*
AA-49020	505	13349 ± 67	15486	*G. bulloides*
AA-49021	735	15302 ± 88	17712	*G. bulloides*
AA-22347	770	15260 ± 140*	17664	*N. pachyderma* (sinistral)
AA-35119	1175.5	17390 ± 190*	20115	*N. pachyderma* (sinistral)
AA-22348	1340	18060 ± 130*	20886	*N. pachyderma* (sinistral)
AA-35120	1411	18680 ± 130*	21600	*N. pachyderma* (sinistral)
AA-35121	1591.5	20390 ± 150*	23567	*N. pachyderma* (sinistral)
CAMS-60835	1941.5	22720 ± 130**	26278	*N. pachyderma* (sinistral)
AA-22349	2020.5	24710 ± 280**	28565	*N. pachyderma* (sinistral)
AA-32312	2173.5	26210 ± 270**	30273	*N. pachyderma* (sinistral)
AA-32313	2288	29400 ± 370**	33860	*G. bulloides*
AA-32314	2418.5	29730 ± 470**	34227	*G. bulloides*
AA-22350	2539	33880 ± 610**	38794	*G. bulloides*
AA-35122	2653.25	42500 ± 1800**	47948	*G. bulloides*
AA-35123	2728.5	47100 ± 3000**	52649	*G. bulloides*
AA-35124	2860	44430 ± 2000**	49936	*G. bulloides*

Tephra	Core Depth (cm)	Calendar age (years)
1 Thol. 2	262.5	12888
NAAZ II	2817	53257.5

Table 7.1. All age (conventional, non-reservoir age corrected and calibrated (calendar) ages) control measurements for core MD95-2006. The Laboratory codes in blue indicate recent dates obtained by L. Wilson. Laboratory codes in red mark the radiocarbon dates obtained by C. Byrne, University of Edinburgh. The two tephra horizons, now clearly identified in core MD95-2006, are also shown.

* Dates which form part of a pair with benthic foraminifera from the same core level (see section 7.2.iii); benthic data not yet available.

Questions regarding the suitability of the Mangerud classification scheme for event correlation between different records have been raised in recent years. An alternative framework has therefore been proposed (Björck *et al.*, 1998) for the N. Atlantic region. This scheme, established by the INTIMATE (Integration of Ice-core, Marine and Terrestrial records) programme in 1997, is based upon the isotopic record of the GRIP ice-core in Greenland. It takes the form of an '*event stratigraphy*' from ca. 22 to 11.5 k GRIP yr BP (ca. 19 to 10 k ^{14}C BP), thus incorporating the last Termination through to the Holocene. The '*events*' are '*short-lived occurrences that have left some trace in the geological record, enabling them to be used as a means of correlation*' (Björck *et al.*, 1998, p.287). The scheme builds on the identification of interstadial events by Johnsen *et al.* (1992) with the inclusion of previously defined stadial/interstadial events. The GRIP isotope record therefore provides the basis to define two Greenland Stadials (GS-1 and GS-2) and two Greenland interstadials (GI-1 and GI-2) through the Lateglacial interval. In addition, GI-1 and GS-2 are sub-divided into GI- 1a, 1b, 1c, 1d and 1e, and GS- 2a, 2b and 2c.

The INTIMATE event stratigraphy is applicable across a series of records, both terrestrial and marine, and has certain advantages over the previously employed lithostratigraphic, biostratigraphic and terrestrially-based radiocarbon chronostratigraphy. The climatic '*events*' are identified, assuming synchrony, within each record and have no clearly defined boundary as their basis for classification. The approach does not work particularly well when records are fragmentary or incomplete and there is the inevitable danger of miss-matching events from differing

proxy records. Equally, synchrony (the underlying assumption of the method) between different climate archives is often difficult to prove (e.g. Chapter 6).

7.1.i.c An interstadial event stratigraphy in core MD95-2006

An increased sampling resolution (every 1cm) through the NAAZII distribution 'window' allows percentage counts of *N. pachyderma (s)* at a very high resolution. The $\delta^{18}O$ record of GISP2 (Grootes and Stuiver, 1997) provides a direct correlation with the relative abundance changes of *N. pachyderma* (sinistral) in core MD95-2006 as it does in many other North Atlantic sediment records (e.g. Bond *et al.*, 1993). The exceptional sub-millennial to centennial-scale resolution of the MD95-2006 record allows the identification of many of the high-frequency features of the GISP2 $\delta^{18}O$ record (e.g. the distinctive, short-lived "warm" event at 52,800 yr BP, between interstadials 15 and 14; Figure 6.3) and confirms that NAAZ II occurs in core MD95-2006 at the interstadial-stadial transition marking the end of interstadial 15 (see chapter 6). Hence, a comparison can be made between core MD95-2006 and the GISP2 ice core record using a series of tie-points between the two records (Figure 6.5).

A revised age-depth model is therefore established which is 'tied' to the GISP2 ice core record. The use of these tie-points between the interstadial maxima of core MD95-2006 and the Meese/Sowers GISP2 timescale (Meese *et al.*, 1994; Bender *et al.*, 1994) transfers the GISP2 timescale onto the marine sediment core

and thus provides a means of correlating between the marine and ice core records (Table 7.2).

By contrast, the variations in atmospheric ^{14}C concentration result in major age differences between the independent GISP2 chronology and the corrected and calendar ages from core MD95-2006 during MIS 3 (Figure 7.3) (e.g. Voelker *et al.* 1998; Beck *et al.*, 2001). Between approximately 21 ka BP and 40 ka BP the calendar age-scale has large dating uncertainty of several thousand years. The calendar – ^{14}C age comparisons are further complicated by the fact that the GISP2 age model also has an error associated with it of $\pm$ 5% (Bender *et al.*, 1994, Meese *et al.*, 1994).

The calibration of the radiocarbon timescale for these older ages remains problematic. The approach adopted by Voelker *et al.* (1998) is promising (Figure 7.4), but failed to highlight and incorporate the calendar age uncertainty in the GISP2 chronology (Figure 7.3). In this method, the difference between the GISP2 age of a marine sample (derived from correlation) and its measured ^{14}C age (corrected for an assumed global average marine reservoir age of 400 years) are considered to be a measure of either changing atmospheric ^{14}C concentration or changing marine reservoir age or some combination of both. Despite the difficulties of radiocarbon calibration, the approach of Voelker *et al.* (1998) has another potential application when two or more marine records are correlated to a GISP2-derived calendar chronology. In this case, if one assumes synchronicity in the

Interstadial (IS) No.	MD95-2006 depth (cm)	GISP2 age (yr BP)	GISP2 depth (m)
IS3	2010.5	27736	2054
IS4	2060	28941	2074
IS 5	2184	32123	2124
IS 6	2233.5	33455	2144
IS 7	2278	35417	2174
IS 8*	2418.5	38201	2228
IS 9	2493	40134	2254
IS 10*	2539	41091	2274
IS 11	2587	42486	2302
IS 12*	2653.25	45283	2356

Table 7.2. Summary of proposed dating levels and the position and GISP2 age of interstadial maxima. Interstadial events marked * have been dated previously (monospecific sub-polar *G.bulloides* (x1,000 specimens, >250μm)) (see Table 7.1 and Figure 7.3).

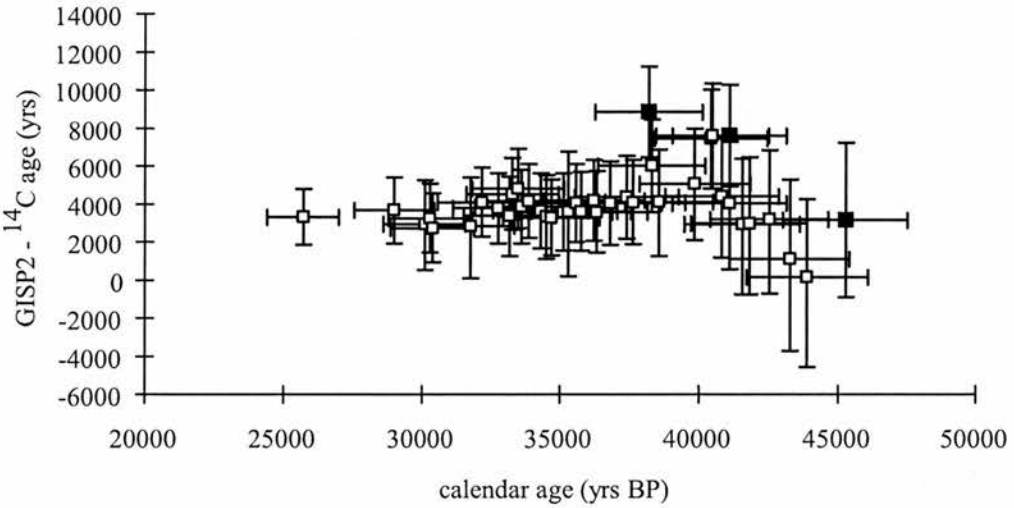

Figure 7.3. Age difference plot (GISP2 calendar age - ^{14}C planktonic foraminiferal age) against the GISP2-derived chronology of marine core PS2644 (open squares) and core MD95-2006 (black squares). Error bars show the combined 5% uncertainty in the GISP2 chronology (Alley *et al.*, 1997) and the 1σ-error of the ^{14}C ages. The PS2644 data are modified after Voelker *et al.* (1998). Note all ^{14}C ages are corrected for a global-average reservoir effect of 400yr.

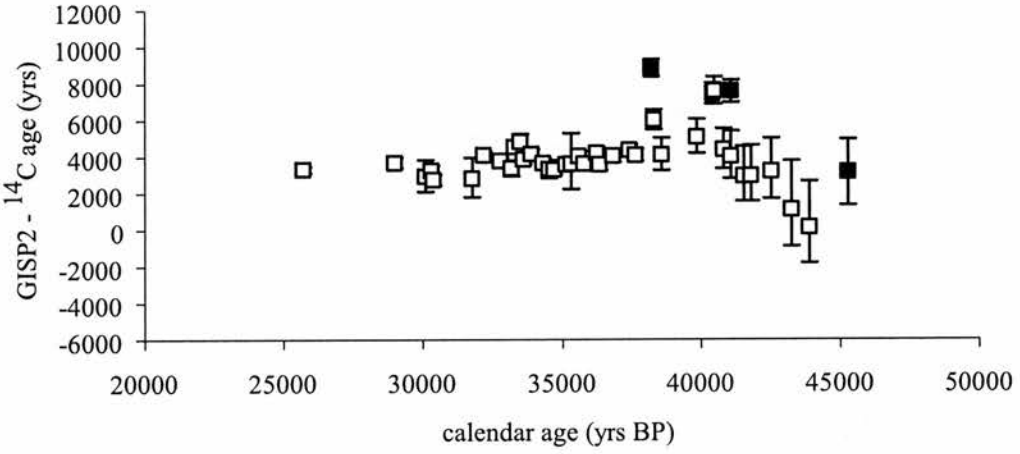

Figure 7.4. Age difference plot (GISP2 calendar age - ^{14}C planktonic foraminiferal age) against the GISP2-derived chronology of marine core PS2644 (open squares) and core MD95-2006 (black squares). Error bars show the 1σ-error of the ^{14}C ages only. The PS2644 data are after Voelker *et al.* (1998). Note all ^{14}C ages are corrected for a global-average reservoir effect of 400yr.

records, age differences in GISP2 age – ^{14}C age between two marine cores at any given calendar age should reflect the difference in marine reservoir age between those core locations at that point in time. The advantage now is that one can significantly reduce any age uncertainty deriving from the GISP2 calendar age chronology (compare Figures 7.3 and 7.4) because both records are tied to the same (synchronous) climate transitions.

The differences between GISP2 age and ^{14}C age for the same interstadial events during MIS 2 and 3 provide the basis for further discussion of the marine reservoir ages at PS2644 and MD95-2006. Core PS2644, located north of Iceland in the Irminger Basin, is strongly influenced by seasonal ice cover and the AMS ^{14}C ages reported are exclusively polar *N. pachyderma* (s). For example, reservoir ages in the surface water of the Southern Ocean increase significantly due to seasonal ice cover, ranging from 1,300 yr (Gordon and Harkness, 1992) to 5,550 yr (Domack *et al.*, 1989).

The three AMS^{14}C dated interstadials of MD95-2006 (Figure 7.4) illustrate the differences in the ^{14}C age shift between the Irminger Basin (PS2644) and the NE Atlantic Ocean (MD95-2006) which are consistent with a large surface ocean reservoir effect north of Iceland during IS 8 and 10 (global-average + 2830 yr and + 3570 yr, respectively). Such increased surface ocean reservoir ages north of Iceland during MIS 2 and 3 are consistent with a reduced THC and diminished ocean ventilation in this region (e.g. Stocker and Wright, 1996). The latter are, of course,

implicated in the underlying large variations of atmospheric ^{14}C concentration which define the $\Delta^{14}C$ excursions (e.g. Beck *et al.*, 2001). As Voelker *et al.* (1998, 524) point out "*..any increase in the reservoir effect would result in an (apparent) ^{14}C age shift*". Significant age differences (GISP2-^{14}C age) between core MD95-2006 and core PS2644 should point to changing regional marine radiocarbon reservoir age gradients between the Iceland Sea and NE Atlantic Ocean. If the surface ocean marine radiocarbon reservoir age of the North Atlantic Current (NAC) does remain close to 400 yr during interstadials 3-12, then it can be argued that any calibration exercise should be conducted at core locations and intervals which record maximum NAC influence.

At present only three of the interstadial events in core MD95-2006 have been AMS^{14}C dated. The identification of the interstadial maxima from the revised age model will now allow further work to be carried out, with the high precision AMS ^{14}C dating from local abundance maxima of planktonic foraminifera *G. bulloides* associated with interstadials 3-12 in core MD95-2006.

In addition to the age and calibration of radiocarbon dates, the palaeoceanographic significance of the GISP2 – ^{14}C age differences through an interstadial could also be tested. Rapid changes in ocean ventilation, as a function of changing ocean ventilation linked to THC variability, have significant implications for the understanding of rapid climate transitions (see section 1.2).

7.1.ii The Hebridean shelf

The chronological study of the 19.35 m long giant piston core MD95-2007, recovered from the St Kilda Basin on the Hebridean Shelf indicated a highly expanded Lateglacial sediment record covering the last 17.5 kyr (Chapter 5, Table 5.1). This confirms the "predictions" based on the seismostratigraphic evidence (Stoker *et al.*, 1993) and the existing understanding of the St Kilda Basin sediment accumulation patterns based upon the short (<5m) BGS vibrocores (Austin *et al.*, 1995; Austin and Kroon, 1996). The glacially overdeepened basin provides a depositional centre for sediments deriving from the retreating ice sheet with average sedimentation rates of >0.5 m/ka. The sixteen AMS ^{14}C dates and two tephra horizons through core MD95-2007 provide a detailed record of the last deglacial period, thus enabling the determination of the timing of regional deglaciation. In the Faroe region of the north east Atlantic the initial deglaciation took place between 15.5 to 15.1 ^{14}C ka BP (Lassen *et al.*, 2002) while a slightly earlier date of 16 ^{14}C ka BP was obtained from a core on the Iceland Plateau (Koç and Jansen, 1994). In contrast the initial deglacial signal core MD95-2007 corresponds closely to the dates obtained from the nearby vibrocores, VE 57/-09/89 and VE 57/-09/46, by Peacock et al. (1992) and Austin and Kroon (1996). A marked lithological change of increased clay and silt in the St Kilda IMAGES core corresponds to an age of 16.8 cal ka BP. However, the longer chronological record of core VE 57/-09/89 demonstrates that deglaciation must have taken place prior to 17.6 cal ka BP. The cold conditions continued in the MD95-2007 record until approximately 15.6 cal ka BP.

7.2 Climate variability of the last British Ice Sheet on the Hebridean continental Shelf and Margin

The marine sediments from cores MD95-2006 (Hebridean slope) and MD95-2007 (Hebridean shelf) record the behaviour of the BIS during the last glacial-interglacial transitional period, thus enabling direct comparisons with other, independently dated marine records from elsewhere in the North Atlantic. In addition, future potential exists to explore the relative timing of IRD with distinctive provenance signatures as it has been emplaced within the MD95-2006 record.

7.2.i MIS 4

Uncertainties remain regarding pre-LGM ice sheet extent and dynamics of most of the major ice sheets, including the BIS. The initial growth and development of the LIS during MIS 5 was followed by an advance of the ice sheet, possibly onto the St Lawrence lowlands, during the early part of MIS 4 (Clark *et al.*, 1993). The area would then have remained ice covered until MIS 2.

The Fennoscandian ice sheet underwent extensive glaciation during MIS 4 through to MIS 3 when it extended out towards the continental shelf. Larsen *et al.*, (1987), for example, proposed a readvance of the ice margin between 47 and 43 ka BP.

The MD95-2006 core records this period and the cooling trend at the end of MIS 4, which is clearly marked in the planktonic $\delta^{18}O$ record. The low concentration of IRD peaks through this period indicates a lack of glacigenic sediment supply to the region. The transition from MIS 4 to MIS 3 is marked by the onset of a warm climate phase, as shown by the marked decrease in the $\delta^{18}O$ of numerous isotope records (e.g. Elliot *et al.*, 1998; Labeyrie *et al.*, 1999; Chapman *et al.*, 2000). Elliot *et al.* (1998) noted the MIS 4 to MIS 3 transition at a date of 59 ka BP in a marine sediment core SU 90-24 from the Irminger Basin. Core MD95-2006 records approximately the same age for this transition at approximately 60 cal ka BP.

7.2.ii MIS 3

During the early stages of the MIS 3 warm climate phase the BIS exhibits aperiodic cycles of expansion and contraction as reflected in the input of IRD of proposed Scottish origin (Knutz *et al.*, 2001). These fluctuations indicate the ice sheet is responding to rapid climate changes on millennial and sub-millennial timescales (Bond *et al.*, 1999; Broecker, 2003). Carbonate-rich, warm interstadial events, operating with a strong D/O cyclicity, punctuate MIS 3 and provide a strong link between the marine and Greenland ice core palaeoclimate records through this interval.

In the later stages of MIS 3 ice rafting events in MD95-2006 operated with a cyclicity of approximately 1500 years. The IRD can be related to ice advances from

this north west sector of the BIS and reflect stadial events which are closely coupled to the 1-2 kyr D/O climate cycles. Despite its proximity to the last BIS, MD95-2006 appears to exhibit eventually the same climatic fluctuations as other North Atlantic deep sea core records, e.g. VM23-81 and site DSDP-609 (Bond and Lotti, 1995).

These cycles were originally assigned to interstadial events 4-14, however, the revised age model now correlates the events to interstadials 4-15 (Figure 7.1). They indicate the very dynamic nature of the BIS throughout this period. Two low $\delta^{18}O$ peaks within MIS 3 indicate the possible influence of meltwater and two major events may correspond to the main Heinrich Events 3 and 4. MIS 3 exhibits an overall cooling trend of perhaps 2-3°C (based on $\delta^{18}O$ measurements) and is characterized by the alternation in abundance of two key foraminiferal species (*G. bulloides* and *N. pachyderma* [s]), indicating the nature of surface water mass reorganisation above the core site.

During MIS 3 sedimentation rates are relatively low (~40cm/ka), particularly during the interstadial periods when glacial retreat would have taken place in response to climate amelioration. Sediment becomes trapped on the continental shelf during interstadials.

7.2.iii MIS 2/1

The transition to MIS 2 is coincident with a marked lithological change from silty-muddy contourites to glacial hemipelagite to muddy contourite sediment indicating the change to a predominantly glacimarine environment. Shortly after 30 ka BP the BIS extended westwards out towards the outer continental shelf break. An increase in sedimentation rates to 200cm/ka at the start of MIS 2 corresponds to an increase in the frequency and amplitude of the ms peaks. This marked increase in sediment delivery to the continental slope indicates the growth of the north west margins of the BIS to the LGM limits at this time.

The chronology of this event cannot be precisely dated but the MD95-2006 radiocarbon age model presented here indicates maximum ice sheet extent on the Hebridean continental margin took place shortly after H2 (24-24.8 cal ka BP). The $\delta^{18}O$ values become increasingly more positive in the later stages of MIS 2 and the *N.pachyderma* (sin.) $\delta^{18}O$ maxima suggest a BIS LGM date between 21 and 17 cal ka BP. This is in agreement with the terrestrial-derived LGM age of between 20 and 25 ka BP for the Irish Sea Basin (McCabe and Clark, 1998) and with the BIS LGM EPILOG date of ca. 22 cal ka BP adopted by Bowen *et al.* (2002). It also closely corresponds with the maximum ice sheet advance in the North Sea between 29.4 and 22 ka BP (Sejrup *et al.*, 1994). The strong millennial scale periodicities recorded in MIS 3 are not observed during MIS 2. Interestingly, the relative abundance of *N. pachyderma* (s) suggest a long-term change towards warmer climates being

somewhere around 22 cal ka BP (Figure 7.1), but predating the most positive $\delta^{18}O$ values between 21-17 cal ka BP.

The main IRD layers observed in core MD95-2006 coincide with a sudden fall in sea surface temperature as indicated by increased *% N. pachyderma* (s), and a reduction in sea surface salinity, as indicated by the reduction in $\delta^{18}O$ values. This is in agreement with the North Atlantic marine core SU90-03 (40 °N, 32 °W) which lies to the south of the main IRD belt (Chapman and Shackleton, 1998b).

Snoeckx *et al.* (1999) and Grousset *et al.* (2000) proposed a European ice sheet trigger for the LIS surging. The Sr-Nd isotope measurements of Grousset *et al.* (2000) from the HE IRD material suggested that the Scandinavian and BIS delivered IRD to the oceans 1.5 ka prior to the LIS deposits. However, it is difficult to determine whether the Barra Fan core indicates a European precursor signal without further analysis. This study has certainly highlighted the potential problem of examining precursor events during MIS 2 when the site is proximal to the BIS. An investigation of a possible precursor to H4, during MIS 3, would add to the phasing debate. H4 represents a more easily definable peak of clearly LIS origin (Figure 1.3a) and therefore represents a favourable candidate for a precursor study. Preliminary high resolution (1cm interval) magnetic susceptibility measurements indicate the presence of a double ms peak for H4 (E. Wadsworth, pers. comm. 2002).

Following the initial phase of deglaciation a number of shifts towards lighter $\delta^{18}O$ values indicates the decay of the BIS around 17 to 16 cal ka BP. The margins of the ice sheet therefore once again became unstable as it extended to the shelf edge delivering both IRD and meltwater. The end of this readvance period is approximately coincident with H1 which is recorded on the Hebridean slope between 15.1-16.6 cal ka BP. This is in agreement with H1 in other north east Atlantic cores, e.g. core NA87-22 and core SU90-08, i.e. approximately 15.3 to 16.7 cal ka BP (13.2 – 14.4 ^{14}C ka BP) (Vidal *et al.*, 1997). Knutz *et al.* (2002b) also records a similar age, approximately 15.6 to 17.4 cal ka BP (13.5 – 15 ^{14}C ka BP), from the north eastern Rockall Trough core DAPC-2 which is proximal to the BIS. McCabe and Clark (1998) propose that the BIS H1 event resulted following the collapse of the LIS at 17.2 – 17.6 cal ka BP (14.6 – 15 ^{14}C ka BP). The readvance of the BIS, associated with H1, may therefore have interrupted the THC and led to a reversal in the deglacial behaviour of the ice sheet. The basal age (approximately 16.8 cal ka BP [14.5 ^{14}C ka BP] (Andrews, 1998)) of H1 from a site proximal to the LIS indicates a possible lag of 500 years between the two potential IRD sources, but such differences are within the dating uncertainty of the method.

It is likely that the majority of the BIS deglacial retreat took place during H1 although coastal temperatures remained cold until 15 cal ka BP, after which time surface waters warmed rapidly. The deglaciation of the outer continental margin is therefore complete sometime before 15 ka BP and there is no evidence of ice rafting

after this date until the cooling that leads into the Younger Dryas (e.g. Kroon *et al.*, 1997).

During this final phase of ice sheet expansion the Hebridean shelf was covered by grounded ice, resulting in the overconsolidated sediments at the base of the shelf core MD95-2007. This marine sediment core lies inside the previously mapped limits of the LGM (Selby, 1989).

The fluctuations in the strength of NADW formation during the last deglacial period could be examined further by establishing how changes in $\Delta^{14}C$ (from paired benthic:planktonic foraminiferal radiocarbon dates) correspond to ventilation changes inferred from the benthic $\delta^{13}C$ reconstructions from the Barra Fan (Austin and Kroon, 2001) and elsewhere. For example, when benthic $\delta^{13}C$ values are positive, NADW formation should be strengthened and the age difference ($\Delta^{14}C_{b\text{-}p}$) reduced.

The continental shelf record MD95-2007 exhibits evidence of the transition to the fully established warm conditions of the interstadial period at 14.3 cal kyr BP, somewhat later than the offshore record MD95-2006. This coincides with the last occurrence of cold water, benthic, indicator species in core VE 57/-09/89 where the initial warm conditions of the interstadial are recorded between approximately 15.6 to 14.7 cal kyr BP (13.5 and 13 ^{14}C ka BP) (Austin and Kroon, 1996). It is also in

broad agreement with core V23-81 (Ruddiman and McIntyre, 1981) which lies to the west of Ireland.

The Younger Dryas to Holocene transition is marked in core MD95-2007 by an increase in coarse sediment delivery and/or winnowing of sediments associated with enhanced bottom currents. However, the precise timing and duration of the Younger Dryas period remain debatable on this continental margin, due in part to the limits placed on the radiocarbon dating method by the presence of a plateau. To overcome this problem, further stable isotope measurements and faunal counts are required from core MD95-2007. Such data will provide a means of direct correlation with, for example, the well-dated Greenland ice cores.

7.3 Summary of Future Work

- Further, higher resolution, residue sampling through the interstadial events of core MD95-2006 could determine an AMS ^{14}C date for each event, thus enabling detailed correlations with the GISP2 $\delta^{18}O$ record (see section 3.4 and section 4.4).

- The obtaining of Nd-Sr measurements and IRD clast counts through H4 in MD95-2006 would enable detailed investigations of the possible BIS/European sourced precursors to the main LIS signal (see section 3.4).

- Paired benthic:planktonic foraminiferal $\Delta^{14}C$ measurements could be obtained to determine a direct, quantitative measure of ocean ventilation. However, limited benthic foraminiferal numbers in core MD95-2006 yield to very small sample weights of monospecific benthic foraminifera and therefore require specialised small sample systems to obtain reliable ^{14}C measurements. This system is currently in development at the NERC Radiocarbon Laboratory, East Kilbride.

- The current AMS ^{14}C dates from core MD95-2007 have confirmed the presence of an expanded Lateglacial section. However, increased dating resolution in combination with foraminiferal taxonomy counts through core MD95-2007 would enable more precise determination of the timing of the interstadial event and onset of the Younger Dryas.

7.4 Conclusions

- Core MD95-2006 covers a longer chronological period than previous proposed by Kroon *et al.* (2000) and Knutz *et al.* (2001). The stratigraphic position of the NAAZII tephra peak (53,260 ± 2,660 yr BP) provides a useful isochrone near the base of the core.

- The BIS was highly responsive to external climate forcing , particularly around 30 cal ka BP. Sediment colour has enabled the characterization of rapid, sub-millennial-scale variability. A series of IRD intervals are present within core MD95-2006 which reflect the pacing of the D/O cyclicity. These IRD peaks are similar in amplitude to the Heinrich Events and indications point to a distinct BIS provenance for each event. A shift occurs at about 30 ka BP to lower amplitude, higher frequency fluctuations and is related to the expansion of the BIS onto the outer continental shelf.

- The recognition of the major ice rafting events of core MD95-2006 are indicative of Scottish IRD provenance and are coincident with the North Atlantic Heinrich Events H1 to H5. The timing of the H1 events is in agreement with other marine core studies of the north east Atlantic. So-called "non-Heinrich" events are recognised and many of these carry similar IRD sediment signatures to the true Heinrich events.

- The identification and timing of the LGM remains unresolved, although it is possible to infer an age from the $\delta^{18}O$ maxima of core MD95-2006 for coldest sea surface temperatures. It can, on this basis, be defined as occurring between 21-17 ka BP for this area off north west Scotland.

- Reliable amphi-Atlantic correlations may be achieved through an event stratigraphy which is based upon the interstadial events. The potential of this correlation was illustrated in comparisons between the MD95-2006 percentage *N. pachyderma* (sinistral) and GISP2 $\delta^{18}O$ records. This method will help to overcome the large dating and calibration uncertainties which are associated with the radiocarbon method and suggest that the major climate transitions are synchronous between the north east Atlantic and Greenland.

- The regional deglaciation of the BIS along the north west continental margin takes place at approximately 16.7 cal ka BP. This deglacial process leads to the rapid, final major retreat of the unstable BIS across the continental shelf area.

- Deglaciation of the entire margin is largely achieved through H1. The BIS probably responded in phase with the LIS during this phase of the deglaciation period.

Appendix A

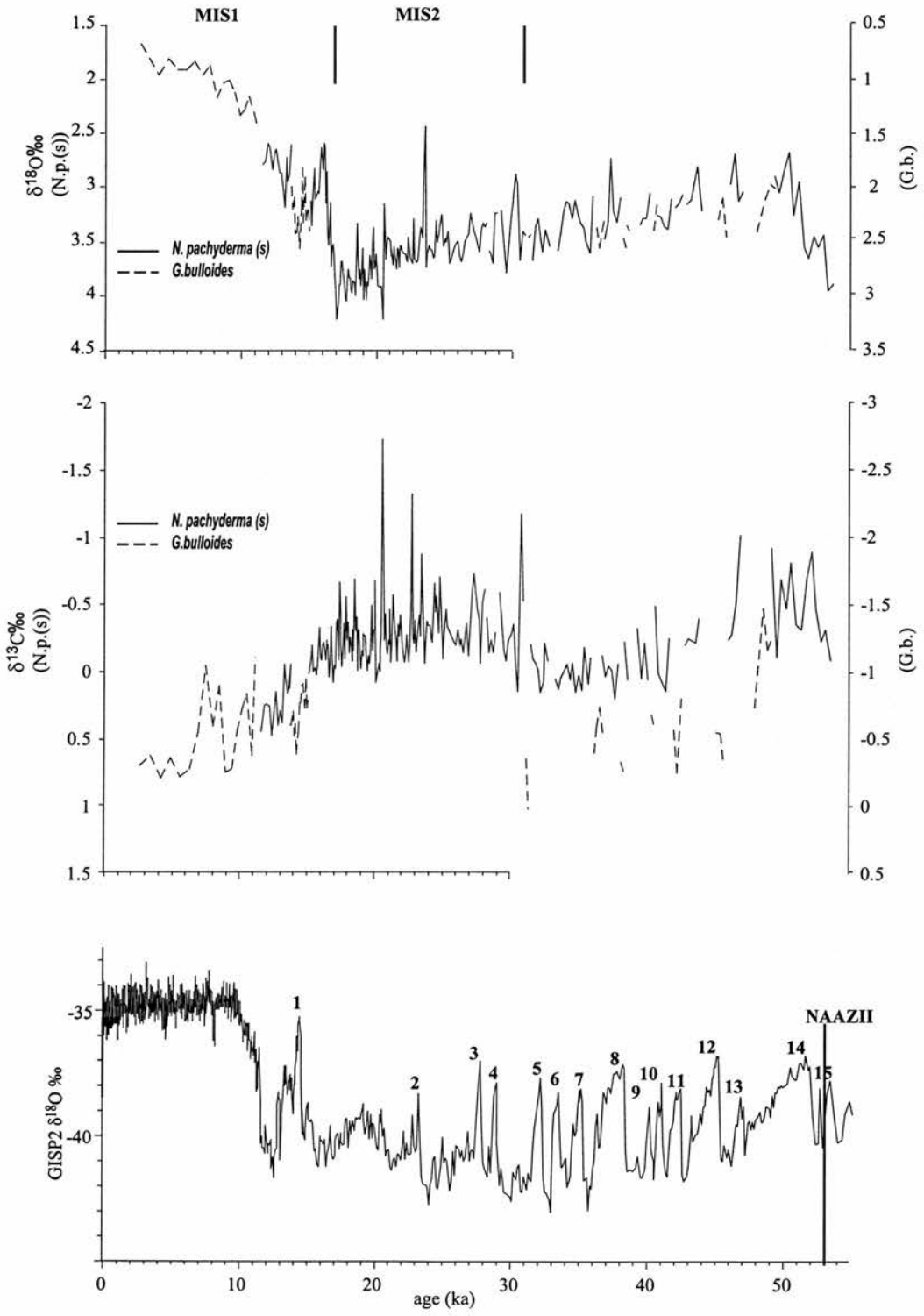

Appendix A. Stratigraphic summary of core MD95-2006 and the Greenland Ice Sheet Project (GISP2) ice core $\delta^{18}O$ (Grootes and Stuiver, 1997). Interstadial events are numbered from figure 3.8 following the identification of NAAZII.

References

Alley, R. B. 2000. The Two-Mile Time Machine. Princeton University Press, Princeton and Oxford. Pp 240.

Alley, R. B., and MacAyeal, D. R. 1994. Ice-rafted debris associated with binge/purge oscillations of the Laurentide Ice Sheet. *Paleoceanography* **9,** 503-511.

Alley, R. B., Shuman, C. A., Meese, D. A., Gow, A. J., Taylor, K. C., Cuffey, K. M., Fitzpatrick, J. J., Grootes, P. M., Zielinski, G. A., Ram, M., Spinelli, G., and Elder, B. 1997. Visual-stratigraphic dating of the GISP2 ice core: Basis, reproducibility, and application. *Journal of Geophysical Research* **102**, C12, 26,367-26,381.

Ammann, B. and Lotter, A. F. 1989. Late-Glacial radiocarbon- and palynostratigraphy on the Swiss Plateau. *Boreas* **18,** 109-126.

Andersen, B. G. 1981. Late Weichselian ice sheets in Eurasia and Greenland. *In:* Denton, G.H. and Hughes, T.J. (eds) *The Last Great Ice Sheets*, Wiley, New York, 1-65.

Andrews, J. T. 1998. Abrupt changes (Heinrich events) in late Quaternary North Atlantic marine environments: a history and review of data and concepts. *Journal of Quaternary Science*, **13**, 3-16.

Andrews, J. T. 2000. Icebergs and iceberg rafted detritus (IRD) in the North Atlantic: Facts and assumptions. *Oceanography* **13**, 100-108.

Andrews, J. T. and Tedesco, K. 1992. Detrital carbonate-rich sediments, northwestern Labrador Sea: implications for ice-sheet dynamics and iceberg rafting (Heinrich) events in the North Atlantic. *Geology* **20**, 1087-1090.

Andrews, J. T., Tedesco, K., and Jennings, A. E. 1993. Heinrich events: chronology and processes, east central Laurentide ice sheet and NW Labrador Sea. *In:* Peltier, W.R. (ed) *Ice in the Climate System*, Springer, Berlin, Heidelberg, 167-186.

Andrews, J. T., Erlenkeuser, H., Tedesco, K., Aksu, A., and Jull, A. J. T. 1994. Late Quaternary (Stage 2 and 3) meltwater and Heinrich like-events, NW Labrador Sea. *Quaternary Research* **41,** 26-34.

Andrews, J. T., Austin, W. E. N., Bergsten, H. and Jennings, A. E. 1996. The Late Quaternary palaeoceanography of North Atlantic margins: an introduction. *In*: Andrews, J.T., Austin, W.E.N., Bergsten, H. and Jennings, A.E. (eds) *Late Quaternary Palaeoceanography of the North Atlantic Margins*, Geological Society, London, Special Publications, **111**, 1-6.

Armishaw, J. E., Holmes, R. and Stow, A. V. 1998. Morphology and sedimentation on the Hebrides Slope and Barra Fan, NW UK continental margin. *In*: Stoker, M.S., Evans, D. and Cramp, A. (eds) *Geological Processes on Continental Margins: Sedimentation, Mass-Wasting and Stability*. Geological Society, London, Special Publications, **129**, 81-104.

Armishaw, J. E., Holmes, R. W., and Stow, D.A.V. 2000. The Barra Fan: A bottom-current reworked, glacially-fed submarine fan system. *Marine and Petroleum Geology* **17,** 219-238.

Austin, W. E. N. 1991. *Late Quaternary benthonic foraminiferal stratigraphy of the western UK continental shelf.* PhD Thesis, University of Wales.

Austin, W. E. N. 1994. Disturbed foraminiferal stratigraphies - a cautionary "tail". *Cushman Foundation Special Publication* **32,** 155-159.

Austin, W. E. N. and Kroon, D. 1996. Late glacial sedimentology, foraminifera and stable isotope stratigraphy of the Hebridean continental shelf, northwest Scotland. *In*: Andrews, J.T., Austin, W.E.N., Bergsten, H. and Jennings, A.E. (eds) *Late Quaternary Palaeoceanography of the North Atlantic Margins*, Geological Society, London, Special Publications, **111**, 187-213.

Austin, W. E. N. and Evans, J. R. 2000. North East Atlantic benthic foraminifera: modern distribution patterns and palaeoecological significance. *Journal of the Geological Society* **157**, 679-691.

Austin, W. E. N. and Kroon, D. 2001. Deep sea ventilation of the northeastern Atlantic during the last 15,000 years. *Global and Planetary Change* **30**, 13-31.

Austin, W. E. N., Bard, E., Hunt, J.B., Kroon, D. and Peacock, J.D. 1995. The ^{14}C age of the Icelandic Vedde Ash: implications for Younger Dryas marine reservoir age corrections. *Radiocarbon* **37**, 53-62.

Ballantyne, C. K. 1990. The Late Quaternary glacial history of the Trotternish Escarpment, Isle of Skye, Scotland, and its implications for ice-sheet reconstruction. *Proceedings of the Geologists' Association* **101** 171-186.

Ballantyne, C. K. and Hallam, G. E. 2001. Maximum altitude of late Devensian glaciation on South Uist, Outer Hebrides, Scotland. *Proceedings of the Geologists' Association* **112**, 155-167

Ballantyne, C. K., McCarroll, D., Nesje, A., Dahl, S. O., and Stone, J. O. 1998. The last ice sheet in north west Scotland: reconstruction and implications. *Quaternary Science Reviews* **17,** 1149-1184.

Balsam, W. L., Damuth, J. E. and Schneider, R. R. 1997. Comparison of shipboard vs. Shore-based spectral data from Amazon Fan cores: implications for interpreting sediment composition. *In*: Flood, R.D., Piper, D.J.W., Klaus, A. and Peterson, L.C. *Proceedings of the Ocean Drilling Program, Scientific Results*, **155**, 193-215.

Bard, E., Arnold, M., Duprat, J., Moyes, J., and Duplessy, J. C. 1987. Retreat velocity of the North Atlantic polar front during the last deglaciation determined by accelerator mass spectrometry. *Nature* **328,** 791-794.

Bard, E., Hamelin, B., and Fairbanks, R. G. 1990a. U-Th ages obtained by mass spectrometry in corals from Barbados: sea level during the past 130,000 years. *Nature* **346,** 456-458.

Bard, E., Hamelin, B., Fairbanks, R. G., and Zindler, A. 1990b. Calibration of the ^{14}C timescale over the past 30,000 years using mass spectrometric U-Th ages from Barbados. *Nature* **345,** 405-410.

Bard, E., Arnold, M., Mangerud, J., Paterne, M., Labeyrie, L., Duprat, J., Mélières, M.-A., Sønstegaard, E., and Duplessy, J. C. 1994. The North Atlantic

atmosphere-sea-surface ^{14}C gradient during the Younger Dryas climatic event. *Earth and Planetary Science Letters* **126,** 275-287.

Bard, E., Arnold, M., Hamelin, B., Tisnerat-Laborde, N. and Cabioch, G. 1998. Radiocarbon calibration by means of mass spectrometric Th^{230}/U^{234} and C^{14} ages of corals: an updated database including samples from Barbados, Mururoa and Tahiti. *Radiocarbon* **40**, 1085-1092.

Barnola, J. M., Raynaud, D., Korotkevich, Y. S. and Lorius, C. 1987. Vostok ice core provides 160,000-year record of atmospheric CO_2. *Nature* **329**, 408-413.

Beck, J. W., Richards, D. A., Edwards, R.L., Silverman, B. W., Smart, P. L., Donahue, D. J., Hererra-Osterheld, S., Burr, G.S., Calsoyas, L., Jull, A.J.T. and Biddulph, D. 2001. Extremely large variations of atmospheric ^{14}C concentration during the last glacial period. *Science* **292**, 2453-2558.

Belderson, R. H., Kenyon, N. H., Stride, A. H. and Stubbs, A. R. 1972. Sonographs of the Sea Floor. Elsevier, Amsterdam.

Bender, M., Sowers, T., Dickson, M. L., Orchardo, J., Grootes, P. M., Mayewski, P. A. and Meese, D. A. 1994. Climate correlations between Greenland and Antarctica during the past 100,000 years. *Nature* **372**, 663-666.

Benn, D. I. 1997. Glacier fluctuations in western Scotland. *Quaternary International* **38/39**, 137-149.

Benn, D. I., Lowe, J. J. and Walker, M. J. C. 1992. Glacier response to climatic-change during the Loch-Lomond Stadial and Early Flandrian: Geomorphological

and palynological evidence from the Isle of Skye, Scotland. *Journal of Quaternary Science* **7**, 125-144.

Berger, W. H., and Heath, G. R. 1968. Vertical mixing in pelagic sediments. *Journal of Marine Research* **26**, 134-143.

Binns, P. E., Harland, R., and Hughes, M. J. 1974. Glacial and postglacial sedimentation in the Sea of the Hebrides. *Nature* **248,** 751-754.

Björck, S., Walker, M. J. C., Cwynar, L. C., Johnsen, S., Knudsen, K.L., Lowe, J. J. and Wohlfarth, B. 1998. An event stratigraphy for the last termination in the North Atlantic region based on the Greenland ice-core record; a proposal by the INTIMATE group. *Journal of Quaternary Science* **13**, 283-292.

Blum, P. 1997. Physical Properties Handbook: A guide to shipboard measurement of physical properties of deep-sea cores. Technical note 26. Ocean Drilling Program.

Boessenkool, K. 2001. Environmental changes in the North Atlantic region during the last deglaciation. Universiteit Utrecht.

Bond, G. C. and Lotti, R. 1995. Iceberg discharges into the North Atlantic on millennial time scales during the last glaciation. *Science* **267**, 1005-1010.

Bond, G. C., Heinrich, H., Broecker, W. S., Labeyrie, L., McManus, J., Andrews, J., Huon, S., Jantschik, R., Clasen, S., Simet, C., Tedesco, K., Klas, M., Bonani, G. and Ivy, S. 1992. Evidence for massive discharges of icebergs into the North Atlantic Ocean during the last glacial period. *Nature* **360**, 245-249.

Bond, G. C., Broecker, W., Johnsen, S., McManus, J., Labeyrie, L., Jouzel, J. and Bonani, G. 1993. Correlations between climate records from North Atlantic sediments and Greenland ice. *Nature* **365**, 143-147.

Bond, G. C., Showers, W.J., Cheseby, M., Lotti, R., Almasi, P., De Menocal, P., Priore, P., Cullen, H., Hajdas, I. and Bonani, G. 1997. A pervasive millennial-scale cycle in North Atlantic Holocene and glacial climates. *Science* **278**, 1257-1266.

Bond, G. C., Showers, W., Elliot, M., Evans, M., Lotti, R., Hajdas, I., Bonani, G. and Johnson, S. 1999. The North Atlantic's 1-2 kyr Climate Rhythm: Relation to Heinrich Events, Dansgaard/Oeschger Cycles and the Little Ice Age. *In*: Clark, P.U., Webb, R.S. and Keigwin, L.D. (eds) *Mechanisms of Global Climate Change at Millennial Time Scales*, Geophysical Monograph, **112**, 35-58.

Bond, G., Mandeville, C., and Hoffmann, S. 2001. Were rhyolitic glasses in the Vedde Ash and in the North Atlantic's Ash Zone 1 produced by the same volcanic eruption? *Quaternary Science Reviews* **20,** 1189-1200.

Borchardt, G. A., Aruscavage, P. J. and Millard, Jr., H. T. 1972. Correlation of the Bishop Ash, a Pleistocene marker bed, Using instrumental neutron activation analysis. *Journal of Sedimentary Petrology* **42**, 301-306.

Boulton, G. S. 1990. Sedimentary and sea level changes during glacial cycles and their control on glacimarine facies architecture. *In*: Dowdeswell, J.A. and Scourse, J.D. (eds) *Glacimarine Environments: Processes and Sediments*, Geological Society, London, Special Publications, **53**, 15-52.

Boulton, G. S., Jones, A. S., Clayton, K. M., and Kenning, M. J. 1977. A British ice-sheet model and patterns of glacial erosion and deposition in Britain. *In:* Shotton, F.W. (ed.) *British Quaternary Studies: Recent Advances*, The Clarendon Press Oxford, 231-246.

Boulton, G. S., Smith, G. D., Jones, A. S., and Newsome, J. 1985. Glacial geology and glaciology of the last mid-latitude ice sheets. *Journal of the Geological Society, London* **142,** 447-474.

Boulton, G. S., Peacock, J. D., and Sutherland, D. G. 1991. Quaternary. *In* Craig, G.Y. (ed) *The Geology of Scotland*, The Geological Society, London, 503-542.

Bowen, D. Q., McCabe, A. M., Rose, J., and Sutherland, D. G. 1986. Correlation of Quaternary glaciations in the England, Ireland, Scotland and Wales. *In* Sibrava, V., Bowen, D.Q. and Richmond, G.M. (eds) *Quaternary Glaciations in the Northern Hemisphere*, International Geological Correlation Programme Project 24. *Quaternary Science Reviews* **5**, 299-340.

Bowen, D. Q., Philips, F. M., McCabe, A. M., Knutz, P. C. and Sykes, G. A. 2002. New data for the Last Glacial Maximum in Great Britain and Ireland. *Quaternary Science Reviews* **21**, 89-101.

Broecker, W. S. 2003. Does the trigger for abrupt climate change reside in the ocean or in the atmosphere? *Science* **300**, 1519-1522.

Broecker, W. and Denton, G. H. 1990. The role of ocean-atmosphere reorganisations in glacial cycles. *Quaternary Science Reviews* **9,** 305-341.

Broecker, W., Andree, M., Wolfli, W., Bonani, G., Kennett, J. P., and Peteet, D. M. 1988. The chronology of the last deglaciation: implications to the cause of the Younger Dryas event. *Paleoceanography* **3,** 1-20.

Broecker, W., Kennett, J. P., Flower, B. P., Teller, J. T., Trumbore, S., Bonani, G., and Wolfli, W. 1989. Routing of meltwater from the Laurentide Ice-Sheet during the Younger Dryas cold episode. *Nature* **341,** 318-321.

Broecker, W., Bond, G., Klas, M., Bonani, G. and Wolfi, W. 1990. A salt oscillator in the glacial Atlantic? *Paleoceanography*, **5**, 469-477.

Broecker, W., Bond, G., Klas, M., Clark, E., and McManus, J. 1992. Origin of the northern Atlantic's Heinrich events. *Climate Dynamics* **6,** 265-273.

Catt, J.A. 1987. Dimlington. *In:* Ellis, S. (ed) *East Yorkshire Field Guide.* Quaternary Research Asssociation. Cambridge. 82-98.

Chapman, M. R. and Shackleton, N. J. 1998a. What level of resolution is attainable in a deep-sea core? Results of a spectrophotometer study. *Paleoceanography*, **13**, 311-315.

Chapman, M. R. and Shackleton, N. J. 1998b. Millennial-scale fluctuations in North Atlantic heat flux during the last 150,000 years. *Earth and Planetary Science Letters*, **159**, 57-70.

Chapman, M. R., Shackleton, N. and Duplessy, J. C. 2000. Sea surface temperature variability during the last glacial-interglacial cycle: assessing the magnitude and

pattern of climate change in the North Atlantic. *Palaeogeography, Palaeoclimatology, Palaeoecology* **157**, 1-25.

Clapperton, C. M. 1997. Greenland ice cores and North Atlantic sediments: implications for the last glaciation in Scotland. *In:* Gordon, J.E. (ed) *Reflections on the Ice Age in Scotland: An Update on Quaternary Studies*. Scottish Association of Geography Teachers & Scottish Natural Heritage, Glasgow. 45-58.

Clark, P. U., and Mix, A. C. 2002. Ice sheets and sea level of the Last Glacial Maximum. *Quaternary Science Reviews* **21,** 1-7.

Clark, P. U., Clague, J. J., Curry, B. B., Dreimanis, A., Hicock, S. R., Miller, G. H., Berger, G. W., Eyles, N., Lamothe, M. and Miller, B. B. 1993. Initiation and development of the Laurentide and Cordilleran Ice Sheets following the last interglaciation. *Quaternary Science Reviews* **12**, 79-114.93

Clark, P. U., Pisias, N. G., Stocker, T. F., and Weaver, A. J. 2002. The role of the thermohaline circulation in abrupt climate change. *Nature* **415,** 863-869.

Cortijo, E., Yiou, P., Labeyrie, L. and Cremer, M. 1995. Sedimentary record of rapid climatic variability in the North Atlantic Ocean during the last glacial cycle. *Paleoceanography* **10,** 911-926.

Curry, W. B., Marchitto, T. M., McManus, J. F., Oppo, D. W. and Laarkamp, K. L. 1999. Millennial-scale changes in ventilation of the thermocline, intermediate, and deep waters of the glacial North Atlantic. *In*: Clark, P.U., Webb, R.S. and Keigwin, L.D. (eds) *Mechanisms of Global Climate Change at Millennial Time Scales*, Geophysical Monograph **112**, 59-76.

Dansgaard, W., Johnsen, S. J., Clausen, H. B., Dahljensen, D., Gundestrup, N. S., Hammer, C. U., Hvidberg, C. S., Steffensen, J. P., Sveinbjornsdottir, A. E., Jouzel, J. and Bond, G. 1993. Evidence for general instability of past climate from a 250-Kyr ice-core record. *Nature* **364**, 218-220.

Davies, H. C., Dobson, M. R., and Whittington, R. J. 1984. A revised seismic stratigraphy for Quaternary deposits on the inner continental shelf west of Scotland between 55°30'N and 57°30'N. *Boreas* **13,** 49-66.

Dearing, J. 1999. Magnetic Susceptibility. *In* Walden, J., Oldfield, F. and Smith, J.P (eds) *Environmental Magnetism: A Practical Guide*, Technical Guide, No. 6., Quaternary Research Association.

Deaton, B.C. 1987. Quantification of rock color from Munsell chips. *Journal of Sedimentary Petrology* **57**, 774-776.

Dokken, T. M. and Jansen, E. 1999. Rapid changes in the mechanisms of ocean convection during the last glacial period. *Nature* **401**, 458-461.

Domack, E.W., Jull, A.J.T., Anderson, J.B., Linick, T.W. and Williams, C.R. 1989. Application of tandem accelerator mass-spectrometer dating to late Pleistocene-Holocene sediments of the East Antarctic continental shelf. *Quaternary Research* **31**, 277-287.

Dowdeswell, J. A., Maslin, M. A., Andrews, J. T. and McCave, I. N. 1995. Iceberg production, debris rafting, and the extent and thickness of Heinrich Layers (H-1, H-2) in North Atlantic Sediments. *Geology* **23**, 4, 301-304.

Dowdeswell, J. A., Elverhøi, A. and Andrews, J. T. 1999. Asynchronous deposition of ice-rafted layers in the Nordic seas and the North Atlantic Ocean. *Nature* **400**, 348-351.

Duplessy, J. C., Delibrias, G., Turon, J. L., Pujol, C., and Duprat, J. 1981. Deglacial warming of the northeastern Atlantic Ocean: correlation with the palaeoclimate evolution of the European continent. *Palaeogeography, Palaeoclimatology, Palaeoecology* **35,** 121-144.

Duplessy, J. C., Arnold, M., Maurice, P., Bard, E., Duprat, J., and Moyes, J. 1986. Direct dating of the oxygen-isotope record of the last deglaciation by ^{14}C accelerator mass spectrometry. *Nature* **320** 350-352.

Eiríksson, J., Knudsen, K. L., Haflidason, H., and Heinemeier, J. 2000. Chronology of late Holocene climatic events in the northern North Atlantic based on AMS ^{14}C dates and tephra markers from the volcano Hekla, Iceland. *Journal of Quaternary Science* **15,** 573-580.

Elliot, M., Labeyrie, L., Bond, G., Cortijo, E., Turon, J. L., Tisnerat, N., and Duplessy, J. C. 1998. Millennial-scale iceberg discharges in the Irminger Basin during the last glacial period: Relationship with Heinrich events and environmental settings. *Paleoceanography* **13,** 433-446.

Evans, D., Stoker, M. S., and Cramp, A. 1998. Geological processes on continental margins: sedimentation, mass-wasting and stability: an introduction. *In* Stoker, M.S., Evans, D. and Cramp, A. *Geological Processes on Continental Margins: Sedimentation, Mass-Wasting and Stability*, Geological Society, London, Special Publications, **129**, 1-4.

Fairbanks, R. G. 1989. A 17,000-year glacio-eustatic sea level record: influence of glacial melting rates on the Younger Dryas event and deep-ocean circulation. *Nature* **342,** 637-642.

Flinn, D. 1978. The glaciation of the Outer Hebrides. *Geological Journal* **13,** 195-199.

Fronval, T., Jansen, E., Bloemendal, J. and Johnsen, S. 1995. Oceanic evidence for coherent fluctuations in Fennoscandian and Laurentide ice sheets on millennium timescales. *Nature*, **374**, 443-447.

Gagnon, A. R. and Jones, G. A. 1993. AMS-graphite target production methods at the Woods Hole Oceanographic Institution during 1986-1991. *Radiocarbon* **35**, 301-310.

Ganachaud, A., and Wunsch, C. R. 2000. Improved estimates of global ocean circulation, heat transport and mixing from hydrographic data. *Nature* **408,** 453-457.

Geikie, J. 1873. On the glacial phenomenon of the Long Isle or Outer Hebrides. *Journal of the Geological Society, London* **29,** 532-545.

Geikie, J. 1878. On the glacial phenomenon of the Long Isle or Outer Hebrides. *Journal of the Geological Society, London* **34,** 819-866.

Grimaldi, F. S., Shapiro, L. and Schnepfe, M. 1966. Determination of carbon dioxide in limestone and dolomite by acid-base titration. *US Geological Survey, Prof. Paper*, **550**, 186-188.

GRIP Greenland Ice-core Project Members 1993. Climate instability during the last interglacial period recorded in the GRIP ice core. *Nature* **364,** 203-207.

Grönvold, K., Óskarsson, N., Johnsen, S. J., Clausen, H. B., Hammer, C. U., Bond, G. and Bard, E. 1995. Express Letter: Ash layers from Iceland in the Greenland GRIP ice core correlated with oceanic and land sediments. *Earth and Planetary Science Letters* **135**, 149-155.

Grootes, P. and Stuiver, M. 1997. Oxygen 18/16 variability in Greenland snow and ice with 10^{-3}-10^{5}-year time resolution. *Journal of Geophysical Research* **102**(C12), 26,455-26,470.

Grootes, P., Stuiver, M., White, J. W. C., Johnsen, S., and Jouzel, J. 1993. Comparison of oxygen isotope records from the GISP2 and GRIP Greenland ice cores. *Nature* **366,** 552-554.

Grousset, F. E., Labeyrie, L., Sinko, J. A., Cremer, M., Bond, G., Duprat, J., Cortijo, E. and Huon, S. 1993. Patterns of ice-rafted detritus in the glacial North Atlantic (40-55^{0}N). *Paleoceanography* **8**, 175-192.

Grousset, F. E., Pujol, C., Labeyrie, L., Auffret, G. and Boelaert, A. 2000. Were the North Atlantic Heinrich events triggered by the behaviour of the European ice sheets? *Geology* **28**, 123-126.

Grousset, F. E., Cortijo, E., Huon, S., Herve, L., Richter, T., Burdloff, D., Duprat, J. and Weber, O. 2001. Zooming in on Heinrich layers. *Paleoceanography* **16**, 240-259.

Gwiazda, R. H.; Hemming, S. R. and Broecker, W. S. 1996. Tracking iceberg sources with lead isotopes: The provenance of ice-rafted debris in Heinrich layer 2, *Paleoceanography* **11**, 77-94.

Haflidason, H., Sejrup, H. P., Klitgaard-Kristensen, D., and Johnsen, S. J. 1995. Coupled response of the late glacial climatic shifts of northwest Europe reflected in Greenland ice cores: Evidence from the northern North Sea. *Geology* **23,** 1059-1062.

Haflidason, H., Eiriksson, J. and van Kreveld, S. 2000. The tephrochronology of Iceland and North Atlantic region during the middle and late Quaternary; a review. *Journal of Quaternary Science* **15**, 3-22.

Hald, M., and Vorren, T. O. 1987. Stable isotope stratigraphy and paleoceanography during the last deglaciation on the continental shelf off Tromso, Northern Norway. *Paleoceanography* **2,** 583-599.

Hall, A. M. (Editor) 1984. Buchan Field Guide. Quaternary Research Association, Cambridge, 120 pp.

Hall, A. M. 1995. Was north west Lewis glaciated during the Late Devensian? *Quaternary Newsletter* **76,** 1-7.

Hall, A., and Bent, A. J. A. 1990. The limits of the last British ice sheet in northern Scotland and the adjacent shelf. *Quaternary Newsletter* **6,** 2-12.

Harkness, D. D. 1983. The extent of natural ^{14}C deficiency in the coastal environment of the United Kingdom. *Proceedings of the First International Symposium on C-14 and Archaeology, PACT* **8,** 351-364.

Heinrich, H. 1988. Origin and consequences of cyclic ice rafting in the Northeast Atlantic Ocean during the past 130,000 years. *Quaternary Research* **29**, 142-152.

Helmke, J. P. and Bauch, H. A. 2001. Glacial-interglacial relationship between carbonate components and sediment reflectance in the North Atlantic. *Geo-Marine Letters* **21** (1), 16-22.

Hemming, S. R., Broecker, W. S., Sharp, W. D., Bond, G. C., Gwiazda, R. H., McManus, J. F., Klas, M., and Hajdas, I. 1998. Provenance of Heinrich layers in core V28-82, northeastern Atlantic: $^{40}Ar/^{39}Ar$ ages of ice-rafted hornblende, Pb isotopes in feldspar grains, and Nd-Sr-Pb isotopes in the fine sediment fraction. *Earth and Planetary Science Letters* **164,** 317-333.

Holmes, R., Long, D. and Dodd, L. R. 1998. Large-scale debrites and submarine landslides on the Barra Fan, west of Britain. *In*: Stoker, M.S., Evans, D. and Cramp, A. (eds) *Geological Processes on Continental Margins: Sedimentation, Mass-Wasting and Stability*. Geological Society, London, Special Publications, **129**, 67-79.

Howe, J. A., Harland, R., Hine, N. M., and Austin, W. E. N. 1998. Late Quaternary stratigraphy and palaeoceanographic change in the northern Rockall Trough, North Atlantic Ocean. *In* Stoker, M.S., Evans, D. and Cramp, A. *Geological*

Processes on Continental Margins: Sedimentation, Mass-Wasting and Stability, Geological Society, London, Special Publications, **129**, 269-286.

Hughen, K. A., Overpeck, J. T., Lehman, S. J., Kashgarian, M., Southon, J. R., and Peterson, L. C. 1998. A new ^{14}C calibration data set for the last deglaciation based on marine varves. *Radiocarbon* **40,** 483-494.

Hughen, K.A., Southon, J.R., Lehman, S.J. and Overpeck, J.T. 2000. Synchronous radiocarbon and climate shifts during the last deglaciation. *Science* **290**, 1951-1954.

Hunt, J.B. 1997. Quaternary tephrology and tephrochronology of the North Atlantic region. unpublished PhD, University of Edinburgh.

Hunt, J. B. and Hill, P. G. 1993. Tephra geochemistry: a discussion of some of the persistent analytical problems, *The Holocene* **3**, 271-278.

Hunt, J. B. and Hill, P. G. 1996. An inter-laboratory comparison of the electron probe microanalysis of glass shards. *Quaternary International* **34-36**, 229-241.

Hunt, J. B. and Hill, P. G. 2001. Tephrological implications of beam size-sample-size effects in electron microprobe analysis of glass shards. *Journal of Quaternary Science* **16**, 105-117.

Hunt, J. B., Fannin, N. G. T., Hill, P. G., and Peacock, J. D. 1995. The tephrochronology and radiocarbon dating of North Atlantic, Late Quaternary sediments: an example from the St. Kilda Basin. *In* Scrutton, R.A., Stoker, M.S., Shimmield, G. and Tudhope, A.W. *The Tectonics, Sedimentation and*

Palaeoceanography of the North Atlantic Region (eds.) Geological Society, London, Special Publication, **90**, 227-248.

Hunt, J.B. and 7 Ocean Drilling Program Participants. 1998. Standardisation of electron probe microanalysis of glass geochemistry. Proceedings of Ocean Drilling Program (Scientific Results) Leg 152, East Greenland Margin.

Huthnance, J. M. 1986. The Rockall slope current and shelf-edge processes. *Proceedings of the Royal Society of Edinburgh* **88B,** 83-101.

Jansen, E., and Erlenkeuser, H. 1985. Ocean circulation in the Norwegian Sea during the last deglaciation: isotopic evidence. *Palaeogeography, Palaeoclimatology, Palaeoecology* **49,** 189-206.

Jansen, E., and Veum, T. 1990. Evidence for a two-step deglaciation and its impact on North Atlantic deep-water circulation. *Nature* **343,** 612-616.

Jehu, T. J., and Craig, R. M. 1934. Geology of the Outer Hebrides. Part 3- North Harris and Lewis. *Transactions of the Royal Society of Edinburgh* **57,** 839-874.

Johnsen, S. J., Clausen, H. B., Dansgaard, W., Fuhrer, K., Gundestrup, N. S., Hammer, C. U., Iversen, P., Jouzel, J., Stauffer, B., and Steffensen, J. P. 1992. Irregular glacial interstadials recorded in a new Greenland ice core. *Nature* **359,** 311-313.

Jouzel, J., Lorius, C., Petit, J. R., Genthon, C., Barkov, N. I., Kotlyakov, V. M. and Petrov, V. M. 1987. Vostok ice core: a continuous isotope temperature record over the last climate cycle (160,000 years). *Nature* **329**, 403-408.

Keigwin, L. D., Jones, G. A., and Lehman, S. J. 1991. Deglacial meltwater discharge, North Atlantic deep circulation, and abrupt climate change. *Journal of Geophysical Research* **96,** 16,811-16,826.

Kellogg, T.B. 1973. Late Pliestocene climatic record in Norwegian and Greenland deep-sea cores. Unpublished PhD thesis. Department of Geology, Columbia University, 544pp.

Kenyon, N. H. 1987. Mass-wasting features on the continental slope of Northwest Europe. *Marine Geology* **74**, 57-77.

Knutz, P. C., Austin, W. E. N. and Jones, E. J. W. 2001. Millennial-scale depositional cycles related to British ice sheet variability and North Atlantic paleocirculation since 45 kyr B.P., Barra Fan, U.K. margin. *Paleoceanography* **16**, 53-64.

Knutz, P. C., Jones, E. J. W., Austin, W. E. N., and van Weering, T. C. E. 2002a. Glacimarine slope sedimentation and formation of contourite drifts on the Barra Fan, UK margin. *Marine Geology* **188,** 129-146.

Knutz, P. C., Hall, I. R., Zahn, R., Rasmussen, T. L., Kuijpers, A., Moros, M. and Shackleton, N. 2002b. Multidecadal ocean variability and NW European ice sheet surges during the last deglaciation. *Geochemistry, Geophysics, Geosystems* **3**, 1077.

Koç, N. and Jansen E. 1994. Response of the high-latitude northern-hemisphere to orbital climate forcing - evidence from the Nordic seas. Geology **22**, 523-526.

Koç, N., Jansen, E. and Haflidason, H. 1993. Paleoceanographic reconstructions of surface ocean conditions in the Greenland, Iceland and Norwegian Seas through the last 14 ka based on diatoms. *Quaternary Science Reviews* **12**, 115-140.

Koç, N., Jansen, E., Hald, M., and Labeyrie, L. 1996. Late glacial-Holocene sea surface temperatures and gradients between the North Atlantic and the Norwegian Sea: implications for the Nordic heat pump. *In*: Andrews, J.T., Austin, W.E.N., Bergsten, H. and Jennings, A.E. (eds) *Late Quaternary Palaeoceanography of the North Atlantic Margins*, Geological Society, London, Special Publications **111**, 177-185.

Kromer, B., and Becker, B. 1993. German oak and pine ^{14}C calibration 7200-9400 BC. *Radiocarbon* **35,** 125-137.

Kroon, D., Austin, W.E.N., Chapman, M.R., and Ganssen, G.M. 1997. Deglacial surface circulation changes in the northeastern Atlantic: Temperature and salinity records off NW Scotland on a century scale. *Paleoceanography* **12**, 755-763.

Kroon, D., Shimmield, G., Austin, W.E.N., Derrick, S., Knutz, P. and Shimmield, T. 2000. Century- to millennial-scale sedimentological-geochemical records of glacial-Holocene sediment variations from the Barra Fan (NE Atlantic). *Journal of the Geological Society* **157**, 643-653.

Kvamme, T., Mangerud, J., Furnes, H., and Ruddiman, W. 1989. Geochemistry of Pleistocene ash zones in cores from the North Atlantic. *Norsk Geologisk Tidsskrift* **69**, 251-272.

Labeyrie, L., Leclaire, H., Waelbroeck, C., Cortijo, E., Duplessy, J. C., Vidal, L., Elliot, M., Le Coat, B. and Auffret, G. 1999. *In*: Clark, P.U., Webb, R.S. and Keigwin, L.D. (eds) *Mechanisms of Global Climate Change at Millennial Time Scales*, Geophysical Monograph, **112**, 77-97.

Lacasse, C. 2001. Influence of climate variability on the atmospheric transport of Icelandic tephra in the subpolar North Atlantic. *Global and Planetary Change* **29**, 31-55.

Lacasse, C., Sigurdsson, Carey, S., Paterne, M. and Guichard, F. 1996. North Atlantic deep-sea sedimentation of Late Quaternary tephra from the Iceland hotspot. *Marine Geology* **129**, 207-235.

Lacasse, C., Werner, R., Paterne, M., Sigurdsson, H., Carey, S. N. and Pinte, G. 1998. Long-range transport of Icelandic tephra to the Irminger Basin, Site 919. *In:* Saunders, A.D., Larsen, H.-C., Clift, P.D., Wise Jr., S.W. (eds.) *Proceedings of the Ocean Drilling Program: Scientific Results*, **152**, Ocean Drilling Program, College Station, TX, 51-65.

Lackschewitz, K. S. and Wallrabe-Adams, H. J. 1997. Composition and origin of volcanic ash zones in Late Quaternary sediments from the Reykjanes Ridge: evidence for ash fallout and ice-rafting. *Marine Geology* **136**, 209-224.

Lambeck, K. 1993a. Glacial rebound of the British Isles- II. A high-resolution, high-precision model. *Geophysical Journal International* **115,** 960-990.

Lambeck, K. 1993b. Glacial rebound of the British Isles- I. Preliminary model results. *Geophysical Journal International* **115,** 941-959.

Lambeck, K. 1995a. Late Devensian and Holocene shorelines of the British Isles and North Sea from models of glacio-hydro-isostatic rebound. *Journal of Quaternary Research* **152,** 437-448.

Lambeck, K. 1995b. Glacial isostacy and water depths in the Late Devensian and Holocene on the Scottish Shelf west of the Outer Hebrides. *Journal of Quaternary Science* **10, 83-86.**

Lambeck, K. 1996. Limits on the areal extent of the Barents Sea ice sheet in Late Wieschelian time. *Palaeogeography, Palaeoclimatology, Palaeoecology* **12,** 41-51.

Lambeck, K., Yokoyama, Y., and Purcell, T. 2002. Into and out of the Last Glacial Maximum: sea-level change during Oxygen Isotope Stages 3 and 2. *Quaternary Science Reviews* **21,** 343-360.

Larsen, E., Gulliksen, S., Lauritzen, S.-E., Lie, R., Lovlie, R. and Mangerud, J. 1987. Cave stratigraphy in western Norway; multiple Weichselian glaciations and interstadial vertebrate fauna. *Boreas* **16**, 267-292.

Larsen, G. 1981. Tephrochronology by microprobe glass analysis, *In:* Self, S. and Sparks, R.S.J., (eds) *Tephra Studies*. Dordrecht, D.Reidel Publishing Company, 95-102.

Larsen, G., Gudmundsson, M. T. and Bjornsson, H. 1998. Eight centuries of periodic volcanism at the center of the Iceland hotspot revealed by glacier tephrostratigraphy.
Geology **26**, 943-946.

Lassen, S., Kuijpers, A., Kunzendorf, H., Lindgren, H., Heinemeier, J., Jansen, E. and Knudsen, K. L. 2002. Intermediate water signal leads surface water response during Northeast Atlantic deglaciation. *Global and Planetary Change* **32**, 111-125.

Le Maitre, R. W. (editor) 1989. A classification of igneous rocks and glossary of terms. Blackwell Scientific Publications, Oxford. Pp193.

Lehman, S. J., and Keigwin, L. D. 1992. Sudden changes in North Atlantic circulation during the last deglaciation. *Nature* **356,** 757-762.

Lehman, S. J., Jones, G. A., Keigwin, L. D., Andersen, E. S., Butenko, G., and Østmo, S.-R. 1991. Initiation of Fennoscandian ice-sheet retreat during the last glaciation. *Nature* **349,** 513-516.

Lowe, J. J. 2001. Abrupt climatic changes in Europe during the last glacial-interglacial transition: the potential for testing hypotheses on the synchroneity of climatic events using tephrochronology. *Global and Planetary Change* **30**, 73-84.

Lowe, J. J., and Walker, M. J. C. 1998. Reconstructing Quaternary Environments. Longman, London. Pp 457.

MacAyeal, D. R. 1993. Binge/Purge oscillations of the Laurentide Ice Sheet as a cause of the North Atlantic's Heinrich Events. *Paleoceanography* **8,** 775-784.

Mangerud, J., Andersen, S. T., Berglund, B. and Donner, J. J. 1974. Quaternary stratigraphy of Norden, a proposal for terminology and classification. *Boreas* **3**, 109-128.

Mangerud, J., Lie, S. E., Furnes, H., Kristiansen, I. L., and Lømo, L. 1984. A Younger Dryas ash bed in Western Norway, and its possible correlations with tephra in cores from the Norwegian Sea and the North Atlantic. *Quaternary Research* **21,** 85-104.

Martinson, D. G., Pisias, N. G., Hays, J. D., Imbrie, J., Moore, T. C. And Shackleton, N. J. 1987. Age dating and the orbital theory of ice ages: development of a high-resolution 0-300,000 year chronostratigraphy. *Quaternary Research* **27**, 1-29.

Mayewski, P. A., Meeker, L. D., Twickler, M. S., Whitlow, S., Yang, Q. Z., Lyons, W. B. and Prentice, M. 1997. Major features and forcing of high-latitude northern hemisphere atmospheric circulation using a 110,000-year-long glaciochemical series. *Journal of Geophysical Research-Oceans* **102**, 26,345-26,366.

McCabe, A. M. and Clark, P. U. 1998. Ice-sheet variability around the North Atlantic Ocean during the last deglaciation. *Nature* **392**, 373-377.

McCabe, M., Knight, J., and McCarron, S. 1998. Evidence for Heinrich event 1 in the British Isles. *Journal of Quaternary Science* **13,** 549-568.

McIntyre, A., and Molfino, B. 1996. Forcing of Atlantic equatorial and subpolar millennial cycles by precession. *Science* **274,** 1867-1870.

Meese, D. A., Alley, R. B., Fiacco, R. J., Germani, M. S., Gow, A. J., Grootes, P. M., Illing, M., Mayewski, P. A., Morrison, M. C., Ram, M., Taylor, K. C., Yang, Q. and Zielinski, G. A. 1994. Preliminary depth-age scale of the GISP2 ice core. Special CRREL Report 94-1, US.

Merrill, R. B. and Beck, J. W. 1996. The ODP color digital system; color logs of Quaternary sediments from the Santa Barbara Basin, Site 893. *Marine Georesources and Geotechnology* **14**, 381-408.

Mitchell, G. F., Penny, L. F., Shotton, F. W. and West, R. G. (eds) 1973. *A Correlation of Quaternary Science Deposits in the British Isles*. Geological Society, London, Special Publications, **4**, 67-80.

Mix, A. C., Bard, E., and Schneider, R. R. 2001. Environmental processes of the ice age: land, oceans, glaciers (EPILOG). *Quaternary Science Reviews* **20,** 627-657.

Munsell, A. H. 1941. A color notation, (9th ed.) Baltimore, Md., Munsell Color Co.

Nagao, S. and Nakashima, S. 1992. The factors controlling vertical color variations of North Atlantic Madeira abyssal plain sediments. The geochemistry of North Atlantic abyssal plains. *Marine Geology* **109**, 83-94.

Nielson, C., and Sigurdsson, H., 1981. Quantitative methods for electron microprobe analysis of sodium in natural and synthetic glasses. *American Mineralogist* **66**, 547-552.

Ortiz, J. D., O'Connell, S. and Mix, A. 1999. Data report; spectral reflectance observations from recovered sediments. Proceedings of the Ocean Drilling Program, scientific results, North Atlantic-Arctic gateways II; covering Leg 162 of the cruises of the drilling vessel JOIDES Resolution, Edinburgh, United Kingdom, to Malaga, Spain, sites 980-987, 7 July- 2 September 1995. Proceedings of the Ocean Drilling Program, Scientific Results **162**, 259-264.

Paillard, D., Labeyrie, L.D. and Yiou, P. 1996. AnalySeries 1.0: a Macintosh software for the analysis of geophysical time-series. *EOS* **77**, 379.

Peacock, J. D. 1984. Quaternary geology of the Outer Hebrides. *British Geological Survey Reports* **16/2,** 26.

Peacock, J. D. 1991. Glacial deposits of the Hebridean region. *In:* Ehlers, J., Gibbard, P.L. and Rose, J. (eds) *Glacial Deposits of Great Britain and Ireland*, Balkema, Rotterdam, 109-119.

Peacock, J. D. and Long, D. 1994. Late Devensian glaciation and deglaciation of Shetland. *Quaternary Newsletter* **74**, 16-21.

Peacock, J. D., Graham, D. K., and Gregory, D. M. 1980. Late-glacial and Post-glacial marine environments in part of the Inner Cromarty Firth, Scotland. *Report of the Institute of Geological Sciences* **80/7**.

Peacock, J. D., Austin, W. E. N., Selby, I., Harland, R., Wilkinson, I. P. and Graham, D. K. 1992. Late Devensian and Holocene palaeoenvironmental changes on the Scottish continental shelf west of the Outer Hebrides. *Journal of Quaternary Science* **7**, 145-161.

Peltier, W. R. 2002. On the post-glacial isostatic adjustment of the British Isles and the shallow visco-elastic structure of the Earth. *Geophysical Journal International* **148,** 443-475.

Pflaumann, U., Duprat, J., Pujol, C. and Labeyrie, L. 1996. SIMMAX: A modern analog technique to deduce Atlantic sea surface temperatures from planktonic foraminifera in deep-sea sediments. *Paleoceanography* **11**, 15-35.

Rahmstorf, S. 1994. Rapid climate transitions in a coupled ocean-atmosphere model. *Nature* **372,** 82-85.

Ram, M. and Gayley, R. I. 1991. Long-range transport of volcanic ash to the Greenland ice sheet. *Nature* **349**, 401-404.

Ram, M., Donarummo, J. and Sheridan, M. 1996. Volcanic ash from Iceland 57,300 yr BP eruption found in GISP2 (Greenland) ice core. *Geophysical Research Letters* **23** (22), 3167-3169.

Raymo, M. E., Ganley, K., Carter, S., Oppo, D. W., and McManus, J. 1998. Millennial-scale climate instability during the early Pleistocene epoch. *Nature* **392,** 699-702.

Revel, M. Sinko, J. A. and Grousset, F. E. 1996. Sr and Nd isotopes as tracers of North Atlantic lithic particles: Paleoclimatic implications. *Paleoceanography* **11**, 95-113.

Richter, T. O., Lassen, S., Van Weering, T. C. E. and Haas, H. De. 2001. Magnetic susceptibility patterns and provenance of ice-rafted material at Feni Drift, Rockall Trough: implications for the history of the British-Irish ice sheet. *Marine Geology* **173**, 37-54.

Robinson, S. G., Maslin, M. A., and McCave, N. I. 1995. Magnetic susceptibility variations in Upper Pleistocene deep-sea sediments of the NE Atlantic: Implications for ice rafting and paleocirculation at the last glacial maximum. *Paleoceanography* **10,** 221-250.

Rochon, A., de Vernal, A., Sejrup, H. P., and Haflidason, H. 1998. Palynological evidence of climatic and oceanographic changes in the North Sea during the last deglaciation. *Quaternary Research* **49,** 197-207.

Rose, J. 1985. The Dimlington Stadial/Dimlington Chronozone: a proposal for naming the main episode of the Late Devensian in Britain. *Boreas* **14**, 225-230.

Ruddiman, W. F. 1977. Late Quaternary deposition of ice-rafted sand in the subpolar North Atlantic (lat 40° to 65°N), *Geological Society of America Bulletin* **88**, 1813-1827.

Ruddiman, W. F. and Glover, L. K. 1972. Vertical mixing of ice-rafted volcanic ash in North Atlantic sediments. *Geological Society of America Bulletin* **83**, 2817-2836.

Ruddiman, W. F., and McIntyre, A. 1981. The North Atlantic Ocean during the last deglaciation. *Palaeogeography, Palaeoclimatology, Palaeoecology* **35,** 145-214.

Sarna-Wojcicki, A. M., Morrison, S. D., Mieyer, C. E. and Hillhouse, J. W. 1987. Correlation of upper Cenozoic tephra layers between sediments of the western United States and eastern Pacific Ocean and comparison with biostratigraphic and magnetostratigraphic age data. *Geological Society of America Bulletin* **98**, 207-223.

Scourse, J. D., and Austin, W. E. N. 2002. Quaternary shelf sea palaeoceanography: recent developments in Europe. *Marine Geology* **191,** 87-94.

Scourse, J. D., Hall, I. R., McCave, I. N., Young, J. R. and Sugdon, C. 2000. The origin of Heinrich layers; evidence from H2 for European precursor events. *Earth and Planetary Science Letters* **182**, 187-195.

Sejrup, H. P., Haflidason, H., Aarseth, I., King, E., Forsberg, C. F., Long, D. and Rokoengen, K. 1994. Late Weichselian glaciation history of the northern North Sea. *Boreas* **23**, 1-13.

Sejrup, H.P., Larsen, E., Landvik, J., King, E.L., Haflidason, H. and Nesje, A. 2000. Quaternary glaciations in southern Fennoscandia: evidence from southwestern Norway and the northern North Sea region. *Quaternary Science Reviews* **19**, 667-685.

Selby, I. 1989. *The Quaternary geology of the Hebridean continental margin.* Ph.D. Thesis, University of Nottingham.

Sigurdsson, H. 1982. Útbreidsla íslenskra gjóskulaga á botni Atlantshafs. Distribution of Icelandic tephra layers on the Atlantic ocean floor. (In Icelandic). *In*: Thorarinsdóttir, H., Oskarsson, O.H., Steinthorsson, S. and Einersson, Th. (eds) *Eldur er í nordri*, Sögufélag, Reykjavik, 119-127.

Sigurdsson, H., McIntosh, W. C., Dunbar, N., Lacasse, C., and Carey, S. N. 1998. Thorsmork Ignimbrite in Iceland; possible source of North Atlantic ash zone 2? *AGU 1998 spring meeting Eos, Transactions, American Geophysical Union* **79**, 377.

Skinner, L.C. and McCave, I.N. 2003. Analysis and modeling of gravity- and piston coring based on soil mechanics. *Marine Geology* **199**, 181-204.

Smith, D. E. 1997. Sea-level Change in Scotland During the Devensian and Holocene. *In:* Gordon, J.E. (ed) *Reflections on the Ice Age in Scotland: An Update on Quaternary Studies*, Scottish Association of Geography Teachers & Scottish Natural Heritage, Glasgow, 136-151.

Smith, D. E. 2000. Relative sea-level rise during the main postglacial transgression in NE Scotland, UK. *Transactions of the Royal Society of Edinburgh* **90,** 1-27.

Smythe, F. M., Ruddiman, W.F. and Lumsden, D.N. 1985. Ice-rafted evidence of long-term North Atlantic Circulation. *Marine Geology* **64**, 131-141.

Snoeckx, H., Grousset, F. E., Revel, M., and Boelaert, A. 1999. European contribution of ice-rafted sand to Heinrich layers H3 and H4. *Marine Geology* **158,** 197-208.

Sparks, R. S. J., Wilson, L. and Sigurdsson, H. 1981. The pyroclastic deposits of the 1875 eruption of Askja, Iceland. *Philosophical Transactions of the Royal Society of London, Series A*, **299**, 241-273.

Stocker, T. F. 2000. Past and future reorganizations in the climate system. *Quaternary Science Reviews* **19,** 301-319.

Stocker, T. F., and Wright, D. G. 1996. Rapid changes in ocean circulation and atmospheric radiocarbon. *Paleoceanography* **11,** 773-795.

Stoker, M. S. 1988. Pleistocene ice-marine glaciomarine sediments in boreholes from the Hebrides Shelf and Wyville-Thomson Ridge, NW UK Continental Shelf. *Scottish Journal of Geology* **24**, 249-262.

Stoker, M. S. 1990. Glacially-influenced sedimentation on the Hebridean slope, northwestern United Kingdom. *In*: Dowdeswell, J.A. and Scourse, J.D. (eds) *Glacimarine Environments: Processes and Sediments*, Geological Society, London, Special Publications, **53**, 349-362.

Stoker, M. S. 1995. The influence of glacigenic sedimentation on slope-apron development on the continental margin off northwest Britain. *In*: Scrutton, R.A., Stoker, M.S. Shimmield, G.B. and Tudhope, A.W. (eds) *The Tectonics, Sedimentation and Palaeoceanography of the North Atlantic Region*, Geological Society, London, Special Publications, **90**, 159-178.

Stoker, M. S. 1998. Sediment-drift development on the continental margin off NW Britain. *In:* Stoker, M.S., Evans, D. and Cramp, A. (eds) *Geological Processes on Continental Margins: Sedimentation, Mass-Wasting and Stability*, Geological Society, London, Special Publications, **129**, 229-254.

Stoker, M. S., and Holmes, R. 1991. Submarine end-moraines as indicators of Pleistocene ice-limits off northwest Britain. *Journal of the Geological Society, London* **148,** 431-434.

Stoker, M. S., Long, D., and Fyfe, J. A. 1985. The Quaternary succession in the central North Sea. *Newsletters on Stratigraphy* **14,** 119-128.

Stoker, M. S., Hitchen, K., and Graham, C. C. 1993. *United Kingdom Offshore Regional Report: the Geology of the Hebrides and West Shetland Shelves, and Adjacent Deep Water Areas*. HMSO for the British Geological Survey, London.

Stoker, M. S., Leslie, A. B., Scott, W. D., Briden, J. C., Hine, N. M., Harland, R., Wilkinson, I. P., Evans, D., and Ardus, D. A. 1994. A record of late Cenozoic stratigraphy, sedimentation and climate change from the Hebrides slope, NE Atlantic Ocean. *Journal of the Geological Society, London* **151,** 235-249.

Stow, D. A. and Tabrez, A. R. 1998. Hemipelagites: processes, facies and model. *In*: Stoker, M.S., Evans, D. and Cramp, A. (eds) *Geological Processes on Continental Margins: Sedimentation, Mass-Wasting and Stability*. Geological Society, London, Special Publications, **129**, 317-337.

Stuiver, M. and Reimer, P. J. 1993. Extended ^{14}C database and revised CALIB 3.0 ^{14}C age calibration program. *In:* Stuiver, M. and Kra, R.S. (eds) *Calibration 1993*, *Radiocarbon* **35**, 215-230.

Stuiver, M. and Grootes, P. 2000. GISP2 Oxygen Isotope Ratios. *Quaternary Research*, **53**, 277-284.

Stuiver, M., Grootes, P., and Braziunas, T. F. 1995. The GISP2 delta O-18 climate record of the past 16,500 years and the role of the sun, ocean, and volcanoes. *Quaternary Research* **44,** 341-354.

Stuiver, M., Reimer, P. J., Bard, E., Beck, J. W., Burr, G. S., Hughen, K. A., Kromer, B., McCormac, G., van der Plicht, J. and Spurk, M. 1998. INTCAL98 radiocarbon age calibration, 24,000-0 cal BP, *Radiocarbon* **40**, 1041-1083.

Sutherland, D. G. 1984. The quaternary deposits and landforms of Scotland and the neighbouring shelves: a review. *Quaternary Science Reviews* **3,** 157-254.

Sutherland, D. G. 1991. Late Devensian glacial deposits and glaciation in Scotland and the adjacent offshore region. *In:* Ehlers, J., Gibbard, P.L. and Rose, J. *Glacial Deposits in Great Britain and Ireland*, Balkema, Rotterdam, 53-60.

Sutherland, D. G., and Walker, M. J. C. 1984. A Late Devensian ice-free area and possible interglacial site on the Isle of Lewis, Scotland. *Nature* **309,** 701-703.

Sutherland, D. G., Ballantyne, C. K., and Walker, M. J. C. 1984. Late Quaternary glaciation and environmental change on St Kilda, Scotland, and their palaeoclimatic significance. *Boreas* **13,** 261-272.

Sweatman T. R. and Long, J. V. P. 1969. Quantitative electron-probe microanalysis of rock-forming minerals. *Journal of Petrology* **10**, 332-379.

Taylor, K. C., Lamorey, G. W., Doyle, G. A., Alley, R. B., Grootes, P., Mayewski, P. A., White, J. W. C. and Barlow, L. K. 1993. The 'flickering switch' of late Pleistocene climate change. *Nature* **361**, 432-436.

Thomson, M. E., and Eden, R. A. 1977. Quaternary deposits of the central North Sea, The Quaternary sequence in the west-central North Sea. *Report of the Institute of Geological Sciences* **77**.

Vidal, L., Labeyrie, L., Cortijo, E., Arnold, M., Duplessy, J. C., Michel, E., Becqué, S. and van Weering, T. C. E. 1997. Evidence for changes in the North Atlantic

Deep Water linked to meltwater surges during the Heinrich events. *Earth and Planetary Science Letters*, **146**, 13-27.

Voelker, A. H. L., Sarnthein, M., Grootes, P.M., Erlenkeuser, H., Laj, C., Mazaud, A., Nadeau, M-J. and Schleicher, M. 1998. Correlation of marine ^{14}C ages from the Nordic Seas with the GISP2 isotope record; implications for ^{14}C calibration beyond 25 ka BP. Proceedings of the 16th international radiocarbon conference; Part 1 *Radiocarbon* **40**, 517-534.

von Weymarn, J. A. 1979. A new concept of glaciation in Lewis and Harries, Outer Hebrides. *Proceedings of the Royal Society of Edinburgh* **77B,** 97-105.

von Weymarn, J. A., and Edwards, K. J. 1973. Interstadial site on the island of Lewis, Scotland. *Marine and Petroleum Geology* **246,** 473-474.

Waelbroeck, C., Duplessy, J. C., Michel, E., Labeyrie, L., Paillard, D., and Duprat, J. 2001. The timing of the last deglaciation in North Atlantic climate records. *Nature* **412,** 724-470.

Walker, M. J. C., Bjork, S., Lowe, J. J., Cwynar, L. C., Johnsen, S., Knudsen, K. L., Wohlfarth, B. and INTIMATE group. 1999. Isotopic 'events' in the GRIP ice core: a stratotype for the late Pleistocene. *Quaternary Science Reviews* **18**, 1143-1150.

Whittington, G., and Hall, A. M. 2002. The Tolsta Interstadial, Scotland: correlation with D-O cycles GI-8 to GI-5? *Quaternary Science Reviews* **21,** 901-915.

Wohlfarth, B. 1996. The chronology of the last termination: A review of radio carbon-dated, high-resolution terrestrial stratigraphies. *Quaternary Science Reviews* **15**, 267-284.

Zaragosi, S., Eynaud, F., Pujol, C., Auffret, G. A., Turon, J. L., and Garlan, T. 2001. Initiation of the European deglaciation as recorded in the northwestern Bay of Biscay slope environments (Meriadzek Terrace and Trevelyan Escarpment); a multi-proxy approach. *Earth and Planetary Science Letters* **188,** 493-507.

Zielinski, G. A., Mayewski, P. A., Meeker, L. D., Gronvöld, K., Germani, M. S., Whitlow, S., Twickler, M. S. and Taylor, K. 1997. Volcanic aerosol records and tephrochronology of the Summit, Greenland, ice cores. *Journal of Geophysical Research* **102**, C12, 26,625-26,640.